TELECONNECTIONS BETWEEN ENSO EVENTS AND GROWING SEASON PRECIPITATION ON THE CANADIAN PRAIRIES

A Thesis

Submitted to the College of Graduate Studies and Research

in Partial Fulfilment of the Requirements

For the Degree of

Doctor of Philosophy

in the

Department of Geography

University of Saskatchewan

Saskatoon

by

Barrie Richard Bonsal

December 1995

UNIVERSITY OF SASKATCHEWAN

College of Graduate Studies and Research

SUMMARY OF DISSERTATION

Submitted in partial fulfilment

of the requirements for the

DEGREE OF DOCTOR OF PHILOSOPHY

by

Barrie Richard Bonsal

Department of Geography
University of Saskatchewan

November 1995

Examining Committee:

Dr. R. McKercher	Associate Dean, Chair, College of Graduate Studies and Research
Dr. D. DeBoer	Chair of Advisory Committee, Department of Geography
Dr. L. Martz	Co-supervisor, Department of Geography
Mr. R. Lawford	Co-supervisor, Department of Geography
Dr. J. Newell	Department of Geography
Dr. A. Chakravarti	Department of Geography
Professor E. Ripley	Department of Crop Science

External Examiner:

Dr. A. Paul
Department of Geography
University of Regina
Regina, Saskatchewan
S4S 0A2

TELECONNECTIONS BETWEEN ENSO EVENTS AND GROWING-SEASON PRECIPITATION ON THE CANADIAN PRAIRIES

Teleconnections between ENSO events and growing-season precipitation variations on the Canadian Prairies are examined. Correlation and composite analyses indicate that between 1948 and 1991, El Niño events were associated with more frequent extended dry spells. Conversely, La Niña events coincided with fewer extended dry spells. Both relationships occurred during the third growing season following the onset of the ENSO events (i.e. approximately a 10-season or 30-month lag). A series of atmosphere - ocean teleconnections over the Pacific Ocean including Pacific North America (PNA) circulation patterns, North Pacific sea-surface temperature anomalies and upper-atmospheric circulation anomalies were found to result in growing-season precipitation variations over the Canadian Prairies. Results of this analysis are incorporated into a conceptual model which may form the basis of a long-range forecasting technique of growing-season precipitation variations on the Canadian Prairies.

ABSTRACT

Teleconnections between ENSO events and growing-season precipitation variations on the Canadian Prairies are examined. Correlation and composite analyses indicate that between 1948 and 1991, El Niño events were associated with more frequent extended dry spells. Conversely, La Niña events coincided with fewer extended dry spells. Both relationships occurred during the third growing season following the onset of the ENSO events (i.e. approximately a 10-season or 30-month lag). A series of atmosphere - ocean teleconnections over the Pacific Ocean including Pacific North America (PNA) circulation patterns, North Pacific sea-surface temperature anomalies and upper-atmospheric circulation anomalies were found to result in growing-season precipitation variations over the Canadian Prairies. Results of this analysis are incorporated into a conceptual model which may form the basis of a long-range forecasting technique of growing-season precipitation variations on the Canadian Prairies.

ACKNOWLEDGEMENTS

I would like to thank Mr. Rick Lawford and Dr. A.K. Chakravarti for their time and effort in supervising, guiding and supporting me in this research project. Thanks is also given to members of my supervisory committee including Professor E.A. Ripley, Dr. L.W. Martz and in particular, Dr. J. Newell who, as a late addition, was an integral part in the completion of this thesis. Acknowledgement is given to Dr. A. Paul of the University of Regina for being external examiner of my thesis.

Many thanks are given to the numerous people (especially from the National Hydrology Research Centre in Saskatoon and the Canadian Meteorological Centre in Dorval, Quebec) who assisted in my data collection and/or analysis. I would also like to acknowledge all the students and faculty in the Department of Geography at the University of Saskatchewan who made my 37,959 hours as a PhD student very enjoyable (especially those who often accompanied me to the local tavern).

Special thanks are given to Jacki, who helped me enjoy the 'ups' and ride through the 'downs' that are associated with completing a PhD degree. Finally, I would like to dedicate this thesis to my good friend Barry, who helped me celebrate many of the early accomplishments of my thesis, but unfortunately, wasn't here to help me party after the completion of the degree.

TABLE OF CONTENTS

LIST OF TABLES

LIST OF FIGURES

TABLE OF ACRONYMS

AES	Atmospheric Environment Service
CMC	Canadian Meteorological Centre
ENSO	El Niño / Southern Oscillation
GCM	general circulation model
GIS	geographic information system
ITCZ	inter-tropical convergence zone
PNA	Pacific North America anomaly
SLP	sea-level pressure
SO	Southern Oscillation
SOI	Southern Oscillation Index
SPANS	spatial analysis system
SPCZ	South Pacific convergence zone
SST	sea-surface temperature

CHAPTER 1

STUDY PROBLEM, HYPOTHESES AND OBJECTIVES

1.1 INTRODUCTION

ENSO (El Niño/Southern Oscillation) events are the largest single source of interannual climatic variability on a global scale (Diaz and Kiladis, 1992). They are often associated with large deviations from climatology of temperature and precipitation in many parts of the world. This study analyzes possible teleconnections between ENSO events and growing-season (May to August) precipitation on the Canadian Prairies.

Environmental processes and economic activity on the Canadian Prairies are highly dependent on precipitation, especially during the growing season when most (up to two thirds) of the annual precipitation is received (Kendrew and Currie, 1955; Chakravarti, 1972; Longley, 1972; Dey, 1982). However, this precipitation is highly variable, both temporally and spatially. Extreme precipitation variations, including wet spells and extended dry spells leading to droughts, are a recurrent feature of the growing-season climate (Kendrew and Currie, 1955; Longley, 1972; Dey, 1976; Dey and Chakravarti, 1976).

Most climatological studies of the Prairies have focused on negative precipitation anomalies. This is because droughts often produce severe environmental and economic impacts on many sectors of society including agriculture (e.g. crop yields), water resources (e.g. streamflow, groundwater, hydroelectric production), forestry (e.g. forest fires), wetlands, waterfowl and wildlife (Wheaton et al., 1992).

In the agricultural areas of the Prairies, drought constitutes one of the most widespread and economically significant natural hazards (Lawford, 1992). As a result, many studies have addressed the environmental and economic impacts of Canadian Prairie droughts (e.g. McKay et al., 1989; Lawford, 1992; Wheaton et al., 1992; Maybank et al., 1995).

Positive precipitation anomalies are less prominent than droughts, likely because they have fewer adverse effects on the Prairie environment and economy than dry periods. Wetter conditions are often beneficial to the semi-arid Prairie climate, producing higher crop yields, greater diversity of crops, fewer forest fires, more hydroelectric production, etc.. However, persistence of wet conditions may lead to adverse effects such as reduced crop yields, delays in planting, higher frequency of crop diseases, less recreation and tourism and, in some areas, even flooding. Therefore, the ability to anticipate or forecast growing-season precipitation variations, especially those which lead to droughts, can provide many environmental and economic benefits to the Canadian Prairies.

The main synoptic characteristic of growing-season dry periods on the Prairies is a persistent mid-tropospheric ridge over the area (Chakravarti, 1972; Dey and Chakravarti, 1976; Dey, 1982; Knox and Lawford, 1990). Conversely, above normal growing-season precipitation is associated with persistent upper-level zonal flow (Dey, 1977,1982; Knox and Lawford, 1990). However, the causes of these persistent patterns are not fully known.

Anomalous surface-boundary conditions such as sea-surface

temperature (SST), soil moisture and snow cover anomalies have the potential to modify and induce persistent anomalies of upper-atmospheric longwave patterns, mainly through changes in latent and sensible heat fluxes from the surface (Walsh et al., 1985; Ripley, 1988). The term teleconnection is used to describe relationships between anomalous surface boundary conditions at one location on the earth's surface and meteorological variables (e.g. upper-atmospheric flow patterns, temperature, precipitation) at other locations (Namias, 1981; Wallace and Gutzler, 1981).

Teleconnections between surface-boundary conditions and variations in growing-season precipitation on the Canadian Prairies have not been extensively researched. Bonsal et al. (1993) showed a significant relationship between persistent (10 months or longer) SST anomalies in the North Pacific Ocean and positive 50 kPa anomalies associated with extended dry spells over the Prairies during the growing season. The SST patterns were characterized by anomalously cold water in the east-central North Pacific and anomalously warm water along the central-west coast of North America (Figure 1.1). It is suggested that the SST anomaly patterns diverted the upper-atmospheric flow producing more positive 50 kPa anomalies (suggesting 50 kPa ridging) and thus, extended dry spells over the Prairies. However, the possible causes of the SST anomaly patterns were not determined.

Large-scale atmospheric circulation influences SSTs mainly through wind stress and associated oceanic mixing and surface ocean currents (Perry and Walker, 1977; Namias and Cayan, 1981). North Pacific SST anomalies are often associated with large-scale circulation anomalies

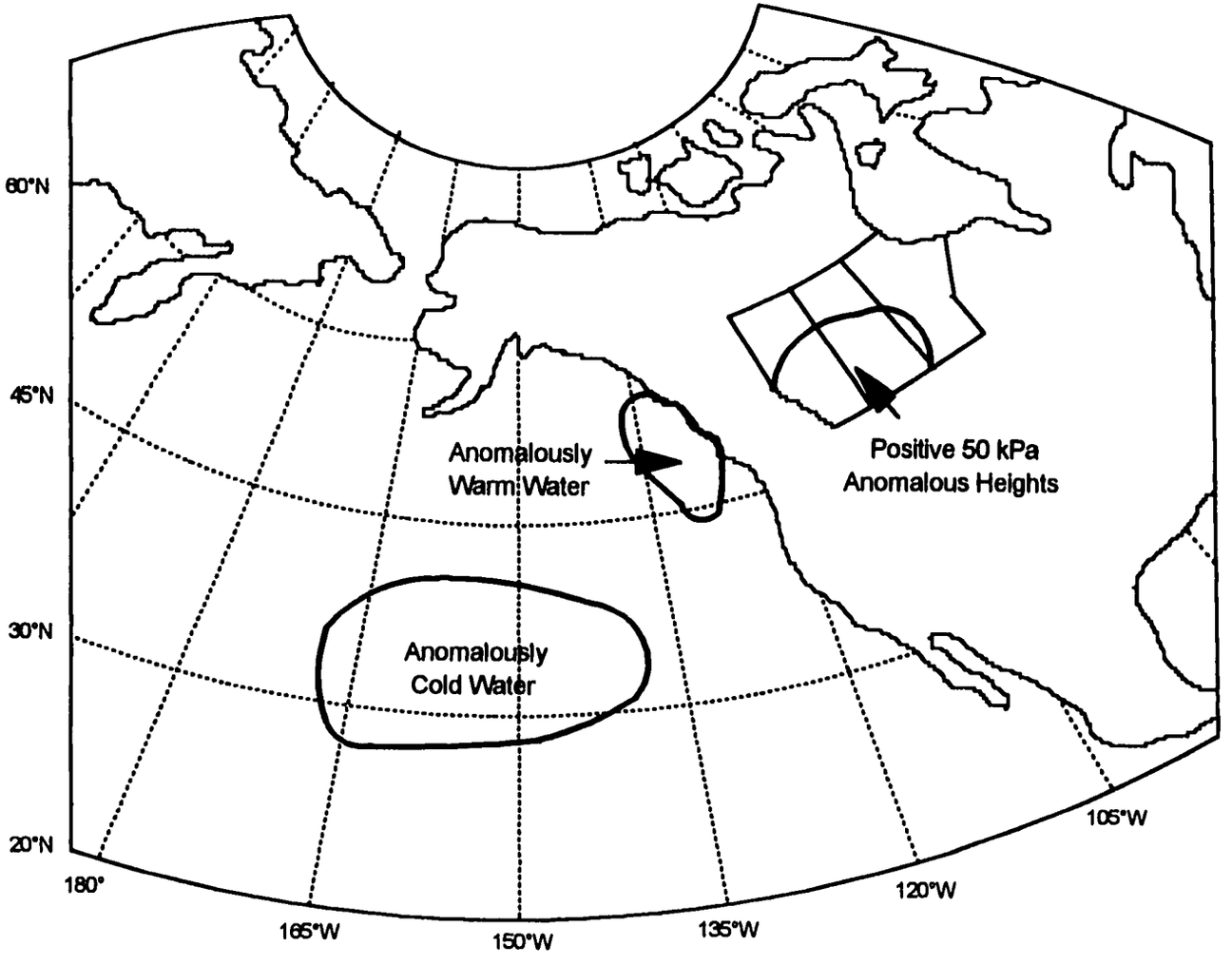

Figure 1.1: Anomalies of North Pacific SSTs and 50 kPa Heights Associated with Growing Season Extended Dry Spells on the Canadian Prairies (Taken from Bonsal et al., 1993)

known as the Pacific North America (PNA) patterns (Simpson, 1983; Wagner, 1984; Emery and Hamilton, 1985; Alexander, 1990,1992). There are two phases of the PNA. The positive phase is characterized by negative height anomalies over the northeastern North Pacific Ocean (i.e. a deeper Aleutian low), positive anomalies over western Canada and negative anomalies over the southeastern United States. The negative phase shows positive height anomalies over the northeastern North Pacific (i.e. a weaker Aleutian low), negative anomalies over western Canada and positive anomalies over the southeastern United States (Yarnal and Diaz, 1986; Leathers et al., 1991).

Several studies have found relationships between positive PNA patterns and North Pacific SST anomaly patterns similar to that depicted in Figure 1.1 (Pan and Oort, 1983,1990; Emery and Hamilton, 1985; Alexander 1990,1992; Weber, 1990). The SST patterns usually occur shortly (i.e. within a season) following the occurrence of positive PNA patterns. It has been suggested that these SST anomalies are generated by the surface circulation of the stronger Aleutian low associated with positive PNA patterns (Simpson, 1983; Wagner, 1984; Mysak, 1986; Yongping and McBean, 1991).

Negative PNA patterns are related to North Pacific SST anomaly patterns opposite to those associated with positive PNA (Emery and Hamilton, 1985; Pan and Oort, 1990). These SST patterns are characterized by anomalously warm water in the east-central North Pacific and anomalously cold water along the central-west coast of North America. It has been suggested that these patterns result from the surface circulation associated with negative PNA patterns, and in

particular, the weaker Aleutian low (Emery and Hamilton, 1985; Yongping and McBean, 1991). However, associations between negative PNA patterns and North Pacific SST anomalies have not been as extensively researched as those involving positive PNA patterns.

ENSO has been shown to influence the development of PNA patterns (Emery and Hamilton, 1985; Ropelewski and Halpert, 1986; Yarnal and Diaz, 1986; Hamilton, 1988; Weber, 1990). ENSO refers to anomalous atmospheric and oceanic conditions in the tropical Pacific. These conditions are associated with a sea-level pressure (SLP) oscillation between the South Pacific sub-tropical high pressure cell in the eastern tropical Pacific and the northern Australian - Indonesian low pressure trough in the western tropical Pacific (known as the Southern Oscillation (SO)) (Walker, 1924; Walker and Bliss, 1932). The phase of the SO is negative with anomalously low SLP in the eastern, and anomalously high SLP in the western tropical Pacific and vice versa (Bjerknes, 1966,1969; Chen, 1982).

There are two modes which make up the ENSO cycle, namely El Niño and La Niña. El Niño refers to a large area of anomalously warm water in the eastern tropical Pacific associated with the negative phase of the SO. El Niño events differ in their timing and duration, however, a typical event begins around December or January and matures approximately one year later (Rasmusson and Carpenter, 1982; Ropelewski and Halpert, 1986,1987,1989; Kiladis and van Loon, 1988; Kiladis and Diaz, 1989).

The second mode, termed La Niña, is opposite to El Niño, and is characterized by a large area of anomalously cold water in the eastern

tropical Pacific associated with the positive phase of the SO (Philander, 1985,1990). The temporal characteristics of a typical La Niña (i.e. onset, maturity, termination, duration) are similar to El Niño (Philander, 1985,1990; van Loon and Shea, 1985; Yarnal and Diaz, 1986; Deser and Wallace, 1990).

During El Niño, the anomalous heat source (caused by the large area of anomalously warm water in the eastern tropical Pacific) produces many teleconnections in both the tropics and extratropics, including positive PNA patterns. These patterns normally develop during the autumn or winter following the onset of El Niño (i.e. near the mature stage) (Horel and Wallace, 1981; Chen, 1983; Yarnal and Diaz, 1986; Hamilton, 1988; Weber, 1990). Conversely, La Niña events are associated with negative PNA patterns which also normally develop during the autumn or winter following the onset of the events (Emery and Hamilton, 1985; Yarnal and Diaz, 1986). However, unlike the link between El Niño and positive PNA patterns, there are relatively few studies examining possible relationships between La Niña and negative PNA patterns.

1.2 HYPOTHESES

1.2.1 EL NIÑO EVENTS

The preceding discussion has indicated possible teleconnections between ENSO events and North Pacific SST anomaly patterns with the PNA acting as a link. In particular, El Niño events are related to positive PNA patterns which normally develop during the following autumn or winter (Emery and Hamilton, 1985; Ropelewski and Halpert, 1986; Yarnal and Diaz, 1986; Hamilton, 1988; Weber, 1990). In addition, positive PNA

patterns are related to SST anomaly patterns similar to that shown in Figure 1.1 (Pan and Oort, 1983,1990; Emery and Hamilton, 1985; Alexander, 1990,1992; Weber, 1990). The SST anomaly patterns normally develop one season after the appearance of positive PNA patterns (which coincides with the winter or spring of the year following the onset of El Niño).

Bonsal et al. (1993) found a significant relationship between North Pacific SST anomaly patterns and positive 50 kPa anomalies associated with growing-season extended dry spells on the Canadian Prairies (especially when the patterns persisted for 10 months or longer). Therefore, it is hypothesized that if North Pacific SST anomaly patterns are related to El Niño events, and growing-season extended dry spells on the Prairies are related to these SST anomalies, then extended dry spells should be related to El Niño events. This relationship occurs through a series of atmosphere - ocean teleconnections over the Pacific Ocean (Figure 1.2 (a)).

It is hypothesized that positive PNA patterns develop during the autumn or winter following the onset of El Niño events (i.e. +3 to +4 seasons) corresponding to the mature stage of these events. The positive PNA patterns then aid in developing North Pacific SST anomaly patterns consisting of negative SST anomalies in the east-central North Pacific and positive anomalies along the central-west coast of North America (see Figure 1.1). These patterns develop around one season following the occurrence of positive PNA patterns (i.e. winter(+4) to spring(+5)).

If these SST anomaly patterns persist for a year or longer (which is usually the case because once SST anomalies are produced, they tend

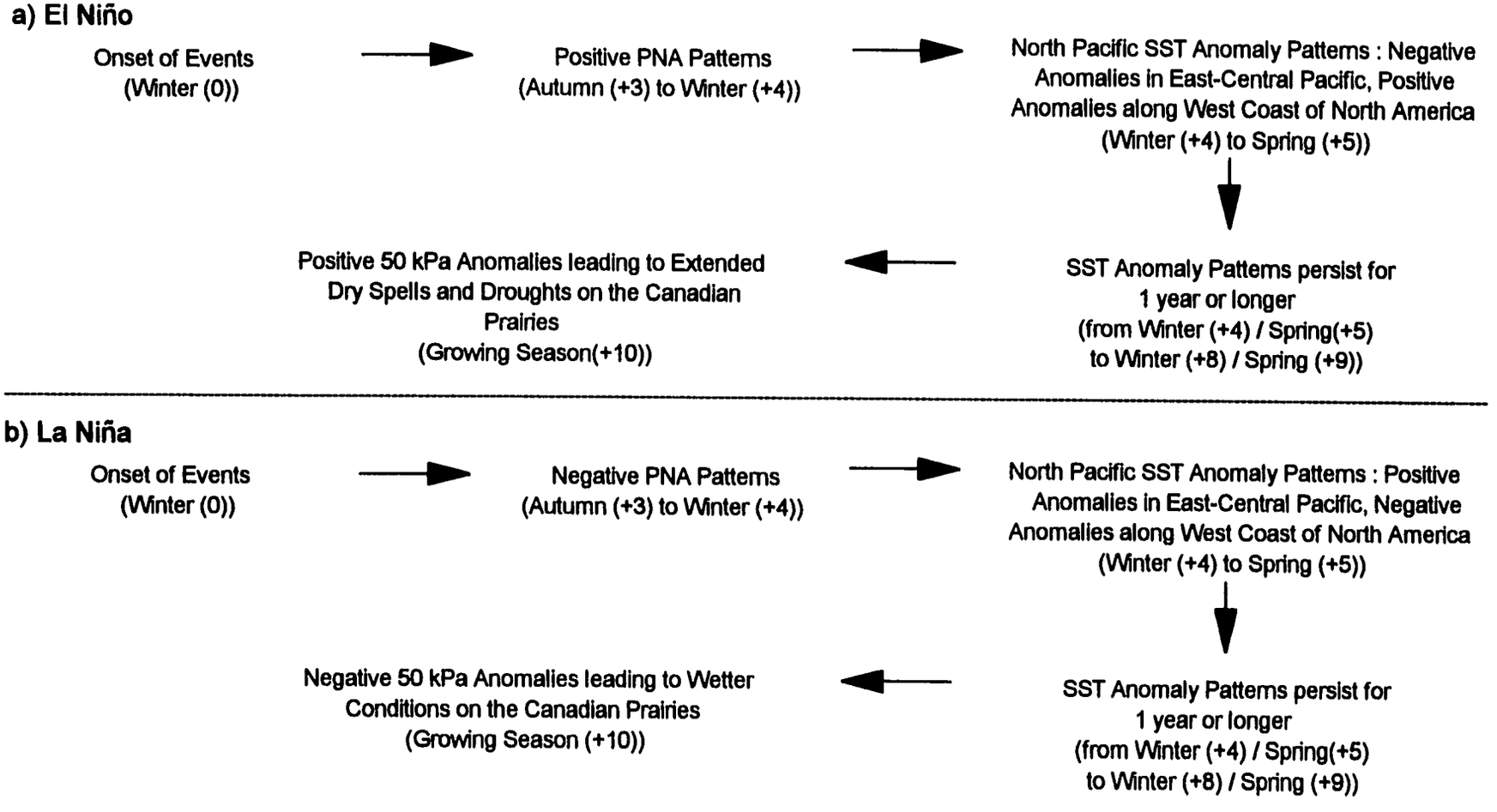

Note: Numbers in brackets refer to the lags (in seasons) with respect to the onset of the ENSO events
Winter refers to December, January, February; Spring to March, April, May; Summer to June, July, August; Autumn to September, October, November; Growing Season to May, June, July, August

Figure 1.2: Hypothesized Atmosphere - Ocean Teleconnections in the Pacific Ocean: a) El Niño and b) La Niña

to persist for several months, or even several years (Namias and Cayan, 1981; Namias et al., 1988)), they could cause positive 50 kPa anomalies leading to extended dry spells on the Canadian Prairies during the growing season (i.e. Bonsal et al., 1993). Taking the SST anomaly persistence into account (i.e. winter(+4)/spring(+5) to winter(+8)/ spring(+9)), positive 50 kPa anomalies and extended dry spells occur during the third growing season following the onset of El Niño events corresponding to a +10 season lag (Figure 1.2).

For example, if an El Niño were to occur during 1996, the hypothesized sequence of events would be as follows: The onset of the El Niño would occur during winter 1996 (December 1995, January and February 1996) (i.e. winter(0)). A positive PNA pattern would develop during autumn 1996 to winter 1997 (i.e. autumn(+3) to winter(+4)). This would coincide with the mature stage of the El Niño. The positive PNA pattern would aid in developing a North Pacific SST anomaly pattern (similar to that presented in Figure 1.1) during winter to spring 1997 (i.e. winter(+4) to spring(+5)). If the SST anomaly pattern were to persist for a year or longer (i.e. winter/spring 1997 to winter/spring 1998), then it would cause positive 50 kPa anomalies leading to extended dry spells on the Canadian Prairies during the growing season of 1998 (i.e. growing season(+10)).

1.2.2 LA NIÑA EVENTS

Many of the previous studies have also indicated teleconnections between La Niña events and North Pacific SST anomalies, with the PNA acting as a link. La Niña events are related to negative PNA patterns

which normally occur during the autumn or winter following the onset of the events (Emery and Hamilton, 1985; Yarnal and Diaz, 1986). In addition, the negative PNA patterns are related to North Pacific SST anomaly patterns opposite to that in Figure 1.1. These SST anomaly patterns also occur approximately one season following the negative PNA patterns corresponding to the winter or spring of the year after the onset of the events (Emery and Hamilton, 1985; Pan and Oort, 1990).

No studies have specifically examined teleconnections between these types of persistent North Pacific SST anomaly patterns and growing-season precipitation variations on the Prairies. However, teleconnections associated with La Niña are often opposite to those with El Niño (e.g. Yarnal and Diaz, 1986; Kiladis and Diaz, 1989; Halpert and Ropelewski, 1992). This study, therefore, hypothesizes that the SST anomaly patterns associated with La Niña cause negative 50 kPa anomalies (suggesting 50 kPa troughing) leading to wetter conditions over the Prairies during the growing season.

Figure 1.2 (b) shows the hypothesized atmosphere - ocean teleconnections over the Pacific Ocean associated with La Niña and growing-season precipitation variations on the Canadian Prairies. The lags are the same as those for El Niño, however, the relationships are opposite. In particular, negative PNA patterns develop during the autumn or winter following the onset of La Niña events (i.e. autumn(+3) to winter(+4)) corresponding to the mature stage of these events. The negative PNA patterns then aid in developing North Pacific SST anomaly patterns consisting of positive SST anomalies in the east-central North Pacific and negative anomalies along the central-west coast of North

America. These patterns develop around one season following the occurrence of negative PNA patterns (i.e. winter(+4) to spring(+5)). If the SST anomaly patterns persist for a year or longer, they could cause negative 50 kPa anomalies leading to wetter conditions on the Canadian Prairies during the growing season. Taking the SST anomaly persistence into account, negative 50 kPa anomalies and wetter conditions occur during the third growing season following the onset of the La Niña events (i.e. a +10 season lag).

1.3 OBJECTIVES

The preceding sections have outlined possible relationships between ENSO events (both El Niño and La Niña) and growing-season precipitation variations on the Canadian Prairies. The main objectives of this study are:

1. **To test the hypothesis that El Niño events are related to growing-season (May to August) dry spells on the Canadian Prairies.**
2. **To test the hypothesis that La Niña events are related to growing-season (May to August) wet conditions on the Canadian Prairies.**

Both relationships are examined by analyzing atmosphere - ocean teleconnections over the Pacific Ocean. These include: i) PNA patterns; ii) North Pacific SST anomaly patterns; iii) growing-season 50 kPa anomalies over the Canadian Prairies; and iv) growing-season precipitation variations on the Prairies. Conceptual models for both El Niño and La Niña are also formulated. These models could help form the

basis of a long-range forecasting technique for growing-season precipitation variations on the Prairies.

1.4 SIGNIFICANCE OF STUDY

Even though many studies have examined teleconnections between ENSO events and weather patterns over North America, none have thoroughly analyzed their possible teleconnections with growing-season precipitation variations on the Canadian Prairies. Furthermore, most of these examined weather patterns only a year or a year and a half (i.e. +4 to +6 seasons) following the onset of ENSO events. Very few examined patterns for a +10 season lag. In addition, the majority only analyzed the El Niño phase of the ENSO cycle. Relatively few have explored teleconnections associated with La Niña. This is the first study to directly analyze and propose physical explanations of relationships between both El Niño and La Niña and growing-season precipitation variations on the Canadian Prairies (through a series of atmosphere - ocean teleconnections over the Pacific Ocean), for up to a +10 season lag.

This investigation aids in understanding the causes of growing-season precipitation variations on the Canadian Prairies as they relate to ENSO events and associated atmosphere - ocean teleconnections over the Pacific Ocean. It also determines whether El Niño and La Niña produce opposite responses in terms of these precipitation variations. Both anomalously dry and wet conditions are examined because extended dry spells and droughts often produce severe impacts on the Prairie environment and economy. As outlined previously, wet conditions can also

have adverse impacts but furthermore, their identification is important because they are representative of non-drought periods. Due to the lags involved (i.e. precipitation could be affected during the third growing season following the onset of ENSO events), the findings may form the basis of a long-range forecasting technique for growing-season precipitation variations on the Prairies.

CHAPTER 2

LITERATURE REVIEW

This chapter reviews literature pertaining to this study. It is presented in three major sections. The first involves a synoptic climatology of growing-season precipitation variations on the Canadian Prairies. The second provides an overview of the ENSO phenomenon, including associated teleconnections. The final section examines teleconnections between North Pacific SST anomalies and weather patterns over North America.

2.1 SYNOPTIC CLIMATOLOGY OF GROWING-SEASON PRECIPITATION VARIATIONS ON THE CANADIAN PRAIRIES

The average annual precipitation on the Canadian Prairies ranges from 60 cm in west-central Alberta to 30 cm in southeastern Alberta and southwestern Saskatchewan (Longley, 1972). These relatively small amounts are mainly due to the Prairie's location in lee of the Rocky Mountains and in the interior of a large continent (Kendrew and Currie, 1955). The Prairies receive most of their precipitation (up to two thirds) during the growing season of May to August (Kendrew and Currie, 1955; Chakravarti, 1972; Longley, 1972; Dey, 1982). This precipitation is mainly determined by storm-track position and associated cyclonic and frontal activity. However, in late spring and summer, convectional precipitation can also occur (Kendrew and Currie, 1955; Kendall and Thomas, 1956; Chakravarti, 1972). Growing-season precipitation is highly

variable on many spatial and temporal scales. As a result, extreme precipitation variations can occur (Kendrew and Currie, 1955; Longley, 1972; Dey, 1976; Dey and Chakravarti, 1976).

2.1.1 NEGATIVE PRECIPITATION ANOMALIES AND DRY SPELLS

The surface climatology of most growing-season dry spells on the Canadian Prairies includes a general eastward displacement of all pressure systems affecting the area (Dey and Chakravarti, 1976). In particular, the sub-tropical North Pacific high extends northeast of its normal position. Tracks of migratory warm anticyclones from this high (which normally remain south of the Prairies) are displaced northward, thus affecting the Prairie region (Dey and Chakravarti, 1976).

The upper-level climatology includes positive 70 kPa height departures of 1.5 to 6.0 dam over the Prairies. These positive anomalies imply strong ridging. The associated subsidence causes low-level divergence and dry conditions at the surface (Dey and Chakravarti, 1976; Dey, 1979,1982). Positive height departures are also found at the 50 kPa level (Dey, 1982; Knox and Lawford, 1990; Bonsal et al., 1993). At this level, large amplitude ridges become quasi-stationary with their north-south axis across the Prairies. This blocks the flow, displacing cyclonic tracks northward, thus creating dry conditions (Chakravarti, 1972,1976; Dey and Chakravarti, 1976; Dey, 1982; AES Study Group, 1986). The 30 kPa level shows a northward displacement of the jet stream which is oriented northwest-southeast over the northeastern Prairies. This results in upper-level convergence and low-level divergence over the Prairie region (Dey and Chakravarti, 1976).

Based on 50 kPa ridge and trough positions, three major synoptic weather types are associated with growing-season dry spells on the Canadian Prairies (see Figures 8, 9 and 10 in Dey and Chakravarti, 1976). The first includes a northeastward extension of the North Pacific sub-tropical high, a strongly developed upper-level ridge over the Pacific coast, an upper-level trough over the eastern Prairies and the jet stream oriented in a northwest-southeast direction over the northeastern Prairies. With this pattern, dry spells are likely in Alberta and Saskatchewan. The second type is similar to the first except for the position of the upper-level ridge axis which is further east over Alberta. There is also an upper-level high pressure cell over the southeastern Prairies. This pattern often creates very dry conditions over all three Prairie Provinces. The third type has an upper-level ridge over the eastern Prairies and an upper-level trough over the western Prairies and British Columbia. It is likely to produce dry conditions in Saskatchewan and Manitoba, but wetter conditions in Alberta. All three weather types intensify meridional flow with an upper-level ridge over some part of western Canada. If these flow patterns become stationary, dry spells are highly probable. Once the first weather type develops, the ridges usually move eastward and therefore, the second and third types will likely follow (Dey and Chakravarti, 1976; Dey, 1982).

Bonsal et al. (1993) found a significant statistical relationship between SST anomaly patterns characterized by anomalously cold water in the east-central North Pacific (30°N to 40°N, 165°W to 135°W) and anomalously warm water along the central-west coast of North America

(45°N to 55°N, 130°W to 125°W), and positive 50 kPa anomalies and extended dry spells over the Prairies during the growing season. The longer these SST anomaly patterns persisted, the greater was the probability of extended dry spells (Bonsal et al., 1993).

Oglesby and Erickson (1989) used a general circulation model (GCM) to examine the effects of contemporaneous soil moisture anomalies on central North American summer climate and drought. Using perpetual July simulations, they concluded a reduction of summer soil moisture over the interior of North America quickly leads to higher surface temperatures, enhanced ridging of up to 5.5 dam at the 50 kPa level and a 10° northward shift in the jet stream (which would affect the Canadian Prairies). Most of the affected regions also showed a sharp decrease in precipitation due to a local reduction in surface evaporation, and ridging aloft which enhanced subsidence and inhibited convection (Oglesby and Erickson, 1989). An extension to this study (Oglesby, 1991) showed that mid to late spring soil moisture reductions could have a significant impact on the climate of the following summer and help induce drought conditions over North America. However, late winter - early spring reductions had little effect beyond a couple of weeks. It was concluded that the timing of soil moisture anomalies can be critical (Oglesby, 1991).

2.1.2 POSITIVE PRECIPITATION ANOMALIES AND WET SPELLS

Wet conditions on the Prairies have not been examined as extensively as dry periods. The surface climatology of most wet growing

seasons includes a well developed Aleutian low and a strong North Pacific sub-tropical high centred off the coast of southern Washington State (which is south of its normal position). These conditions result in stronger than normal westerly winds thus increasing the flow of moist Pacific air into western Canada (Dey, 1977).

The upper-level climatology includes a higher frequency of zonal flow and negative height departures at both the 70 kPa and 50 kPa levels over the Prairie region. These conditions are associated with increased cyclogenesis, thus causing wet conditions at the surface (Dey, 1977, 1982). At the 30 kPa level, the jet stream is displaced southward in an west-east direction along the Canada - United States border causing low-level cyclones to be steered over the Prairies (Dey, 1977).

Knox and Lawford (1990) found that periods of higher than normal growing-season precipitation were associated with negative 50 kPa height anomalies over the Prairie region. These periods were often associated with blocking over the Baffin Island area. When this occurred, the semi-permanent northeastern Canadian low pressure was significantly displaced from its normal position thereby affecting precipitation regimes over large portions of Canada, including the Canadian Prairies (Knox and Lawford, 1990).

2.2 ENSO EVENTS

ENSO events are the largest single source of interannual climatic variability on a global scale. Their effects are wide ranging and often severe. They are associated with a large-scale redistribution of atmospheric mass, heat and momentum within the tropical Pacific ocean -

atmosphere system. This is often associated with large deviations from climatology of monthly, seasonal and annual values of temperature and precipitation in many parts of the world (Diaz and Kiladis, 1992). Teleconnections associated with ENSO occur in the tropics and extratropics (Glantz, 1991; Tribbia, 1991; Fraedrich and Muller, 1992; Diaz and Kiladis, 1992). However, for the purpose of this study, only extratropical teleconnections associated with PNA patterns, North Pacific SST anomaly patterns and weather patterns over North America are reviewed.

2.2.1 MEAN CONDITIONS IN THE TROPICAL PACIFIC

To explain ENSO, mean atmospheric and oceanic conditions in the tropical Pacific are first described. The northeast and southeast trade winds move toward the equator along the coasts of North and South America and converge at the Inter-Tropical Convergence Zone (ITCZ) (Figures 2.1 and 2.2). Moist air rises from the ITCZ, diverges poleward in the upper troposphere and descends over both sub-tropical high pressure cells. This completes the meridional (north-south) Hadley circulation (Philander, 1990) (Figure 2.2).

Superimposed on the Hadley Circulation is the zonal (east-west) Walker Circulation. It involves ascending motion over the western tropical Pacific in the area associated with the South Pacific Convergence Zone (SPCZ). The SPCZ results from convergence of easterly trade winds from the South Pacific high and southwesterly winds generated by migratory surface anticyclones in the Australian region (Kiladis et al., 1989) (see Figure 2.1). The rising air from the SPCZ

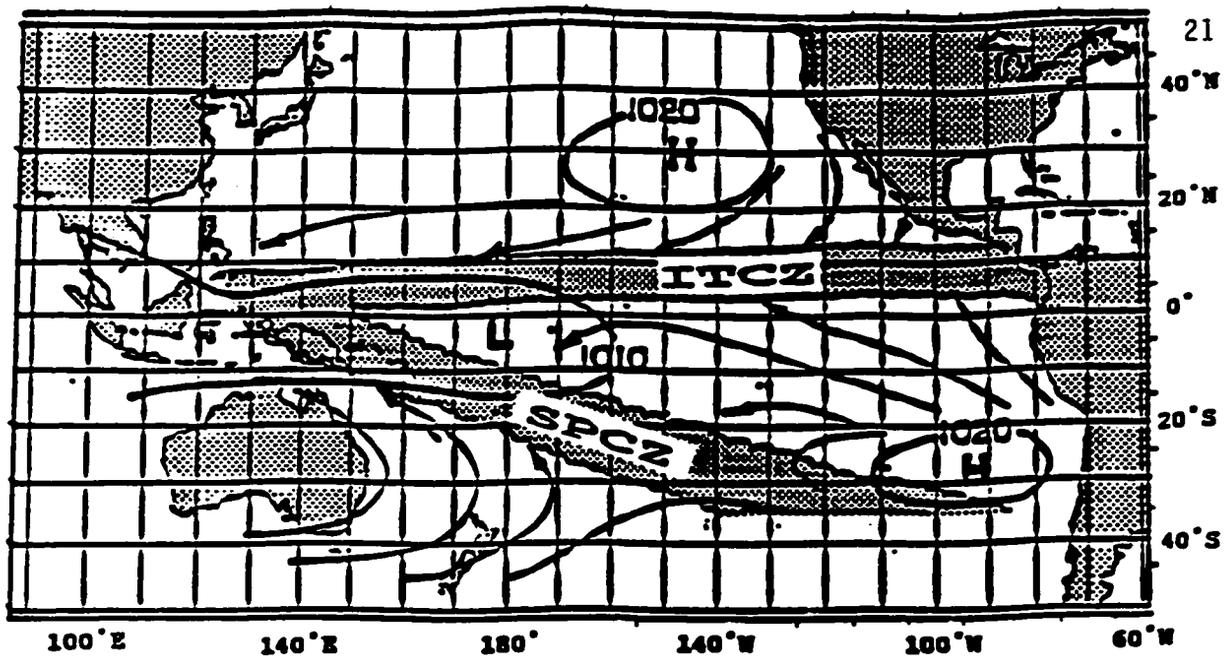

Figure 2.1: Schematic Diagram of Mean Annual Sea Level Pressure Systems, Surface Wind Streamlines and Positions of the ITCZ and SPCZ (Taken from Trenberth, 1991)

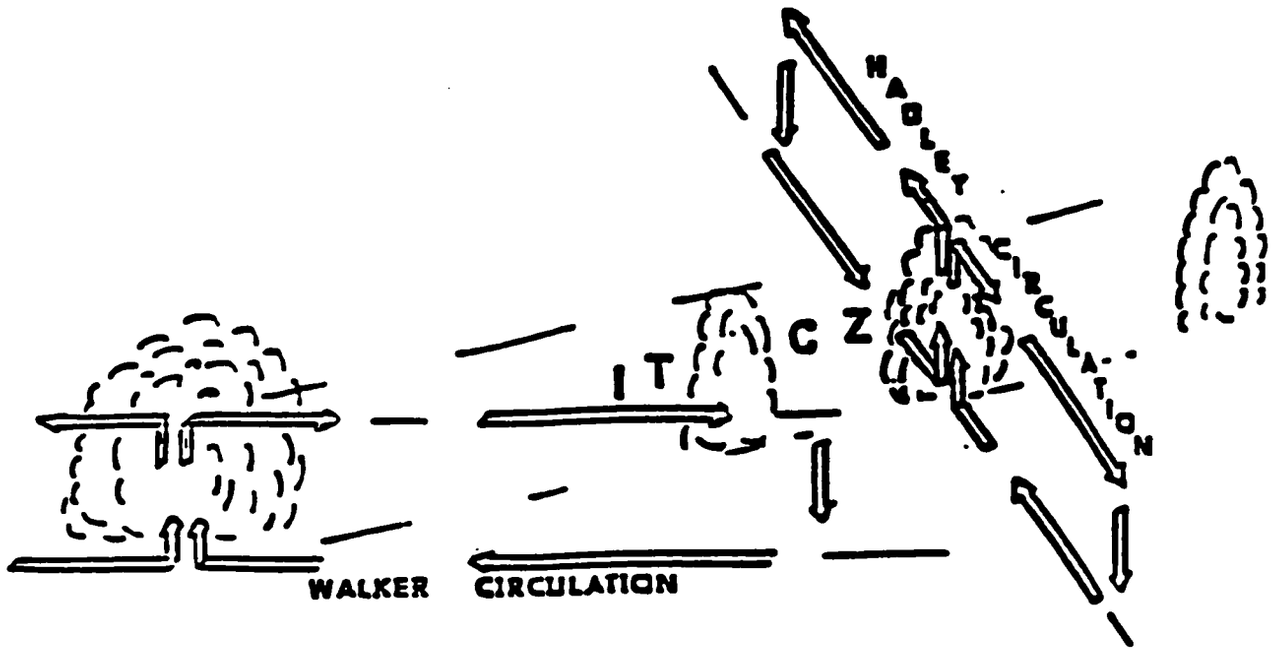

Figure 2.2: Schematic Diagram of the Meridional Hadley and the Zonal Walker Circulations (Taken from Philander, 1990)

diverges eastward and westward in the upper troposphere. The eastward component descends over the South Pacific sub-tropical high. From this region, surface easterly winds move along the equator completing the circulation (Philander, 1990) (Figures 2.1 and 2.2). The Walker Circulation results in a trans-Pacific SLP gradient with lower pressure over Australia and Indonesia and higher pressure off the west coast of South America (Bigg, 1990).

The atmospheric circulation patterns directly influence ocean currents and SSTs (Figure 2.3). Along the western coast of South America, counter-clockwise circulation associated with the South Pacific high drives the Peru Current. Due to the alignment of the coast, this current pushes surface water offshore resulting in upwelling of cold water (Ramage, 1986). Surface easterly winds associated with the Walker Circulation drive the strong westward South Equatorial Current (Philander, 1990). The current transports cold water (that upwells along the South American coast) westward to the central tropical Pacific. Therefore, along the equator, there is an increase in SST from east to west (Figure 2.3). This current causes an accumulation of water in the western tropical Pacific which deepens the warm surface layer of the ocean and depresses the thermocline (the boundary between the well mixed surface and colder deeper layers) (Ramage, 1986; Bigg, 1990). North of the South Equatorial Current is the eastward flowing Equatorial Countercurrent. It results in warm surface waters north of the equator that extend along the entire equatorial Pacific and are associated with the ITCZ (Philander, 1990) (Figure 2.3).

The distribution of strong convection and subsidence in the

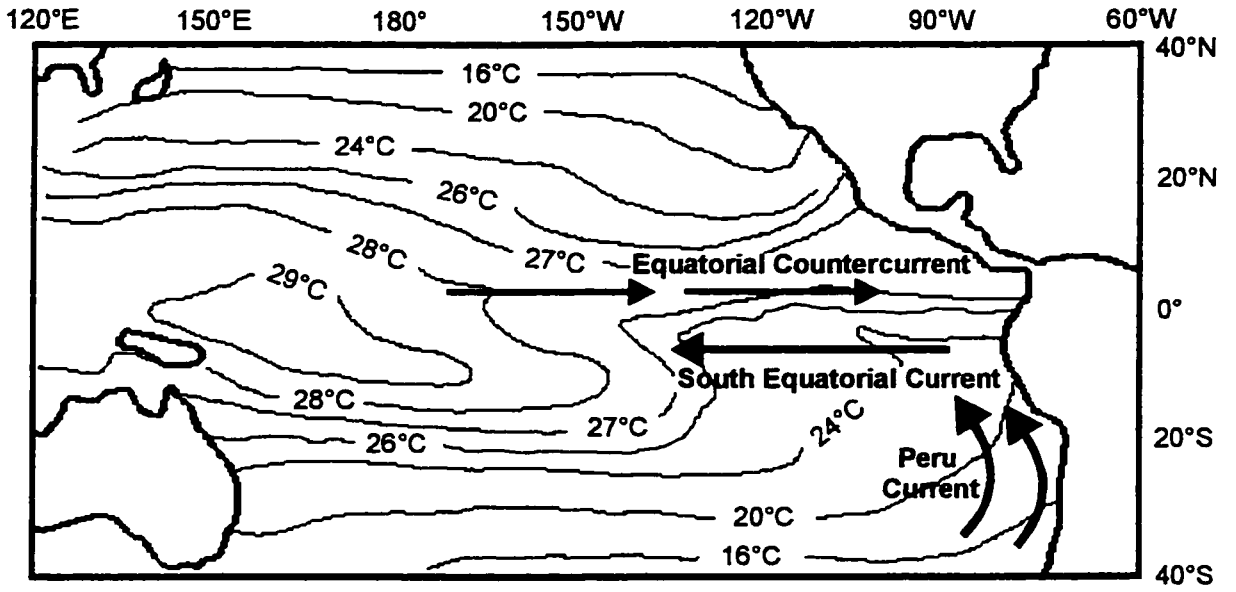

Figure 2.3: Schematic Diagram of the Mean Annual SSTs and Ocean Currents in the Tropical Pacific Ocean (Adapted from Trenberth, 1991)

tropical Pacific is largely determined by the SST pattern and the two convergence zones (which typically lie over the regions of highest SST). High SSTs (which normally heat the atmosphere from below), coupled with moisture convergence from the trade winds, lead to strong convection over the ITCZ and SPCZ. Conversely, due to cooling from below, lower SSTs in the eastern tropical Pacific stabilize the atmosphere. This, along with an absence of moisture convergence, leads to large-scale subsidence in this region (Trenberth, 1991).

2.2.2 INTERANNUAL VARIABILITY

The dominant mode of interannual variability in the tropical Pacific is in direct response to ENSO (Philander, 1990). Interannual

movements of convective zones are mostly influenced by SST variations. Warm surface waters expand eastward during El Niño and contract westward during La Niña. The increase of SSTs in the eastern tropical Pacific during the early stages of El Niño is caused by a local weakening of the southeast trades. As the El Niño evolves, eastward advection of warm surface waters maintains the high SSTs even though the southeast trades initially start to intensify. Therefore, the convective zones in Figure 2.1 begin to merge (i.e. the ITCZ shifts southward and the SPCZ north and eastward). This weakens the Walker Circulation and as a result, the southeast trades weaken and retreat eastward. The warm eastward Equatorial Countercurrent intensifies while the cold South Equatorial Current relaxes (Philander, 1990).

During La Niña, the opposite generally occurs. The southeast trade winds initially intensify, thus strengthening the South Equatorial Current. As a result, the low SSTs in the eastern tropical Pacific (Figure 2.3) move westward. The Equatorial Countercurrent relaxes and the convective zones begin to diverge with the ITCZ moving northward and the SPCZ south and westward. These events cause the Walker Circulation to intensify including a strengthening of both the South Pacific sub-tropical high and Australian - Indonesian low (Philander, 1990). Therefore, both El Niño and La Niña involve perturbations to the direct thermal Walker Circulation which influences the interannual movements of convective zones, variations in surface winds, ocean currents and SST patterns (Philander, 1990).

2.2.3 TYPICAL ENSO EVENTS

Amplitudes of ENSO events can vary significantly, however, their phases are remarkably similar. As a result, a composite or typical event can be described. For El Niño, this composite is presented in Figure 2.4 (Rasmusson and Carpenter, 1982; Ramage, 1986; Ropelewski and Halpert, 1986,1987,1989; Kiladis and van Loon, 1988; Kiladis and Diaz, 1989). Near the end of the year preceding an event (i.e. October or November), SLP in the eastern tropical Pacific decreases and the southeast trades weaken. No longer supported by the trade winds, warm water in the western tropical Pacific (which has a higher sea level than the east) begins to flow eastward. The flow occurs via sub-surface Kelvin waves which flow along the equator and reach the western coast of South America in two or three months (Wyrtki, 1975; Ramage, 1986; Cane, 1991). Kelvin waves tend to warm surface waters by physically transporting warm water from the west but more importantly, they depress the thermocline and thus, prevent upwelling of cold water along the west coast of South America.

SSTs in the eastern tropical Pacific begin to warm around December or January when the first Kelvin waves reach the South American coast (Wyrtki, 1975; Ramage, 1986; Cane, 1991). This is known as the onset of the event and often referred to as year 0. High SST anomalies then begin to spread westward along the equator (Figure 2.4(a) and (b)). Since the ITCZ remains over the warmest waters, its normal seasonal northward migration is inhibited (Rasmusson and Carpenter, 1982; Philander, 1985, 1990; Ramage, 1986).

As the El Niño develops, the trade winds continue to relax and are

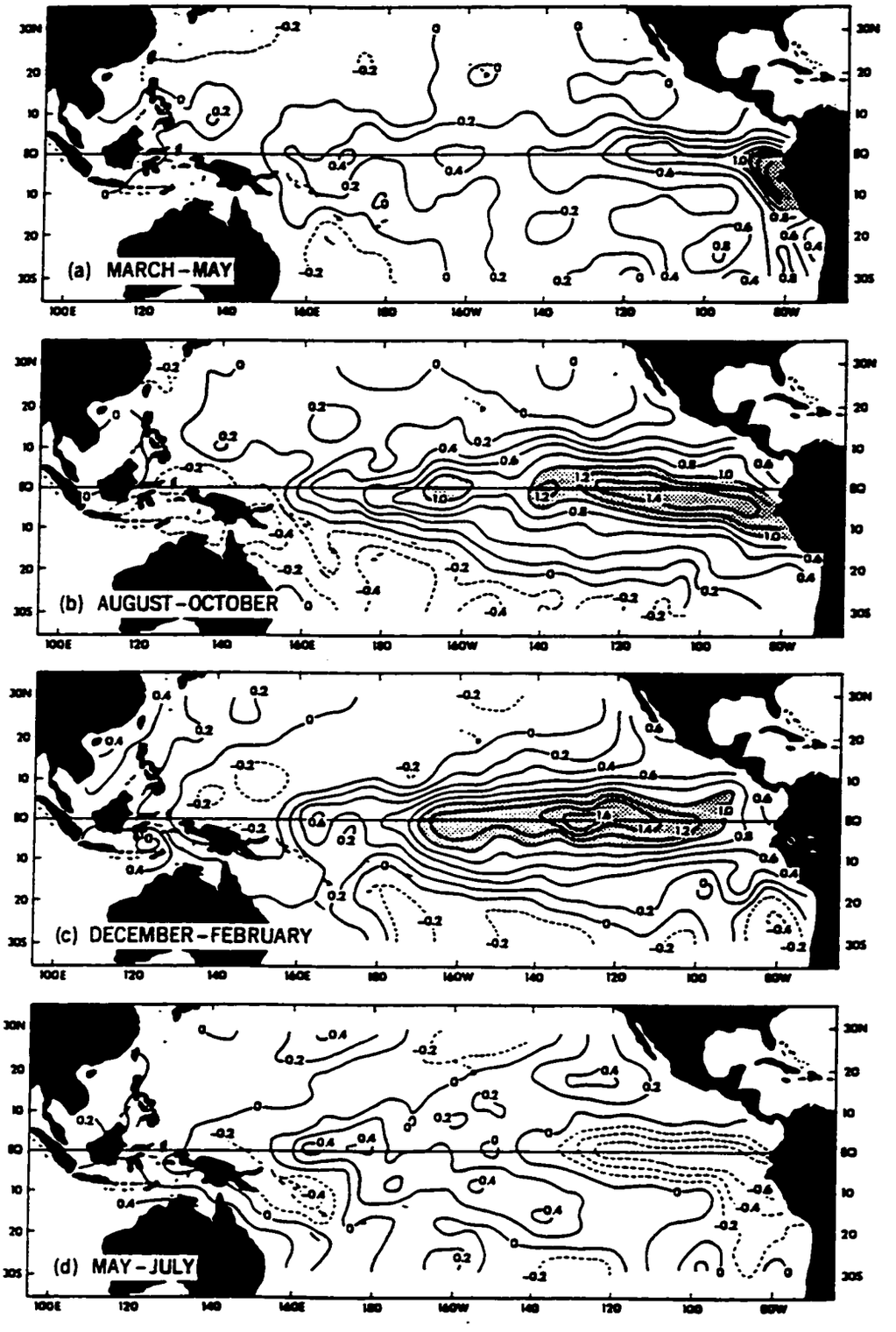

Figure 2.4: SST Anomalies (°C) during Typical El Niño Events Between 1950 and 1973 a) March to May after onset, b) the following August to October, c) the following December to February, and d) May to July more than a year after onset (Taken from Rasmusson and Carpenter, 1982)

eventually replaced by surface westerlies. These westerlies trigger more Kelvin waves which further depress the thermocline when they reach the South American coast. The SPCZ moves northward and eastward toward the higher SSTs and eventually merges with the ITCZ (Rasmusson and Carpenter, 1982; Philander, 1985,1990; Ramage, 1986). These anomalous conditions continue through year 0 and reach their peak early in year +1 when SSTs and negative SOI values also reach their maximum anomalies (Figure 2.4(c)). The peak is referred to as the mature stage of the El Niño. The appearance of cold surface waters in the eastern tropical Pacific near the middle of year +1 marks the end of an event (Figure 2.4(d)) (Rasmusson and Carpenter, 1982; Philander, 1985,1990). The duration of a typical El Niño is around 18 months and the recurrence interval averages four years, but can be from two to ten years (Rasmusson and Carpenter, 1982; Ropelewski and Halpert, 1986,1987,1989; Kiladis and van Loon, 1988; Kiladis and Diaz, 1989).

La Niña events were not fully recognized until the mid 1980s and therefore, have not been as extensively researched (van Loon and Shea, 1985; Philander, 1990). However, typical La Niña events are generally opposite to those of El Niño. The onset of La Niña is initially caused by a strengthening of the southeast trades. As a result, the upwelling of cold water along the west coast of South America increases, the thermocline becomes shallower and the South Equatorial Current intensifies. The negative SST anomalies in the eastern tropical Pacific increase the SST gradient along the equatorial Pacific and enhance the Walker Circulation (Trenberth, 1991). The SST anomaly pattern is further amplified because the strengthened South Pacific high causes more

upwelling of cold water which is physically transported westward by the strengthened South Equatorial Current. As a result, sea levels are unusually high in the west and low in the east. The colder region of water, which normally only extends to approximately 150°W (see Figure 2.3), often extends to 170°E causing the ITCZ to be displaced northward and the SPCZ south and westward (Philander, 1985,1990; van Loon and Shea, 1985, Trenberth, 1991).

Unlike El Niño, the timing of a typical La Niña event is difficult to define because each La Niña differs greatly in terms of onset and duration. However, several studies which analyzed teleconnections associated with both El Niño and La Niña, proposed that typical La Niña events also tend to develop near the beginning of the calendar year, mature during the winter following their onset and last around 18 months (Philander, 1985; van Loon and Shea, 1985; Yarnal and Diaz, 1986; Bradley et al., 1987; Lau and Sheu, 1988; Kiladis and Diaz, 1989; Ropelewski and Halpert, 1989; Deser and Wallace, 1990).

El Niño and La Niña are two extremes of the ENSO cycle. There is a tendency for the system to go from one extreme to the other in adjacent years. Therefore, El Niño and La Niña frequently follow one another (van Loon and Shea, 1985; Meehl, 1987; Kiladis and Diaz, 1989; Rasmusson et al., 1990). Each ENSO event (both El Niño and La Niña) can also vary significantly in terms of timing, evolution, amplitude, duration and spatial extent. These differences can be key factors in determining teleconnection patterns associated with individual ENSO events (Diaz and Kiladis, 1992).

2.2.4 TELECONNECTIONS ASSOCIATED WITH ENSO

2.2.4.1 PNA PATTERNS

For extratropical teleconnections to occur, the heating associated with the positive SST anomalies in the tropical Pacific must be extended vertically to the troposphere and then horizontally to the extratropics (Tribbia, 1991). An early theory proposed the anomalous heat source in the eastern tropical Pacific (i.e. El Niño) causes increased convection and release of latent heat. The anomalous heating of the tropical troposphere intensifies transports of heat and momentum to the mid-latitudes and subsequently, strengthens the sub-tropical jet stream and westerlies (Bjerknes, 1966).

Simple numerical models showed the typical response of a three-dimensional spherical atmosphere to thermal forcing associated with El Niño included Rossby wave trains of alternating high and low pressure around the globe (Opsteegh and van den Dool, 1980; Hoskins and Karoly, 1981; Webster, 1981). Further modelling studies showed that heating of upper levels of the tropical Pacific troposphere by latent heat release appeared to be the driving mechanism of the Rossby wave train (Simmons, 1982; Webster, 1982; Webster and Holton, 1982; Lim and Chang, 1983; Simmons et al., 1983; Hanna et al., 1984; Lau and Lim, 1984). These, along with many observational (Horel and Wallace, 1981; van Loon and Madden, 1981; Chen, 1983; Yarnal, 1985; Ropelewski and Halpert, 1986; Yarnal and Diaz, 1986; Hamilton, 1988; Weber, 1990) and other modelling (Keshavamurty, 1982; Blackmon, et al., 1983; Shukla and Wallace, 1983; Pitcher et al., 1988) studies, showed the typical Northern Hemisphere mid-latitude response to El Niño events was a Rossby wave train

resembling a positive PNA pattern. This pattern, first described by Wallace and Gutzler (1981), includes a deep Aleutian low extending from the surface to the upper troposphere in the northeastern Pacific Ocean, an upper-level ridge centred over western Canada and a deeper than normal upper-level trough over the southeastern United States (Figure 2.5) (Horel and Wallace, 1981; Yarnal and Diaz, 1986).

Several studies have confirmed that strong teleconnections can only be propagated to the extratropics when the anomalous heat source is overlain by upper-level westerlies (Simmons, 1982; Webster, 1982; Webster and Holton, 1982; Lim and Chang, 1983; Lau and Lim, 1984). As a result, the response is dependent on the position of the tropical heat source which is dependent on the type of ENSO event. During El Niño, the heat source is over the central tropical Pacific where weak upper-level westerlies occur during winter. During La Niña, the heat source is displaced westward near Australia and Indonesia which experience continuous upper-level easterly flow (Lau and Chan, 1983a,1983b). Therefore, during El Niño, strong teleconnections should develop in the winter hemisphere as the westerly winds move equatorwards. Teleconnections during summer are weak or non-existent because the latent heat source is embedded in upper-level tropical easterlies (Webster, 1982). In fact, the observational and modelling studies outlined previously confirm that positive PNA patterns associated with El Niño occur during the late fall or early winter following the onset of the events (i.e. near the mature stage).

This implies extratropical teleconnections to the Northern Hemisphere are only associated with El Niño. However, a distinctive

Figure 2.5: Schematic Diagram of the PNA Pattern of Middle to Upper-Tropospheric Geopotential Height Anomalies during a Northern Hemisphere Winter coinciding with the Maturity of El Niño Events (Taken from Horel and Wallace, 1981)

pattern over the North Pacific/North American region (i.e. a negative PNA pattern) also occurs during the winter following the onset of most La Niña events (Yarnal and Diaz, 1986). The teleconnection pattern does not appear to be forced directly by the tropical Pacific heat source (which is displaced westward during La Niña). Rather, it occurs in conjunction with cold air surges from east Asia southward into the region of convection over the western tropical Pacific. These cold surges increase convection (and thus release of latent heat) which intensifies the speed and momentum of the Hadley Circulation. This

enhances the east Asian jet stream setting up a ridge and trough system over the North Pacific and North America resembling negative PNA patterns (Emery and Hamilton, 1985; Yarnal and Diaz, 1986).

2.2.4.2 NORTH PACIFIC SST ANOMALY PATTERNS

Several studies have associated anomalous SST patterns in the North Pacific Ocean with ENSO events and related extremes in PNA patterns. During the Northern Hemisphere fall and winter following the onset of El Niño, a cold pool of water develops in the central North Pacific and warm water extends along most of the west coast of North America (Reynolds and Rasmusson, 1983; Pan and Oort, 1983,1990; Emery and Hamilton, 1985; Alexander, 1990,1992; Weber, 1990). Two major processes may lead to this pattern. First, is the northward propagation of Kelvin waves along the west coast of North America. As outlined previously, during El Niño, Kelvin waves travel from the western tropical Pacific to the east. When they reach the west coast of South America, northward and southward Kelvin waves may be generated. The northward waves propagate up the west coast of North America (McCreary, 1976; Enfield and Allen, 1980; Clarke, 1983; Johnson and O'Brien, 1990). They depress the thermocline and reduce upwelling of cold water, thus resulting in higher than normal SSTs. However, these waves are confined to a narrow region near the shore. Therefore, this process does not explain basin wide SST anomalies in the North Pacific, although it may play a significant role in the high coastal anomalies (Emery and Hamilton, 1985; Alexander, 1990,1992).

The second process is related to positive PNA patterns. These

patterns are associated with an intensification and southeastward displacement of the Aleutian low which extends from the surface to the upper troposphere (Horel and Wallace, 1981; Yarnal and Diaz, 1986). The resultant strengthened cyclonic surface winds alter the oceanic fluxes, vertical mixing and surface currents to produce the observed SST anomalies (Simpson, 1983; Wagner, 1984; Emery and Hamilton, 1985; Mysak, 1986; Alexander, 1990,1992). In particular, the stronger north to northwest flow behind the low brings colder air and stronger winds to the central North Pacific causing more heat transfer from the ocean to the atmosphere and thus, lower SSTs in this region. Ahead of the low, a strengthened south to southwesterly flow of warmer air causes less heat transfer from the ocean to the atmosphere and thus, higher SSTs along the central-west coast of North America (Yongping and McBean, 1991).

Teleconnections between La Niña and North Pacific SST anomalies have not been as extensively researched. However, similar SST patterns associated with El Niño are also associated with La Niña, except that for the latter, the two regions of SST anomalies have opposite signs (i.e. an anomalously warm pool of water in the central North Pacific and anomalously cold water along the west coast of North America). These SST patterns are likely the result of the circulation associated with a weaker Aleutian low that is characteristic of negative PNA patterns (Weare et al., 1976; Pan and Oort, 1983,1990; Emery and Hamilton, 1985).

2.2.4.3 WEATHER PATTERNS OVER NORTH AMERICA

Numerous studies have examined teleconnections between ENSO events and surface weather patterns (e.g. temperature, precipitation) over

North America. During El Niño, northwestern North America generally has warmer, drier conditions while the southeastern United States are cooler and wetter. These patterns normally occur late in year 0 or early in year +1 and are mainly attributable to the circulation associated with positive PNA patterns (Ropelewski and Halpert, 1986, Yarnal and Diaz, 1986; Kiladis and Diaz, 1989; Halpert and Ropelewski, 1992). However, the storm track position for each El Niño can differ significantly and as a result, displacements of only a few 100 km can cause large spatial differences in surface weather patterns (especially precipitation) (Yarnal and Diaz, 1986).

Specifically over Canada, December of year 0 to March of year +1 shows statistically significant above normal temperatures over most of the country (Shabbar, 1993). The highest anomalies occur over the Prairies, northern Ontario and the Yukon. However, during the following summer (i.e. June to September of year +1), no significant temperature anomalies are observed. For precipitation, December of year 0 to March of year +1 is below normal over most of the Prairies, Ontario and the Atlantic region while the west coast, northeastern Canada and southwestern Quebec are above normal. However, these results are not statistically significant (Shabbar, 1993).

For La Niña events, patterns of temperature and precipitation over North America tend to be generally opposite to those associated with El Niño (Yarnal and Diaz, 1986; Kiladis and Diaz, 1989; Ropelewski and Halpert, 1989; Halpert and Ropelewski, 1992). In particular, northwestern North America generally has cooler, wetter conditions while the southeastern United States are warmer and drier from December of

year 0 to March of year +1 (Yarnal and Diaz, 1986; Kiladis and Diaz, 1989; Ropelewski and Halpert, 1989; Halpert and Ropelewski, 1992). These patterns are attributed to the circulation associated with negative PNA patterns which are normally associated with La Niña (Yarnal and Diaz, 1986).

Over most of Canada, temperatures during December of year 0 to March of year +1 are significantly below normal including strong negative anomalies in northern Manitoba and the Mackenzie District of the Northwest Territories. This pattern is basically opposite to El Niño (Shabbar, 1993). In fact, many Canadian Prairie stations (e.g. Edmonton and Winnipeg) are on average more than 3°C warmer during El Niño as opposed to La Niña (Kiladis and Diaz, 1989). However, no significant differences are found for precipitation over any regions of Canada during December of year 0 to March of year +1. Temperature and precipitation during summer of year +1 also show no significant differences from normal (Shabbar, 1993).

Trenberth et al. (1988) analyzed the 1988 summer drought over the central plains of North America that was contemporaneously associated with the 1988 La Niña. They suggested the anomalously cold water in the eastern tropical Pacific (associated with the La Niña), along with anomalously warm water southeast of Hawaii, caused the ITCZ to be displaced northward of its usual position. The displaced zone forced anomalous upper-atmospheric longwaves over the Northern Hemisphere which subsequently caused the sub-tropical jet stream to shift northward over central North America thereby causing the summer drought conditions (Trenberth et al., 1988). However, Namias (1991) composited summer North

American upper-atmospheric patterns associated with seven La Niña events and determined the composite anomaly showed little resemblance to the 1988 case. He suggested the 1988 La Niña was unique in its effects on upper-atmospheric anomalies over North America (Namias, 1991).

2.3 TELECONNECTIONS BETWEEN NORTH PACIFIC SST ANOMALIES AND WEATHER PATTERNS OVER NORTH AMERICA

Numerous studies have found associations between anomalous SST patterns in the North Pacific and surface weather patterns over North America. In particular, the winter SST anomaly pattern associated with El Niño is associated with a long-standing Rossby wave pattern that produces warm, dry conditions over western, and cold, wet conditions over eastern North America during the same winter (Namias, 1969,1972, 1978, 1986; Wick, 1973; Harnack, 1979; Dixon and Harnack, 1986). If these SST anomalies are reversed (i.e. the winter SST anomaly pattern associated with La Niña), winter weather patterns over North America are also reversed (Namias, 1972).

Summer droughts over the north and central United States Great Plains are also significantly related to contemporaneous North Pacific SST anomalies (Namias, 1982). The SST pattern includes anomalously warm water in the northern and western parts, and anomalously cold water in the northeastern parts of the North Pacific. It is suggested the anomalous cold pool assists in the development of a stronger than normal North Pacific sub-tropical high. Through longwave amplifications, the west coast trough, Great Plains ridge and east coast troughs are intensified. The stronger Great Plains ridge is responsible for drought

conditions over the north and central United States Great Plains (Namias, 1982).

As outlined previously, Bonsal et al. (1993) found a statistically significant correlation between North Pacific SST anomaly patterns characterized by negative SST anomalies in the east-central North Pacific and positive anomalies along the central-west coast of North America and positive 50 kPa anomalies leading to growing-season extended dry spells on the Canadian Prairies. It was hypothesized the persistent SST anomaly patterns aided in diverting the upper-atmospheric flow to produce these positive 50 kPa anomalies (Bonsal et al., 1993).

The physical basis for these relationships includes the fact that SST anomalies cover very large areas (e.g. hundreds of thousands of square kilometres) and persist for several months, or even several years (Harnack and Broccoli, 1979; Namias and Cayan, 1981). The long persistence implies a significant change in ocean to atmosphere heat exchanges (both latent and sensible), especially during winter. These changes can affect intensity of weather disturbances and the nature of mean upper-atmospheric circulation patterns over the adjacent ocean and continents (Namias and Cayan, 1981).

During winter, SST anomaly patterns in the North Pacific are strongly correlated with SLP and mid-tropospheric height fields over the same region (Davis, 1976; Lanzante, 1984; Iwasaka et al., 1987; Wallace and Jiang, 1987; Wallace et al., 1990). The effect of these anomalies is increased if a SST anomaly gradient (i.e. adjacent pools of high and low SST anomalies) is present. The gradients produce and maintain enhanced baroclinicity (through differential latent and sensible heat fluxes)

which leads to anomalous SLPs both locally and downstream (Namias, 1978). Anomalous meridional mid-tropospheric flows over the North Pacific and North America are associated with anomalous east-west SST anomaly gradients in the North Pacific Ocean. The associations occur on both monthly and seasonal time scales and are strongest during the winter, but are also strong during summer. However, it is not entirely clear whether the ocean is forcing the atmosphere or vice versa (Harnack and Broccoli, 1979).

A few GCM studies examined relationships between mid-latitude SST anomalies and atmospheric flow patterns. Palmer and Sun (1985) used the United Kingdom Meteorological Office GCM to analyze the effect of North Atlantic SST anomalies on atmospheric circulation (using 50 kPa height anomalies). They found a statistically significant response which included positive (negative) height anomalies approximately 20° longitude downstream from positive (negative) SST anomalies. A wave train of height anomalies of alternating sign and decreasing amplitude was observed farther downstream. The magnitude of the 50 kPa response scaled almost linearly with that of the SST anomaly (Palmer and Sun, 1985). GCM studies between North Pacific SST anomalies and atmospheric circulation patterns observed that SLP tended to increase (decrease) over low (high) SST anomalies. However, in the mid to upper troposphere, the atmospheric pressure tended to increase (decrease) over and to the east of high (low) SST anomalies (Huang, 1978; Chervin, 1980; Lau and Nath, 1990).

The preceding sections have reviewed literature pertaining to the atmosphere - ocean teleconnections presented in Figure 1.2. Based on

this literature, it appears that ENSO events (El Niño and La Niña) can be related to growing-season precipitation on the Canadian Prairies through a series of atmosphere - ocean teleconnections over the Pacific Ocean. However, no studies have thoroughly analyzed possible teleconnections between ENSO events and growing-season precipitation on the Prairies.

CHAPTER 3

STUDY AREA, DATA SOURCES AND METHODOLOGY

This chapter describes the methodology used in this investigation. It begins with a description of the study area. Data sources and related variables are then discussed in four sub-sections headed Canadian Prairie precipitation, Northern Hemisphere upper-atmospheric circulation, North Pacific SSTs and ENSO events. Each sub-section describes nature of the data, variables derived from this data and mapping procedures. The chapter concludes with a discussion of the methodology incorporated in the study.

3.1 STUDY AREA

As outlined in chapter 1, teleconnections involving ENSO events, PNA patterns, North Pacific SST anomalies and growing-season 50 kPa anomalies and associated precipitation variations over the Canadian Prairies are analyzed. As a result, the study area includes the Canadian Prairies, the North Pacific/North American region and the tropical Pacific. The Canadian Prairie study area is the agricultural region of the Prairies which includes the southern portions of Alberta, Saskatchewan and Manitoba (Figure 3.1). It is bounded on the east by the Manitoba - Ontario border and on the west by the foothills of the Rocky Mountains. To the north, it extends to the southern limit of the boreal forest while the United States border forms the southern boundary (Dey, 1976). This region has been used in many studies which examined

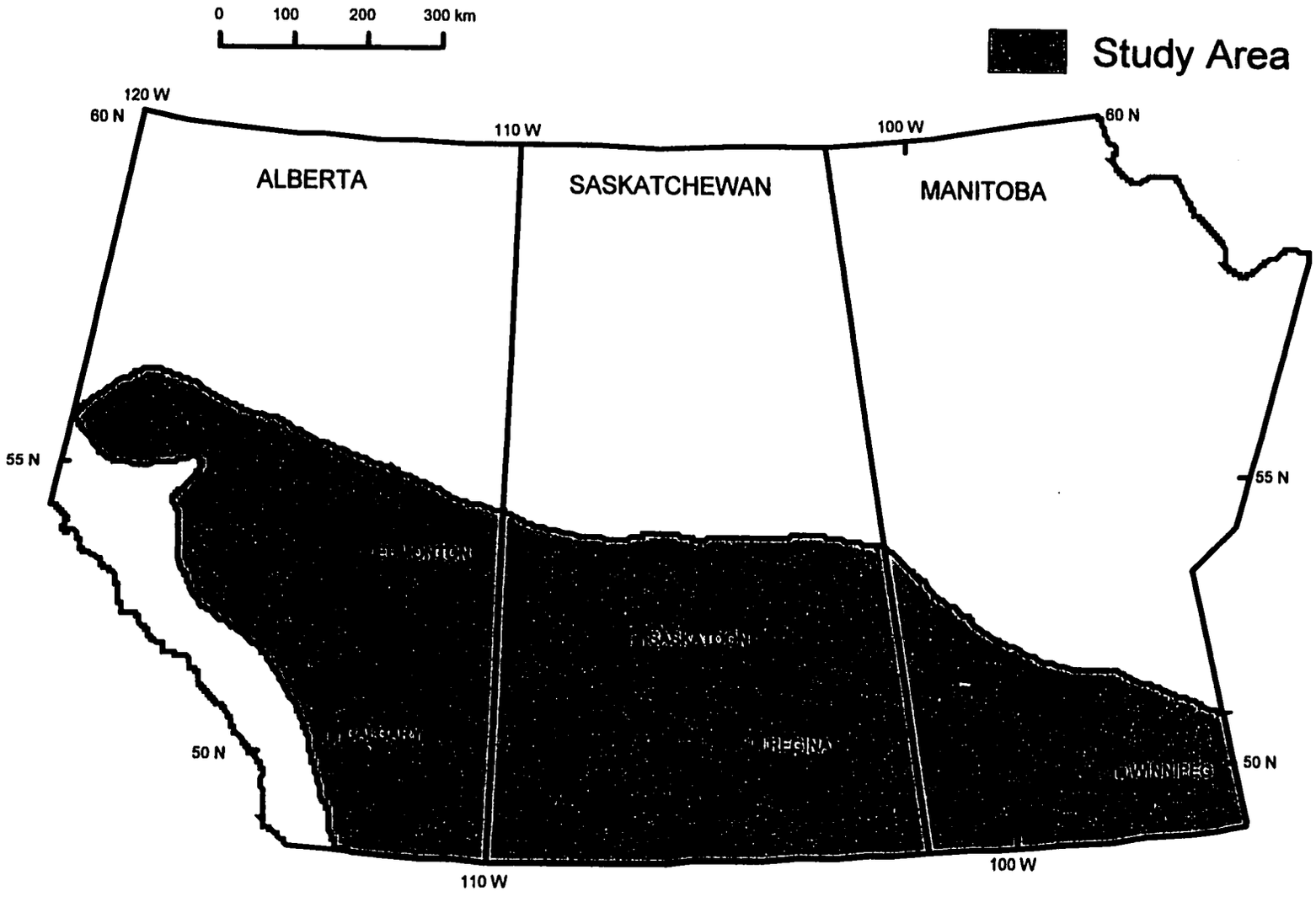

Figure 3.1: Canadian Prairie Study Area

precipitation variations on the Canadian Prairies (e.g. Chakravarti, 1976; Dey, 1982; Bonsal et al., 1993).

The North Pacific/North American region extends from 15°N to 75°N and 120°E to 60°W. This region encompasses the entire North Pacific Ocean and most of North America. Therefore, both North Pacific SST anomaly patterns and upper-atmospheric circulation patterns such as the PNA can be identified. The tropical Pacific study area includes the region that experiences SST and SLP anomalies associated with ENSO events. From previous investigations (e.g. Ramage, 1986; Philander, 1990), this region extends across the tropical Pacific from the west coast of South America to the Australian - Indonesian sector (approximately 15°N to 15°S and 120°E to 70°W).

3.2 DATA SOURCES AND VARIABLE DESCRIPTIONS

For this analysis, several variables are required. The study period chosen is 1948-1991 because comprehensive North Pacific SST data and Northern Hemisphere 50 kPa data only date back to 1948. This 44-year period also encompasses ten El Niño and seven La Niña events.

3.2.1 CANADIAN PRAIRIE PRECIPITATION

3.2.1.1 PRECIPITATION DATA

Canadian Prairie precipitation variations are analyzed during the growing season (May to August). The precipitation data were obtained from 63 stations across the Prairie study area (Figure 3.2). These stations were chosen for two reasons. Firstly, they had a relatively continuous record of daily precipitation amounts from May through August

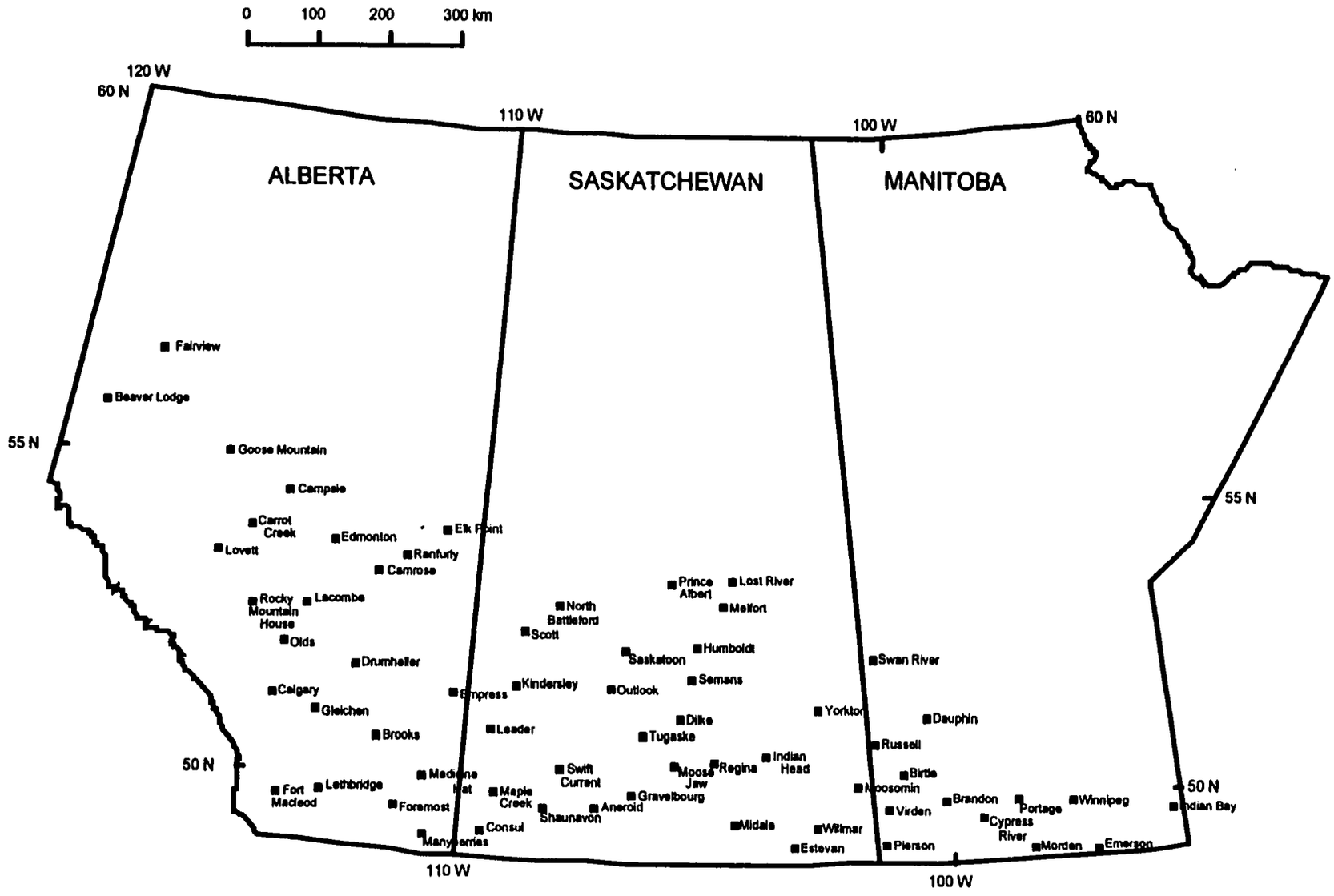

Figure 3.2: Precipitation Stations Used in this Study

during 1948-1991. Secondly, they provided the most uniform coverage of the study area possible. A list of these stations, their identification numbers and the periods for which they were used are given in Appendix A - Table A.1.

Daily precipitation data were obtained from the Atmospheric Environment Service (AES) archives in Downsview, Ontario. Some values for certain stations were missing. This problem was handled by substituting data from the nearest station that had data for that time. As a result, a complete precipitation time series for every growing season from 1948-1991 was developed for every station. The insertion of replacement values should not have a significant effect on the analysis because large-scale (i.e. entire Canadian Prairie study area) precipitation variations are being analyzed. Since the replacement stations are near the actual stations, and the highest number of these stations used for any given day was only three (3/63 = 4.8%), the identification of large area precipitation variations should not be significantly affected. A list of the replacement stations, periods for which they were used and their distance from the actual stations are given in Appendix A - Table A.2.

Two variables are defined to describe growing-season precipitation variations on the Prairies. Each one quantifies these variations over the entire Prairie study area for the total growing season and each month within the growing season. Both variables indicate large-scale precipitation variations, however, each shows different characteristics of these variations.

3.2.1.2 TOTAL NUMBER OF 10-DAY DRY SPELLS

The first variable is the total number of 10-day dry spells. A 10-day dry spell is defined as a period of 10 consecutive days during which no measurable precipitation is recorded. This definition is similar to the one utilized by Dey and Chakravarti (1976), Dey (1982) and Bonsal et al. (1993) who outlined individual growing-season extended dry spells on the Canadian Prairies. However, in this study, total number of dry spells are determined for every growing season during 1948-1991.

The total number of 10-day dry spells for each month (during the study period) is calculated by first determining the number of dry spells for each station. If a station has only one consecutive 10-day period without any precipitation, the value is "1". If it has two separate periods with this condition, the value is "2"; and so on. However, if the consecutive days without precipitation exceeds 10, the number of 10-day dry spells increases. For example, if a station has 11 consecutive dry days, the value is "2"; 12 consecutive dry days, the value is "3"; and so on. As a result, the longer the consecutive dry period (i.e. the greater the likelihood it will lead to drought), the higher the total number of 10-day dry spells.

For example, if a station has no precipitation during all of May, the number of 10-day dry spells is "22" (i.e. the first 10 days is "1" while the remaining 21 days are "21" 10-day dry spells). However, the dry spell can continue from one month to the next (e.g. May into June). If this occurs, the dry spells are given to the month which has the most consecutive dry days. For example, if a 10-day dry spell occurs from May 25th to June 3rd, the dry spell is classified as occurring in May

(because more dry days occurred in May). Conversely, if the spell lasts from May 29th to June 7th, it is classified as occurring in June.

Therefore, the maximum number of 10-day dry spells for May (i.e. if all of May and the first five days of June have no precipitation) is 22 + 5 = "27" (i.e. the original 22 dry spells plus the 5 that continued into June). From this definition, the maximum number of 10-day dry spells for June is "30" and for July is "31". However, the maximum number for August is only "27" (since September data are not used, dry spells cannot continue from the end of August into September). Therefore, if a station has no precipitation for the entire growing season (i.e. May 1st to August 31st), the number of 10-day dry spells is 27 + 30 + 31 + 27 = "115".

This procedure is carried out for all 63 stations. The total number of 10-day dry spells (for the entire Prairies) is determined by summing the values for each station. As an extreme example, if all stations experience no precipitation for all of May and the first five days of June, the total number of 10-day dry spells is 27 x 63 = "1701". The maximum for June is 30 x 63 = "1890"; for July is 31 x 63 = "1953"; and for August is 27 x 63 = "1701". Conversely, if there are no consecutive 10-day dry periods for any stations during a particular month, the value is "0". Total number of 10-day dry spells for the entire growing season are determined by simply summing the individual months within the growing season. Therefore, the maximum is 1701 + 1890 + 1953 + 1701 = "7245".

Total number of 10-day dry spells (including averages and standard deviations) for the entire growing season and months within the growing

season from 1948-1991 are given in Appendix A - Table A.3. Growing-season values range from "1956" in 1961 to "137" in 1982 while monthly values range from "729" in July 1961 to "2" in May 1974. Standardized values are also included. They are standardized by subtracting the 44-year mean from the actual value and then dividing by the standard deviation (Ebdon, 1985).

Total number of 10-day dry spells indicate extended dry periods which often lead to droughts on the Prairies. Therefore, larger values indicate large-scale extended dry periods over the entire Prairie study area while smaller values indicate relatively few large-scale extended dry periods (and presumably large-scale wet periods). As a result, this variable is a temporal representation of precipitation variations on the Prairies.

3.2.1.3 AREALLY-AVERAGED PRECIPITATION ANOMALIES

The second variable is the areally-averaged precipitation anomaly. The values are also determined for the entire growing season and months within the growing season and are calculated in the following manner. Individual monthly and total growing-season precipitation values are determined for each station by summing the daily precipitation amounts. Precipitation anomalies are calculated by subtracting the 44-year mean from these values. From these anomalies, precipitation anomaly maps are produced for the entire Prairie study area. The maps are generated using the *SPANS* Geographic Information System (GIS) (version 5.3). The 63 precipitation anomalies (i.e. from the 63 stations) are used as point data which are linearly interpolated and contoured to create the anomaly

maps. From these maps, areally-averaged precipitation anomalies are calculated (in millimetres) for the entire Prairie study area. This procedure is carried out for the total growing season and each month within the growing season for all 44 years within the study period.

Areally-averaged precipitation anomalies (and standardized values) over the Canadian Prairie study area are given in Appendix A - Table A.4. Total growing-season values range from -110.9 mm in 1967 to +81.3 mm in 1954 while monthly values range from -47.3 mm in August 1961 to +63.7 mm in May 1977.

Areally-averaged precipitation anomalies indicate overall precipitation with respect to normal over the Prairie study area. Larger negative values indicate large-scale below normal precipitation or drier conditions while larger positive values indicate large-scale above normal precipitation or wetter conditions. However, these values do not always indicate the length of the anomalously dry or wet periods (i.e. they do not indicate extended dry or wet periods). They are more representative of total amounts of precipitation on the Prairies.

3.2.2 NORTHERN HEMISPHERE UPPER-ATMOSPHERIC CIRCULATION

Northern Hemisphere upper-atmospheric circulation data are used to quantify anomalous upper-atmospheric heights over the Canadian Prairies and PNA patterns. The 50 kPa level is used because it provides good representation of mid-tropospheric flow patterns and has been used in several investigations that studied synoptic causes of growing-season precipitation variations on the Canadian Prairies (e.g. Chakravarti, 1972; Dey, 1982; Knox and Lawford, 1990; Bonsal et al., 1993) and PNA

patterns (e.g. Wallace and Gutzler, 1981; Knox and Lawford, 1990).

3.2.2.1 50 KPA DATA

The data used to derive these variables consisted of daily (1200 UTC) 50 kPa heights for the Northern Hemisphere on a 455 point 5° latitude by 10° longitude grid. The majority of these data (1948-1981) are originally from the National Centre for Atmospheric Research in Boulder, Colorado and the remainder (1982-1991) from the Canadian Meteorological Centre in Montreal, Quebec (Knox et al., 1988). For this study, the complete data set was obtained from the AES archives in Downsview, Ontario.

The area examined is 15°N to 75°N and 120°E to 60°W (i.e. the North Pacific/North American region) which includes 230 grid points. For each of these points, daily 50 kPa heights are averaged by month and 50 kPa anomalies are calculated by subtracting the 44-year mean from the actual values.

3.2.2.2 AREALLY-AVERAGED 50 KPA ANOMALIES OVER THE CANADIAN PRAIRIES

The 50 kPa anomaly values are used to generate monthly 50 kPa anomaly maps for each month within the growing season (using *SPANS*). From these maps, areally-averaged 50 kPa anomalies (in decametres) are calculated for the Canadian Prairie study area. These anomalies (and standardized values) over the Prairie study area for each month within the growing season from 1948-1991 are given in Appendix B - Table B.1. The values range from +6.36 dam in June 1988 to -6.32 dam in May 1974. Larger positive values indicate upper-atmospheric ridging over the

Prairies while larger negative values indicate a more zonal flow. Total growing-season anomalies are not provided because these anomalies are quite variable for periods as long as the entire growing season. As a result, the value for this period tends to be near zero.

3.2.2.3 PNA INDICES

Monthly 50 kPa data are also used to identify PNA patterns. This teleconnection pattern was first identified by Wallace and Gutzler (1981) and involves four major centres of action in the Northern Hemisphere including the sub-tropical Pacific, the east-central North Pacific, western Canada and the southeastern United States (see Figure 2.5). Since the main focus of this study is the North Pacific/North American region, the area over the sub-tropical Pacific is omitted. Several studies that focused on the North Pacific/North American region have also omitted this centre and used the other three (e.g. Yarnal and Diaz, 1986; Leathers et al., 1991; Leathers and Palecki, 1992; Henderson and Robinson, 1994).

Several different indices (which incorporate these three main centres) are used to quantify PNA patterns. The indices vary slightly depending on the purpose of the study and data availability. For this investigation, the winter PNA index designed by Knox (1991) is used (Equation 3.1).

Equation 3.1: PNA Index Used in this Study

$$PNA = 1/3\ [-z(45^{\circ}N,160^{\circ}W) + z(55^{\circ}N,110^{\circ}W) - z(35^{\circ}N,80^{\circ}W)]$$

where z is the standardized monthly 50 kPa anomaly at each grid point.

Note that Knox (1991) defined three PNA indices (for spring, autumn and winter) accounting for the seasonal migration of pressure systems. However, for the purpose of this study, the winter PNA index is used because PNA patterns are most often associated with ENSO events during winter (Horel and Wallace, 1981; Emery and Hamilton, 1985; Yarnal and Diaz, 1986; Weber, 1990). The three main centres in this index correspond very closely to those used by Wallace and Gutzler (1981), Yarnal and Diaz (1986), Leathers et al., (1991) and Henderson and Robinson (1994).

From Equation 3.1, monthly PNA indices for the study period are calculated. However, this study uses the four standard seasons of winter (December, January, February), spring (March, April, May), summer (June, July, August) and autumn (September, October, November) for the PNA analysis for several reasons. Firstly, the other variables (i.e. North Pacific SST anomaly gradients and SOI values defined later in this chapter) are also analyzed on a seasonal basis because once these patterns establish themselves, they tend to persist for several months (e.g. Namias and Cayan, 1981; Philander, 1990). As a result, seasonal values should be representative of the months within the season. In fact, Trenberth (1976,1984) suggested that seasonal values are more effective in monitoring the SOI because monthly data often contain noise and also have significant autocorrelations when used in time series analysis. Secondly, many investigations used seasonal data when analyzing PNA patterns (e.g. Hansen et al., 1993; Henderson and Robinson, 1994), North Pacific SSTs (e.g. Emery and Hamilton, 1985; Yongping and McBean, 1991) and ENSO events (e.g. Fu et al., 1986;

Handler, 1990; Fraedrich and Muller, 1992).

Seasonal PNA indices are determined by averaging the three monthly values within each season. These indices (and standardized values) from 1948-1991 are given in Appendix C - Table C.1. The indices range from +1.44 in autumn 1976 to -2.12 in autumn 1985. Larger positive PNA values indicate a strong meridional flow over the North Pacific and North America with negative anomalies in the east-central North Pacific, positive anomalies over western Canada and negative anomalies over the southeastern United States. Larger negative values indicate more zonal flow with the anomalies being opposite to those in the positive cases (Leathers et al., 1991; Henderson and Robinson, 1994).

3.2.3 NORTH PACIFIC SSTS

3.2.3.1 SST DATA

The area of the North Pacific Ocean considered extends from 20°N to 60°N and 120°E to 110°W. This area has been used in previous investigations of North Pacific SSTs (e.g. Namias, 1970; Davis, 1976; Namias et al., 1988). The SST data were based on approximately eight million ship observations over the North Pacific Ocean which were compiled by the Bureau of Commercial Fisheries, United States Weather Bureau reports and National Marine Fisheries Service. These SSTs were then computed as monthly averages over a 5° latitude-longitude grid (181 grid points) (Namias, 1970; Davis, 1976; Namias et al., 1988). This data set was obtained from Scripps Institute of Oceanography in La Jolla, California. Monthly SST anomalies are calculated by subtracting the 44-year average value from the actual value for each grid point.

3.2.3.2 NORTH PACIFIC SST ANOMALY GRADIENTS

For statistical analysis, North Pacific SST anomaly patterns were quantified using the procedure designed by Bonsal et al. (1993). They determined SST anomaly gradients between two main regions in the North Pacific were associated with growing-season extended dry spells on the Canadian Prairies. The regions were the east-central North Pacific (30°N to 40°N, 165°W to 135°W) and the central-west coast of North America (45°N to 55°N, 130°W to 125°W) (see Figure 1.1). The SST anomaly gradients were quantified by subtracting the largest absolute anomaly found in the east-central North Pacific from the largest absolute anomaly found along the central-west coast of North America. Positive gradients occurred when SST anomalies along the central-west coast are higher than those in the east-central North Pacific and vice versa.

Monthly SST anomaly gradients are determined (in °C) using the above procedure. Seasonal gradients are calculated by averaging the three monthly values within each season. These gradients (and standardized values) from 1948-1991 are given in Appendix D - Table D.1. The values range from +3.97 °C in spring 1983 to -4.63 °C in winter 1949. It is realized that the term gradient implies a difference in SST over a given distance. However, since the regions used to calculate these differences are fixed, the distances remain relatively constant. Therefore, the gradients are simply presented as SST differences.

In addition to the gradients, some seasonal North Pacific SST anomaly patterns are examined. Using *SPANS*, seasonal SST anomaly maps are generated from the 181 grid points in the North Pacific Ocean. An example is shown in Figure 5.2.

3.2.4 ENSO EVENTS

Since the SO affects the entire ocean - atmosphere system in the tropical Pacific, a measure of this variable is often sufficient to quantify ENSO events (i.e. El Niño and La Niña) (Aceituno, 1992; Halpert and Ropelewski, 1992). Several indices have been used, however, the most common is the SOI. It is defined as the normalized difference in monthly mean SLP between Tahiti, French Polynesia (18°S, 150°W) (i.e. the eastern tropical Pacific) and Darwin, Australia (12°S, 131°E) (i.e. the western tropical Pacific) (Chen, 1982). The SOI is calculated as Tahiti SLP minus Darwin SLP. Negative values (i.e. anomalously low pressure in the eastern and anomalously high pressure in the western tropical Pacific) represent El Niño conditions, while positive values (i.e. anomalously high pressure in the eastern and anomalously low pressure in the western tropical Pacific) represent La Niña conditions. Numerous investigations have used the SOI to quantify ENSO events (e.g. Fu et al., 1986; Kiladis and Diaz, 1989; Halpert and Ropelewski, 1992) and therefore, this investigation also incorporates this index.

3.2.4.1 SOI DATA

Monthly SOI data were obtained from the Climatic Diagnostic Data Base at the National Oceanic and Atmospheric Administration in Washington, D.C. Seasonal values are determined by averaging the three monthly values within each season. These values (and standardized values) from 1948-1991 are given in Appendix E - Table E.1. They range from -5.96 in winter 1983 to +3.64 in winter 1974.

3.2.4.2 INDIVIDUAL ENSO EVENTS

The identification of individual ENSO events is also required. Several definitions have been used to outline these events. Most incorporate SOI and tropical Pacific SST anomalies (e.g. Quinn et al., 1978; van Loon and Madden, 1981; Rasmusson and Carpenter, 1982; Trenberth, 1984). This investigation uses the ENSO events defined by Kiladis and Diaz (1989). Their definition employed seasonal standardized SOI values and a seasonal tropical Pacific SST anomaly index for the region 4°N to 4°S and 160°W to the South American coast. For an El Niño (La Niña) event, the SST anomaly in this region had to be positive (negative) for at least three consecutive seasons and be at least 0.5°C above (below) the mean for at least one of these seasons. The seasonal SOI also had to remain below -1.0 (above +1.0) for the same three seasons. This criterion was also used in other ENSO related studies (e.g. Bradley et al., 1987; Kiladis and van Loon, 1988). Based on this definition, ten El Niño and seven La Niña events occurred from 1948-1991 (Table 3.1). The years in the table refer to the onset of the events (i.e. year 0).

It is realized that each ENSO event (both El Niño and La Niña) can differ significantly in terms of onset, evolution, amplitude, duration and spatial extent (Rasmusson et al., 1983; van Loon and Shea, 1985; Fu et al., 1986; Ropelewski and Halpert, 1986,1987,1989; Philander, 1990). However, for the purpose of the analyses used in this study, it is assumed that each event roughly corresponds to the composite or typical event described in chapter 2. The implications of this assumption will be discussed in chapter 7.

Table 3.1: ENSO Events Used in this Study

EL NIÑO	LA NIÑA
1951	1949
1953	1954
1957	1964
1963	1970
1965	1973
1969	1975
1972	1988
1976	
1982	
1986	

Note: Each year refers to onset of the event.

3.3 METHODOLOGY

The preceding sections have described the variables used in this investigation. The ones that pertain to the Canadian Prairies (i.e. total number of 10-day dry spells, areally-averaged precipitation anomalies, areally-averaged 50 kPa anomalies) are determined only for the growing seasons. They include monthly and entire growing-season (i.e. May through August) values. Conversely, PNA indices, North Pacific SST anomaly gradients and SOI values are seasonal variables that are determined for the entire year. The individual ENSO events occur irregularly throughout the period 1948-1991.

Two methods are used to analyze the relationships between ENSO events and growing-season precipitation variations on the Canadian Prairies. The first is a correlation analysis which determines the strength and significance of relationships between two variables over a specified period. It has been used in several investigations involving

SOI values (i.e. ENSO events) and related meteorological variables (e.g. Trenberth, 1984; Leathers and Palecki, 1992; Henderson and Robinson, 1994). The statistical procedure is Pearson's product-moment correlation. The strength of association is measured by a correlation coefficient (r) which is tested for significance using a two-tailed critical value table (Ebdon, 1985).

The correlation analysis determines the strength and significance of relationships between SOI values (ENSO events) and the variables associated with the atmosphere - ocean teleconnections over the Pacific Ocean during the entire study period 1948-1991. This includes correlations between SOI and the following: PNA indices, North Pacific SST anomaly gradients, areally-averaged 50 kPa anomalies, total number of 10-day dry spells and areally-averaged precipitation anomalies. The results are presented in chapter 4.

The second method includes a composite analysis. PNA indices, North Pacific SST anomaly gradients, areally-averaged 50 kPa anomalies, total number of 10-day dry spells and areally-averaged precipitation anomalies are composited or averaged for both the ten El Niño and seven La Niña events in Table 3.1. The purpose is to determine if there are any significant differences between El Niño and non-El Niño periods, La Niña and non-La Niña periods and El Niño and La Niña events for each variable. The analysis also examines average characteristics of these variables associated with both El Niño and La Niña events.

In the composite analysis, the two-tailed Student's t test determines the difference between two samples. A test statistic (t) is calculated from the mean, sample size and standard deviation of the

samples (Ebdon, 1985). Composite analysis and Student's t test have been used in several studies that examined relationships between ENSO events and meteorological variables (e.g. Yarnal and Diaz, 1986; Hamilton, 1988; Kiladis and Diaz, 1989; Halpert and Ropelewski, 1992). The results of this analysis are presented in chapter 5.

To summarize and provide possible physical explanations of the results of the correlation and composite analyses, conceptual models for El Niño and La Niña are formulated and discussed. Each model displays characteristics and lags involved in the atmosphere - ocean teleconnections over the Pacific Ocean associated with ENSO events and growing-season precipitation variations on the Canadian Prairies. These models are tested by determining the strength (i.e. very strong, strong, weak, very weak) and the consistency of responses of PNA patterns, North Pacific SST anomaly patterns, growing-season areally-averaged 50 kPa anomalies and total number of 10-day dry spells on the Prairies for the ten El Niño and seven La Niña events occurring between 1948 and 1991. Finally, two case studies (i.e. for El Niño and La Niña) are presented. The conceptual models, testing of these models and case studies are presented in chapter 6.

CHAPTER 4

CORRELATION ANALYSIS

Chapters 4 and 5 analyze teleconnections between ENSO events and growing-season precipitation variations on the Canadian Prairies focusing on the interpretation of the results. Although some discussion of physical processes is included, most will be presented in the modelling and case studies (chapter 6) and discussion (chapter 7) chapters.

This chapter presents results of a correlation analysis used to determine the strength and significance of relationships between ENSO events (as measured by SOI values) and the atmosphere - ocean teleconnections over the Pacific Ocean described in chapter 1. In addition, the lags involved with these relationships are determined (see Figure 1.2). Included are correlations between SOI values and the following: PNA indices, North Pacific SST anomaly gradients, areally-averaged 50 kPa anomalies over the Prairies, total number of 10-day dry spells on the Prairies and areally-averaged precipitation anomalies over the Prairies. As outlined in chapter 3, the statistical procedure used is Pearson's product-moment correlation.

4.1 SOI AND PNA INDICES

The first relationship examined is between ENSO events and PNA patterns. A line graph comparing standardized seasonal values of SOI and PNA indices from 1948 to 1991 is given in Figure 4.1. Standardization

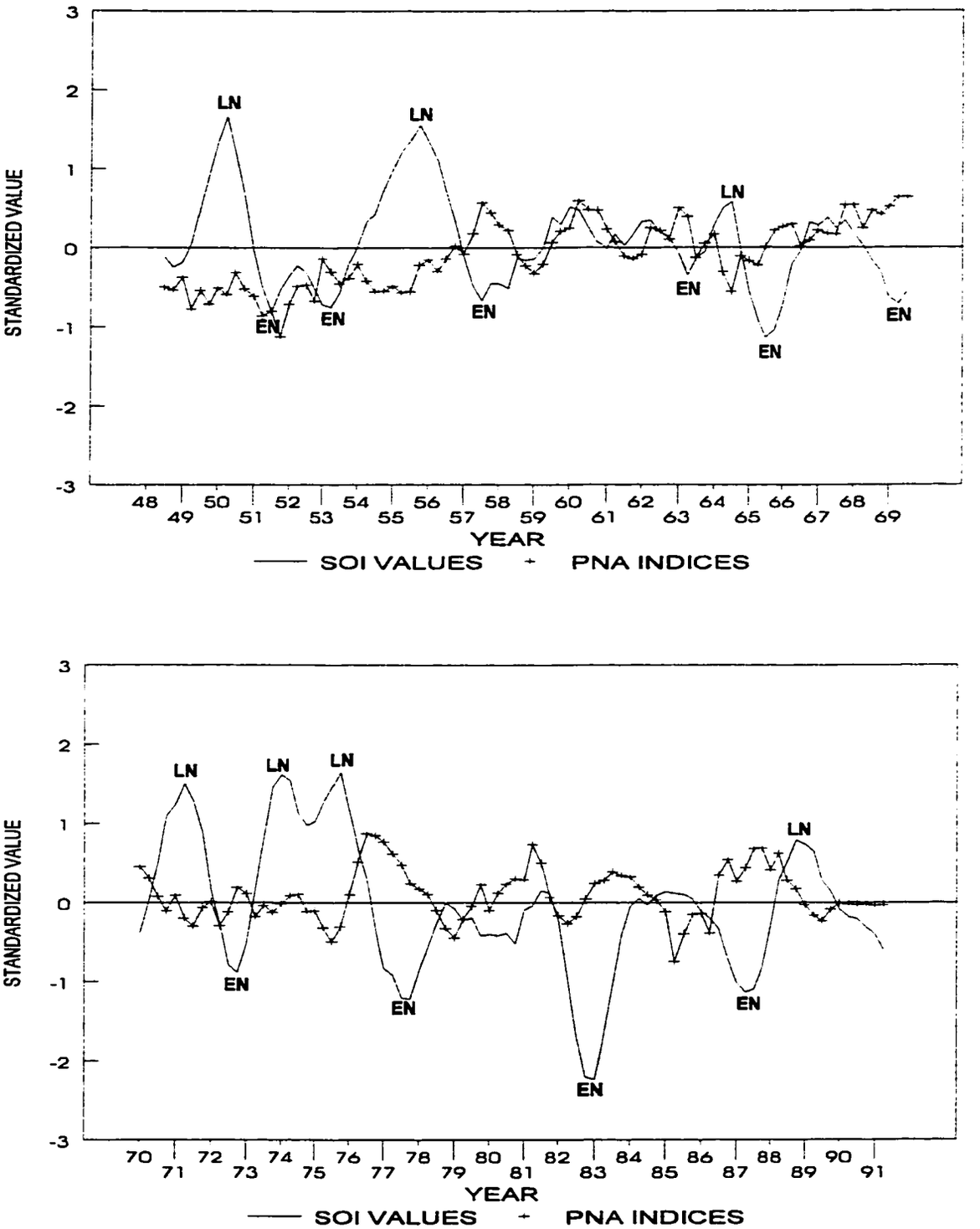

EN represents El Niño event
LN represents La Niña event

Figure 4.1: Seasonal SOI Values and PNA Indices (1948-1991)

facilitates comparison of the variables. The data are also filtered using a three-season running mean which is calculated by averaging the current observation with those from the previous and subsequent seasons. This smoothing procedure is commonly used to reduce noise (e.g. Trenberth, 1984; Leathers and Palecki, 1992). The mature stages of the ten El Niño and seven La Niña events occurring during the study period (Table 3.1) are also indicated.

An inverse relationship between SOI and PNA is shown with El Niño events coinciding with positive PNA indices and La Niña events with negative indices. To determine if this relationship is statistically significant, correlations between actual (i.e. unsmoothed) seasonal SOI values and seasonal PNA indices are calculated (Table 4.1). The lags (in seasons) with respect to the SOI values are also presented.

With continuous time series data, there may be significant autocorrelations within each series which reduce the degrees of freedom (e.g. Trenberth, 1984). Using a procedure designed by Davis (1976) it is determined that autocorrelations have a minimal effect on the significance levels in all of the correlation analyses presented in this chapter.

Table 4.1 shows a significant negative correlation for a 0 season lag (i.e. a significant contemporaneous correlation). The negative correlation suggests El Niño events (negative SOI values) are associated with positive PNA patterns and La Niña (positive SOI values) are associated with negative PNA patterns. Since the strongest SOI signal (i.e. negative for El Niño and positive for La Niña) tends to be associated with the mature stage of ENSO events (Rasmusson and

Table 4.1: Correlations Between Seasonal SOI Values and Seasonal PNA Indices (1948-1991).

VARIABLES	LAG (SEASONS)	R VALUE
SOI vs PNA(-1)	-1	-0.12
SOI vs PNA(0)	0	-0.22***
SOI vs PNA(+1)	+1	-0.17
SOI vs PNA(+2)	+2	-0.09

*** significant at 0.01 level
Note: Lags are with respect to the SOI values.

Carpenter, 1982; Philander, 1985,1990), the 0 season lag suggests the different PNA patterns (i.e. positive and negative) are strongest near the mature stages of these events. As outlined in chapter 2, typical ENSO events (both El Niño and La Niña) mature during the winter following their onset (i.e. winter(+4)).

The preceding correlations indicate significant, but weak relationships for the entire study period. A possible reason is the inclusion of all seasons. It has been shown that the PNA teleconnection associated with ENSO events tends to be strongest during winter (e.g. Simmons, 1982; Webster, 1982; Lau and Lim, 1984). Since ENSO events typically mature (and thus experience their most anomalous SOI values) during winter, correlations associated with winter SOI should be strongest. However, because ENSO events typically last around 18 months, the associated SOI anomalies should also have the same duration. Therefore, spring, summer and autumn SOI may also be associated with strong correlations (Rasmusson and Carpenter, 1982; Philander, 1985,1990; Kiladis and Diaz, 1989). Correlations between SOI values and PNA indices for each season (i.e. winter, spring, summer, autumn) are

thus calculated, to determine if certain seasons show stronger associations (Table 4.2).

All significant correlations are associated with winter PNA. Winter SOI has a significant negative correlation for a 0 season lag. Since strongest SOI correlations are normally associated with the mature stage of ENSO (which typically occurs during winter(+4)), the 0 season lag suggests PNA patterns occur near the mature stages (i.e. the winter following the onset).

Spring shows a significant correlation for a -1 season lag. As outlined previously, strong SOI correlations can also be associated with periods other than winter (because ENSO events typically last around 18 months). Therefore, the -1 season lag could indicate the ENSO events are in their later stages during spring, but the PNA patterns have already occurred during the preceding winter (i.e. the winter coinciding with the mature stage of ENSO events). For summer and autumn, the significant +2 and +1 season lags likely indicate that ENSO events are in their earlier stages during summer and autumn and the PNA patterns occur during the following winter.

The preceding analysis suggests PNA patterns have strongest associations with ENSO events during the winter coinciding with the mature stage of these events (i.e. winter(+4)). The significant negative correlations imply that El Niño events are associated with positive PNA patterns and La Niña are associated with negative PNA patterns.

4.2 SOI AND NORTH PACIFIC SST ANOMALY GRADIENTS

The next relationship examined is between ENSO events and North

Table 4.2: Correlations Between Seasonal SOI Values and Seasonal PNA Indices for each Season (1948-1991).

VARIABLES	LAG (SEASONS)	R VALUE
WINTER		
Winter SOI vs Autumn PNA	-1	-0.20
Winter SOI vs Winter PNA	0	-0.34**
Winter SOI vs Spring PNA	+1	-0.15
Winter SOI vs Summer PNA	+2	+0.13
Winter SOI vs Autumn PNA	+3	+0.18
SPRING		
Spring SOI vs Winter PNA	-1	-0.36**
Spring SOI vs Spring PNA	0	-0.24
Spring SOI vs Summer PNA	+1	+0.02
Spring SOI vs Autumn PNA	+2	-0.05
Spring SOI vs Winter PNA	+3	-0.13
SUMMER		
Summer SOI vs Spring PNA	-1	-0.04
Summer SOI vs Summer PNA	0	+0.07
Summer SOI vs Autumn PNA	+1	-0.13
Summer SOI vs Winter PNA	+2	-0.32**
Summer SOI vs Spring PNA	+3	-0.01
AUTUMN		
Autumn SOI vs Summer PNA	-1	+0.03
Autumn SOI vs Autumn PNA	0	-0.22
Autumn SOI vs Winter PNA	+1	-0.38**
Autumn SOI vs Spring PNA	+2	+0.03
Autumn SOI vs Summer PNA	+3	+0.19

** significant at 0.05 level
Note: Lags are with respect to the SOI values.

Pacific SST anomaly patterns. Figure 4.2 is a line graph comparing standardized seasonal values of SOI and North Pacific SST anomaly gradients from 1948 to 1991 (using a three-season running mean). The mature stages of the El Niño and La Niña events are also presented showing a distinct inverse relationship with El Niño events coinciding with positive SST anomaly gradients and La Niña with negative gradients.

Table 4.3 presents correlations between seasonal SOI values and

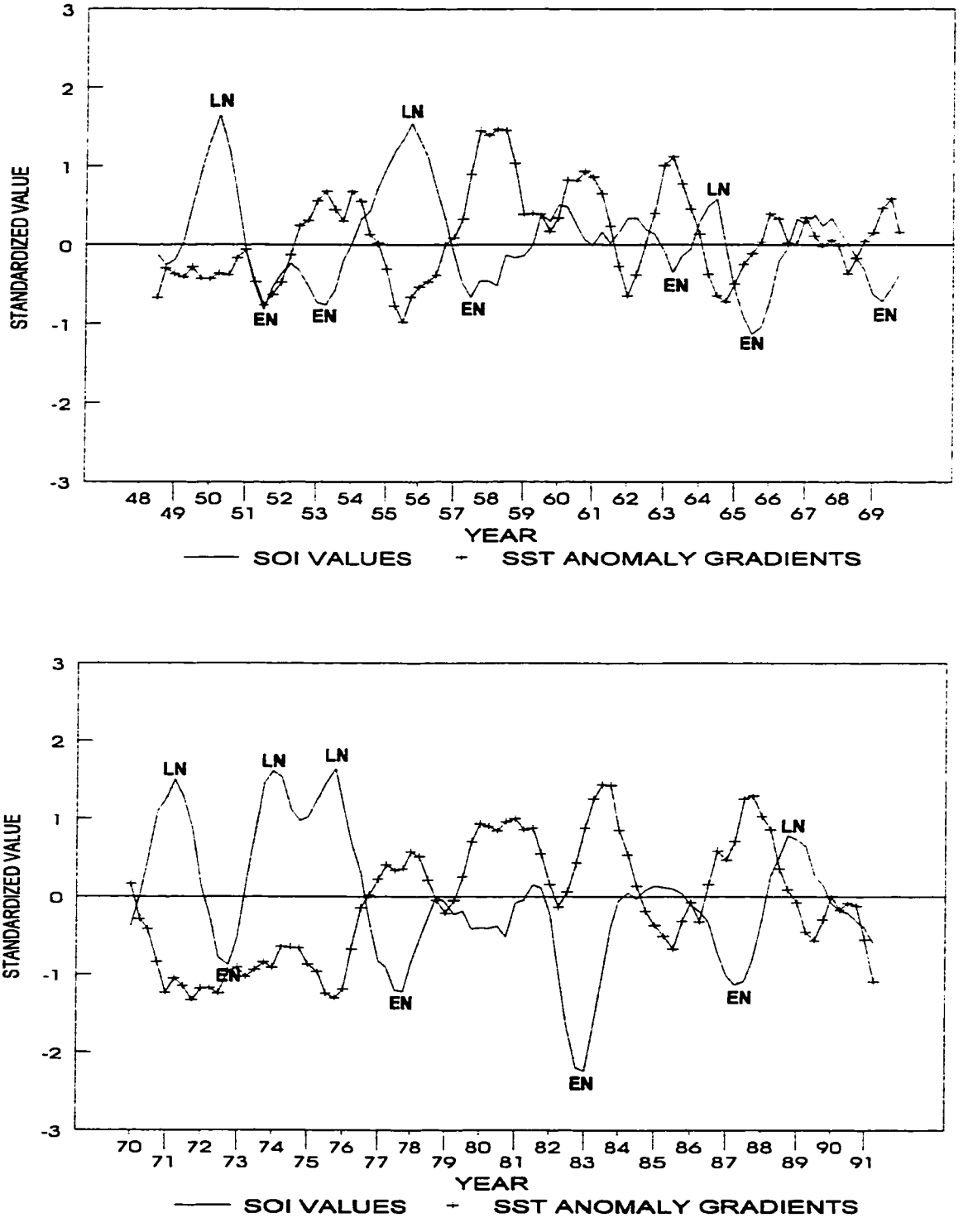

EN represents El Niño events
LN represents La Niña events

Figure 4.2: Seasonal SOI Values and North Pacific SST Anomaly Gradients (1948-1991)

Table 4.3: Correlations Between Seasonal SOI Values and Seasonal North Pacific SST Anomaly Gradients (1948-1991).

VARIABLES	LAG (SEASONS)	R VALUE
SOI vs SST(-2)	-2	-0.13
SOI vs SST(-1)	-1	-0.21***
SOI vs SST(0)	0	-0.28***
SOI vs SST(+1)	+1	-0.40***
SOI vs SST(+2)	+2	-0.35***
SOI vs SST(+3)	+3	-0.28***
SOI vs SST(+4)	+4	-0.23***
SOI vs SST(+5)	+5	-0.16

*** significant at 0.01 level
Note: Lags are with respect to the SOI values.

seasonal North Pacific SST anomaly gradients. The analysis shows several significant negative correlations for a number of lags. Negative r values suggest El Niño events (negative SOI values) are associated with positive SST anomaly gradients (i.e. anomalously cold water in the east-central North Pacific and anomalously warm water along the central-west coast of North America (see Figure 1.1)), while La Niña are associated with opposite SST anomaly patterns. The strongest correlation occurs with a +1 season lag. Since strongest SOI signals tend to be associated with the mature stage of ENSO events, the +1 season lag suggests the SST anomaly patterns are strongest around one season following the mature stages (i.e. the spring following the mature stages). There are also significant negative correlations persisting for up to a +4 season lag suggesting that once the SST anomaly patterns are produced, they generally persist for several seasons.

Correlations between SOI values and SST anomaly gradients for each season are also calculated to determine if certain seasons show stronger

associations (Table 4.4). There are many significant negative r values occurring during all seasons. However, the strongest SOI correlations (for each season) are associated with spring SST. Winter SOI has significant r values for a 0, +1 and +2 season lag corresponding to winter, spring and summer SST respectively. As outlined in the previous section, the strongest SOI correlations are normally associated with the mature stage of ENSO (i.e. winter(+4)). Therefore, these results suggest North Pacific SST anomaly patterns are strongest during the winter associated with, and the spring and summer following the maturity.

For spring SOI, significant negative r values occur during lags of -1, 0, +1, +2, +3 and +4 seasons. As was the case with spring SOI vs PNA, the significant correlation associated with a -1 season lag (i.e. winter SST) could indicate ENSO events are in their later stages during spring, however, the SST anomaly patterns are observed during the preceding winter. The 0, +1, +2, +3 and +4 season lags would therefore indicate that these SST anomaly patterns persist for several seasons (i.e. the next spring, summer, autumn, winter and spring).

However, typical ENSO events begin during winter, strengthen during spring, summer and autumn, mature during the following winter and terminate during spring (Rasmusson and Carpenter, 1982; Philander, 1985, 1990; Kiladis and Diaz, 1989). Therefore, strong SOI correlations can also be associated with springs prior to the mature stage of ENSO events. As a result, the significant -1, 0, +1, +2, +3 and +4 correlations could also indicate the SST anomaly patterns occur during the winter, spring, summer and autumn prior to, the winter coinciding with, and the spring following the mature stage of ENSO events. From

Table 4.4: Correlations Between Seasonal SOI Values and Seasonal North Pacific SST Anomaly Gradients for each Season (1948-1991).

VARIABLES	LAG (SEASONS)	R VALUE
WINTER		
Winter SOI vs Autumn SST	-1	-0.12
Winter SOI vs Winter SST	0	-0.37**
Winter SOI vs Spring SST	+1	-0.57***
Winter SOI vs Summer SST	+2	-0.40***
Winter SOI vs Autumn SST	+3	-0.13
Winter SOI vs Winter SST	+4	-0.22
Winter SOI vs Spring SST	+5	-0.13
SPRING		
Spring SOI vs Winter SST	-1	-0.32**
Spring SOI vs Spring SST	0	-0.45***
Spring SOI vs Summer SST	+1	-0.37**
Spring SOI vs Autumn SST	+2	-0.33**
Spring SOI vs Winter SST	+3	-0.37**
Spring SOI vs Spring SST	+4	-0.35**
Spring SOI vs Summer SST	+5	-0.07
SUMMER		
Summer SOI vs Spring SST	-1	-0.15
Summer SOI vs Summer SST	0	-0.17
Summer SOI vs Autumn SST	+1	-0.23
Summer SOI vs Winter SST	+2	-0.34**
Summer SOI vs Spring SST	+3	-0.43***
Summer SOI vs Summer SST	+4	-0.17
Summer SOI vs Autumn SST	+5	-0.12
AUTUMN		
Autumn SOI vs Summer SST	-1	-0.20
Autumn SOI vs Autumn SST	0	-0.25
Autumn SOI vs Winter SST	+1	-0.37**
Autumn SOI vs Spring SST	+2	-0.45***
Autumn SOI vs Summer SST	+3	-0.25
Autumn SOI vs Autumn SST	+4	-0.16
Autumn SOI vs Winter SST	+5	-0.16

*** significant at 0.01 level
** significant at 0.05 level
Note: Lags are with respect to the SOI values.

this analysis, it is difficult to separate correlations representing periods prior to the mature stage and those following the mature stage for spring SOI.

Both summer and autumn SOI have significant negative values associated with winter and spring SST. Since strong SOI correlations are often associated with summers and autumns preceding the mature stage of ENSO events, these results suggest the SST anomaly patterns occur during the winter coinciding with, and spring following, the mature stage. From Table 4.4, negative r values are associated with every season for lags of up to, and including +5 seasons. Even though some of these values are not significant, the persistence of negative correlations suggests that once these SST anomaly patterns occur, they persist for several (up to +5) seasons.

Both the continuous and seasonal comparisons between SOI values and North Pacific SST anomaly gradients show several significant negative correlations. Those using each season (Table 4.4) show highest r values with winter and spring SST implying that SST anomaly patterns associated with ENSO events are strongest during, and shortly after, the maturity of the events (i.e. winter(+4) to spring(+5)). The negative correlations suggest El Niño events are associated with SST anomaly patterns consisting of anomalously cold water in the east-central North Pacific and anomalously warm water along the central-west coast of North America and La Niña are associated with opposite patterns.

4.2.1 PNA INDICES AND NORTH PACIFIC SST ANOMALY GRADIENTS

The preceding sections have indicated significant associations between SOI values and North Pacific SST anomaly gradients. As outlined in chapter 1 (Figure 1.2), it is hypothesized that this association occurs with the PNA acting as a link (i.e. ENSO events cause PNA

patterns which cause North Pacific SST anomalies). If this is the case, then significant correlations between PNA indices and North Pacific SST anomaly gradients should be observed.

Figure 4.3 compares standardized seasonal values of PNA indices and North Pacific SST anomaly gradients from 1948 to 1991 (using a three-season running mean). A positive association between the variables is shown. To determine if this relationship is statistically significant, and the lags involved, correlations between seasonal PNA indices and seasonal North Pacific SST anomaly gradients are calculated (Table 4.5). There are significant positive r values for a 0 and +1 season lag indicating positive PNA patterns are associated with positive SST anomaly gradients and vice versa. The results also indicate the SST anomaly patterns are strongest during, and shortly after, the occurrence of PNA patterns.

Table 4.6 presents correlations between PNA indices and North Pacific SST anomaly gradients for each season. Significant positive correlations are also observed, although not for every season. Winter PNA has highly significant r values for a 0 and +1 season lag (i.e. winter and spring SST). Spring PNA has a significant correlation for a 0 season lag (i.e. spring SST), but it is not as strong as those associated with winter PNA. Summer PNA has no significant correlations, while autumn PNA has significant correlations for a 0 and +1 season lag (i.e autumn and winter SST). These correlations are stronger than for spring PNA, but not as strong as winter PNA.

The preceding suggests relationships between PNA patterns and North Pacific SST anomaly patterns, especially during autumn and winter.

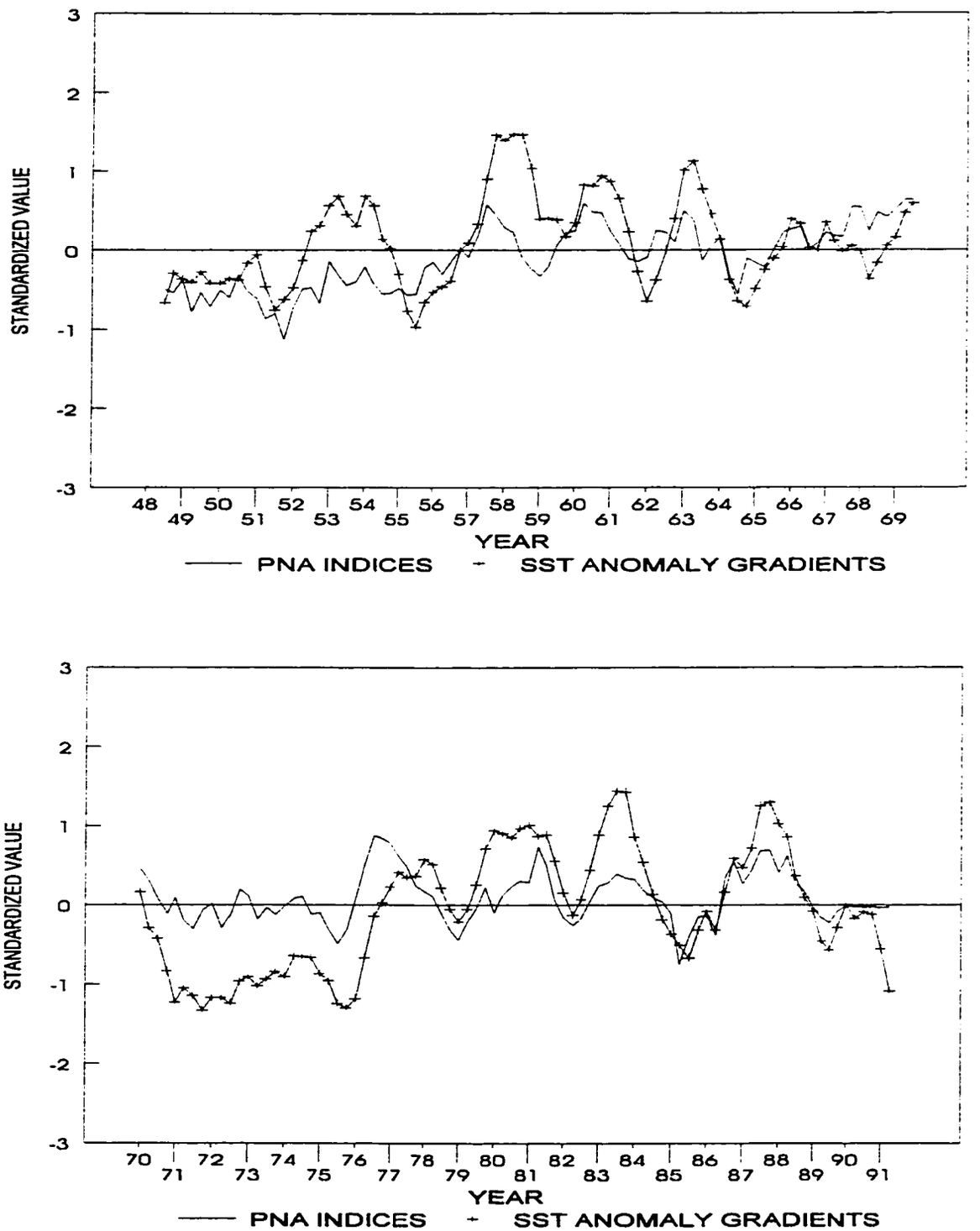

Figure 4.3: Seasonal PNA Indices and North Pacific SST Anomaly Gradients (1948-1991)

Table 4.5: Correlations Between Seasonal PNA Indices and Seasonal North Pacific SST Anomaly Gradients (1948-1991).

VARIABLES	LAG (SEASONS)	R VALUE
PNA vs SST(-1)	-1	+0.09
PNA vs SST(0)	0	+0.50***
PNA vs SST(+1)	+1	+0.36***
PNA vs SST(+2)	+2	+0.04

*** significant at 0.01 level
Note: Lags are with respect to the PNA indices.

However, this investigation is only concerned with PNA patterns associated with ENSO events (i.e. both positive and negative PNA patterns can be generated by other forcing mechanisms such as orography, land/sea heating contrasts and barotropic instability (e.g. Lau, 1981; Leathers et al., 1991)). The correlation analysis between SOI and PNA (section 4.1) suggested PNA patterns associated with ENSO events occur during the winter coinciding with the mature stages of the events. Therefore, due to the hypothesized atmosphere - ocean teleconnections in this study (Figure 1.2), winter PNA patterns are most relevant.

Winter PNA indices have significant positive r values for a 0 and +1 season lag (Table 4.6) suggesting North Pacific SST anomaly patterns are strongest during the same winter, and the spring following, the occurrence of PNA patterns. This also coincides with periods during or shortly after the mature stage of the ENSO events (i.e. winter(+4) to spring(+5)). The significant positive correlations suggest that positive PNA patterns are associated with positive SST anomaly gradients and vice versa.

In summary, a significant association has been shown between ENSO

Table 4.6: Correlations Between Seasonal PNA Indices and Seasonal North Pacific SST Anomaly Gradients for each Season (1948-1991).

VARIABLES	LAG (SEASONS)	R VALUE
WINTER		
Winter PNA vs Autumn SST	-1	+0.21
Winter PNA vs Winter SST	0	+0.67***
Winter PNA vs Spring SST	+1	+0.64***
Winter PNA vs Summer SST	+2	+0.19
SPRING		
Spring PNA vs Winter SST	-1	-0.06
Spring PNA vs Spring SST	0	+0.32**
Spring PNA vs Summer SST	+1	+0.20
Spring PNA vs Autumn SST	+2	-0.11
SUMMER		
Summer PNA vs Spring SST	-1	+0.05
Summer PNA vs Summer SST	0	+0.03
Summer PNA vs Autumn SST	+1	-0.05
Summer PNA vs Winter SST	+2	-0.11
AUTUMN		
Autumn PNA vs Summer SST	-1	+0.14
Autumn PNA vs Autumn SST	0	+0.56***
Autumn PNA vs Winter SST	+1	+0.45***
Autumn PNA vs Spring SST	+2	+0.11

*** significant at 0.01 level
** significant at 0.05 level
Note: Lags are with respect to the PNA values.

and winter PNA which, in turn, is associated with winter and spring North Pacific SST anomalies. This suggests that the PNA acts as a link between ENSO and North Pacific SST anomalies.

4.3 SOI AND GROWING-SEASON AREALLY-AVERAGED 50 KPA ANOMALIES OVER THE CANADIAN PRAIRIES

In section 4.2, an association was shown between SOI and persistent North Pacific SST anomaly gradients. As outlined in chapter 1, these persistent gradients may be associated with 50 kPa anomalies

leading to precipitation variations on the Canadian Prairies. To test this hypothesis, correlations are calculated between SOI values and growing-season precipitation parameters (i.e. 50 kPa anomalies, 10-day dry spells and precipitation anomalies) on the Canadian Prairies.

The first analysis involves SOI and growing-season areally-averaged 50 kPa anomalies over the Prairies. Correlations between SOI values for each season and monthly areally-averaged 50 kPa anomalies over the Canadian Prairies during the growing season are determined (Table 4.7). To test the hypothesized atmosphere - ocean teleconnections in Figure 1.2, 50 kPa anomalies during the third growing season following the onset of ENSO events (i.e. +10 seasons) are analyzed. As discussed earlier in this chapter, the strongest SOI correlations are normally associated with the mature stage of ENSO events (i.e. the winter corresponding to +4 seasons with respect to the onset). Since 50 kPa anomalies are analyzed with a lag of +10 seasons with respect to the onset of an ENSO, this corresponds to a +6 season lag with respect to the mature stage. Therefore, correlations between winter SOI and 50 kPa anomalies are determined for a +6 season lag.

However, strong SOI correlations can also be associated with periods other than winter. Therefore, spring, summer and autumn SOI values are also examined. The strongest SOI correlations would be associated with the springs, summers and autumns preceding the mature stage (i.e. spring(+1), summer(+2), autumn(+3)) and springs following the mature stage (i.e. spring(+5)) of ENSO events (Rasmusson and Carpenter, 1982; Trenberth, 1984; Kiladis and Diaz, 1989). Since 50 kPa anomalies are analyzed with a +10 season lag with respect to the onset

Table 4.7: Correlations Between Seasonal SOI Values and Growing-Season Areally-Averaged 50 kPa Anomalies Over the Canadian Prairies (1948-1991).

VARIABLES	LAG (SEASONS)	R VALUE
SPRING		
Spring(+1) SOI vs May(+10)	+9	+0.37**
Spring(+1) SOI vs June(+10)	+9	-0.02
Spring(+1) SOI vs July(+10)	+9	-0.32**
Spring(+1) SOI vs August(+10)	+9	-0.06
SUMMER		
Summer(+2) SOI vs May(+10)	+8	+0.44***
Summer(+2) SOI vs June(+10)	+8	-0.08
Summer(+2) SOI vs July(+10)	+8	-0.30**
Summer(+2) SOI vs August(+10)	+8	-0.20
AUTUMN		
Autumn(+3) SOI vs May(+10)	+7	+0.47***
Autumn(+3) SOI vs June(+10)	+7	-0.11
Autumn(+3) SOI vs July(+10)	+7	-0.19
Autumn(+3) SOI vs August(+10)	+7	-0.17
WINTER		
Winter(+4) SOI vs May(+10)	+6	+0.42***
Winter(+4) SOI vs June(+10)	+6	-0.12
Winter(+4) SOI vs July(+10)	+6	-0.33**
Winter(+4) SOI vs August(+10)	+6	-0.14

*** significant at 0.01 level
** significant at 0.05 level
Note: Lags are with respect to the SOI values.
: In this analysis, May is considered a summer month.

of ENSO, this corresponds to a +8 season lag with summer SOI (i.e. summer(+2)) and a +7 season lag with autumn SOI (i.e. autumn(+3)). However, since spring SOI can be associated with periods prior to (i.e. spring(+1)) and following (i.e. spring(+5)) the mature stage of ENSO, growing season(+10) can either correspond to a +9 or +5 season lag. However, the +5 season lags do not show any significant correlations and as a result, only the +9 season lags are presented. Note that according to the definition of seasons, May occurs during spring. However, since

May is also part of the growing season, it is included as a summer (i.e. +10) month in the correlation and composite analyses.

In Table 4.7, positive r values indicate that negative SOI (i.e. El Niño events) are associated with negative 50 kPa anomalies over the Prairies and positive SOI are associated with positive 50 kPa anomalies. Negative values imply the opposite. Every May is associated with a significant positive correlation, while most Julys have significant negative correlations. The only exception is the July associated with autumn SOI. Furthermore, with the exception of May, every other month has negative r values (however, not always significant).

These results indicate that during El Niño, May is associated with negative 50 kPa anomalies over the Canadian Prairies and July with positive anomalies. Though not significant, the signs of the correlation values suggest that June and August are also associated with positive 50 kPa anomalies. During La Niña, the 50 kPa anomalies are opposite to those associated with El Niño. It therefore appears that during growing season(+10), 50 kPa anomalies associated with ENSO events are strongest during May and July. The associations with May tend to be opposite to those of the rest of the growing season.

4.4. SOI AND GROWING-SEASON PRECIPITATION VARIATIONS ON THE CANADIAN PRAIRIES

The previous section showed significant associations between SOI values and areally-averaged 50 kPa anomalies. Since 50 kPa anomalies often lead to precipitation variations over the Prairies (Dey and Chakravarti, 1976; Dey, 1982; Knox and Lawford, 1990), significant

associations between SOI values and these variations should also be observed. As outlined in chapter 3, this study defines two variables to identify precipitation variations including total number of 10-day dry spells and areally-averaged precipitation anomalies.

Table 4.8 presents correlations between SOI values and growing-season total number of 10-day dry spells on the Prairies. For reasons outlined in the previous section, the lags are the same as those in Table 4.7. A total growing-season value is also examined in the 10-day dry spell analysis. Negative values indicate negative SOI (i.e. El Niño events) are associated with more 10-day dry spells (i.e. dry conditions) and positive SOI are associated with fewer 10-day dry spells (i.e. wet conditions). Conversely, positive values indicate negative SOI are associated with fewer 10-day dry spells and positive SOI are associated with more 10-day dry spells.

Table 4.8 shows every June and most of the Julys have significant negative correlations. The only exception is the correlation between July and spring SOI. Furthermore, every June, July, August and total growing season have negative correlations. Conversely, every May has a positive correlation, but only the one associated with summer SOI is statistically significant. This agrees with the correlation analysis between SOI and 50 kPa anomalies which indicated correlations with May are opposite to those with the rest of the growing season.

The results of this analysis suggest El Niño events are associated with fewer extended dry spells during May and more extended dry spells during June and July (and perhaps August). Conversely, La Niña are associated with opposite conditions (i.e. more extended dry spells

Table 4.8: Correlations Between Seasonal SOI Values and Growing-Season Total Number of 10-Day Dry Spells on the Canadian Prairies (1948-1991).

VARIABLES	LAG (SEASONS)	R VALUE
SPRING		
Spring(+1) SOI vs Total(+10)	+9	-0.02
Spring(+1) SOI vs May(+10)	+9	+0.24
Spring(+1) SOI vs June(+10)	+9	-0.32**
Spring(+1) SOI vs July(+10)	+9	-0.05
Spring(+1) SOI vs August(+10)	+9	-0.01
SUMMER		
Summer(+2) SOI vs Total(+10)	+8	-0.16
Summer(+2) SOI vs May(+10)	+8	+0.30**
Summer(+2) SOI vs June(+10)	+8	-0.41***
Summer(+2) SOI vs July(+10)	+8	-0.35**
Summer(+2) SOI vs August(+10)	+8	-0.24
AUTUMN		
Autumn(+3) SOI vs Total(+10)	+7	-0.16
Autumn(+3) SOI vs May(+10)	+7	+0.16
Autumn(+3) SOI vs June(+10)	+7	-0.30**
Autumn(+3) SOI vs July(+10)	+7	-0.35**
Autumn(+3) SOI vs August(+10)	+7	-0.22
WINTER		
Winter(+4) SOI vs Total(+10)	+6	-0.16
Winter(+4) SOI vs May(+10)	+6	+0.18
Winter(+4) SOI vs June(+10)	+6	-0.36**
Winter(+4) SOI vs July(+10)	+6	-0.36**
Winter(+4) SOI vs August(+10)	+6	-0.16

*** significant at 0.01 level
** significant at 0.05 level
Note: Lags are with respect to the SOI values.

during May and fewer extended dry spells during June and July (and perhaps August)). These associations occur during the third growing season following the onset of ENSO events.

Growing-season precipitation variations are also identified by areally-averaged precipitation anomalies. Table 4.9 presents correlations between SOI values and these precipitation anomalies. The analysis shows no significant correlations. However, every May has a

Table 4.9: Correlations Between Seasonal SOI Values and Growing-Season Areally Averaged Precipitation Anomalies over the Canadian Prairies (1948-1991).

VARIABLES	LAG (SEASONS)	R VALUE
SPRING		
Spring(+1) SOI vs Total(+10)	+9	+0.05
Spring(+1) SOI vs May(+10)	+9	-0.10
Spring(+1) SOI vs June(+10)	+9	+0.21
Spring(+1) SOI vs July(+10)	+9	0.00
Spring(+1) SOI vs August(+10)	+9	+0.05
SUMMER		
Summer(+2) SOI vs Total(+10)	+8	+0.24
Summer(+2) SOI vs May(+10)	+8	-0.13
Summer(+2) SOI vs June(+10)	+8	+0.16
Summer(+2) SOI vs July(+10)	+8	+0.22
Summer(+2) SOI vs August(+10)	+8	+0.17
AUTUMN		
Autumn(+3) SOI vs Total(+10)	+7	+0.13
Autumn(+3) SOI vs May(+10)	+7	-0.06
Autumn(+3) SOI vs June(+10)	+7	+0.01
Autumn(+3) SOI vs July(+10)	+7	+0.08
Autumn(+3) SOI vs August(+10	+7	+0.20
WINTER		
Winter(+4) SOI vs Total(+10)	+6	+0.11
Winter(+4) SOI vs May(+10)	+6	-0.09
Winter(+4) SOI vs June(+10)	+6	+0.06
Winter(+4) SOI vs July(+10)	+6	+0.21
Winter(+4) SOI vs August(+10)	+6	+0.16

Note: Lags are with respect to the SOI values.

negative r value and every June, July, August and total growing season have positive values. This also suggests that May has an opposite response to the rest of the growing season. The question of why May is generally opposite from the rest of the growing season will be discussed in chapter 7.

Recall that the total number of 10-day dry spells variable is a temporal representation of precipitation variations on the Prairies while areally-averaged precipitation anomalies are more representative

of total amounts of precipitation (see chapter 3). Therefore, this analysis suggests that ENSO events are associated more with number of extended dry spells (i.e. length of dry periods) as opposed to actual precipitation amounts on the Prairies. Further discussion of extended dry spells versus precipitation anomalies will also be provided in chapter 7.

4.5 SUMMARY

Figure 4.4 summarizes the results of the correlation analysis between ENSO events and growing-season precipitation variations on the Canadian Prairies. Except for a few minor differences (e.g. lags, May versus the rest of the growing season), the results agree with the hypothesis of chapter 1 (Figure 1.2).

During El Niño events, positive PNA patterns develop during the winter following the onset of the events (i.e. winter(+4)). This coincides with the mature stage of El Niño events. Shortly following the appearance of these patterns (i.e. 0 to +1 seasons), North Pacific SST anomaly patterns consisting of anomalously cold water in the east-central North Pacific and anomalously warm water along the central-west coast of North America are observed. This corresponds to the period of winter(+4) to spring(+5). These SST anomaly patterns then persist for up to +5 seasons (i.e. from winter(+4)/spring(+5) to spring(+9)/summer(+10)). During growing season(+10) (i.e. the third growing season following the onset of El Niño events), positive 50 kPa anomalies and more extended dry spells occur during June, July and August. Conversely,

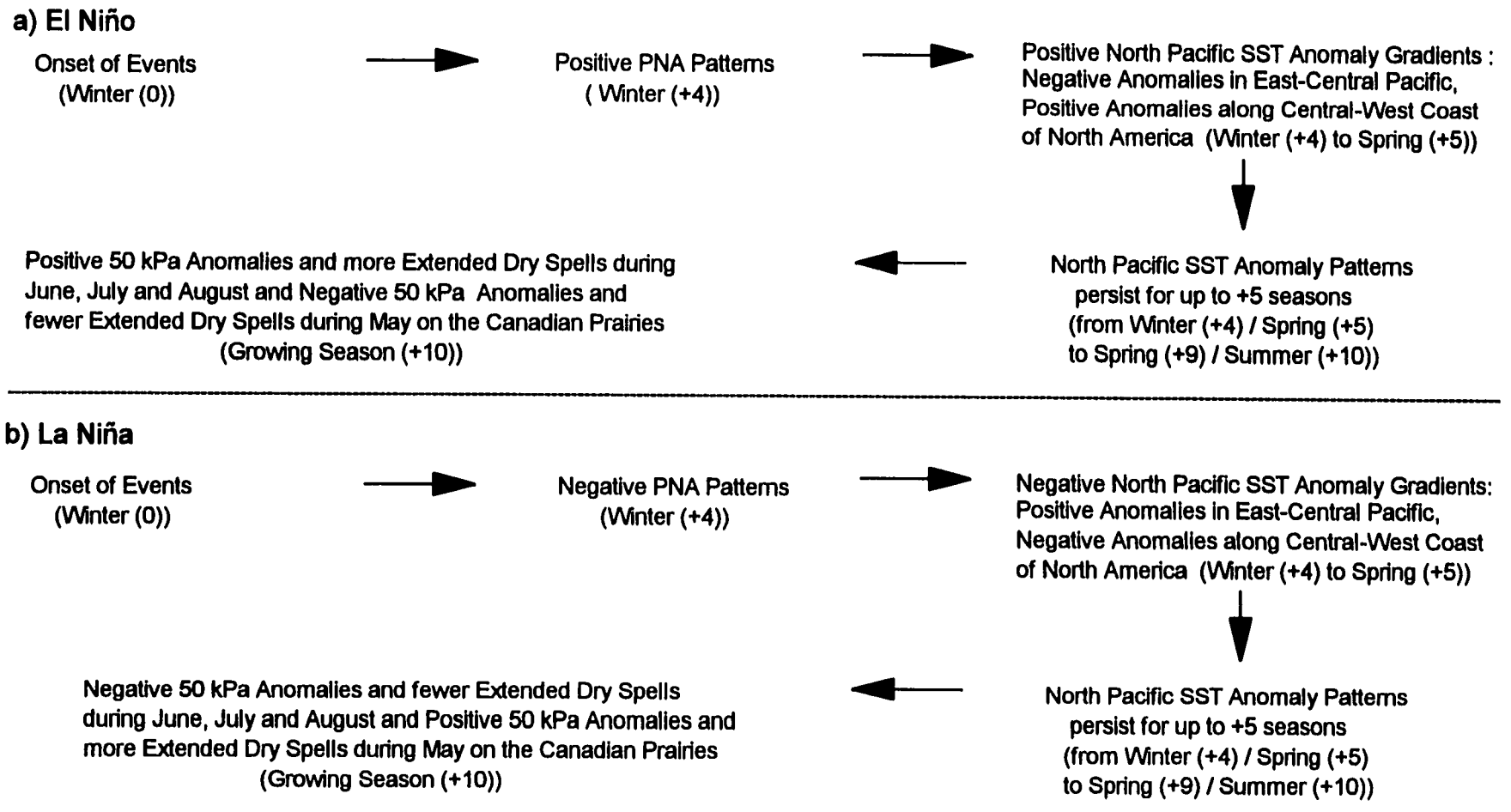

Note: Numbers in brackets refer to the lags (in seasons) with respect to the onset of the ENSO events
Winter refers to December, January, February; Spring to March, April, May; Summer to June, July, August;
Autumn to September, October, November; Growing Season to May, June, July, August

Figure 4.4: Results of the Correlation Analysis Between ENSO Events and Growing Season Precipitation Variations on the Canadian Prairies: a) El Niño and b) La Niña

during May, negative 50 kPa anomalies and fewer extended dry spells occur.

For La Niña events, the results are opposite (i.e. because these events are associated with positive SOI values). In particular, negative PNA patterns develop during the winter following the onset of the events (i.e. winter(+4)) corresponding to the mature stage. North Pacific SST anomaly patterns consisting of anomalously warm water in the east-central North Pacific and anomalously cold water along the central-west coast of North America are observed during the winter and/or spring following the mature stage of La Niña events (i.e. winter(+4) to spring(+5)). These SST anomaly patterns also tend to persist for up to +5 seasons (i.e. from winter(+4)/spring(+5) to spring(+9)/summer(+10)). During growing season(+10), June, July and August are associated with negative 50 kPa anomalies and fewer extended dry spells, while May is associated with positive 50 kPa anomalies and more extended dry spells on the Prairies.

In conclusion, correlation analyses have shown significant correlations between SOI values and variables used to describe the atmosphere - ocean teleconnections over the Pacific Ocean hypothesized in Figure 1.2. The significant correlations suggest relationships between ENSO events and growing-season precipitation variations on the Canadian Prairies through a series of these teleconnections. However, a weakness of the correlation analysis is that all situations (i.e. El Niño events, La Niña events and periods when no ENSO events occur) are included. Even though strongest SOI correlations should be associated with periods when ENSO events are occurring, they can also be influenced

by other periods. This could mask many of the effects, thus explaining why the correlation coefficients (although significant) are not very high. In some instances, it is difficult to determine what the SOI correlations using each season represent (e.g. the spring SOI in Table 4.4 could be representative of periods prior to, or following, the mature stage of ENSO events).

Even though the correlation analysis does indicate association between SOI and growing-season precipitation on the Canadian Prairies for the overall period 1948-1991, it does not provide details of relationships with actual ENSO events (both El Niño and La Niña). For this, further analysis examining actual ENSO events is required. The results of this analysis will be presented in the next chapter.

CHAPTER 5

COMPOSITE ANALYSIS

This chapter describes a composite analysis of teleconnections between ENSO events and growing-season precipitation variations on the Canadian Prairies. This analysis differs from the correlation analysis in that it examines the teleconnections during actual ENSO events as opposed to the entire period of 1948-1991. As was the case with the correlation analysis, the variables include PNA indices, North Pacific SST anomaly gradients and growing-season areally-averaged 50 kPa anomalies, total number of 10-day dry spells and areally-averaged precipitation anomalies over the Prairies. Each variable is composited or averaged for the ten El Niño and the seven La Niña events presented in Table 3.1. The analysis examines the average characteristics and also, determines if there are any significant differences between El Niño and non-El Niño periods, La Niña and non-La Niña periods and El Niño and La Niña events for each of the variables. As outlined in chapter 3, the statistical procedure used to analyze these differences is the two-tailed Student's t test.

5.1 PNA PATTERNS

Composite PNA indices associated with the ten El Niño and the seven La Niña events are presented in Table 5.1. Differences between the events (i.e. El Niño minus La Niña) are also given. The PNA indices are composited for each season from the onset of a typical ENSO event

Table 5.1: Composite PNA Indices Associated with ENSO Events.

SEASON	EL NIÑO	LA NIÑA	DIFFERENCE (EL NIÑO - LA NIÑA)
Winter(0)	-1.17	-0.53	-0.64
Spring(+1)	-0.23	-1.83	+1.60
Summer(+2)	+0.27	-0.53	+0.80
Autumn(+3)	+1.43	-0.87	+2.30**
Winter(+4)	+2.83**	-4.30**	+7.13***
Spring(+5)	-0.37	-0.13	-0.24
Summer(+6)	-0.17	+0.10	-0.27
Autumn(+7)	-0.60	+0.80	-1.40
Winter(+8)	-0.10	-1.70	+1.60
Spring(+9)	-0.70	-0.33	-0.37
Summer(+10)	-0.17	+0.63	-0.80

*** significant at 0.01 level
** significant at 0.05 level
Note: Numbers in brackets refer to lags (in seasons) with respect to the onset of ENSO events.

(i.e. winter(0)) to the end of the third growing season following the onset (i.e. summer(+10)).

Table 5.1 indicates that during El Niño, positive PNA patterns occur during autumn(+3) and strengthen during winter(+4). These patterns then disappear during the following season. This agrees with the correlation analysis which suggested positive PNA patterns occur during the winter following the onset of El Niño. The composite PNA index for winter(+4) is significant. Therefore, the ten winter(+4) PNA indices associated with El Niño events are significantly different from all other winter PNA indices during the study period. This suggests that positive PNA patterns fully develop during winter(+4) (i.e. near the mature stage of typical El Niño events).

For La Niña, a very strong negative composite PNA index occurs

during winter(+4). This value is also significant (i.e. the seven winter(+4) PNA indices associated with La Niña events are significantly different from all other winter PNA indices during the study period). This result also supports the correlation analysis. The differences in composite PNA indices between El Niño and La Niña for autumn(+3) and especially for winter(+4), are also significant. Therefore, the ten autumn(+3) PNA indices associated with El Niño are significantly different from the seven autumn(+3) PNA indices associated with La Niña. The same holds true for winter(+4).

To visualize the composite PNA patterns, winter(+4) composite 50 kPa anomaly maps for both El Niño and La Niña are presented in Figure 5.1(a) and (b). Figure 5.1(a) clearly shows a typical positive PNA pattern with negative height anomalies over the northeastern Pacific Ocean, positive anomalies over western Canada and negative anomalies over the southeastern United States. Conversely, Figure 5.1(b) shows an opposite pattern (i.e. a typical negative PNA pattern). It includes positive height anomalies over the northeastern Pacific Ocean, negative anomalies over western Canada and positive anomalies over the southeastern United States. In fact, this pattern is much stronger than the one associated with El Niño.

The preceding indicates that during El Niño events, positive PNA patterns start to develop during autumn(+3) and fully develop during winter(+4). The winter(+4) pattern is significantly different from those associated with non-El Niño periods. Conversely, during La Niña, strong negative PNA patterns develop during winter(+4). These patterns are also significantly different from non-La Niña periods. Furthermore, the PNA

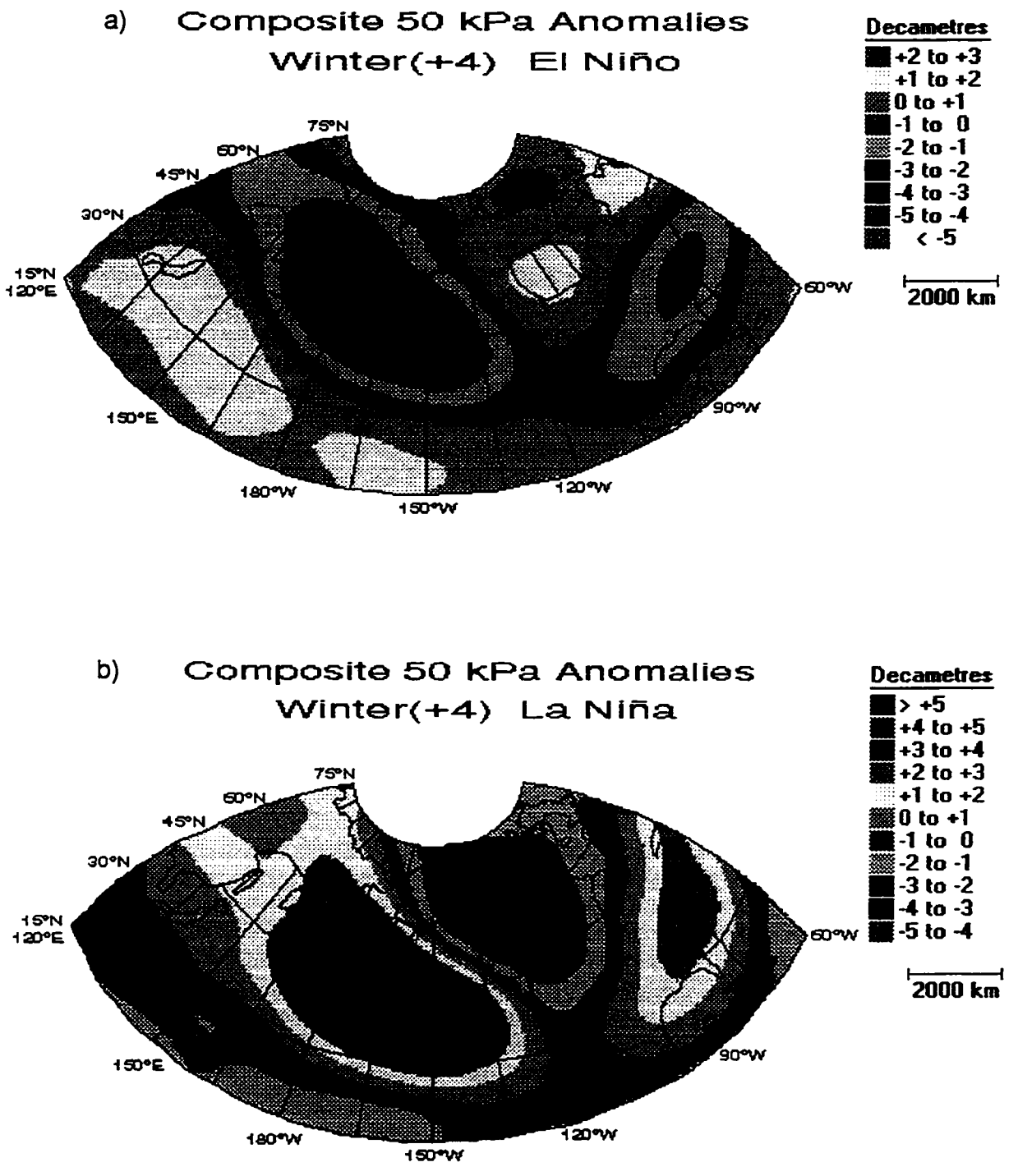

Figure 5.1: Northern Hemisphere Composite 50 kPa Anomaly Maps Associated with Winter (+4): a) El Niño and b) La Niña

patterns associated with El Niño are significantly different from those associated with La Niña during autumn(+3) and winter(+4). All of these results support those of the correlation analysis.

5.2 NORTH PACIFIC SST ANOMALY PATTERNS

Composite SST anomaly gradients (in °C) associated with El Niño, La Niña and the difference between the events are given in Table 5.2. The periods are the same as those for the composite PNA analysis (i.e. winter(0) to summer(+10)). With regards to El Niño, there are many positive gradients (i.e. negative SST anomalies in the east-central North Pacific and positive anomalies along the central-west coast of North America). A positive composite gradient occurs during autumn(+3), weakens during winter(+4), and weakens further during spring(+5) and summer(+6). However, the gradients remain positive. During autumn(+7), the positive gradient strengthens, and this stronger gradient persists through winter(+8), spring(+9) and summer(+10) (i.e. four seasons). Therefore, on average, positive SST anomaly gradients occur from autumn(+3) until summer(+10); a total of eight seasons.

Positive SST anomaly gradients first occur during autumn(+3). This is slightly different from the correlation analysis which suggested the positive gradients develop during winter(+4) or spring(+5). However, the composite analysis did suggest that positive SST anomaly gradients occur during the same periods as when positive PNA patterns start to develop (i.e. autumn(+3)) (see Table 5.1). There is also a long persistence of positive gradients (eight seasons for positive and four seasons for stronger positive). This long persistence was also evident in the

Table 5.2: Composite North Pacific SST Anomaly Gradients (°C) Associated with ENSO Events.

SEASON	EL NIÑO	LA NIÑA	DIFFERENCE (EL NIÑO - LA NIÑA)
Winter(0)	+0.40	+0.10	+0.30
Spring(+1)	0.00	-0.10	+0.10
Summer(+2)	-0.20	-0.30	+0.10
Autumn(+3)	+0.80	-0.10	+0.90
Winter(+4)	+0.40	0.00	+0.40
Spring(+5)	+0.10	-0.90***	+1.00**
Summer(+6)	+0.20	+0.20	0.00
Autumn(+7)	+0.50	-0.10	+0.60
Winter(+8)	+0.60	-0.40	+1.00
Spring(+9)	+0.60	-0.10	+0.70
Summer(+10)	+0.40	+0.30	+0.10

*** significant at 0.01 level
** significant at 0.05 level
Note: Numbers in brackets refer to lags (in seasons) with respect to the onset of ENSO events.

correlation analysis.

Table 5.2 shows no significant composite SST anomaly gradients associated with El Niño (i.e. there are no significant differences between any of the seasonal SST anomaly gradients associated with the ten El Niño events and all other seasonal SST anomaly gradients during the study period). This is likely because these SST anomaly patterns also occur in the absence of El Niño events (i.e. they can be forced by other factors) (Davis, 1976; Namias and Cayan, 1981; Namias et al., 1988).

A question that arises is why do strong positive SST anomaly gradients appear during autumn(+3), weaken during winter(+4), spring(+5) and summer(+6), and then strengthen during autumn(+7). To aid in determining this, seasonal composite North Pacific SST anomaly maps

associated with El Niño events for the eight seasons where positive SST anomaly gradients persist (i.e. autumn(+3) to summer(+10)) are presented (Figure 5.2(a) through (h)). Figure 5.2(a) shows the positive composite gradient occurring during autumn(+3). This gradient includes negative SST anomalies in the east-central North Pacific Ocean and positive anomalies along the central-west coast of North America. During winter(+4), the gradient weakens because the positive SST anomalies begin to disappear. Even though the negative anomalies are weaker and cover a smaller area, they continue to persist. Spring(+5) and summer(+6) show an even weaker SST anomaly gradient due to the positive SST anomalies completely disappearing. The negative anomalies expand to cover a larger area.

It also appears that during spring(+5), a pool of positive SST anomalies starts to detach from the large area of anomalously warm water in the tropical Pacific (which is associated with El Niño). This pool is located at approximately 30°N to 35°N, 120°W. It then appears to move up the west coast of North America during summer(+6) (see Figure 5.2(d) at approximately 40°N, 125°W). By autumn(+7), this pool appears to move even further up the coast (approximately 45°N, 130°W), thus leading to the stronger positive composite SST anomaly gradient observed during this period. The stronger positive gradient persists from autumn(+7) until summer(+10) (Figure 5.2(e) through (h)). During summer(+10), the negative SST anomalies in the east-central North Pacific begin to disappear. By autumn(+11) (not shown), these negative SST anomalies completely disappear and as a result, the positive gradient also disappears.

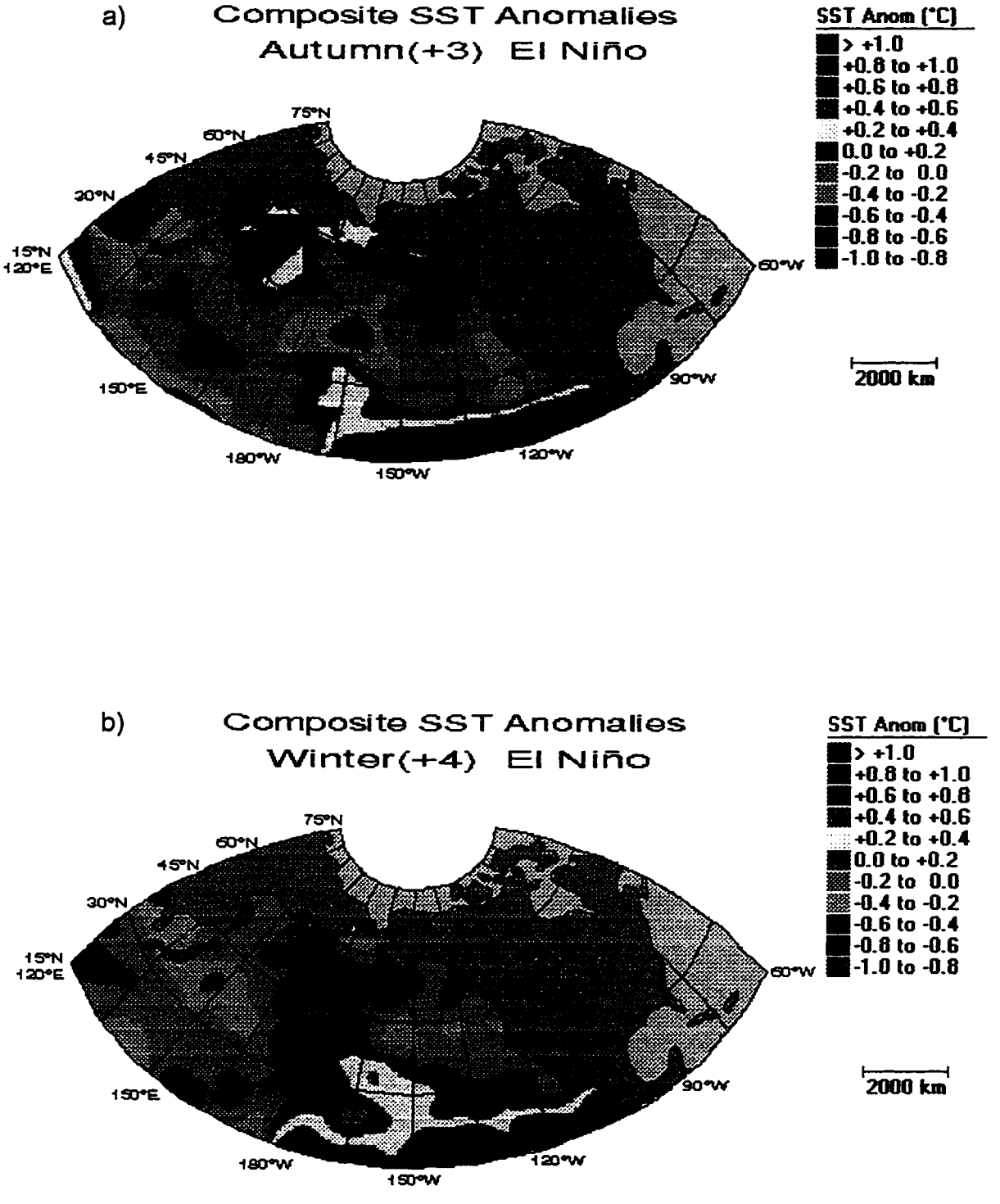

Figure 5.2: North Pacific Composite SST Anomaly Maps Associated with El Niño: a) Autumn(+3) and b) Winter(+4)

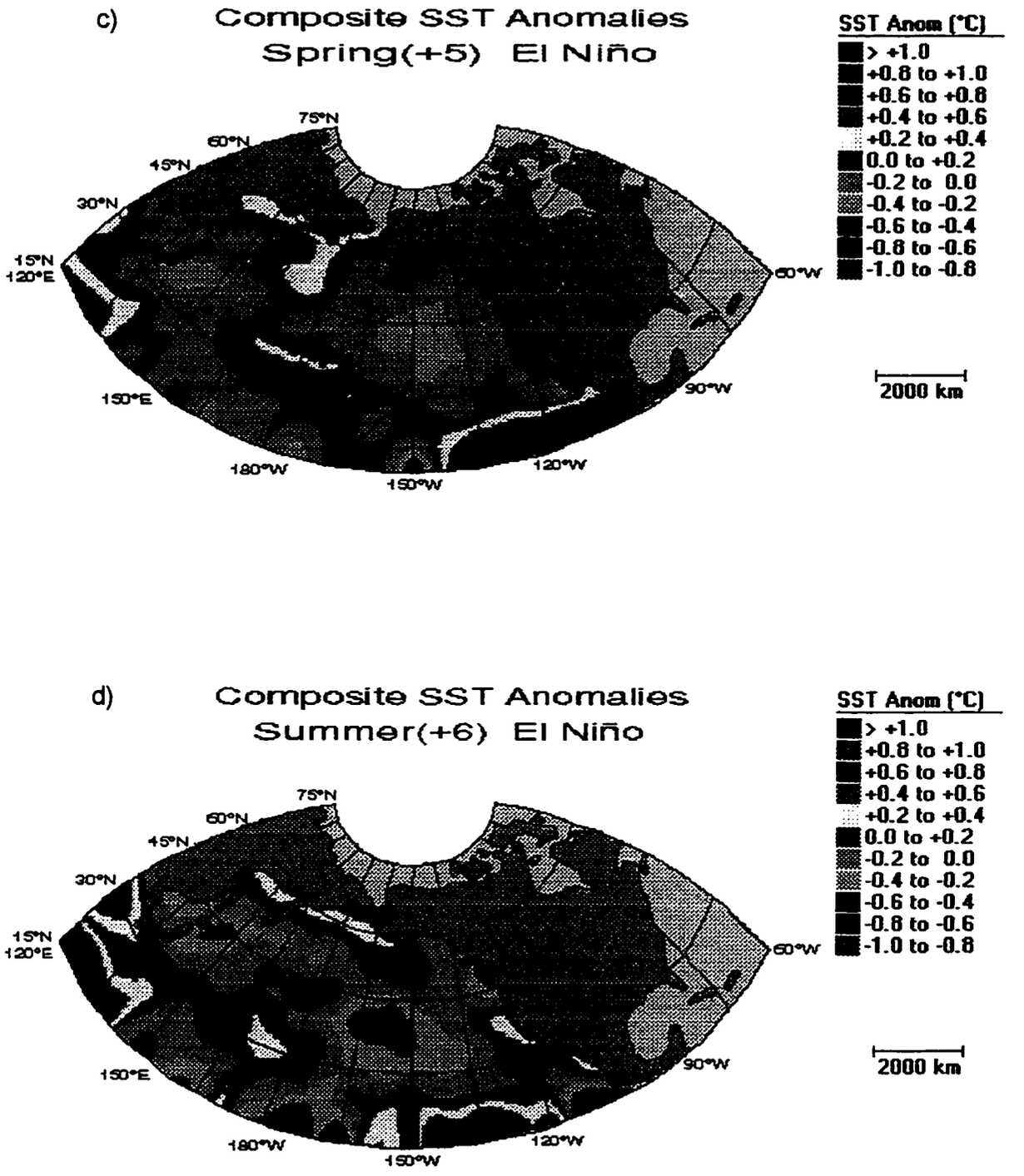

Figure 5.2: Continued: c) Spring(+5) and d) Summer(+6)

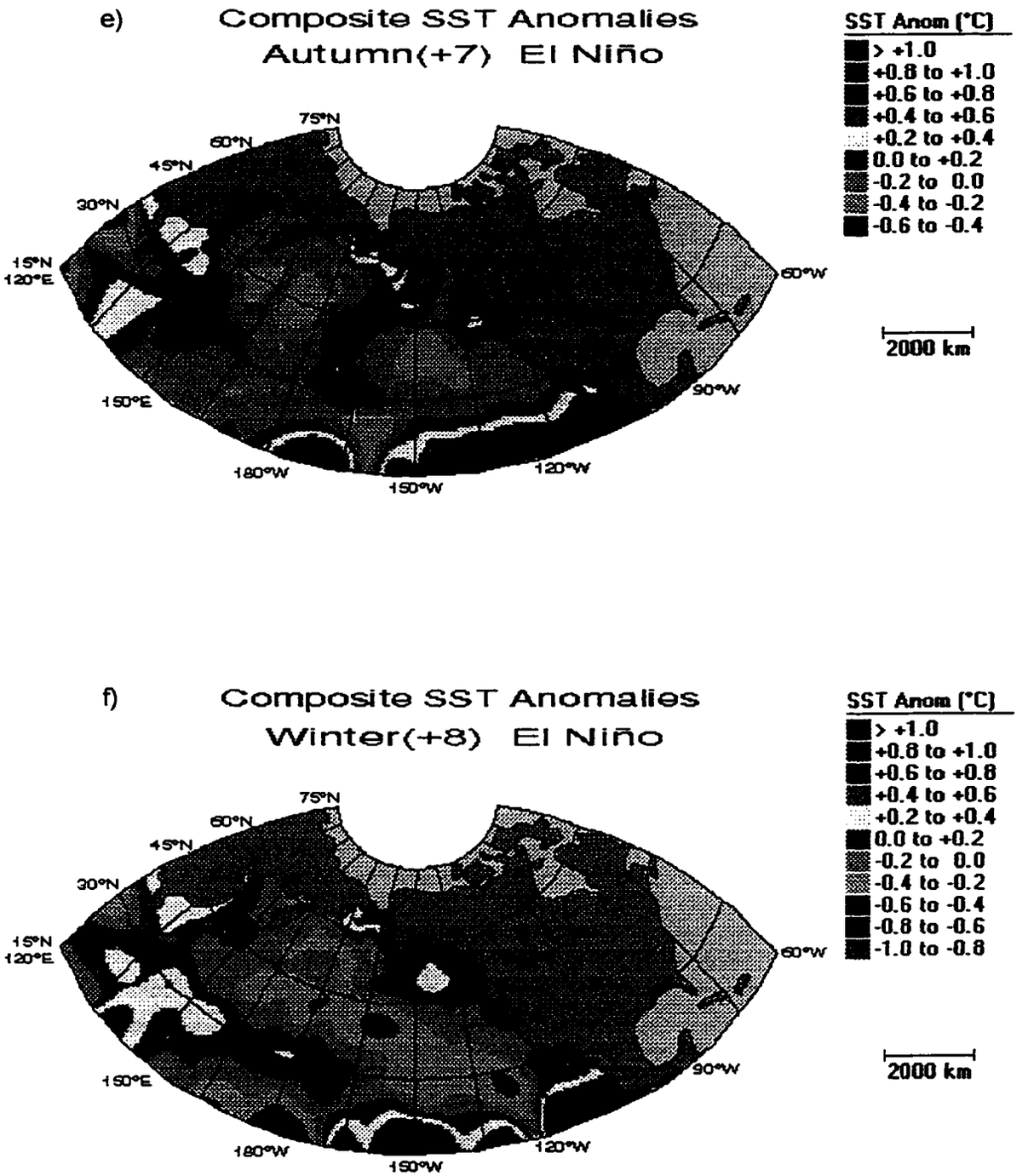

Figure 5.2: Continued: e) Autumn(+7) and f) Winter(+8)

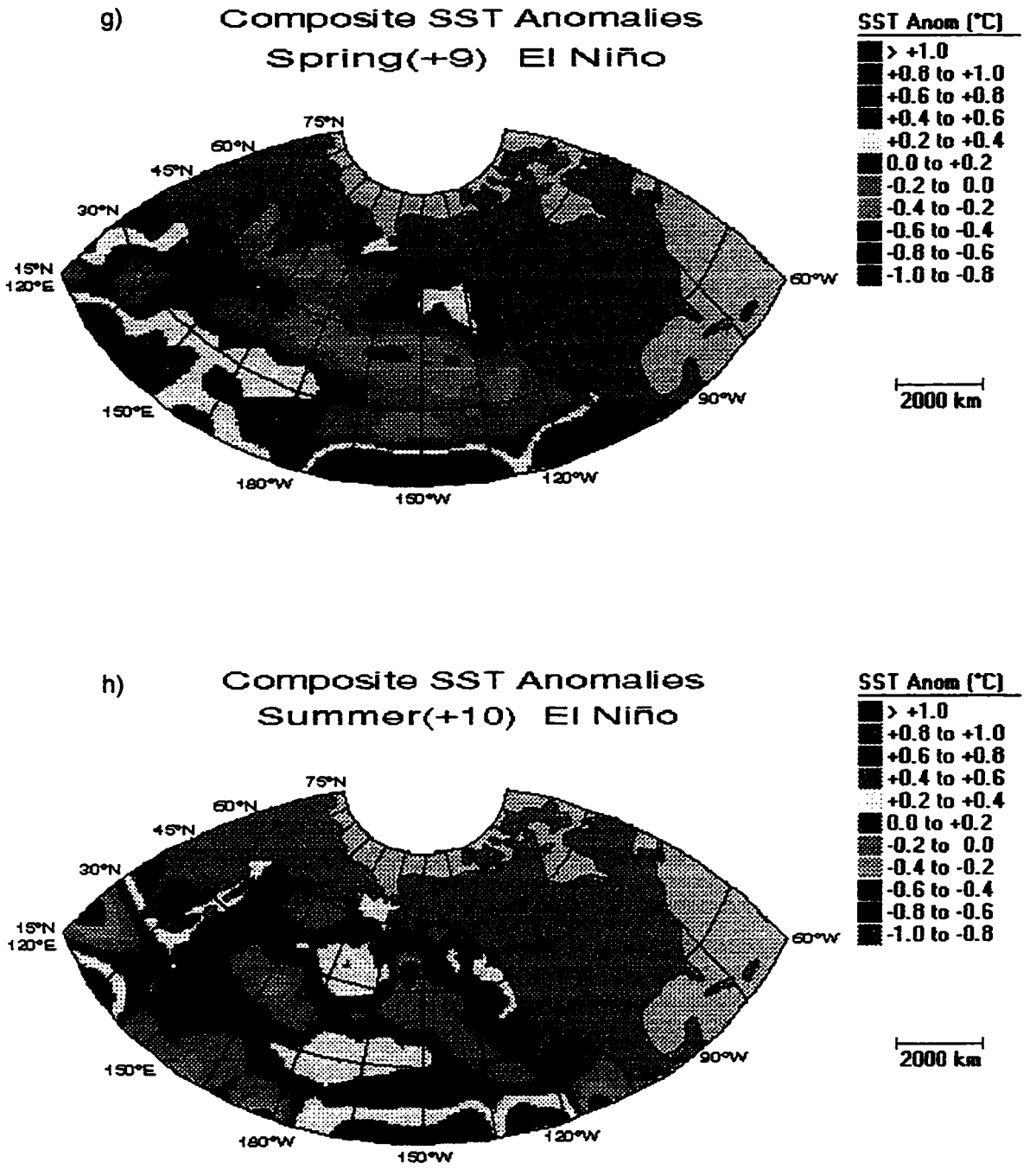

Figure 5.2: Continued: g) Spring(+9) and h) Summer(+10)

From the preceding analysis, it is suggested that the positive SST anomaly gradients that occur during autumn(+3), are initially induced by the circulation associated with the positive PNA patterns (which also begin to develop during autumn(+3)) (see Table 5.1). As outlined in chapter 2, positive PNA patterns are associated with an intensification and a southeastward displacement of the Aleutian low (Simpson, 1983; Wagner, 1984; Emery and Hamilton, 1985; Mysak, 1986; Alexander, 1990, 1992). The resultant increased north to northwest flow behind the low, brings colder air and stronger winds to the central North Pacific Ocean causing more heat transfer from the ocean to the atmosphere and thus, anomalously low SSTs in this region. The opposite condition occurs in front of the low (i.e. an increased south to southwesterly flow, brings warmer winds to the central-west coast of North America causing less heat transfer from the ocean to the atmosphere and thus, anomalously high SSTs in this region) (Simpson, 1983; Wagner, 1984; Emery and Hamilton, 1985; Mysak, 1986; Alexander, 1990,1992; Yonping and McBean, 1991).

The anomalously warm water weakens during winter(+4) and disappears during spring(+5). However, the anomalously cold water persists. As a result, the positive SST anomaly gradient weakens. During spring(+5), summer(+6) and autumn(+7), a pool of anomalously warm water appears to detach from the large area of positive SST anomalies in the tropical Pacific and moves up the west coast of North America. As mentioned in chapter 2, studies have suggested that during El Niño events, anomalously warm water can propagate northward up the west coast of North America via Kelvin waves. These waves are confined to a narrow

region near the coast and can play a significant role in developing high SST anomalies off the west coast of North America (McCreary, 1976; Enfield and Allen, 1980; Clarke, 1983; Emery and Hamilton, 1985; Alexander, 1990,1992; Johnson and O'Brien, 1990). By autumn(+7), the anomalously warm water moves up to the central-west coast of North America thus leading to stronger positive SST anomaly gradients. These stronger gradients persist from autumn(+7) to summer(+10).

For composite La Niña events, Table 5.2 does not show a persistence of negative SST anomaly gradients as hypothesized in chapter 1 and suggested by the correlation analysis. However, during spring(+5), there is a strong significant negative gradient which indicates the spring(+5) SST anomaly gradients associated with the seven La Niña events, are significantly different from all other spring SST anomaly gradients during the entire study period. Figure 5.3 presents the composite North Pacific SST anomaly map associated with La Niña for spring(+5). The map shows a typical negative SST anomaly gradient consisting of a large area of positive SST anomalies in the east-central North Pacific and negative SST anomalies along the central-west coast of North America. This finding is similar to the correlation analysis which suggested negative SST anomaly gradients occur during winter(+4) to spring(+5). Even though they do not persist, there is a higher frequency of negative gradients (i.e. more negative than positive) from spring(+5) to summer(+10) (see Table 5.2). As a result, the SST anomaly gradients associated with La Niña, are different from those associated with El Niño (i.e. they are not persistently positive).

From these results, it is suggested the strong negative PNA

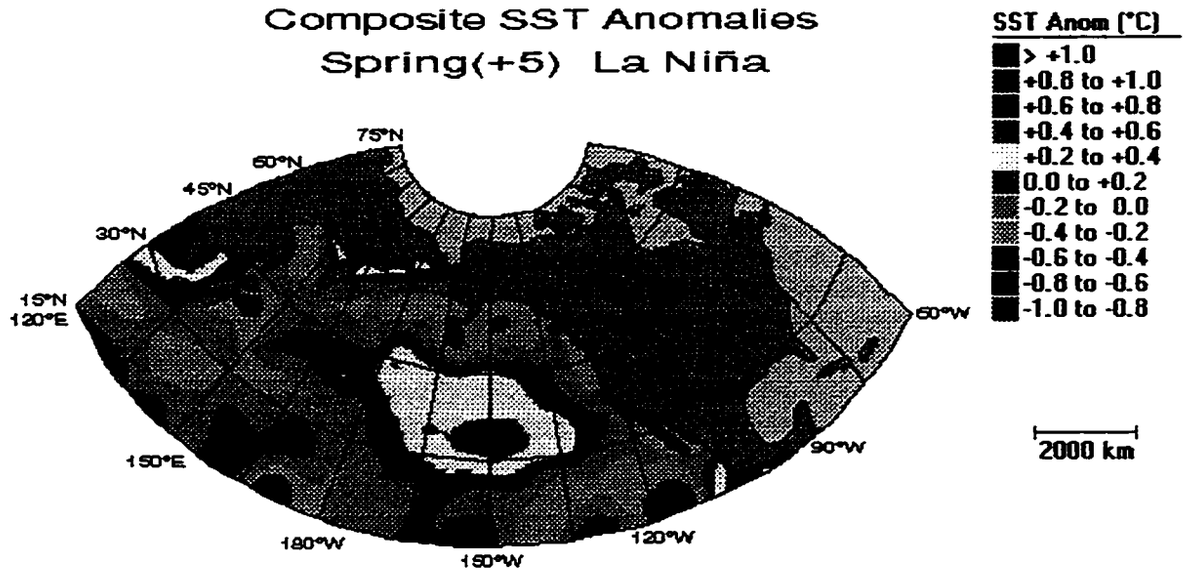

Figure 5.3: North Pacific Composite SST Anomaly Map Associated with La Niña: Spring(+5)

patterns which occur during winter(+4) (see Table 5.1 and Figure 5.1(b)) aid in the development of strong negative SST anomaly gradients during spring(+5). Negative PNA patterns are associated with a weaker Aleutian low (Weare et al., 1976; Pan and Oort, 1983,1990; Emery and Hamilton, 1985). As a result, there is a lower frequency of north to northwesterly flow behind the low and over the east-central North Pacific. This results in less than normal heat transfer from the ocean to the atmosphere and thus, anomalously warm water in this region. Ahead of the low, there is a weakening of the warmer south to southwesterly flow which normally occurs along the central-west coast of North America. As a result, higher than normal heat transfer from the ocean to the

atmosphere occurs, thus lowering SSTs in this region (Weare et al., 1976; Pan and Oort, 1983,1990; Emery and Hamilton, 1985). This agrees with the results of the correlation analysis which suggested negative SST anomaly gradients occur 0 to +1 seasons after the occurrence of negative PNA patterns (i.e. during winter(+4) to spring(+5)).

The difference between composite SST anomaly gradients associated with El Niño and La Niña (Table 5.2) shows the majority of the values are positive. This indicates that for these periods, North Pacific SST anomaly gradients associated with El Niño tend to be higher (i.e more positive) than those associated with La Niña. The only significant value occurs during spring(+5) signifying the SST anomaly gradients associated with the ten El Niño events are significantly different from those associated with the seven La Niña events. However, this significant difference is likely attributable to the large negative SST anomaly gradient associated with La Niña.

5.3 GROWING-SEASON AREALLY-AVERAGED 50 KPA ANOMALIES OVER THE CANADIAN PRAIRIES

The preceding section has indicated that El Niño events are associated with persistent positive SST anomaly gradients in the North Pacific Ocean. As hypothesized in chapter 1, these persistent gradients should be associated with positive 50 kPa anomalies and drier conditions over the Canadian Prairies during the growing season (Bonsal et al., 1993). Since this persistence occurs prior to growing season(+10), 50 kPa anomalies and precipitation variations are examined during this growing season. Even though there was no indication of persistence of

negative SST anomaly gradients associated with La Niña, growing-season 50 kPa anomalies and precipitation variations are analyzed to determine if they are different from those associated with El Niño.

Table 5.3 presents the monthly composite growing-season areally-averaged 50 kPa anomalies (in decametres) over the Canadian Prairies associated with ENSO events during growing season(+10). For El Niño, a negative composite value occurs during May and smaller positive values during June, July and August. The signs of the values suggest that once again, May is different from the rest of the growing season (which agrees with the correlation analysis). There is also an indication that June, July and August are associated with slightly positive 50 kPa anomalies and May, with slightly negative anomalies.

However, none of these anomalies is significant (i.e. there are no significant differences between the 50 kPa anomalies associated with El Niño events and those for non-El Niño periods). This could be due to several reasons. Firstly, monthly data are used in the analysis and persistent 50 kPa anomalies may not occur during the entire month. For example, a particular month may have strong positive 50 kPa anomalies for the first two weeks and the rest of the month has average or negative 50 kPa anomalies. As a result, the overall monthly 50 kPa anomaly is lowered. However, the strong positive anomalies during the first two weeks may have initiated an extended dry spell on the Prairies. Secondly, for any month, persistent 50 kPa anomalies may not cover the very large Prairie study area. Since the data are areally-averaged, the overall 50 kPa anomaly value could be affected. Finally, there are several factors other than ENSO events that affect upper-

Table 5.3: Composite Growing-Season Areally-Averaged 50 kPa Anomalies (dam) over the Canadian Prairies Associated with ENSO Events.

MONTH	EL NIÑO	LA NIÑA	DIFFERENCE (EL NIÑO - LA NIÑA)
May(+10)	-1.85	+0.63	-2.48
June(+10)	+0.43	-0.53	+0.96
July(+10)	+0.08	-0.19	+0.27
August(+10)	+0.28	-1.53	+1.81

Note: Numbers in brackets refer to lags (in seasons) with respect to the onset of ENSO events.

atmospheric flow patterns (and thus persistent 50 kPa anomalies) over the Canadian Prairies (e.g. soil moisture anomalies, anomalous snow and ice cover over Northern Canada and the Arctic, etc.) (e.g. Walsh et al., 1982; Oglesby and Erickson, 1989; Ripley, 1991).

For La Niña, the signs of the 50 kPa anomalies are opposite to those for El Niño. This includes slightly positive 50 kPa anomalies during May and slightly negative anomalies during June, July and August. These results also agree with those of the correlation analysis. However, once again none of the values is significant (perhaps due to the reasons outlined previously). The composite difference between El Niño and La Niña once again, shows that May has an opposite sign from June, July and August.

5.4 GROWING-SEASON PRECIPITATION VARIATIONS ON THE CANADIAN PRAIRIES

Two variables identify growing-season precipitation variations on the Prairies (i.e. total number of 10-day dry spells and areally-averaged precipitation anomalies). Table 5.4 presents the composite

Table 5.4: Composite Growing-Season Total Number of 10-Day Dry Spells on the Canadian Prairies Associated with ENSO Events (expressed as percentage of average).

MONTH	EL NIÑO	LA NIÑA	DIFFERENCE (EL NIÑO - LA NIÑA)
Total(+10)	112.4	66.9***	+45.5**
May(+10)	69.2**	73.7	-4.5
June(+10)	136.2**	67.2**	+69.0**
July(+10)	141.0**	63.0***	+78.0***
August(+10)	126.3	57.1**	+69.2**

*** significant at 0.01 level
** significant at 0.05 level
Note: Numbers in brackets refer to lags (in seasons) with respect to the onset of ENSO events.

total number of 10-day dry spells associated with ENSO events for growing season(+10). The composite values are expressed as a percentage of the 44-year average. Therefore, if a value for a particular month is greater than 100%, it experienced a greater than normal total number of 10-day dry spells and vice versa. A total growing-season value is also computed.

Table 5.4 shows many significant results for El Niño, La Niña and differences between the events. For El Niño, both June and July have significantly more 10-day dry spells (136.2% and 141.0% respectively). This indicates the number of 10-day dry spells during June(+10) associated with the ten El Niño events is significantly different from all other June 10-day dry spells for the entire study period. The same holds true for July. The results also show August and the total growing season with more 10-day dry spells (126.3% and 112.4% respectively), however, they are not significant. Conversely, May shows significantly

fewer 10-day dry spells (69.2%). These results agree with those of the correlation analysis which suggested June, July and August are associated with more extended dry spells and May, with fewer extended dry spells.

For La Niña, June, July, August and the total growing season show significantly fewer 10-day dry spells (67.2%, 63.0%, 57.1% and 66.9% respectively). This signifies that for these periods, the total number of 10-day dry spells associated with the seven La Niña events is significantly different from those for the entire study period. However, unlike El Niño, May is not different from the rest of the growing season. In fact, it also shows fewer 10-day dry spells (73.7%). This does not correspond to the correlation analysis which suggested the May(+10)s associated with La Niña events should have more 10-day dry spells. The reasons for this are not entirely clear. However, June, July and August do agree with the correlation analysis of 10-day dry spells. The significantly fewer dry spells not only represent wetter than normal conditions on the Prairies, but are also representative of non-drought conditions.

The preceding has shown significantly fewer 10-day dry spells during most of growing season(+10) associated with La Niña. However, these fewer dry spells are not associated with persistent negative North Pacific SST anomaly gradients (as hypothesized in chapter 1). A possible reason is that as outlined previously, there is a higher frequency of negative SST anomaly gradients from spring(+5) to summer(+10). In other words, La Niña events are associated with SST anomaly gradients that are different from El Niño (i.e. they are not persistently positive). These

differences may explain the opposite responses in terms of growing-season extended dry spells on the Prairies. This will be discussed further in chapters 6 and 7.

The difference between composite El Niño and La Niña shows significant positive values for June, July, August and the total growing season. The positive values indicate there are significantly more 10-day dry spells associated with the ten El Niño events as opposed to the seven La Niña events. The value for May is very small indicating virtually no difference between El Niño and La Niña. This also suggests May is different from the rest of the growing season in terms of the number of 10-day dry spells associated with ENSO events.

Therefore, ENSO events are significantly related to growing-season number of extended dry spells, but not significantly related to 50 kPa anomalies over the Prairies. There are, however, indications of slightly positive (negative) 50 kPa anomalies during June, July and August associated with El Niño (La Niña). Conversely, May shows slightly negative (positive) 50 kPa anomalies associated with El Niño (La Niña). A possible reason for this is that the North Pacific SST anomaly gradients may not necessarily cause strong 50 kPa anomalies (as hypothesized in chapter 1), but rather, may act in conjunction with, weaker anomalies to affect the number of extended dry spells on the Prairies. Further analysis and discussion of this topic will be presented in chapters 6 and 7.

With regards to the second precipitation variable, Table 5.5 presents the areally-averaged precipitation anomalies (in millimetres) over the Prairies for growing season(+10) associated with ENSO events.

Table 5.5: Composite Growing-Season Areally-Averaged Precipitation Anomalies (mm) Over the Canadian Prairies Associated with ENSO Events.

MONTH	EL NIÑO	LA NIÑA	DIFFERENCE (EL NIÑO - LA NIÑA)
Total(+10)	-4.20	+13.10	-17.30
May(+10)	+5.00	+3.58	+1.42
June(+10)	+0.52	+3.16	-2.64
July(+10)	-6.69	-0.47	-6.22
August(+10)	-4.70	+8.20	-12.90

Note: Numbers in brackets refer to lags (in seasons) with respect to the onset of ENSO events.

As with the correlation analysis of precipitation anomalies, this analysis also shows no significant results. The signs of the differences between El Niño and La Niña again suggest May is different from the rest of the growing season.

The fact that there are no significant values in Table 5.5 also suggests that ENSO events are significantly associated with number of extended dry spells as opposed to precipitation anomalies. Since the total number of 10-day dry spells is a temporal representation of precipitation variations, while areally-averaged precipitation anomalies are more representative of total amounts, the composite analysis indicates that ENSO events are associated more with length of dry periods as opposed to actual precipitation amounts. As mentioned in chapter 4, extended dry spells versus precipitation anomalies will be discussed further in chapter 7.

5.5 SUMMARY

Figure 5.4 summarizes the results of the composite analysis between El Niño events and growing-season precipitation variations on the Canadian Prairies. The results indicate that positive PNA patterns start to develop during autumn(+3) and fully develop during winter(+4). This period roughly coincides with the mature stage of El Niño events. During autumn(+3), positive SST anomaly gradients also occur. It is suggested these gradients develop due to the circulation associated with positive PNA patterns (and associated stronger Aleutian low), which also begin to develop during this period. These SST anomaly gradients begin to weaken during winter(+4) because the positive SST anomalies along the central-west coast of North America start to disappear. The gradients weaken even further during spring(+5) and summer(+6), due to the complete disappearance of the positive SST anomalies.

During spring(+5), summer(+6) and autumn(+7), positive SST anomalies appear to move up the west coast of North America. In particular, during spring(+5), the positive SST anomalies are located at approximately 30°N to 35°N, 120°W; during summer(+6), they move up the coast to approximately 40°N, 125°W; and during autumn(+7), they move further up the coast to approximately 45°N, 130°W. It also appears that these positive SST anomalies originate from the large area of anomalously warm water situated in the tropical Pacific Ocean during El Niño events. It is suggested that the positive anomalies move up the coast via sub-surface Kelvin waves. The positive SST anomalies reach the central-west coast of North America by autumn(+7). As a result, the positive gradients strengthen. The stronger gradients persist through

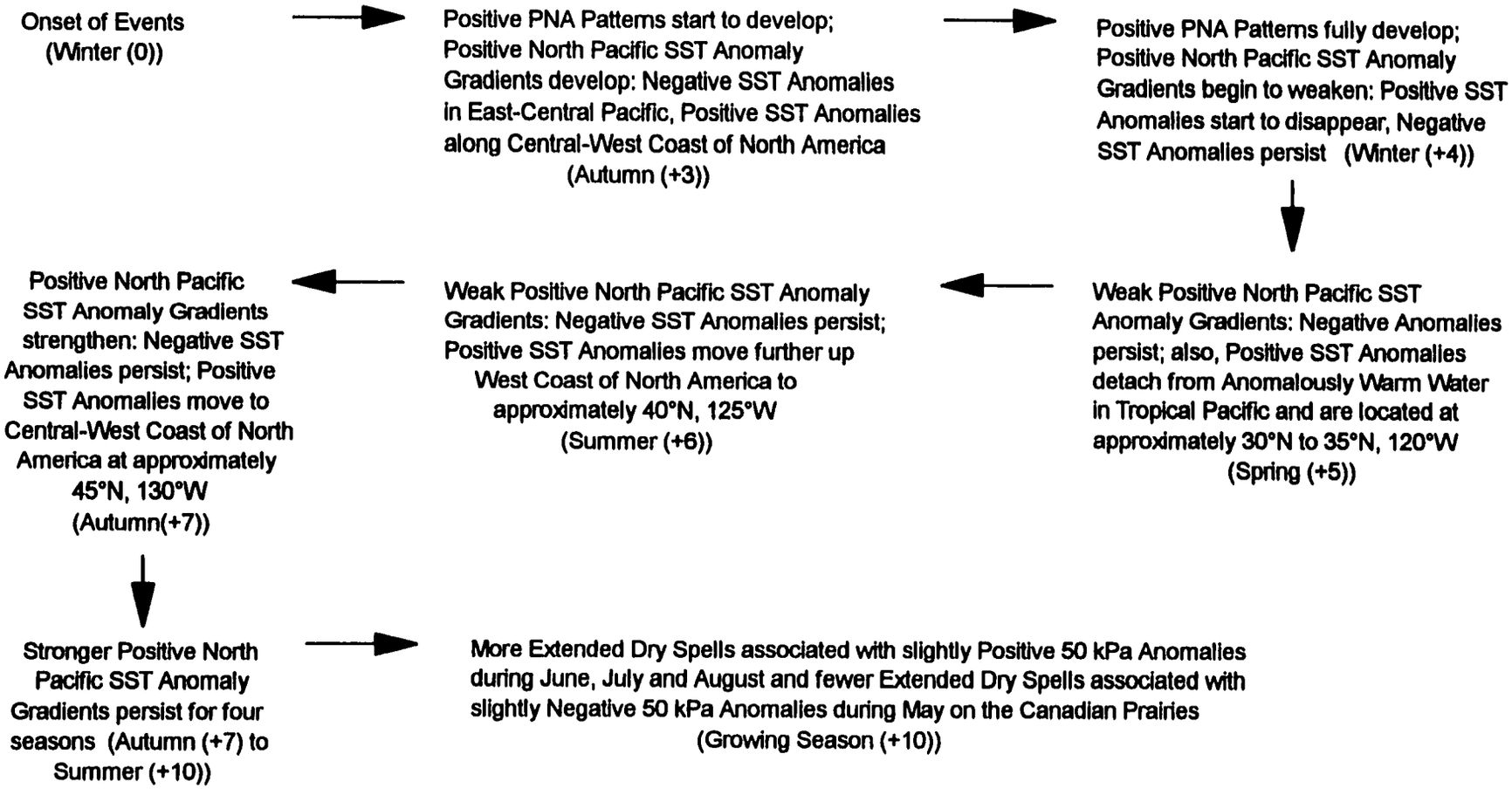

Note: Numbers in brackets refer to the lags (in seasons) with respect to the onset of the El Niño events
Winter refers to December, January, February; Spring to March, April, May; Summer to June, July, August; Autumn to September, October, November; Growing Season to May, June, July, August

Figure 5.4: Results of the Composite Analysis Between El Niño Events and Growing Season Precipitation Variations on the Canadian Prairies

winter(+8), spring(+9) and summer(+10). Therefore, positive SST anomaly gradients persist for a total of eight seasons (i.e. autumn(+3) to summer(+10)) while stronger positive gradients persist for four seasons (i.e. autumn(+7) to summer(+10)).

It is hypothesized that these persistent positive gradients are associated with positive 50 kPa anomalies (suggesting upper-level ridging) and extended dry spells on the Canadian Prairies during growing season(+10). Although June, July and August show only slightly positive 50 kPa anomalies, they are associated with significantly more extended dry spells which could lead to droughts on the Prairies. It is suggested that the persistent positive SST anomaly gradients may not necessarily cause strong positive 50 kPa anomalies, but rather, may act in conjunction with, weaker positive anomalies to produce the greater number of extended dry spells. Conversely, during May, there are significantly fewer extended dry spells associated with slightly negative 50 kPa anomalies.

Figure 5.5 summarizes the results of the composite analysis between La Niña events and growing-season precipitation variations on the Canadian Prairies. For the most part, these results tend to be opposite from those associated with El Niño. In fact, most of the variables show significant differences between El Niño and La Niña. For La Niña events, strong negative PNA patterns develop during winter(+4), which roughly corresponds to the mature stage of the events. It is suggested the circulation associated with the negative PNA patterns (and in particular the weakened Aleutian low) aids in the development of strong negative SST anomaly gradients that are observed during

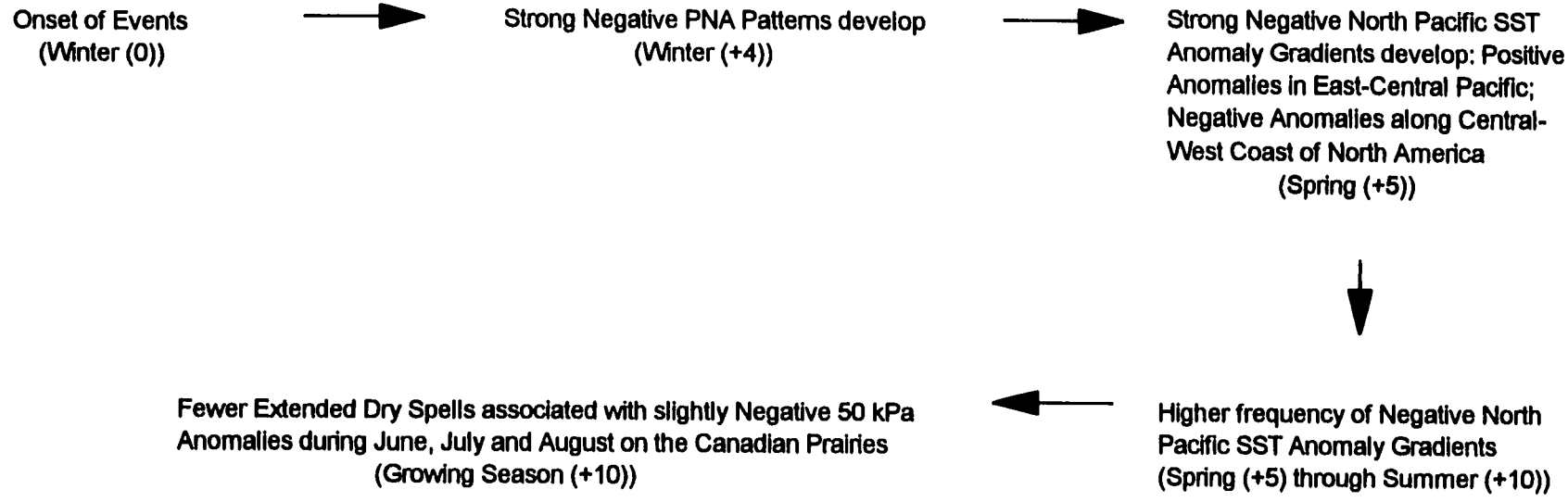

Note: Numbers in brackets refer to the lags (in seasons) with respect to the onset of the La Niña events
Winter refers to December, January, February; Spring to March, April, May; Summer to June, July, August; Autumn to September, October, November; Growing Season to May, June, July, August

Figure 5.5: Results of the Composite Analysis Between La Niña Events and Growing Season Precipitation Variations on the Canadian Prairies

spring(+5). These negative gradients represent SST anomaly patterns opposite to those associated with El Niño (i.e. positive anomalies in the east-central North Pacific and negative anomalies along the central-west coast of North America). The negative SST anomaly gradients do not persist. However, there is a higher frequency of negative gradients from spring(+5) to summer(+10).

It is hypothesized that the higher frequency is associated with negative 50 kPa anomalies (suggesting upper-level troughing) and wetter conditions on the Prairies during growing season(+10). Although June, July and August show only slightly negative 50 kPa anomalies, they are associated with significantly fewer extended dry spells. It is once again suggested that the higher frequency of negative SST anomaly gradients may not necessarily cause strong negative 50 kPa anomalies, but rather, may act in conjunction with, weaker negative anomalies to produce fewer extended dry spells. May shows slightly positive 50 kPa anomalies but fewer extended dry spells. Once again, May tends to show a different response from the rest of the growing season. As indicated previously, May versus the rest of the growing season will be discussed in chapter 7.

CHAPTER 6

MODELLING AND CASE STUDIES

This chapter focuses on the statistical modelling of teleconnections between ENSO events and growing-season precipitation variations on the Canadian Prairies. It consists of three main sections. The first describes the development of conceptual models for El Niño and La Niña events which summarize the results of the correlation and composite analyses. Possible physical explanations of these results are also proposed. The second deals with testing these models by examining the strength and consistency of the results suggested by them. The strength and consistency are determined by analyzing the ten El Niño and seven La Niña events occurring between 1948 and 1991. The chapter concludes with two case studies (for El Niño and La Niña) which are examples where the conceptual models worked well.

6.1 CONCEPTUAL MODELS

The results of the correlation (Figure 4.4) and composite analyses (Figures 5.4 and 5.5) suggested relationships between ENSO events and growing-season precipitation on the Canadian Prairies through a series of atmosphere - ocean teleconnections over the Pacific Ocean. Even though minor differences existed between these analyses (e.g. lags, strength of relationships, characteristics of the persistence of North Pacific SST anomaly patterns), both showed similar results. From these results, conceptual models for El Niño and La Niña events are

formulated. The purpose is to visually present and also suggest possible physical explanations of the typical relationships. These models could also help form the basis of a long-range forecasting technique of growing-season precipitation variations on the Canadian Prairies as they relate to ENSO events.

6.1.1 EL NIÑO EVENTS

Figure 6.1 displays the conceptual model showing the typical atmosphere - ocean teleconnections associated with El Niño events. The model suggests that El Niño are related to growing-season precipitation variations on the Canadian Prairies through a series of six stages. Stage one involves the development of a positive PNA pattern during the autumn to winter following the onset of an El Niño (i.e. autumn(+3) to winter(+4)). This period also corresponds to the mature stage of the event. The positive PNA pattern is characterized by negative pressure anomalies over the northeastern Pacific Ocean (i.e. a stronger Aleutian low), positive anomalies over western Canada and negative anomalies over the southeastern United States.

The correlation and composite analyses demonstrated significant associations between El Niño events and positive PNA patterns. The results indicated that positive PNA patterns start to develop during autumn(+3) and fully develop during winter(+4). This finding is similar to numerous other studies (both observational and modelling) that examined relationships between El Niño events and atmospheric circulation patterns over the Northern Hemisphere (Horel and Wallace, 1981; van Loon and Madden, 1981; Keshavamurty, 1982; Simmons, 1982;

Stage 1: Positive PNA Pattern - Autumn(+3) to Winter(+4)

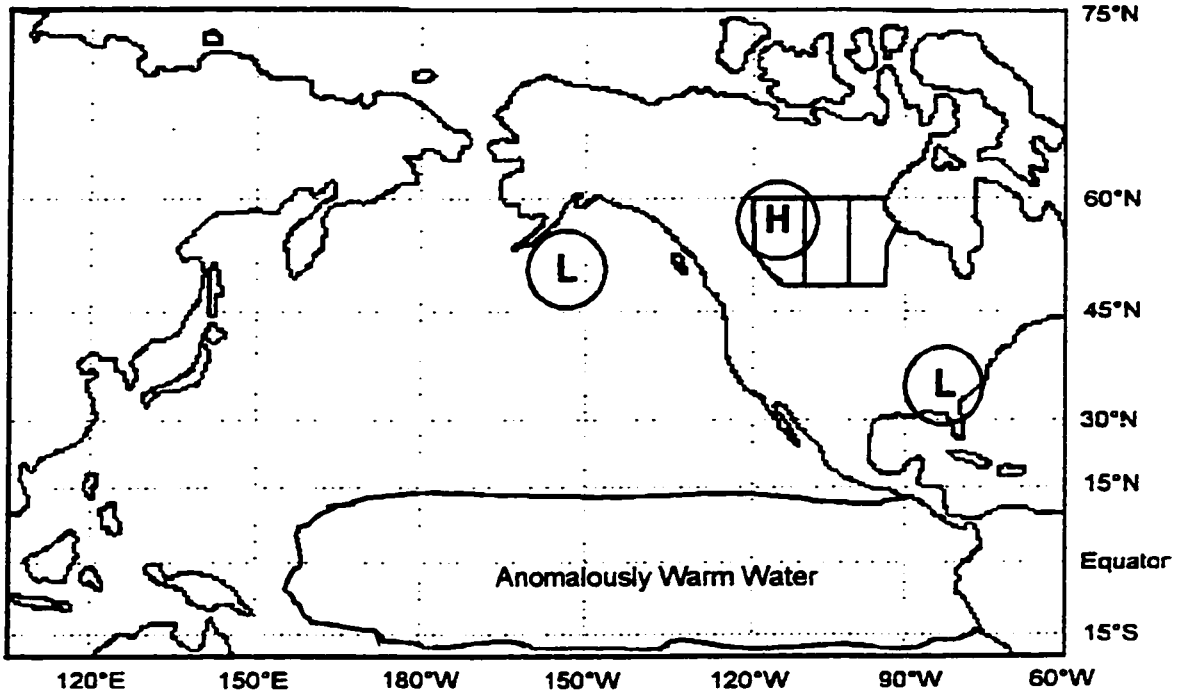

Stage 2: Positive North Pacific SST Anomaly Gradient - Autumn(+3) to Winter(+4)

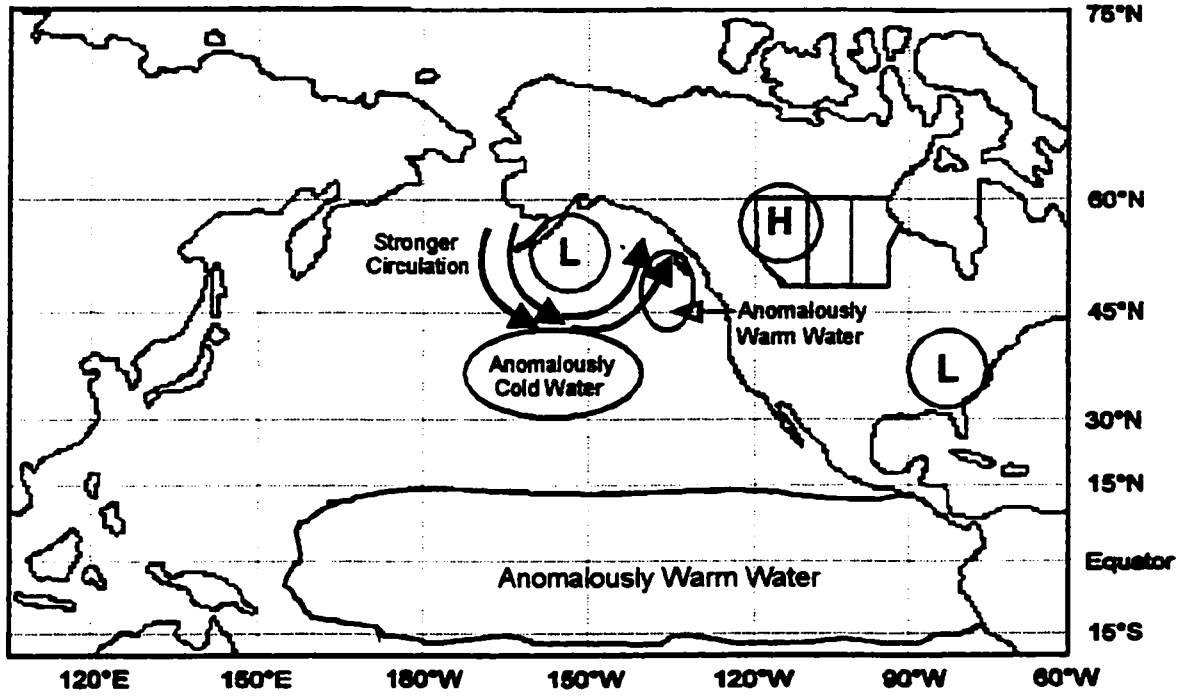

Figure 6.1: Conceptual Model of the Typical Atmosphere - Ocean Teleconnections Associated with El Niño Events

Stage 3: Anomalously Cold Water Remains, Anomalously Warm Water Disappears - Winter(+4) to Spring(+5)

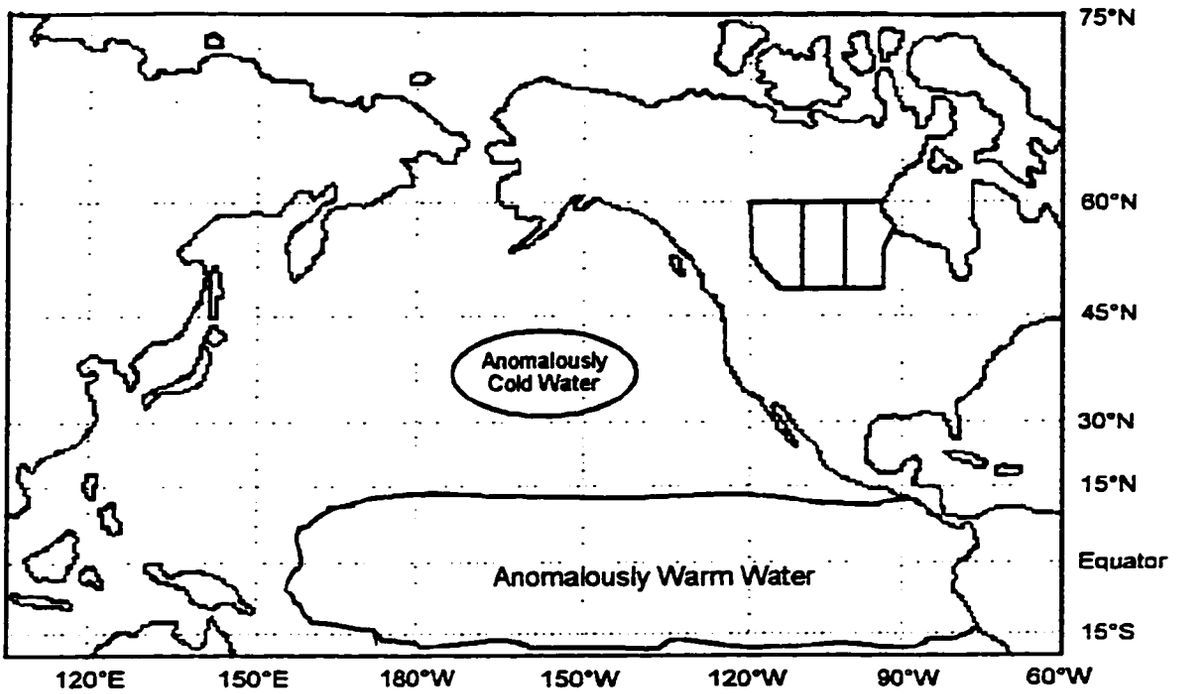

Stage 4: Anomalously Cold Water Remains, Pool of Anomalously Warm Water Moves up West Coast of North America - Spring(+5) to Autumn(+7)

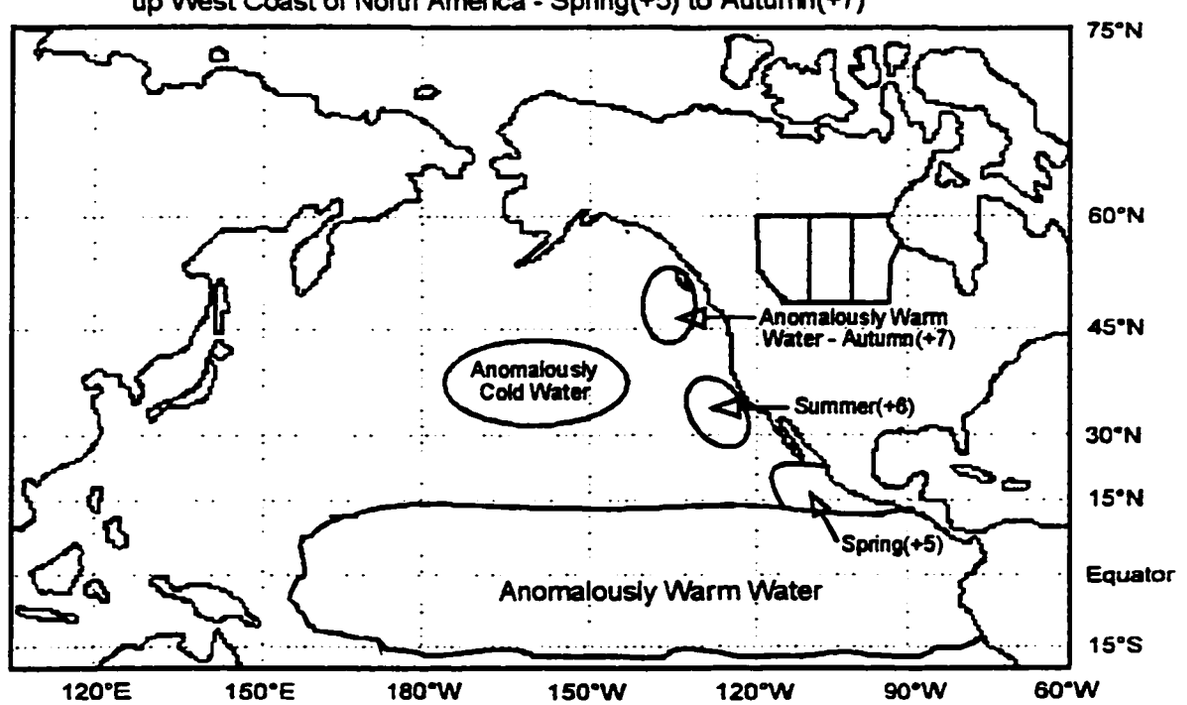

Figure 6.1: Continued

Stage 5: Positive North Pacific SST Anomaly Gradient Persists - Autumn(+7) to Summer(+10)

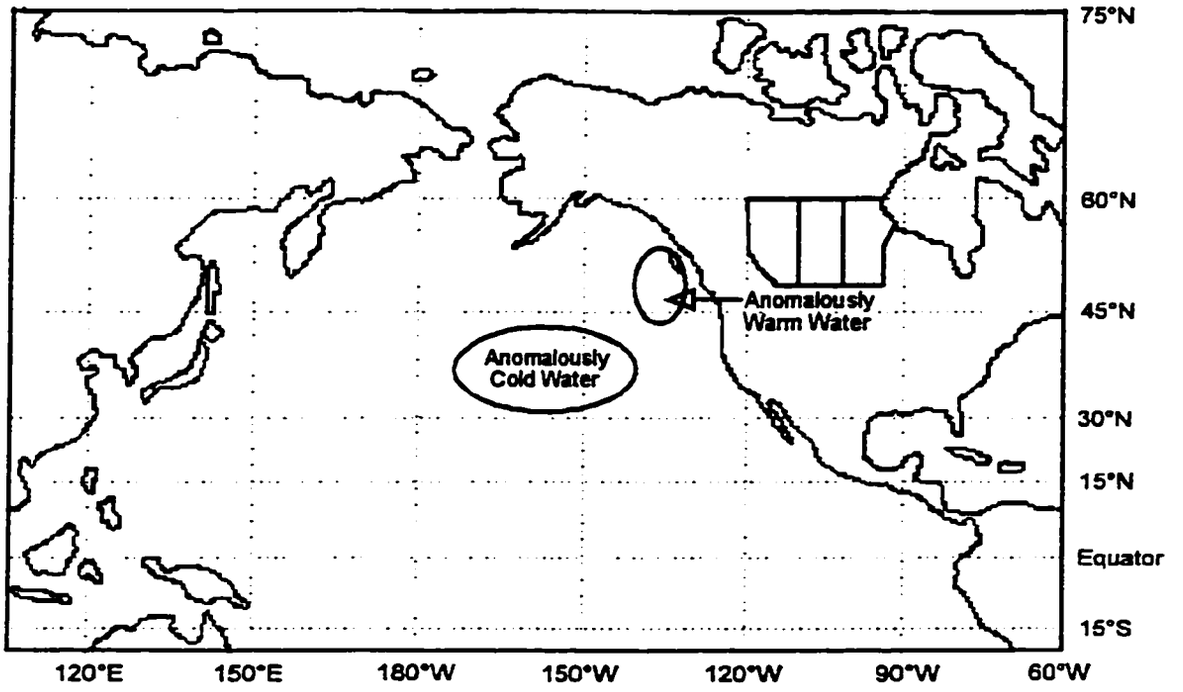

Stage 6: Positive North Pacific SST Anomaly Gradient and Associated Positive 50 kPa Anomalies Leading to Extended Dry Spells on the Canadian Prairies - June(+10), July(+10), August(+10)

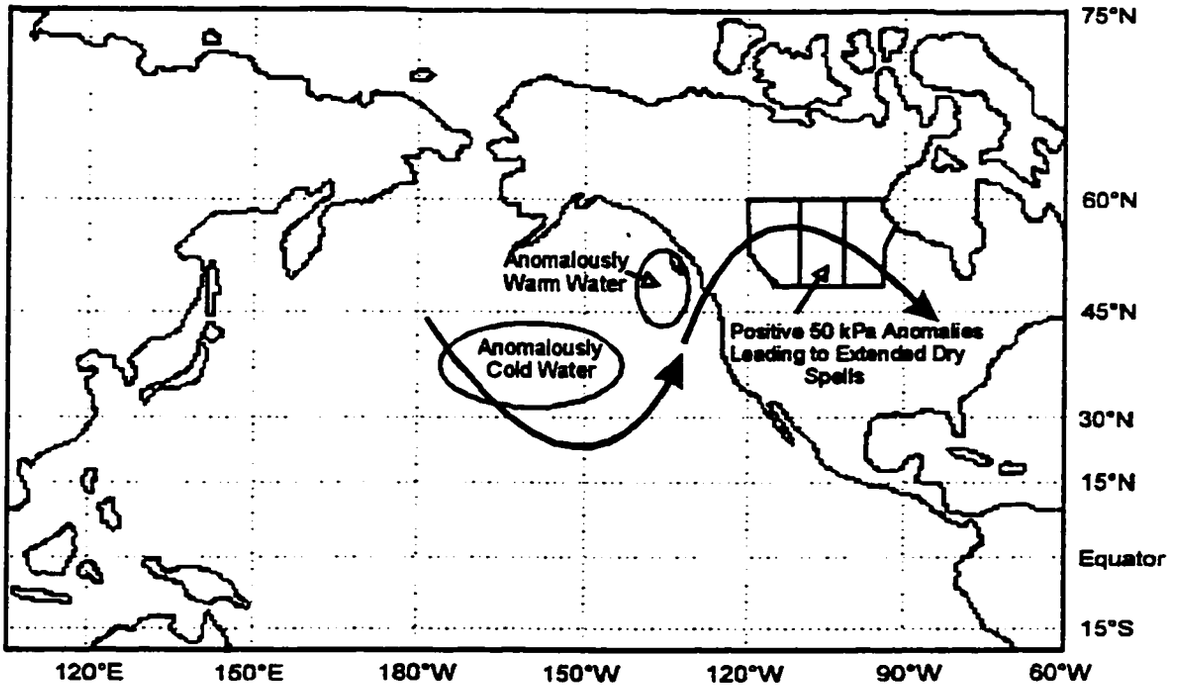

Figure 6.1: Continued

Webster, 1982; Webster and Holton, 1982; Blackmon et al., 1983; Chen, 1983; Lim and Chang, 1983; Shukla and Wallace, 1983; Simmons et al., 1983; Hanna et al., 1984; Lau and Lim, 1984; Yarnal, 1985; Ropelewski and Halpert, 1986; Yarnal and Diaz, 1986; Hamilton, 1988; Pitcher et al., 1988; Weber, 1990).

The physical basis for relationships between El Niño and large-scale atmospheric circulation patterns over the Northern Hemisphere (including positive PNA patterns) includes the premise that the atmospheric heating associated with the large area of anomalously warm water in the tropical Pacific Ocean (associated with El Niño), must be extended by some mechanism vertically to the troposphere and then horizontally to the extratropics (Tribbia, 1991). It is theorized this occurs in the following manner. The anomalously warm water in the tropical Pacific heats surface air which rises, reducing surface pressure and leading to low-level convergence. This enhances precipitation which increases latent heat release (and thus energy) to the atmosphere. At upper levels, the temperature of the rising air eventually reaches equilibrium with its surroundings and it spreads horizontally outward, thus inducing anomalous upper-level divergence (Tribbia, 1991).

Several studies have demonstrated that if the anomalous divergence is embedded in upper-level westerly flow, it can affect the Rossby wave pattern over the Northern Hemisphere (Haurwitz, 1940; Yeh, 1949; Hoskins et al., 1977; Hoskins and Karoly, 1981). Over the North Pacific/North American region, the resultant Rossby wave train resembles a positive PNA pattern. However, if the anomalous divergence is embedded in upper-

level easterly flow, the effects are confined to the tropics (Hoskins et al., 1977). As a result, teleconnections to the Northern Hemisphere can normally only occur during its winter, when upper-level westerlies move equatorward and therefore, over the anomalous heat source in the tropical Pacific (Simmons, 1982; Webster, 1982; Webster and Holton, 1982; Lim and Chang, 1983; Lau and Lim, 1984). Positive PNA patterns are thus observed during periods closely associated with the Northern Hemisphere winter (i.e. autumn(+3) to winter(+4)). This is also when warm SST anomalies in the tropical Pacific normally reach their maximum extent and intensity (i.e. the mature stage of the El Niño events) (Rasmusson and Carpenter, 1982; Philander, 1985,1990).

As outlined previously, positive PNA patterns are associated with a stronger Aleutian low that extends from the surface to the upper troposphere (Horel and Wallace, 1981; Yarnal and Diaz, 1986). The associated surface atmospheric circulation leads to stage two of the model, which includes the development of a positive North Pacific SST anomaly gradient. As shown in Figure 6.1, the stronger Aleutian low is associated with a strengthened surface counterclockwise circulation. The resultant stronger north to northwesterly flow behind the low brings colder air and higher winds to the central North Pacific Ocean causing more heat transfer from the ocean to the atmosphere (including more evaporation) and thus, resulting in anomalously low SSTs in this region. Ahead of the low, a strengthened south to southwesterly flow brings warmer winds to the regions along the central-west coast of North America. These winds cause less heat transfer from the ocean to the atmosphere and thus, anomalously high SSTs in this region (Yongping and

McBean, 1991). Therefore, a positive North Pacific SST anomaly gradient is produced.

Several studies have observed similar SST anomaly patterns associated with a stronger Aleutian low and positive PNA patterns (which are associated with El Niño events). The SST anomaly patterns normally occurred within a season following the development of positive PNA patterns and thus, within a season following the mature stage of El Niño events (Reynolds and Rasmusson, 1983; Pan and Oort, 1983,1990; Simpson, 1983; Wagner, 1984; Emery and Hamilton, 1985; Mysak, 1986; Alexander, 1990,1992; Yongping and McBean, 1991). This coincides with the period of autumn(+3) to winter(+4). The correlation analysis showed significant associations between SOI values and positive North Pacific SST anomaly gradients and positive PNA patterns and these gradients. The composite analysis also showed positive North Pacific SST anomaly gradients occurring during autumn(+3) associated with El Niño.

In stage three, the positive SST anomaly gradient weakens due to the anomalously warm water along the central-west coast of North America disappearing. However, the anomalously cold water in the east-central North Pacific persists. According to the composite analysis, the positive gradient weakens during winter(+4) to spring(+5). The correlation analysis did not indicate this weakening. A possible reason is that this analysis examined the entire period of 1948-1991 and as a result, examined all situations (i.e. El Niño, La Niña and periods when no ENSO events occurred). The composite analysis is likely more accurate since it examined SST anomaly patterns associated with only the ten El Niño events. Therefore, stage three of the model is based mainly on the

results of the composite analysis.

Once produced, mid-latitude SST anomalies tend to persist for long periods (i.e. several months or even, several years) due to the large thermal capacity and slow movement of the ocean (e.g. Davis, 1976; Namias and Cayan, 1981; Namias et al., 1988). This could explain the persistence of negative SST anomalies in the east-central North Pacific. In fact, anomalously cold water in this region is a very common and persistent feature of North Pacific SST anomaly patterns (Davis, 1976; Namias et al., 1988; Alexander, 1990,1992; Yongping and McBean, 1991; Kushnir and Lau, 1992). Reasons for the disappearance of anomalously warm water along the central-west coast of North America are not clear. As shown by both the correlation and composite analyses, positive PNA patterns associated with El Niño disappear following winter(+4). Therefore, the circulation around the Aleutian low weakens. This may aid in the disappearance of these SST anomalies. There may also be other atmospheric and oceanic factors (outside the scope of this study) that aid in the persistence of low SSTs and the disappearance of high SSTs. This topic will be discussed further in chapter 7.

Stage four occurs over the next three seasons (i.e. spring(+5) to autumn(+7)). A pool of anomalously warm water detaches from the large area of positive SST anomalies in the tropical Pacific (associated with El Niño) and moves up the west coast of North America. According to the composite analysis, the warm pool detaches during spring(+5) and by summer(+6), has moved to approximately 40°N, 125°W. By autumn(+7), these SST anomalies are at approximately 45°N, 130°W. During this entire period, the anomalously cold water in the east-central North Pacific

persists. Therefore, a weak positive SST anomaly gradient occurs during spring(+5) and summer(+6). The gradient strengthens during autumn(+7) because anomalously warm water is now located along the central-west coast of North America.

As outlined in chapter 5, it is suggested that the anomalously warm water moves up the west coast of North America via Kelvin waves (e.g. McCreary, 1976; Johnson and O'Brien, 1990). During typical El Niño events, warm water normally located in the western tropical Pacific, begins to flow eastward in the form of sub-surface Kelvin waves. These waves warm surface waters by physically transporting warm water and more importantly, by depressing the thermocline and thus preventing cold upwelling (Wyrtki, 1975; Ramage, 1986; Cane, 1991). Once they reach the South American coast, northward and southward Kelvin waves may be generated. The northward component propagates up the west coast of North America and is confined to a narrow region along the coast. The waves depress the thermocline and thus reduce the normal upwelling of cold water (due to the cold California Current). Therefore, warm water does not physically move up the coast but rather, the normal cold upwelling is suppressed. As a result, higher than normal SSTs are associated with these waves (McCreary, 1976; Enfield and Allen, 1980; Clarke, 1983; Emery and Hamilton, 1985; Johnson and O'Brien, 1990). In fact, the large-scale anomalous warming off the west coast of North America associated with the 1982-83 El Niño was attributed, in part, to northward moving Kelvin waves (Norton et al., 1985).

In stage five, the positive North Pacific SST anomaly gradient persists from autumn(+7) to summer(+10). The correlation and composite

analyses suggested El Niño events are associated with persistent positive gradients. Persistent SST anomaly patterns consisting of negative anomalies in the east-central North Pacific and positive anomalies along the central-west coast of North America have been observed in many studies involving North Pacific SSTs (e.g. Davis, 1976; Namias et al., 1988; Alexander, 1990, 1992; Yongping and McBean, 1991; Bonsal et al., 1993).

Stage six suggests the persistent positive SST anomaly gradient is associated with positive 50 kPa anomalies (i.e. ridging) over the Canadian Prairies during June(+10), July(+10) and August(+10). These two conditions lead to more extended dry spells during these periods. From the composite analysis, there was no clear evidence that the SST anomaly gradients caused strong positive 50 kPa anomalies. However, it did appear that when these SST anomalies occurred in conjunction with slightly positive 50 kPa anomalies, significantly more extended dry spells were observed. Whether the SST anomalies caused these slightly positive 50 kPa anomalies is unclear.

The physical basis for an association between North Pacific SST anomalies and upper-atmospheric circulation patterns is not entirely understood. Several studies have suggested that North Pacific SST anomalies affect mean atmospheric circulation patterns (both locally and downstream) because the SST anomalies imply significant changes in ocean to atmosphere heat exchanges, especially if they persist for long periods (Davis, 1976; Namias and Cayan, 1981; Namias et al., 1988). The effect of these anomalies may be increased if SST anomaly gradients (i.e. adjacent pools of anomalously warm and cold water) are present.

These gradients produce and maintain enhanced baroclinicity (through differential latent and sensible heat fluxes) which can lead to anomalous atmospheric flow patterns both locally and downstream (Harnack, 1979; Harnack and Broccoli, 1979; Dixon and Harnack, 1986).

Many studies have observed significant relationships between North Pacific SST anomaly patterns resembling positive SST anomaly gradients and long-standing Rossby wave patterns consisting of ridging over western, and troughing over eastern North America (Namias, 1969,1972, 1978,1986; Wick, 1973; Harnack, 1979; Harnack and Broccoli, 1979; Dixon and Harnack, 1986). Bonsal et al. (1993) also found a statistically significant relationship between positive North Pacific SST anomaly gradients and positive 50 kPa anomalies and extended dry spells on the Canadian Prairies during the growing season. The longer these positive SST anomaly gradients persisted, the higher the probability of more severe extended dry spells.

A few GCM studies have indicated relationships between mid-latitude SST anomalies and upper-atmospheric flow patterns both locally and downstream. In the mid to upper troposphere (including the 50 kPa level), the atmospheric pressure tended to increase (decrease) over and to the east (up to 20° of longitude) of high (low) SST anomalies (Huang, 1978; Chervin, 1980; Palmer and Sun, 1985; Lau and Nath, 1990). From these results, the upper-atmospheric flow pattern associated with persistent positive North Pacific SST anomaly gradients may be similar to that in stage six of Figure 6.1 (i.e. higher atmospheric pressure or ridging to the east of the high SST anomalies (thus over the Canadian Prairies) and lower atmospheric pressure or troughing to the east of the

low SST anomalies). Further discussion of relationships among positive SST anomaly gradients, upper-atmospheric flow patterns and extended dry spells on the Prairies will be provided in chapter 7.

Note, May(+10) is not incorporated into the conceptual model. This is because it showed an opposite response to the rest of the growing season. The correlation and composite analyses of El Niño suggested slightly negative 50 kPa anomalies and significantly fewer 10-day dry spells during May. As noted previously, relationships between May and the rest of the growing season will also be discussed in chapter 7. In summary, the majority of growing season(+10) (i.e. June, July and August) corresponds to the hypothesis that El Niño events are related to more growing-season extended dry spells on the Prairies.

6.1.2 LA NIÑA EVENTS

Figure 6.2 presents the conceptual model showing the typical atmosphere - ocean teleconnections associated with La Niña events. As with El Niño, this model also suggests that La Niña are related to growing-season precipitation variations on the Canadian Prairies through a series of stages. However, in this case, only four stages are involved. During stage one, a negative PNA pattern develops during the autumn or winter following the onset of the events (i.e. autumn(+3) to winter(+4)). The pattern includes positive height anomalies over the northeastern Pacific Ocean (i.e. a weaker Aleutian low), negative anomalies over western Canada and positive anomalies over the southeastern United States. Note that Figure 6.2 shows the weaker Aleutian low as an area of high pressure. This is because the map shows

Stage 1: Negative PNA Pattern - Autumn(+3) to Winter(+4)

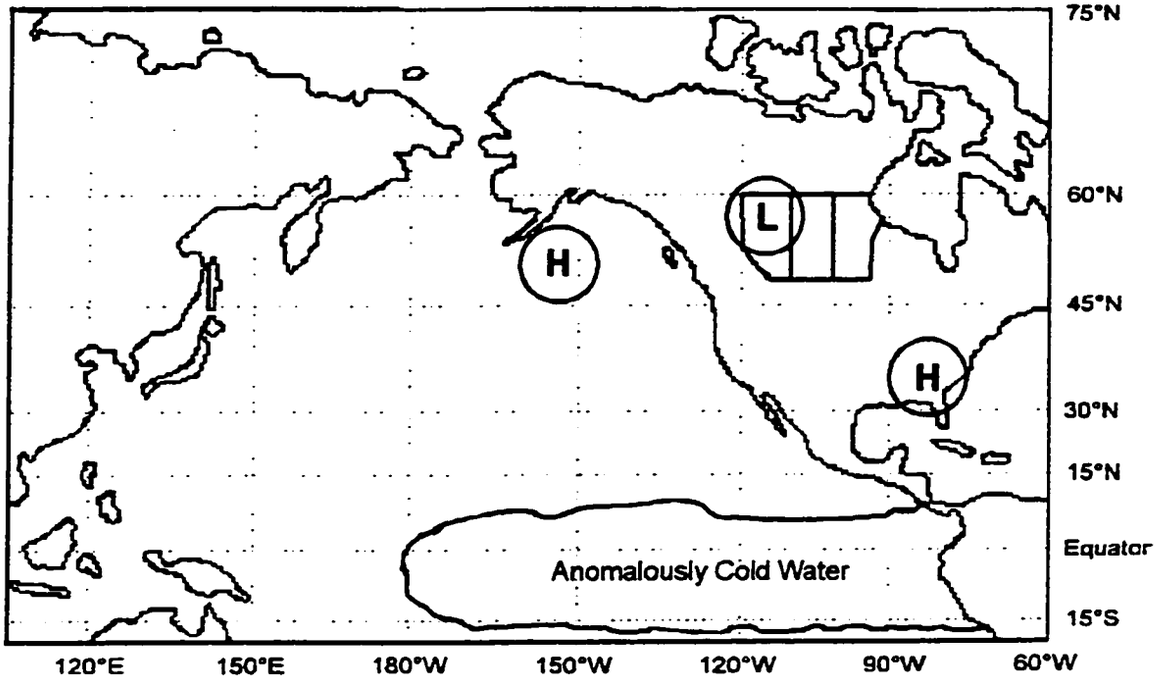

Stage 2: Negative North Pacific SST Anomaly Gradient - Winter(+4) to Spring(+5)

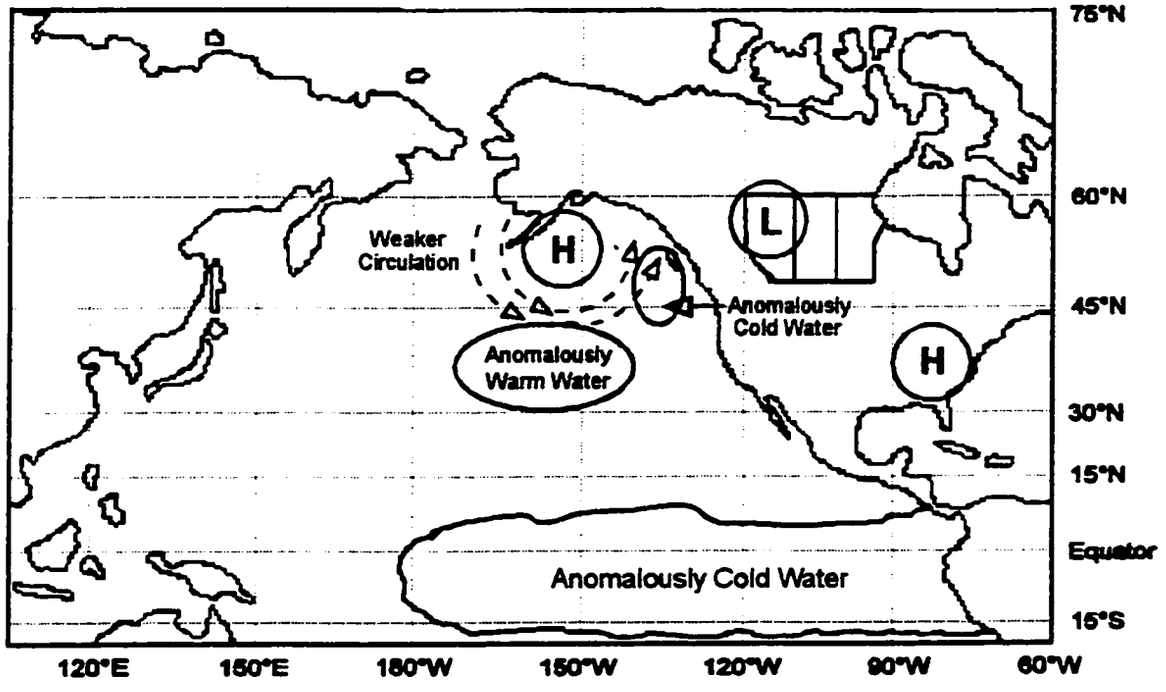

Figure 6.2: Conceptual Model of the Typical Atmosphere - Ocean Teleconnections Associated with La Niña Events

Stage 3: Higher Frequency of Negative North Pacific SST Anomaly Gradients - Spring(+5) to Summer(+10)

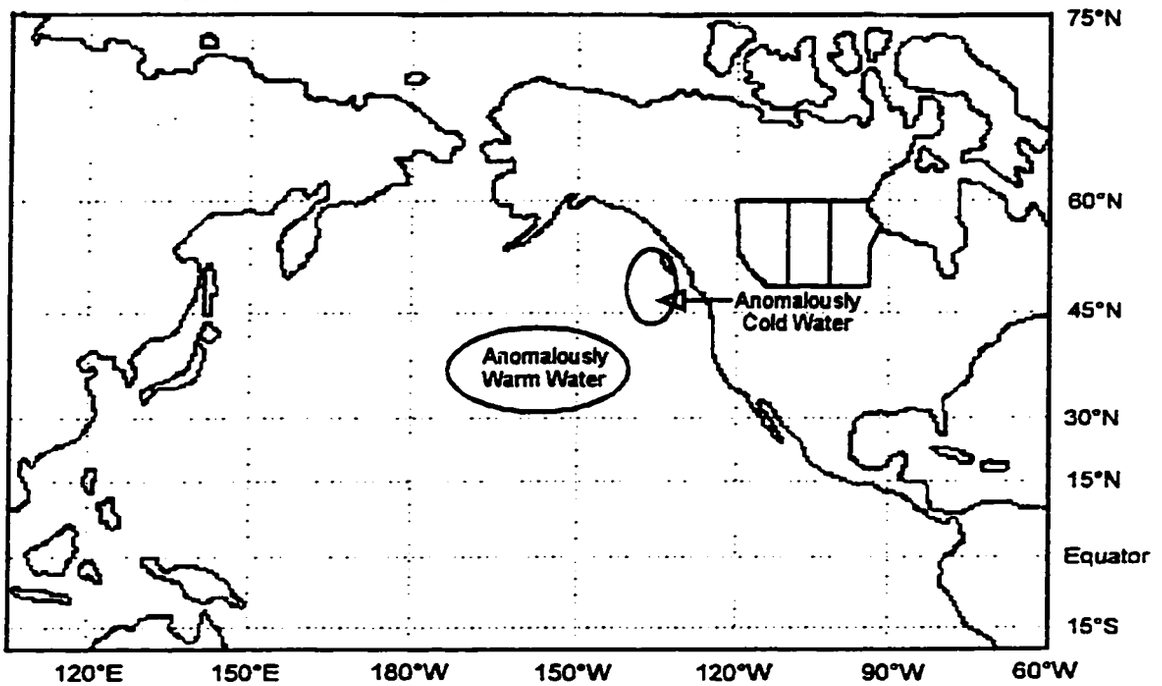

Stage 4: Negative North Pacific SST Anomaly Gradient and Associated Negative 50 kPa Anomalies Leading to Fewer Extended Dry Spells on the Canadian Prairies - June(+10), July(+10), August(+10)

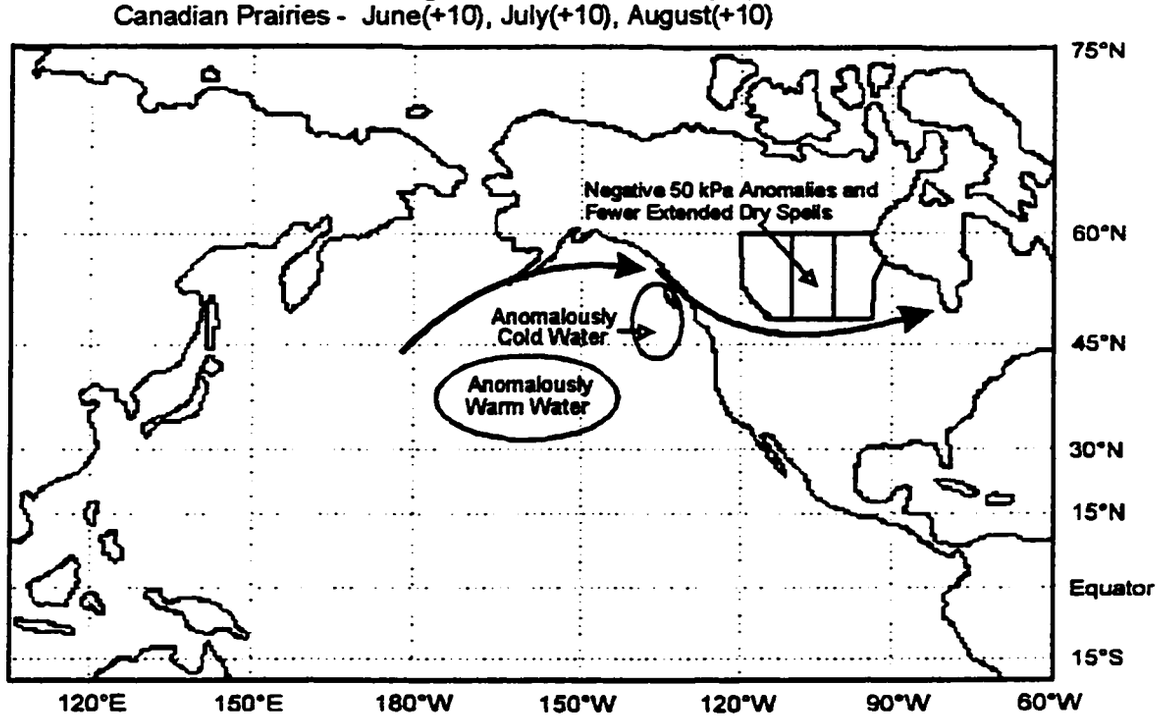

Figure 6.2: Continued

pressure anomalies. Since a weaker Aleutian low represents positive anomalies, it appears as an area of high pressure on the figure.

Significant associations between La Niña and winter negative PNA patterns were shown in the correlation and composite analyses. Relationships between La Niña and upper-atmospheric circulation patterns over the Northern Hemisphere have not been extensively researched. However, a few studies observed that negative PNA patterns developed during the autumn or winter following the onset of most La Niña events (Emery and Hamilton, 1985; Yarnal and Diaz, 1986).

The physical basis for this relationship differs from El Niño events and positive PNA patterns in that negative PNA patterns do not appear to be forced directly by the tropical Pacific heat source (which is displaced westward during La Niña). Rather, Yarnal and Diaz (1986) hypothesized that these patterns are associated with complex ocean - atmosphere interactions that stimulate convection over the westward displaced heat source. In particular, cold air surges (which often sweep southward from the east-Asian mainland across the East and South China Seas), sometimes penetrate as far south as the equator and thus, over the tropical Pacific heat source associated with La Niña. The cold surges increase convection and release of latent heat and as a result, the upper-level northward branch of the Hadley Cell picks up speed and momentum. This in turn enhances the east-Asian jet stream setting up a ridge and trough system across the North Pacific and North America which resembles a negative PNA pattern. Since these cold surges occur most often during late autumn and winter, negative PNA patterns also tend to develop during these periods (Yarnal and Diaz, 1986).

The development of a negative North Pacific SST anomaly gradient (i.e. anomalously warm water in the east-central North Pacific and anomalously cold water along the central-west coast of North America) during winter(+4) to spring(+5), signifies stage two of the model. The correlation and composite analyses showed significant associations between La Niña and negative SST anomaly gradients, especially during spring(+5).

It is suggested these negative gradients develop due to the circulation associated with negative PNA patterns and in particular, the weaker Aleutian low. This situation causes a weaker surface counterclockwise circulation resulting in lower frequencies of cold north to northwesterly flow behind the low. Therefore, less than normal heat transfer from the ocean to the atmosphere results in anomalously warm water in the east-central North Pacific. Ahead of the low, lower frequencies of warmer south to southwesterly flows result in a higher than normal heat transfer from the ocean to the atmosphere and thus, anomalously cold water along the central-west coast of North America (Yongping and McBean, 1991). The result is a negative North Pacific SST anomaly gradient. These types of North Pacific SST anomaly patterns have often been observed during winters and springs following the onset of La Niña events (Weare et al., 1976; Pan and Oort, 1983,1990; Emery and Hamilton, 1985).

Stage three indicates a higher frequency of negative North Pacific SST anomaly gradients (i.e. more negative than positive) during spring(+5) to summer(+10). The composite analysis showed no persistence of negative SST anomaly gradients. However, a higher frequency of these

gradients was observed to be associated with La Niña events indicating that the SST anomaly gradients associated with La Niña, were different from those associated with El Niño (i.e. they were not persistently positive). Further discussion of possible reasons why negative SST anomalies do not persist will be provided in chapter 7.

Stage four suggests that the higher frequency of negative SST anomaly gradients is associated with negative 50 kPa anomalies over the Canadian Prairies during June(+10), July(+10) and August(+10). These two conditions lead to fewer extended dry spells (i.e. wetter conditions) during these periods. From the composite analysis, there was no clear evidence that the SST anomalies caused strong negative 50 kPa anomalies. However, it did appear that when these SST anomalies occurred in conjunction with slightly negative 50 kPa anomalies, significantly fewer extended dry spells were observed. Once again, whether the SST anomalies caused these slightly negative 50 kPa anomalies is unclear.

As with El Niño, the physical basis for an association between these North Pacific SST anomalies and upper-atmospheric circulation patterns is also not entirely understood. As discussed previously, several studies suggested mid-latitude SST anomalies affect mean atmospheric circulation patterns (both locally and downstream) because the anomalies imply significant changes in ocean to atmosphere heat exchanges (Davis, 1976; Namias and Cayan, 1981; Namias et al., 1988). Namias (1972) observed a significant relationship between North Pacific SST anomaly patterns resembling negative SST anomaly gradients and a long-standing Rossby wave pattern that consisted of troughing over western, and ridging over eastern North America. If the SST anomalies

were reversed, the areas of ridging and troughing were also reversed (Namias, 1972). However, unlike relationships between positive SST anomaly gradients and positive 50 kPa anomalies and extended dry spells on the Canadian Prairies (e.g. Bonsal et al., 1993), no studies have examined relationships between negative SST anomaly gradients and 50 kPa anomalies and precipitation variations.

Recall GCM studies showed that in the mid to upper troposphere, atmospheric pressure tended to increase (decrease) over and to the east (up to 20° of longitude) of high (low) mid-latitude SST anomalies (Huang, 1978; Chervin, 1980; Palmer and Sun, 1985; Lau and Nath, 1990). Therefore, the upper-atmospheric flow pattern associated with a higher frequency of negative SST anomaly gradients may be similar to that in stage four of Figure 6.2 (i.e. lower atmospheric pressure or troughing to the east of the low SST anomalies (thus over the Canadian Prairies) and higher atmospheric pressure or ridging to the east of the high SST anomalies) (i.e. a pattern opposite to that associated with positive SST anomaly gradients).

As with El Niño, May(+10) is not incorporated into the model because it showed an opposite response to the rest of the growing season. Nonetheless, the majority of the growing season corresponds to the hypothesis that La Niña events are related to fewer extended dry spells (i.e. wetter conditions) on the Canadian Prairies during the growing season.

6.2 TESTING OF CONCEPTUAL MODELS

In the preceding section, two conceptual models showing

teleconnections between ENSO events and growing-season precipitation variations on the Canadian Prairies were developed. However, these models were based on typical or average relationships for the period 1948-1991. As discussed in chapter 2, individual ENSO events (both El Niño and La Niña) often differ in terms of timing, evolution, amplitude, duration and spatial extent (Rasmusson et al., 1983; van Loon and Shea, 1985; Fu et al., 1986; Ropelewski and Halpert, 1986,1987,1989; Kiladis and Diaz, 1989; Philander, 1990). These differences can be key factors in determining the strength and consistency of the anomalies associated with teleconnection patterns during individual ENSO events (Diaz and Kiladis, 1992).

Therefore, concerns may arise with regard to the accuracy of the conceptual models. For example, the typical response could be dominated by a few large events. The consistency of the anomalies from event to event is also unclear (i.e. are they always positive, negative, or both). To address these concerns, the conceptual models are tested by examining the strength and consistency of the responses for each variable associated with the teleconnections in these models. These variables include PNA indices, North Pacific SST anomaly gradients and growing-season areally-averaged 50 kPa anomalies and total number of 10-day dry spells on the Prairies. The responses are tested using the ten El Niño and seven La Niña events occurring between 1948 and 1991 (Table 3.1).

Ideally, this testing procedure should use an independent set of El Niño and La Niña events because the models were based on the events between 1948 and 1991. However, due to data limitations (e.g. Northern

Hemisphere upper-air and North Pacific SST data only date back to 1948 and the period from 1992 to the present is too short), the use of an independent set of events is not possible. Nonetheless, this testing procedure is beneficial because it will aid in determining the accuracy of each conceptual model. The testing is broken up into two main sections including the El Niño model and the La Niña model.

6.2.1 EL NIÑO MODEL

6.2.1.1 PNA PATTERNS

The conceptual model of El Niño events showed positive PNA patterns occurring near the mature stage of the events (i.e. autumn(+3) to winter(+4)). To determine the strength and consistency of the relationships between these two variables, the strengths and signs of PNA indices associated with the ten El Niño events occurring between 1948 and 1991 are presented in Table 6.1. The period examined is autumn(+3) to winter(+4) because this is when positive PNA patterns associated with El Niño events normally occur. The PNA indices are categorized into six different strengths including very strong negative, strong negative, weak negative, weak positive, strong positive and very strong positive. These categories are determined using standardized PNA indices given in Appendix C - Table C.1. They are chosen as follows. Very strong negative has a standardized value of less than -1.00; strong negative between -1.00 and -0.50; weak negative between -0.50 and 0.00; weak positive between 0.00 and +0.50; strong positive between +0.50 and +1.00; and very strong positive greater than +1.00.

According to the normal probability table, the probability that an

Table 6.1: Strength of PNA Indices Associated with the Ten El Niño Events Between 1948 and 1991.

TIME PERIOD	VERY STRONG NEG.	STRONG NEG.	WEAK NEG.	WEAK POS.	STRONG POS.	VERY STRONG POS.
Autumn(+3) to Winter(+4)	0	1	1	0	2	6

individual has a standardized value less than -1.00 is 0.16. The probability of a value between -1.00 and -0.50 is 0.15; between -0.50 and 0.00 is 0.19; between 0.00 and +0.50 is 0.19; between +0.50 and +1.00 is 0.15; and greater than +1.00 is 0.16 (Ebdon, 1985). Therefore, very strong negative values correspond to the lowest 16% of the PNA indices (i.e. values less than -1.00); strong negative to the next lowest 15%; and weak negative to the next lowest 19%. Conversely, very strong positive values correspond to the highest 16% of the PNA indices (i.e. values greater than +1.00); strong positive to the next highest 15%; and weak positive to the next highest 19%. This procedure is similar to the one used by Yarnal and Diaz (1986) who examined the strength and consistency of meteorological variables (e.g. PNA patterns, temperature, precipitation) associated with ENSO events.

Table 6.1 shows that autumn(+3) to winter(+4) was associated with PNA indices that included six very strong positive, two strong positive, one weak negative and one strong negative. Therefore, eight of ten or 80% of El Niño events were associated with positive PNA indices during autumn(+3) to winter(+4). Of these, six were very strong positive PNA indices (i.e. the highest 16%) and two were strong positive (i.e. the

next highest 15%). Therefore, the majority (80%) of El Niño events were associated with either strong or very strong positive PNA patterns during autumn(+3) to winter(+4) indicating a consistent relationship between the two variables.

6.2.1.2 NORTH PACIFIC SST ANOMALY PATTERNS

The conceptual model suggested that during autumn(+3) to winter(+4), positive North Pacific SST anomaly gradients develop. It also suggested the positive gradients weaken during spring(+5) and summer(+6), strengthen during autumn(+7), and then persist until summer(+10). The strengths and signs of the North Pacific SST anomaly gradients associated with the eight El Niño events having positive PNA patterns are presented in Table 6.2. The gradients are only analyzed for these eight events because according to both the hypothesis in chapter 1 and the model in Figure 6.1, positive SST anomaly gradients are generated due to the circulation associated with positive PNA patterns. The analysis uses the same categories as for PNA patterns and the strengths of the gradients are determined using standardized SST anomaly gradients in Appendix D - Table D.1. The period examined is from autumn(+3) to summer(+10).

Positive SST anomaly gradients should develop during autumn(+3) to winter(+4). During autumn(+3), seven of eight (88%) El Niño events were associated with positive gradients and six were strong or very strong. During winter(+4), all eight had strong or very strong positive gradients. Therefore, every El Niño that had a positive PNA pattern, was also associated with stronger positive North Pacific SST anomaly

Table 6.2: Strength of North Pacific SST Anomaly Gradients Associated with the Eight El Niño Events having Positive PNA Patterns.

TIME PERIOD	VERY STRONG NEG.	STRONG NEG.	WEAK NEG.	WEAK POS.	STRONG POS.	VERY STRONG POS.
Autumn(+3)	0	0	1	1	4	2
Winter(+4)	0	0	0	0	4	4
Spring(+5)	0	1	1	2	1	3
Summer(+6)	1	0	1	3	1	2
Autumn(+7)	1	0	1	0	2	4
Winter(+8)	0	1	1	1	3	2
Spring(+9)	0	3	1	0	1	3
Summer(+10)	2	1	3	0	2	0

gradients during autumn(+3) to winter(+4).

The gradients should then weaken (but still remain positive) during spring(+5) and summer(+6). Spring(+5) shows only six events associated with positive gradients including three very strong, one strong and two weak. The other two events had negative gradients. During summer(+6), there were still six events with positive gradients. Two were very strong, one was strong and three were weak. Once again, two events had negative gradients.

This indicates many of the stronger positive gradients occurring during autumn(+3) and winter(+4) have either weakened or even become negative. However, three events were still associated with strong or very strong positive gradients. Upon closer examination of these eight events, those of 1953, 1965 and 1976 agreed with the model because the gradients weakened but remained positive during spring(+5) and summer(+6). During those of 1957, 1982 and 1986, the gradients did not weaken, but rather remained strong positive. The two events that had

negative gradients were 1963 and 1969. In fact, following summer(+6), the gradients associated with these events remained negative for several seasons.

During autumn(+7), the model suggested the positive gradients strengthen and persist until summer(+10). Autumn(+7) shows that all six events that had positive gradients during the preceding summer, were associated with strong or very strong positive gradients. In fact, during the three events that showed a weakening of positive gradients (i.e. 1953, 1965, 1976), the gradients did strengthen. During the other three (i.e. 1957, 1982, 1986), strong positive gradients persisted from autumn(+3) to autumn(+7). Therefore, all six of these events did not exactly correspond to the conceptual model. Nonetheless, they were all associated with stronger positive gradients during autumn(+7).

Winter(+8) still shows these six events associated with positive gradients. Two were very strong, three were strong and one was weak. During spring(+9), only four events (1957, 1976, 1982, 1986) were associated with positive gradients including three very strong and one strong. The following summer had only two events (1976 and 1986) with positive gradients (both were strong).

This indicates a weakening of the gradients for the majority of events during spring(+9) and summer(+10) (i.e. positive gradients did not persist from autumn(+7) to summer(+10) as suggested by the model). Nonetheless, these six events had positive gradients for long periods. This included six seasons (i.e. autumn(+3) to winter(+8)) for the events of 1953 and 1965; seven seasons (i.e. autumn(+3) to spring(+9)) for those of 1957 and 1982; and eight seasons (i.e. autumn(+3) to

summer(+10)) for those of 1976 and 1986. Therefore, this analysis has shown the majority (i.e. six of eight or 75%) of El Niño events having positive PNA patterns, were also associated with persistent positive North Pacific SST anomaly gradients.

6.2.1.3 GROWING-SEASON 50 KPA ANOMALIES OVER THE CANADIAN PRAIRIES

It was suggested the persistent positive North Pacific SST anomaly gradients are associated with positive 50 kPa anomalies and more extended dry spells over the Canadian Prairies during June(+10), July(+10) and August(+10). To determine this, the strengths and signs of areally-averaged 50 kPa anomalies over the Prairies (using standardized values in Appendix B - Table B.1) associated with the six El Niño events having positive PNA patterns and persistent positive North Pacific SST anomaly gradients are presented for months within growing season(+10) (Table 6.3). The categories are the same as those used in the previous analyses.

During June, only two events were associated with positive 50 kPa anomalies, however, both were very strong. July and August had only three events associated with positive 50 kPa anomalies. Therefore, it appears the positive 50 kPa anomaly response to these events was not very consistent. In fact, of the 18 Junes, Julys and Augusts considered, only eight experienced positive anomalies, and only five were strong or very strong positive.

However, this analysis examines all six El Niño events as a group. Individual events may show stronger and more consistent responses. These events are therefore further analyzed to determine which ones had the

Table 6.3: Strength of Growing-Season Areally-Averaged 50 kPa Anomalies over the Canadian Prairies Associated with the Six El Niño Events having Positive PNA Patterns and Persistent Positive North Pacific SST Anomaly Gradients.

TIME PERIOD	VERY STRONG NEG.	STRONG NEG.	WEAK NEG.	WEAK POS.	STRONG POS.	VERY STRONG POS.
May(+10)	3	1	1	1	0	0
June(+10)	0	0	4	0	0	2
July(+10)	1	0	2	2	1	0
August(+10)	1	1	1	1	1	1

strongest responses in terms of positive 50 kPa anomalies over the Canadian Prairies during June(+10), July(+10) and August(+10) (Table 6.4). As outlined previously, the six events having positive PNA patterns and persistent positive SST anomaly gradients included 1953, 1957, 1965, 1976, 1982 and 1986. Note that only strong and very strong positive (i.e. standardized values greater than +0.50 and +1.00 respectively) 50 kPa anomalies are considered because they would most likely lead to extended dry spells and droughts on the Prairies.

Table 6.4 shows that during four of these six events, strong or very strong positive 50 kPa anomalies were observed during either June(+10), July(+10) or August(+10). The only exceptions were the events of 1957 and 1976. In fact, these two events experienced strong negative 50 kPa anomalies during June(+10), July(+10) and August(+10) (see Appendix B). This indicates that the majority of the events were associated with strong or very strong positive anomalies during at least one of these months. However, the strong positive anomalies were not consistent through the entire period. In fact, the average 50 kPa

Table 6.4: Positive 50 kPa Anomaly Response over the Canadian Prairies during the Months of June(+10), July(+10) and August(+10) Associated with the Six El Niño Events Which Experienced Positive PNA Patterns and Persistent Positive North Pacific SST Anomaly Gradients.

EL NIÑO EVENT	POSITIVE 50 KPA ANOMALY RESPONSE
1953	Very strong during June; strong during July.
1957	No strong or very strong positive anomalies.
1965	Very strong during August.
1976	No strong or very strong positive anomalies.
1982	Strong during August.
1986	Very strong during June.

anomalies for June, July and August associated with these four events were near normal or only slightly positive (see Appendix B). This suggests that the persistent positive SST anomaly gradients do not cause consistently strong positive 50 kPa anomalies over the Prairies.

Finally, May(+10) is also examined because the correlation and composite analyses suggested it should experience negative 50 kPa anomalies over the Prairies. Table 6.3 shows that during May, five of six (83%) events were associated with negative 50 kPa anomalies. Three were very strong, one was strong and one was weak. The other event was associated with only weak positive anomalies. Therefore, the majority of El Niño events (83%) having positive PNA patterns and persistent positive North Pacific SST anomaly gradients, were associated with negative 50 kPa anomalies over the Canadian Prairies during May(+10). Furthermore, many of these were strong or very strong negative. This once again indicates that May has an opposite response from the rest of the growing season.

6.2.1.4 GROWING-SEASON EXTENDED DRY SPELLS ON THE CANADIAN PRAIRIES

Even though strong positive 50 kPa anomalies did not show a consistent response during June(+10), July(+10) and August(+10), extended dry spells are examined to determine if they showed more consistent responses. The strengths and signs of the total number of 10-day dry spells on the Prairies (using standardized values in Appendix A - Table A.3) associated with the six El Niño events having positive PNA patterns and persistent positive North Pacific SST anomaly gradients are presented for months within growing season(+10) (Table 6.5). As was the case with correlation and composite analyses, a total growing-season value is also analyzed.

During June, five of six events were associated with positive total number of 10-day dry spells. Three were very strong and two were weak. July shows four events with positive values including two very strong, one strong and one weak. August had only two events with positive values, however, both were very strong. The total growing season was associated with four positive values including two strong and two very strong. Therefore, there is a more consistent response of positive total number of 10-day dry spells (as opposed to positive 50 kPa anomalies). The strongest response occurred during June when five of six events had positive values with three being very strong.

As with the positive 50 kPa anomaly response, total number of 10-day dry spells are further analyzed to determine which events had the strongest responses. Table 6.6 shows the positive total number of 10-day dry spells response on the Canadian Prairies during June(+10), July(+10), August(+10) and the total growing season(+10). Once again,

Table 6.5: Strength of Growing-Season Total Number of 10-Day Dry Spells on the Canadian Prairies Associated with the Six El Niño Events having Positive PNA Patterns and Persistent Positive North Pacific SST Anomaly Gradients.

TIME PERIOD	VERY STRONG NEG.	STRONG NEG.	WEAK NEG.	WEAK POS.	STRONG POS.	VERY STRONG POS.
Total(+10)	0	1	1	0	2	2
May(+10)	2	1	0	3	0	0
June(+10)	0	1	0	2	0	3
July(+10)	0	0	2	1	1	2
August(+10)	0	1	3	0	0	2

only strong and very strong positive responses are considered because these represent more severe dry spells that could lead to drought on the Prairies.

Four of six (67%) of these events had strong or very strong positive responses during June(+10), July(+10), August(+10) or the total growing season(+10). As with positive 50 kPa anomalies, the only exceptions were the events of 1957 and 1976. Most of the events having stronger positive responses, also experienced them for a period of more than one month and in all four cases, the total growing season. Therefore, the majority (67%) of El Niño events having positive PNA patterns and persistent positive North Pacific SST anomaly gradients also had strong or very strong positive responses in terms of 10-day dry spells during either June(+10), July(+10), August(+10) or the total growing season(+10). The responses during these four events also tended to be somewhat persistent (i.e. they often occurred during more than one month and the total growing season itself showed strong or very strong positive responses).

Table 6.6: Positive Total Number of 10-Day Dry Spell Response on the Canadian Prairies Associated with the Six El Niño Events having Positive PNA Patterns and Persistent Positive North Pacific SST Anomaly Gradients.

EL NIÑO EVENT	POSITIVE TOTAL NUMBER OF 10-DAY DRY SPELL RESPONSE
1953	Very strong during July, August and the total growing season.
1957	No strong or very strong positive values.
1965	Very strong during June, July, August and the total growing season.
1976	No strong or very strong positive values.
1982	Very strong during June; strong during July and the total growing season.
1986	Very strong during June; strong during the total growing season.

In summary, the testing of the positive 50 kPa anomaly and extended dry spell responses during June(+10), July(+10) and August(+10) showed no clear evidence that persistent positive SST anomaly gradients caused consistently strong positive 50 kPa anomalies or ridging over the Canadian Prairies. However, it does appear that the nature of the associated 50 kPa anomalies does influence whether these SST anomalies lead to more extended dry spells. For example, when the SST anomalies occurred in conjunction with positive or near normal 50 kPa anomalies, consistent strong positive responses in terms of extended dry spells were observed (i.e. the events of 1953, 1965, 1982 and 1986). On the other hand, when these SST anomalies occurred in conjunction with strong negative 50 kPa anomalies, strong positive extended dry spell responses did not occur (i.e. the 1957 and 1976 events). Therefore, it appears that persistent positive SST anomaly gradients (associated with El Niño) in conjunction with positive or near normal 50 kPa anomalies, are

required to lead to a higher frequency of extended dry spells on the Prairies.

Once again, May(+10) is analyzed to determine if it had an opposite (i.e. negative) response in terms of extended dry spells. Table 6.5 shows that during May, only three events had negative values (two very strong and one strong) while the other three had weak positive values. Therefore, only half of the events were associated with negative total number of 10-day dry spells. However, they all experienced either strong or very strong negative responses.

6.2.1.5 SUMMARY

The testing of the conceptual model of El Niño events showed that eight of ten (80%) of the El Niño events were associated with strong or very strong positive PNA patterns during autumn(+3) to winter(+4). Of these, six (75%) were associated with persistent positive North Pacific SST anomaly gradients. However, these six events did not all exhibit the same persistence. Some events agreed with the conceptual model (i.e. stronger positive SST anomaly gradients occurred during autumn(+3) to winter(+4), weakened during spring(+5) and summer(+6), strengthened during autumn(+7) and persisted through summer(+10)). However, others developed stronger positive gradients during autumn(+3) to winter(+4) and these stronger gradients persisted for several seasons.

Four of the six (67%) El Niño events with positive PNA patterns and persistent positive North Pacific SST anomaly gradients had positive 50 kPa anomalies during June(+10), July(+10) and August(+10) (although not consistently strong positive). These events also had strong or very

strong positive responses in terms of total number of 10-day dry spells (i.e. drier conditions). Furthermore, the dry spell responses tended to be somewhat persistent (i.e. they covered more than one month and in all four cases, the total growing season).

In conclusion, this testing procedure has shown eight of ten El Niño events experienced strong or very strong positive PNA patterns. Of these, six experienced persistent positive North Pacific SST anomaly gradients. Therefore, six of ten or 60% of the events experienced both positive PNA patterns and persistent positive North Pacific SST anomaly gradients. Of these six, four experienced both positive 50 kPa anomalies and extended dry spells over the Prairies during June(+10), July(+10) and August(+10). Therefore, four of ten or 40% of the original El Niño events corresponded to the conceptual model in that they experienced positive PNA patterns, persistent positive North Pacific SST anomaly gradients and positive 50 kPa anomalies with associated extended dry spells during June(+10), July(+10) or August(+10). As outlined previously, these events included 1953, 1965, 1982 and 1986. Even though only four of ten events corresponded to the model, these four had very strong and consistent responses in terms of growing-season extended dry spells (which could lead to drought conditions) on the Canadian Prairies.

6.2.2 LA NIÑA MODEL

This section tests the conceptual model of La Niña events. The procedure is the same as in the testing of the El Niño conceptual model.

6.2.2.1 PNA PATTERNS

The La Niña conceptual model suggested a relationship between these events and negative PNA patterns. The patterns occurred near the mature stage of the events (i.e. autumn(+3) to winter(+4)). Table 6.7 presents the strengths and signs of PNA indices associated with the seven La Niña events between 1948 and 1991 for the period of autumn(+3) to winter(+4). During this period, all seven events were associated with negative PNA indices and six (86%) were strong or very strong negative patterns. This indicates a very consistent response between the two variables.

6.2.2.2 NORTH PACIFIC SST ANOMALY PATTERNS

Once negative PNA patterns fully develop, negative North Pacific SST anomaly gradients should be observed approximately one season later (i.e. spring(+5)). The model then suggested a higher frequency of these negative gradients (i.e. more negative than positive) from spring(+5) to summer(+10). The strength and signs of the North Pacific SST anomaly gradients associated with the seven La Niña events having negative PNA patterns are given in Table 6.8. The periods examined are spring(+5) to summer(+10). During spring(+5), all seven events had negative SST anomaly gradients including four very strong, two strong and one weak. Therefore, 100% of the La Niña events that had negative PNA patterns also experienced negative SST anomaly gradients during spring(+5) and of these, six (86%) were strong or very strong negative.

Regarding the higher frequency of negative gradients, summer(+6) showed six events having negative gradients (three very strong and three

Table 6.7: Strength of PNA Indices Associated with the Seven La Niña Events Between 1948 and 1991.

TIME PERIOD	VERY STRONG NEG.	STRONG NEG.	WEAK NEG.	WEAK POS.	STRONG POS.	VERY STRONG POS.
Autumn(+3) to Winter(+4)	4	2	1	0	0	0

strong); autumn(+7) had three (two very strong and one strong); winter(+8) had four (one very strong and three strong); spring(+9) had six (two very strong, one strong and three weak); and summer(+10) had five events (one strong and four weak). Upon closer examination, the events of 1954 and 1970 had persistent negative gradients during all six of these seasons (i.e. from spring(+5) to summer(+10)). During the 1973 La Niña, five of six seasons had negative gradients with only autumn(+7) being positive. The 1949, 1964 and 1975 events showed four seasons having negative gradients with autumn(+7) and winter(+8) being positive. During the 1988 event, three seasons had negative gradients with autumn(+7), spring(+9) and summer(+10) being positive. Therefore, all seven events were associated with a higher frequency of negative gradients during spring(+5) to summer(+10) and during two of these (1954 and 1970), negative gradients persisted for all six seasons.

6.2.2.3 GROWING-SEASON 50 KPA ANOMALIES OVER THE CANADIAN PRAIRIES

According to the model, the higher frequency of negative North Pacific SST anomaly gradients is associated with negative 50 kPa anomalies and fewer extended dry spells during June(+10), July(+10) and

Table 6.8: Strength of North Pacific SST Anomaly Gradients Associated with the Seven La Niña Events having Negative PNA Patterns.

TIME PERIOD	VERY STRONG NEG.	STRONG NEG.	WEAK NEG.	WEAK POS.	STRONG POS.	VERY STRONG POS.
Spring(+5)	4	2	1	0	0	0
Summer(+6)	3	3	0	1	0	0
Autumn(+7)	2	1	0	1	3	0
Winter(+8)	1	3	0	0	2	1
Spring(+9)	2	1	3	0	1	0
Summer(+10)	1	0	4	1	0	1

August(+10). Table 6.9 presents the strengths and signs of growing season areally-averaged 50 kPa anomalies over the Canadian Prairies for each month within growing season(+10) associated with the seven La Niña events having negative PNA patterns and a higher frequency of negative SST anomaly gradients. June was associated with four events having negative 50 kPa anomalies including two very strong, one strong and one weak. During July, only three events had negative anomalies (two very strong and one strong) while August had four events including two strong and two weak. This response is more consistent than that for positive 50 kPa anomalies associated with El Niño, however, of the 18 Junes, Julys and Augusts considered here, only 11 experienced negative anomalies and only eight were strong or very strong negative.

As with El Niño events, the seven La Niña events (i.e. 1949, 1954, 1964, 1970, 1973, 1975 and 1988) are further analyzed to determine which events showed the strongest responses in terms of negative 50 kPa anomalies during June(+10), July(+10) and August(+10) (Table 6.10). Six of seven of these events had strong or very strong negative 50 kPa

Table 6.9: Strength of Growing-Season Areally-Averaged 50 kPa Anomalies over the Canadian Prairies Associated with the Seven La Niña Events having Negative PNA Patterns and a Higher Frequency of Negative North Pacific SST Anomaly Gradients.

TIME PERIOD	VERY STRONG NEG.	STRONG NEG.	WEAK NEG.	WEAK POS.	STRONG POS.	VERY STRONG POS.
May(+10)	0	2	0	2	1	2
June(+10)	2	1	1	1	2	0
July(+10)	2	1	0	0	2	2
August(+10)	2	0	2	1	2	0

anomalies during either June(+10), July(+10) or August(+10). The only exception was the event of 1954 which experienced strong positive anomalies during these periods (see Appendix B). This indicates that the majority of these events were associated with strong or very strong negative anomalies during at least one of these months. However, the strong negative anomalies were not consistently strong through the entire period. Some events, (i.e. 1964, 1973 and 1975) were associated with strong negative anomalies for two of these three months, however, the average 50 kPa anomalies for June, July and August for the other events were near normal or only slightly negative (see Appendix B). As with El Niño (and associated positive SST anomaly gradients), these results also suggest that the higher frequency of negative SST anomaly gradients associated with La Niña do not cause consistently strong and negative 50 kPa anomalies over the Prairies.

May(+10) is again examined to determine if it had an opposite response. Table 6.9 shows that during this period, five of seven (71%) events were associated with positive 50 kPa anomalies including two very

Table 6.10: Negative 50 kPa Anomaly Response over the Canadian Prairies Associated with the Seven La Niña Events having Negative PNA and a Higher Frequency of Negative North Pacific SST Anomaly Gradients.

LA NIÑA EVENT	NEGATIVE 50 KPA ANOMALY RESPONSE
1949	Strong during June.
1954	No strong or very strong negative anomalies.
1964	Strong during June and July.
1970	Very strong during July.
1973	Very strong during June and August.
1975	Very strong during July and August.
1988	Strong during June.

strong, one strong and two weak. This indicates once again that May(+10) tends to be opposite from the rest of growing season(+10).

6.2.2.4 GROWING-SEASON EXTENDED DRY SPELLS ON THE CANADIAN PRAIRIES

The strengths and signs of the total number of 10-day dry spells on the Prairies for the months within growing season(+10) associated with the seven La Niña events having negative PNA patterns and a higher frequency of negative North Pacific SST anomaly gradients are presented in Table 6.11. A total growing-season value is also analyzed. In terms of negative responses, June had six of seven events including four strong and two weak. July showed all seven events associated with negative values. One was very strong, four were strong and two were weak. August had six events including four strong and two weak. The total growing season(+10) had negative values associated with all seven events. One was very strong, three were strong and three were weak.

This analysis shows a very consistent result in terms of negative responses to total number of 10-day dry spells for these periods. The

Table 6.11: Strength of Growing-Season Total Number of 10-Day Dry Spells on the Canadian Prairies Associated with the Seven La Niña Events having Negative PNA Patterns and a Higher Frequency of Negative North Pacific SST Anomaly Gradients.

TIME PERIOD	VERY STRONG NEG.	STRONG NEG.	WEAK NEG.	WEAK POS.	STRONG POS.	VERY STRONG POS.
Total(+10)	1	3	3	0	0	0
May(+10)	2	1	1	2	1	0
June(+10)	0	4	2	1	0	0
July(+10)	1	4	2	0	0	0
August(+10)	0	4	2	1	0	0

strongest responses occurred during July and the total growing season when all seven La Niña events were associated with negative values. Even June and August showed the majority (six of seven) of La Niña events having negative values.

The responses of the seven events are further analyzed to determine which had the strongest negative responses in terms of the total number of 10-day dry spells during June(+10), July(+10), August(+10) and the total growing season(+10) (Table 6.12). Six of seven (86%) had strong or very strong negative 10-day dry spell responses during these periods. The only exception was the La Niña of 1954. This event also did not show any stronger responses in terms of negative 50 kPa anomalies. With the exception of 1970, every event had stronger negative responses for more than one month and in some cases, the total growing season. Therefore, 86% of the La Niña events having negative PNA patterns and a higher frequency of negative North Pacific SST anomaly gradients also had stronger negative responses in terms of extended dry spells during June(+10), July(+10), August(+10) or the total growing

Table 6.12: Negative Total Number of 10-Day Dry Spell Response on the Canadian Prairies Associated with the Seven La Niña Events having Negative PNA Patterns and a Higher Frequency of Negative North Pacific SST Anomaly Gradients.

LA NIÑA EVENT	NEGATIVE TOTAL NUMBER OF 10-DAY DRY SPELL RESPONSE
1949	Strong during July, August and the total growing season.
1954	No strong or very strong negative values.
1964	Strong during June, July and August.
1970	Strong during June.
1973	Strong during July, August and the total growing season.
1975	Very strong during July and the total growing season; strong during June and August.
1988	Strong during June, July and the total growing season.

season(+10). Furthermore, the responses to most of these events tended to be somewhat persistent (i.e. they covered a period of more than one month and in some instances, the total growing season).

In summary, the testing of the negative 50 kPa anomaly and extended dry spell responses during June(+10), July(+10) and August(+10) to La Niña events suggests similar results to those of the positive 50 kPa anomaly and extended dry spell responses to El Niño events. There was no clear evidence that the higher frequency of negative SST anomaly gradients caused consistently strong negative 50 kPa anomalies or troughing over the Canadian Prairies. However, it does appear that the nature of the associated 50 kPa anomalies does influence whether these SST anomalies lead to fewer extended dry spells. For example, when the SST anomalies occurred in conjunction with negative or near normal 50 kPa anomalies, consistently strong negative responses in terms of extended dry spells were observed (i.e. the events of 1949, 1964, 1970,

1973, 1975 and 1988). Conversely, in the case where the SST anomaly occurred in conjunction with a strong positive 50 kPa anomaly, a strong negative extended dry spell response did not occur (i.e. the 1954 event). Therefore, it appears that the higher frequency of negative SST anomaly gradients (associated with La Niña) in conjunction with negative or near normal 50 kPa anomalies, is required to lead to fewer extended dry spells on the Prairies.

For May(+10), Table 6.11 shows only three events had positive values including one strong and two weak. The other four events were associated with negative values including two very strong, one strong and one weak. This indicates that May(+10) is not entirely opposite from the rest of the growing season. In fact, four of seven (57%) events showed negative values including three strong or very strong. This agrees with the composite analysis of total number of 10-day dry spells (section 5.4) which showed that May(+10) was associated with fewer extended dry spells. Therefore, with regards to La Niña events, May(+10) is not generally opposite to the rest of the growing season in terms of extended dry spells on the Canadian Prairies.

6.2.2.5 SUMMARY

The testing of the conceptual model of La Niña events showed all seven events associated with negative PNA patterns during autumn(+3) to winter(+4). Furthermore, six had strong or very strong negative patterns. Every event was also associated with negative North Pacific SST anomaly gradients during spring(+5) (six were strong or very strong negative). The seven events also had a higher frequency of negative

gradients (i.e. more negative than positive) during spring(+5) to summer(+10).

Of the seven La Niña events having negative PNA patterns and a higher frequency of negative North Pacific SST anomaly gradients, six showed negative 50 kPa anomaly responses during June(+10), July(+10) and August(+10) (although not consistently strong negative). These six events had strong or very strong negative responses in terms of total number of 10-day dry spells. The dry spell responses were also somewhat persistent (i.e. stronger negative responses covered a period of more than one month and in some cases, the total growing season).

In conclusion, this testing procedure has shown that all seven of the La Niña events experienced negative PNA patterns. Of these, every one also experienced a higher frequency of negative North Pacific SST anomaly gradients. Therefore, 100% experienced both negative PNA patterns and a higher frequency of negative North Pacific SST anomaly gradients. Of these seven, six had negative responses in terms of both 50 kPa anomalies and extended dry spells on the Prairies during June(+10), July(+10) or August(+10). The only exception was the event of 1954. Therefore, the conceptual model of La Niña events appears to work very well. In fact, 86% of the La Niña events occurring between 1948 and 1991 agreed with the model and were therefore associated with fewer extended dry spells on the Canadian Prairies during most of growing season(+10). These fewer extended dry spells suggest wet conditions but are also representative of non-drought periods on the Canadian Prairies.

6.3 CASE STUDIES

In this section, case studies for El Niño and La Niña are examined as examples where the conceptual models presented in section 6.1 worked well. For El Niño, the event of 1986 was chosen because it was associated with a positive PNA pattern and persistent positive North Pacific SST anomaly gradients. Strong positive 50 kPa anomalies and very dry conditions during the 1988 growing season were also observed on the Canadian Prairies. The 1973 La Niña event is used because it was associated with a negative PNA pattern and persistent negative North Pacific SST anomaly gradients. Also, strong negative 50 kPa anomalies and wetter than normal conditions occurred on the Canadian Prairies during the 1975 growing season. For each case study, variables including SOI values, PNA indices, North Pacific SST anomaly gradients and growing-season areally-averaged 50 kPa anomalies and total number of 10-day dry spells on the Prairies are presented and discussed as they relate to the conceptual models.

6.3.1 THE 1986 EL NIÑO EVENT

6.3.1.1 SOI VALUES

Table 6.13 presents actual and standardized seasonal SOI values from autumn 1985 through winter 1988 associated with the 1986 El Niño event. SOI values became negative (i.e. anomalously low pressure in the eastern, and anomalously high pressure in the western tropical Pacific) during winter 1986. This period likely coincided with the onset of the event. The SOI remained slightly negative through spring and summer 1986. During autumn 1986, the value became stronger and continued to

Table 6.13: Seasonal SOI Values Associated with the 1986 El Niño Event.

TIME PERIOD	ACTUAL SOI VALUE	STANDARDIZED SOI VALUE
Autumn 1985	+0.20	+0.12
Winter 1986	-0.16	-0.09
Spring 1986	-0.24	-0.18
Summer 1986	-0.15	-0.10
Autumn 1986	-0.63	-0.51
Winter 1987	-1.64	-0.96
Spring 1987	-2.23	-2.01
Summer 1987	-1.07	-0.88
Autumn 1987	-0.23	-0.51
Winter 1988	+0.10	+0.06

strengthen through winter 1987. It reached its peak during spring. The period of winter to spring 1987 likely represented the mature stage of the event which is approximately one season later than the composite or typical El Niño described in chapter 2. Following spring, the negative SOI value weakened during summer 1987 and this trend continued into autumn. The value became positive during winter 1988 signifying the end of the event.

6.3.1.2 PNA INDICES

According to the conceptual model of El Niño events, a positive PNA pattern should occur during autumn(+3) to winter(+4) (i.e. autumn 1986 to winter 1987). Table 6.14 presents actual and standardized seasonal PNA indices from autumn 1986 to summer 1987. The PNA index was negative during autumn 1986. However, during winter, the index became very strong positive (i.e. a standardized value of greater than +1.00). The positive PNA index weakened greatly during spring 1987 and became

Table 6.14: Seasonal PNA Indices Associated with the 1986 El Niño Event.

TIME PERIOD	ACTUAL PNA INDEX	STANDARDIZED PNA INDEX
Autumn 1986	-0.35	-0.55
Winter 1987	+0.96	+1.23
Spring 1987	+0.13	+0.20
Summer 1987	-0.10	-0.24

negative during summer.

Therefore, a very strong positive PNA pattern developed during winter 1987 (i.e. winter(+4)) which agrees with the conceptual model. To visualize this pattern, a Northern Hemisphere 50 kPa anomaly map for winter 1987 is presented in Figure 6.3. The figure shows the general characteristics of a positive PNA pattern including negative height anomalies over the north-central North Pacific Ocean (suggesting a stronger Aleutian low) and positive height anomalies over western Canada. However, there is a slight difference from the winter(+4) composite 50 kPa anomaly map associated with El Niño events (Figure 5.1(a)) and stage one of the conceptual model of El Niño events (Figure 6.1) in that, the negative anomalies over the North Pacific Ocean were displaced northward, the positive anomalies over western Canada were displaced westward and there was an absence of negative anomalies over the southeastern United States. Nonetheless, winter 1987 does show the main characteristics of a strong positive PNA pattern including the likelihood of a stronger Aleutian low.

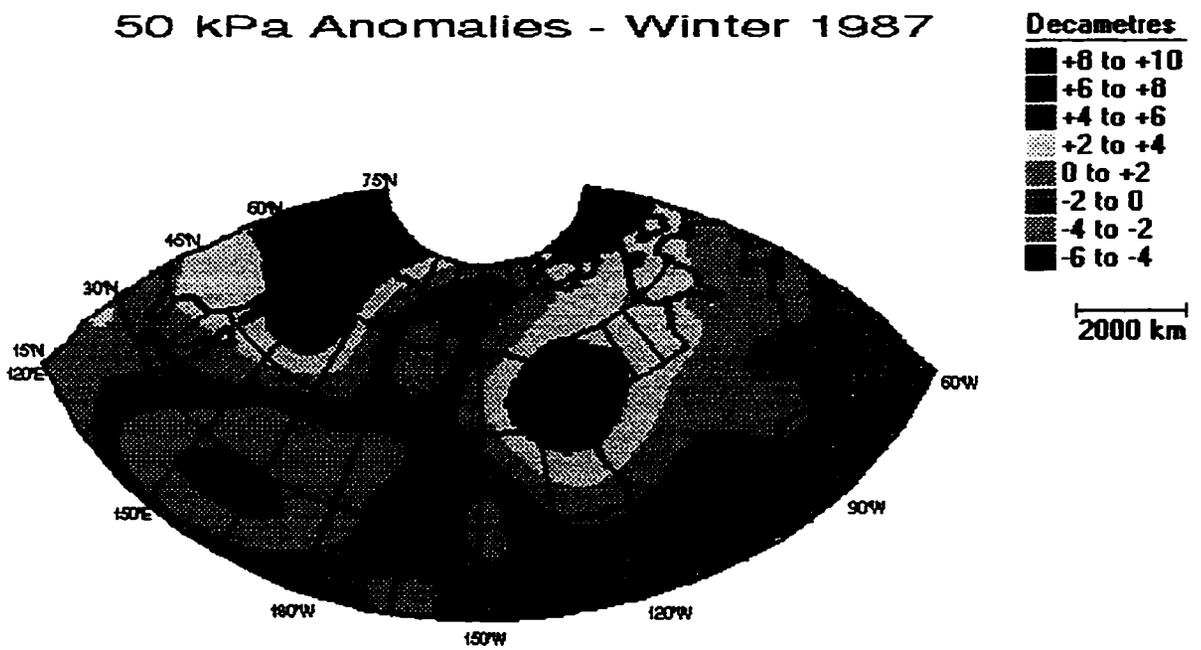

Figure 6.3: Northern Hemisphere 50 kPa Anomaly Map Showing the Positive PNA Pattern Associated with the 1986 El Niño: (Winter 1987)

6.3.1.3 NORTH PACIFIC SST ANOMALY GRADIENTS

The conceptual model suggested a stronger positive PNA pattern during winter(+4) (i.e. winter 1987) would aid in the development of a positive North Pacific SST anomaly gradient during the same winter. The positive gradient should weaken during spring(+5) to summer(+6) (i.e. spring to summer 1987), strengthen during autumn(+7) (i.e. autumn 1987) and then persist from autumn(+7) to summer(+10) (i.e. autumn 1987 to summer 1988).

Actual and standardized seasonal North Pacific SST anomaly gradients from autumn 1986 to autumn 1988 are given in Table 6.15.

Table 6.15: Seasonal North Pacific SST Anomaly Gradients Associated with the 1986 El Niño Event.

TIME PERIOD	ACTUAL SST ANOMALY GRADIENT (°C)	STANDARDIZED SST ANOMALY GRADIENT
Autumn 1986	-0.37	-0.18
Winter 1987	+2.97	+1.50
Spring 1987	+1.92	+1.25
Summer 1987	+1.85	+1.28
Autumn 1987	+2.57	+1.61
Winter 1988	+2.17	+1.13
Spring 1988	+2.17	+1.38
Summer 1988	+0.57	+0.50
Autumn 1988	-0.57	-0.30

Autumn 1986 had a negative SST anomaly gradient. However, during winter 1987, the gradient became very strong positive. It weakened slightly during spring and summer but remained very strong positive. The gradient strengthened during autumn 1987 and continued very strong positive through winter and spring 1988. It weakened during summer, but remained strong positive. It became negative during autumn 1988.

To visualize these persistent positive North Pacific SST anomaly gradients, North Pacific SST anomaly maps from winter 1987 to summer 1988 are given in Figure 6.4(a) through (g). Winter 1987 clearly shows a strong positive SST anomaly gradient consisting of a large area of anomalously cold water in the east-central North Pacific and an area of anomalously warm water along the central-west coast of North America. The pattern differs slightly from the winter(+4) composite SST anomaly map associated with El Niño events (Figure 5.2(b)) and stage two of the conceptual model of El Niño events (Figure 6.1) in that, the region of anomalously cold water was much larger and extended farther westward.

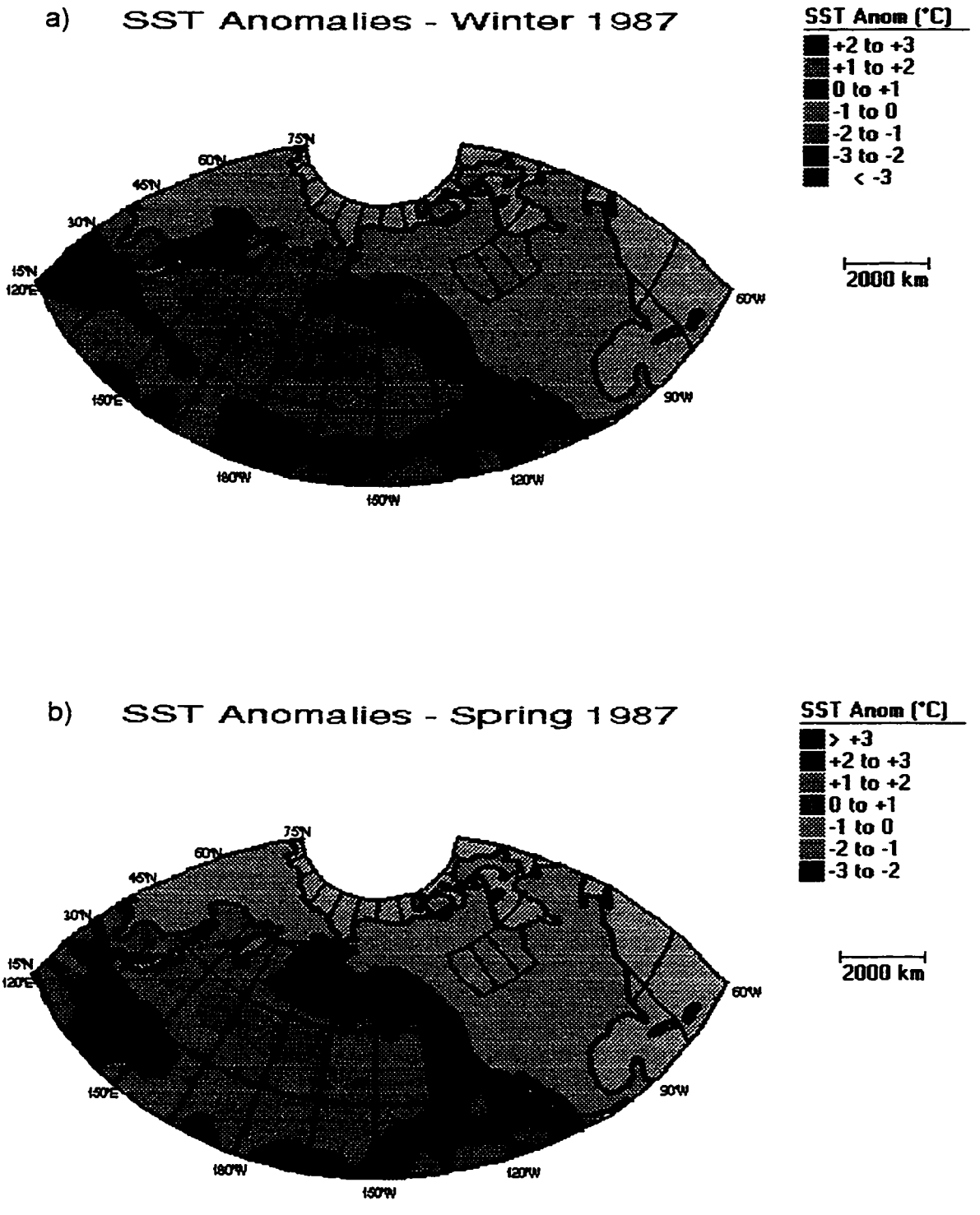

Figure 6.4: North Pacific SST Anomaly Maps Showing the Persistent Positive SST Anomaly Gradients Associated with the 1986 El Niño: a) Winter 1987 and b) Spring 1987

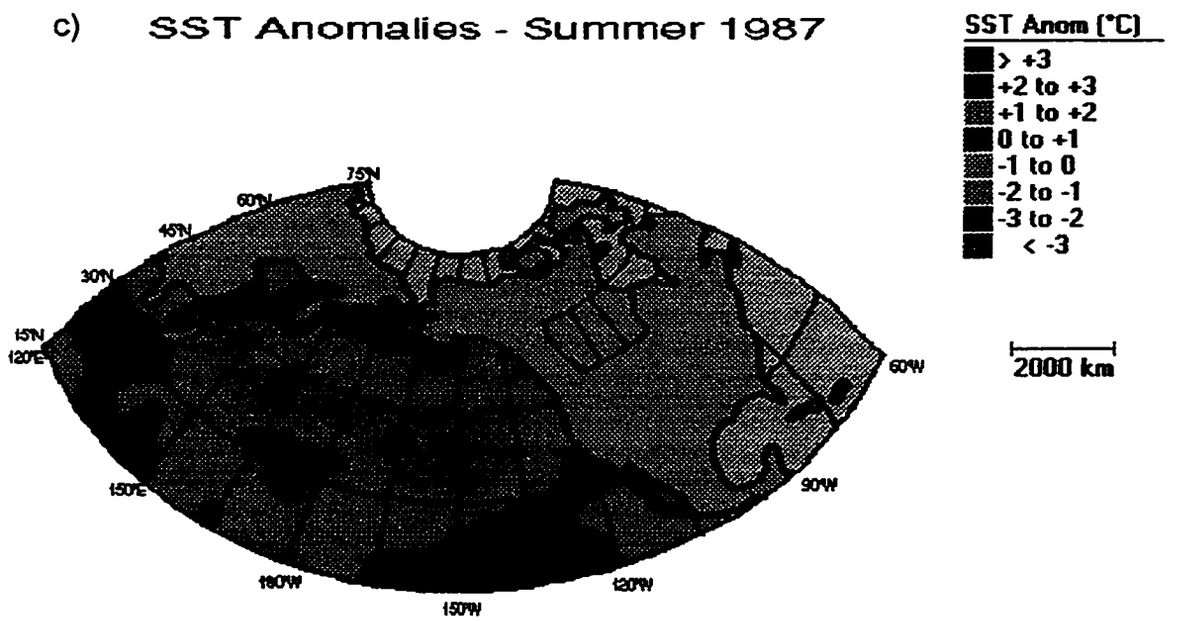

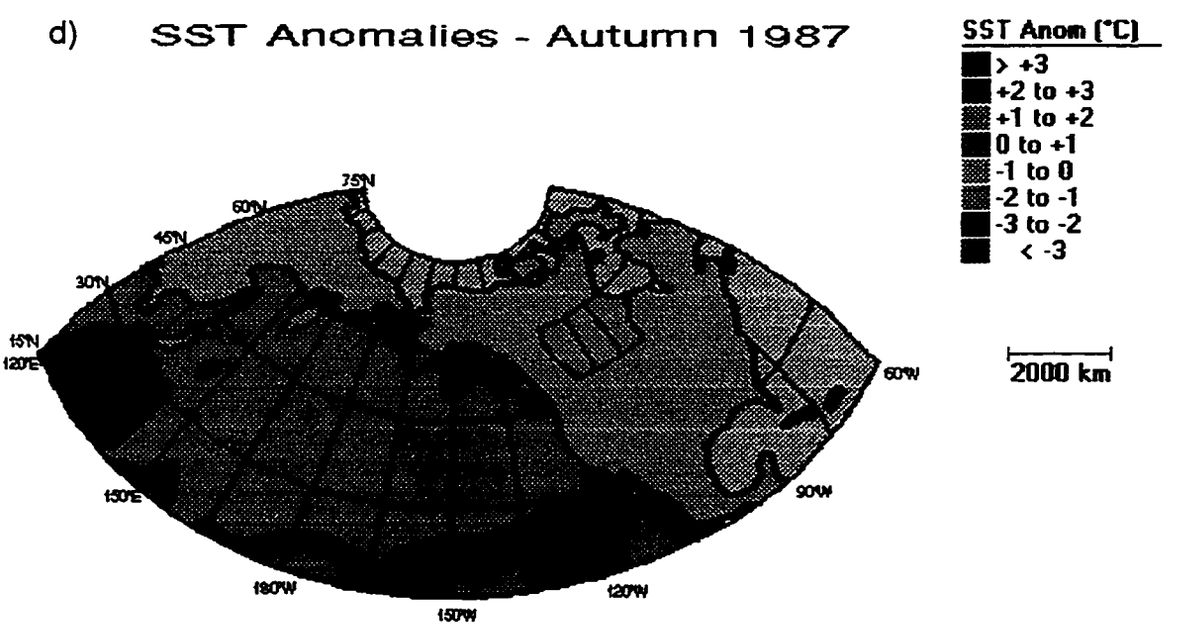

Figure 6.4: Continued: c) Summer 1987 and d) Autumn 1987

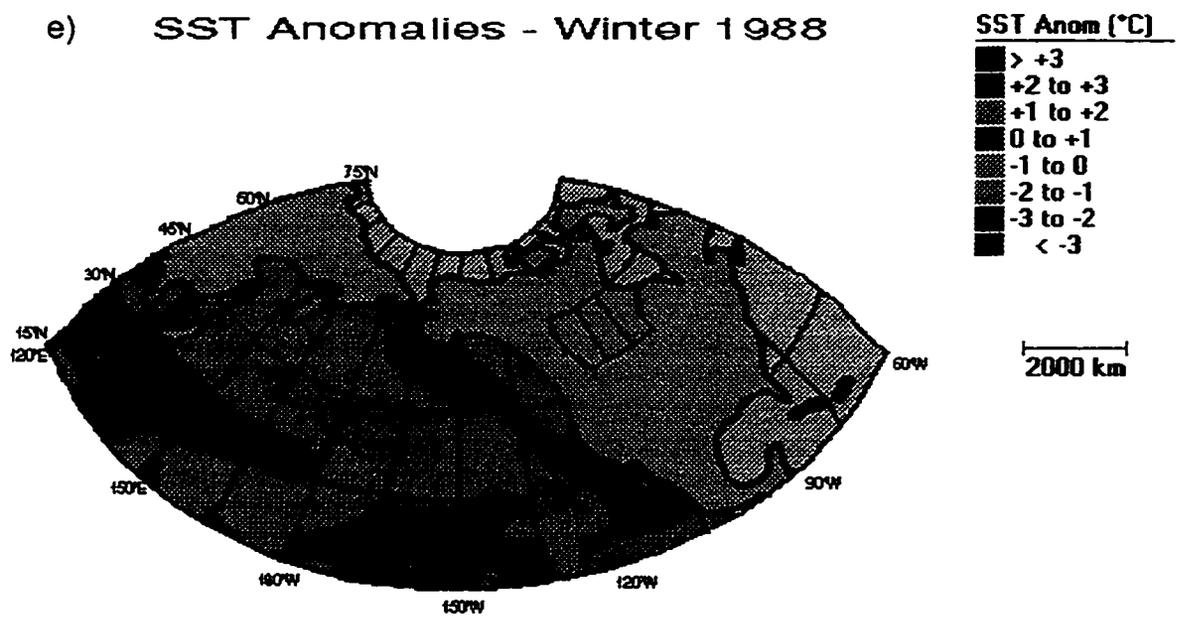

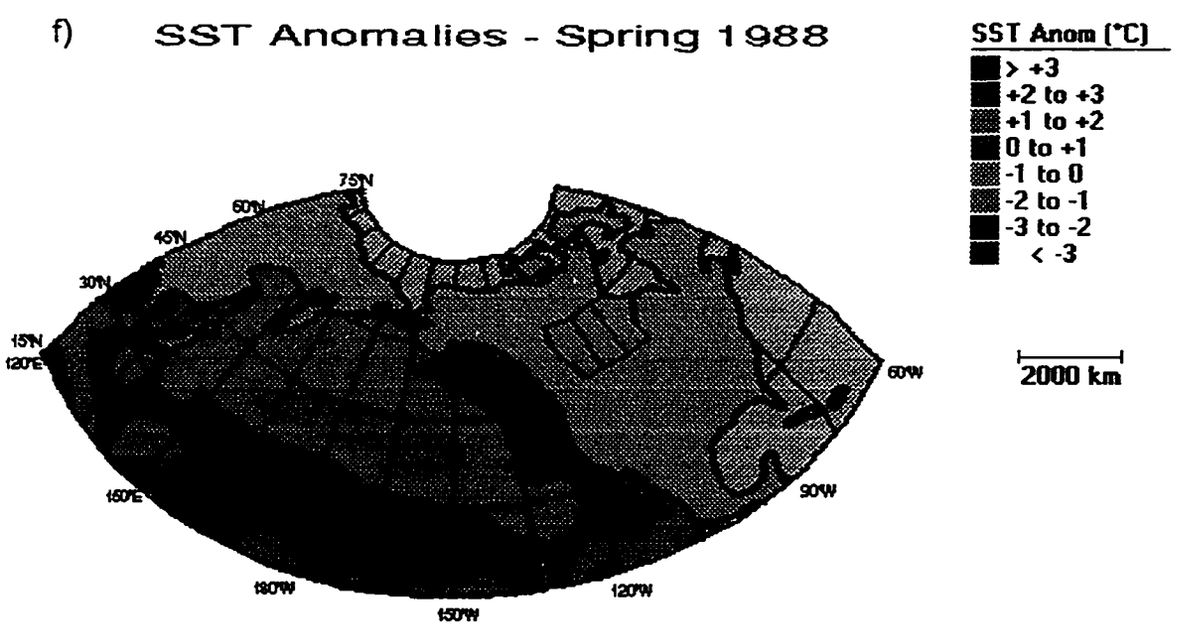

Figure 6.4: Continued: e) Winter 1988 and f) Spring 1988

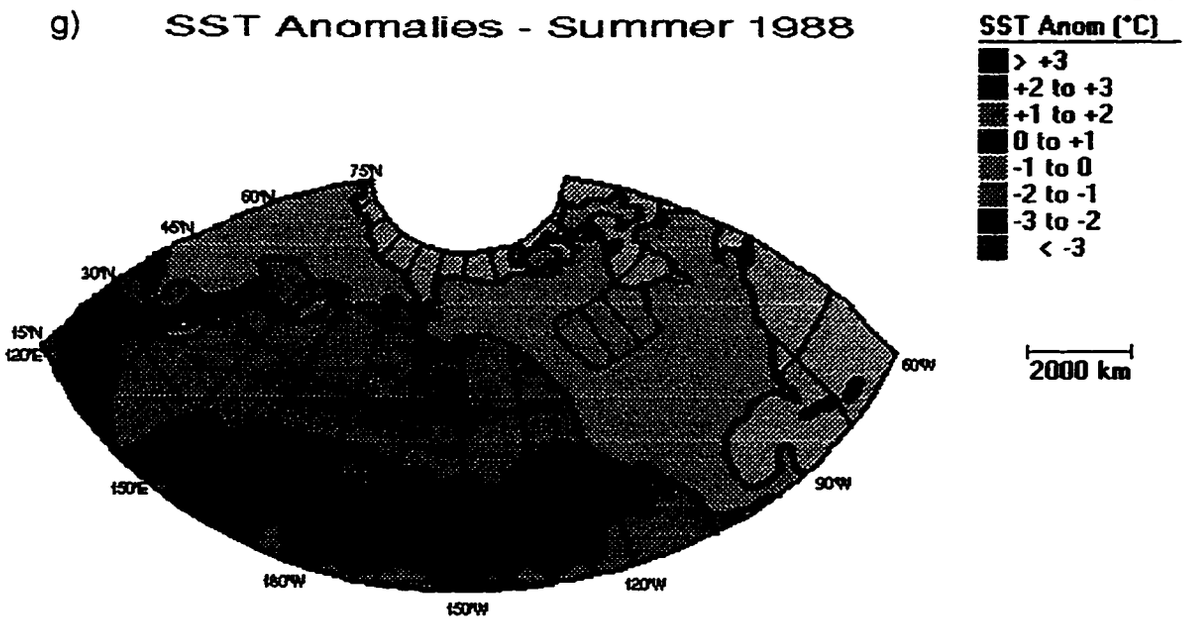

Figure 6.4: Continued: g) Summer 1988

Spring 1987 still showed a strong positive gradient including the large area of anomalously cold water. However, the positive gradient was slightly weaker because the anomalously warm water along the central-west coast of North America was weaker. During summer 1987, the anomalously warm water has disappeared. However, the anomalously cold water intensified and as a result, a strong positive SST anomaly gradient was still observed. This is similar to stage three of the conceptual model which suggested the anomalously cold water remains and the anomalously warm water disappears. However, during the 1986 El Niño, this occurred during summer(+6) (i.e. summer 1987) as opposed to spring(+5) as suggested by the model.

Autumn 1987 showed a reappearance of anomalously warm water along

the central-west coast of North America while the anomalously cold water persisted. As a result, the positive SST anomaly gradient strengthened. Stage four of the conceptual model suggested a pool of anomalously warm water detaches from the large area of positive SST anomalies in the tropical Pacific and moves up the west coast of North America via Kelvin waves during spring(+5), summer(+6) and autumn(+7). However, this is not clearly shown in the SST anomaly maps associated with the 1986 El Niño. The positive anomalies along the central-west coast of North America did disappear during summer 1987 and reappeared during autumn. However, it is not clear whether the reappearance was due to a pool of anomalous warm water moving up the west coast of North America. Further discussion of this topic will be provided in chapter 7.

Winter and spring 1988 showed the continued persistence of a stronger positive SST anomaly gradient. During summer 1988, the positive gradient weakened because the positive SST anomalies along the central-west coast of North America have disappeared. As shown in Table 6.15, the SST anomaly gradient became negative during the following autumn. Therefore, for the 1986 El Niño, a very strong positive SST anomaly gradient developed during winter 1987 and persisted through summer 1988 (seven seasons).

6.3.1.4 GROWING-SEASON AREALLY-AVERAGED 50 KPA ANOMALIES OVER THE CANADIAN PRAIRIES

It was suggested that if these persistent stronger positive SST anomaly gradients are associated with positive 50 kPa anomalies over the Prairies during June(+10), July(+10) and August(+10) (i.e. June, July

and August 1988), then a higher frequency of extended dry spells will occur during these periods. Actual and standardized areally-averaged 50 kPa anomalies over the Prairies for June, July and August 1988 are given in Table 6.16. June was associated with very strong positive 50 kPa anomalies. However, July had only weak positive anomalies and August experienced weak negative anomalies.

Therefore, the 1986 event was associated with very strong positive 50 kPa anomalies during June 1988. To visualize this upper-atmospheric anomaly pattern, Figure 6.5 shows the Northern Hemisphere 50 kPa anomaly map of June 1988. The map clearly shows positive 50 kPa anomalies over the Canadian Prairies. These positive anomalies were also centred near the area of anomalously warm water shown in the North Pacific SST anomaly maps (Figure 6.4). There was also a region of negative 50 kPa anomalies over the central North Pacific Ocean. It appears these negative anomalies were associated with the anomalously cold water in Figure 6.4. Therefore, in this case, the SST anomaly pattern may have played a role in initiating or amplifying the upper-atmospheric circulation pattern.

This 50 kPa anomaly pattern corresponded quite closely to the hypothesized upper-atmospheric flow pattern in stage six of the El Niño conceptual model (Figure 6.1), with the exception that the centre of the positive 50 kPa anomalies (i.e. ridging) and negative 50 kPa anomalies (i.e. troughing) were shifted westward. This could be due to the region of negative SST anomalies in the central North Pacific (associated with the 1986 El Niño) being much larger and displaced westward from that shown in stage six of the model.

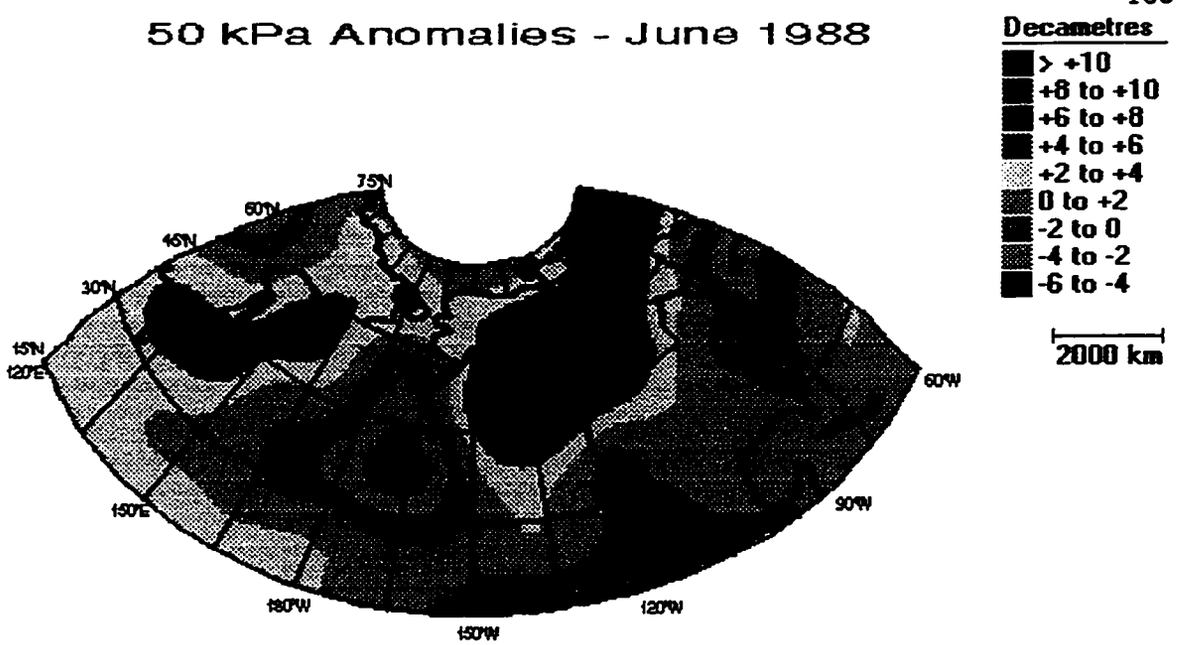

Figure 6.5: Northern Hemisphere 50 kPa Anomaly Map Showing the Positive 50 kPa Anomalies over the Canadian Prairies Associated with the 1986 El Niño: (June 1988)

6.3.1.5 GROWING-SEASON TOTAL NUMBER OF 10-DAY DRY SPELLS ON THE CANADIAN PRAIRIES

The persistent positive SST anomaly gradients and positive 50 kPa anomalies should lead to more extended dry spells and thus drier conditions on the Canadian Prairies. Table 6.17 presents the percentage of average total number of 10-day dry spells on the Canadian Prairies (as defined in chapter 5) along with standardized values for June, July, August and the total growing season of 1988. During June, there was a very strong positive standardized value. In fact, it experienced 178.4% of its normal 10-day dry spells. This result is most likely due to the very strong positive 50 kPa anomalies during this period. July

Table 6.16: Growing-Season Areally-Averaged 50 kPa Anomalies over the Canadian Prairies Associated with the 1986 El Niño Event.

TIME PERIOD	ACTUAL 50 KPA ANOMALY (dam)	STANDARDIZED 50 KPA ANOMALY
June 1988	+6.36	+2.66
July 1988	+0.22	+0.14
August 1988	-0.32	-0.12

experienced a near normal number of 10-day spells and August was slightly below normal. The total growing season showed a strong positive standardized value. Therefore, June 1988 experienced many more extended dry spells (i.e. drier conditions) than would normally occur.

6.3.1.6 SUMMARY

The preceding has examined the 1986 El Niño event as a case study demonstrating relationships between El Niño events and growing-season precipitation variations on the Canadian Prairies through a series of atmosphere - ocean teleconnections over the Pacific Ocean. The 1986 El Niño began during winter 1986, matured during winter to spring 1987 and ended around autumn 1987. This was similar to a typical El Niño event with the exception that it matured approximately one season later and lasted a couple of seasons longer. During winter 1987, a very strong positive PNA pattern developed. It is suggested the circulation associated with this pattern aided in the development of a very strong positive North Pacific SST anomaly gradient observed during the same winter. The positive gradient weakened slightly during the following spring and summer because the anomalously warm water along the central-

Table 6.17: Growing-Season Total Number of 10-Day Dry Spells on the Canadian Prairies Associated with the 1986 El Niño Event.

TIME PERIOD	PERCENTAGE OF AVERAGE TOTAL NUMBER OF 10-DAY DRY SPELLS	STANDARDIZED TOTAL NUMBER OF 10-DAY DRY SPELLS
Total 1988	112.2	+0.52
June 1988	178.4	+1.03
July 1988	103.3	+0.05
August 1988	82.1	-0.27

west coast of North America disappeared. During autumn 1987, the gradient strengthened due to the reappearance of this water. However, it was unclear whether the warm water moved up the west coast of North America via Kelvin waves as suggested by the conceptual model. The very strong positive gradient persisted through winter and spring 1988. It weakened during summer, but remained strong positive.

This persistence was associated with an upper-atmospheric flow pattern that produced very strong positive 50 kPa anomalies over the Canadian Prairies during June 1988. This period was also associated with 178.4% of normal 10-day dry spells on the Prairies. Even though the rest of the growing season months had near normal 50 kPa anomalies and number of 10-day dry spells, the very dry conditions during June led to a severe drought on the Canadian Prairies which had adverse impacts on agriculture, water resources, forestry, waterfowl and fisheries (Wheaton et al., 1988; Lawford, 1992).

6.3.2 THE 1973 LA NIÑA EVENT

6.3.2.1 SOI VALUES

Table 6.18 presents actual and standardized seasonal SOI values from winter 1973 to winter 1975 associated with the 1973 La Niña event. The SOI values became slightly positive (i.e. anomalously high pressure in the eastern and anomalously low pressure in the western tropical Pacific) during spring 1973 and highly positive during summer. The period of spring to summer 1973 likely coincided with the onset of this event which is approximately one season later than a typical La Niña described in chapter 2. The values continued to become more positive through autumn 1973 and reached their peak during winter 1974. This likely represented the mature stage of the La Niña. The values began to decrease during spring 1974 and continued this trend through summer and autumn of that year. They became negative during winter 1975 signifying the end of the event.

6.3.2.2 PNA INDICES

The conceptual model of La Niña events suggested a negative PNA pattern should occur during winter(+4) (i.e. winter 1974). Actual and standardized seasonal PNA indices from autumn 1973 to summer 1974 are presented in Table 6.19. During autumn 1973, the PNA index was positive. However, during the following winter, it became very strong negative. The negative index weakened during spring 1974 and became positive during the next summer.

Therefore, a very strong negative PNA pattern developed during the winter of 1974. To visualize this pattern, the Northern Hemisphere 50

Table 6.18: Seasonal SOI Values Associated with the 1973 La Niña Event.

TIME PERIOD	ACTUAL SOI VALUE	STANDARDIZED SOI VALUE
Winter 1973	-2.02	-1.18
Spring 1973	+0.03	+0.06
Summer 1973	+1.45	+1.15
Autumn 1973	+2.90	+1.99
Winter 1974	+3.64	+2.13
Spring 1974	+2.10	+1.96
Summer 1974	+1.05	+0.83
Autumn 1974	+1.00	+0.72
Winter 1974	-0.09	-0.05

kPa anomaly map for winter 1974 is shown in Figure 6.6. The map shows the main characteristics of a negative PNA pattern including positive height anomalies over the central North Pacific Ocean (suggesting a weaker Aleutian low), negative anomalies over western Canada and positive heights over the southeastern United States. This is similar to the winter(+4) composite 50 kPa anomaly map associated with La Niña events (Figure 5.1(b)) and stage one of the La Niña conceptual model (Figure 6.2) with the exception that during winter 1974, the three main centres of the PNA pattern were displaced westward.

6.3.2.3 NORTH PACIFIC SST ANOMALY GRADIENTS

It was suggested the stronger negative PNA pattern during winter(+4) (i.e. winter 1974) would aid in the development of a negative North Pacific SST anomaly gradient during spring(+5) (i.e. spring 1974). A higher frequency of negative SST anomaly gradients during summer(+6) to summer(+10) (i.e. summer 1974 to summer 1975) would then occur. Table 6.20 presents actual and standardized North Pacific SST anomaly

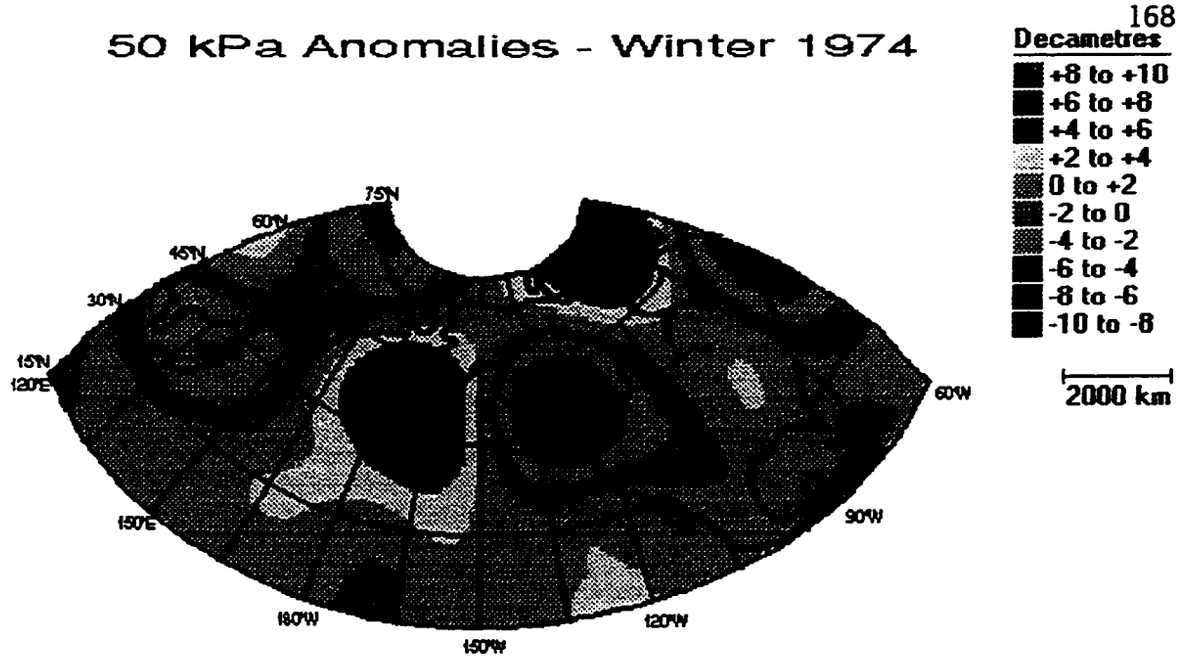

Figure 6.6: Northern Hemisphere 50 kPa Anomaly Map Showing the Negative PNA Pattern Associated with the 1973 La Niña: (Winter 1974)

gradients from winter 1974 to autumn 1975. A weak negative gradient occurred during winter 1974. The gradient strengthened during spring and this trend continued into summer. However, it turned positive during autumn 1974. A strong negative gradient was observed once again during winter 1975 and continued to strengthen through the ensuing spring and summer. It weakened slightly but still remained strong negative during autumn 1975.

Therefore, there was a higher frequency of negative gradients from spring 1974 through summer 1975 and also, a persistence of stronger negative gradients from winter through summer 1975. To visualize these gradients, North Pacific SST anomaly maps for spring 1974 to summer 1975

Table 6.19: Seasonal PNA Indices Associated with the 1973 La Niña Event.

TIME PERIOD	ACTUAL PNA INDEX	STANDARDIZED PNA INDEX
Autumn 1973	+0.12	+0.11
Winter 1974	-0.84	-1.13
Spring 1974	-0.13	-0.31
Summer 1974	+0.14	+0.09

are shown in Figure 6.7(a) through (f). Spring 1974 had a stronger negative gradient consisting of a large region of anomalously warm water in the east-central North Pacific and anomalously cold water along the central-west coast of North America. This pattern is similar to the spring(+5) composite SST anomaly map associated with La Niña (Figure 5.3) and stage two of the La Niña conceptual model (Figure 6.2). Summer 1974 also showed a strong negative gradient similar to the pattern of the preceding spring. However, during the autumn, the region of anomalously warm water in the east-central North Pacific appears to have moved northeastward towards the central-west coast of North America. As a result, the SST anomaly gradient became positive.

The region of anomalously warm water along the central-west coast of North America appeared to move back southwestward towards the east-central North Pacific during winter 1975. As a result, a strong negative SST anomaly gradient occurred during this period. During spring 1975, the warm water in the east-central North Pacific had strengthened and therefore, the negative SST anomaly gradient also strengthened. During summer, the negative gradient intensified because the cold water along the central-west coast of North America became stronger. Therefore, the

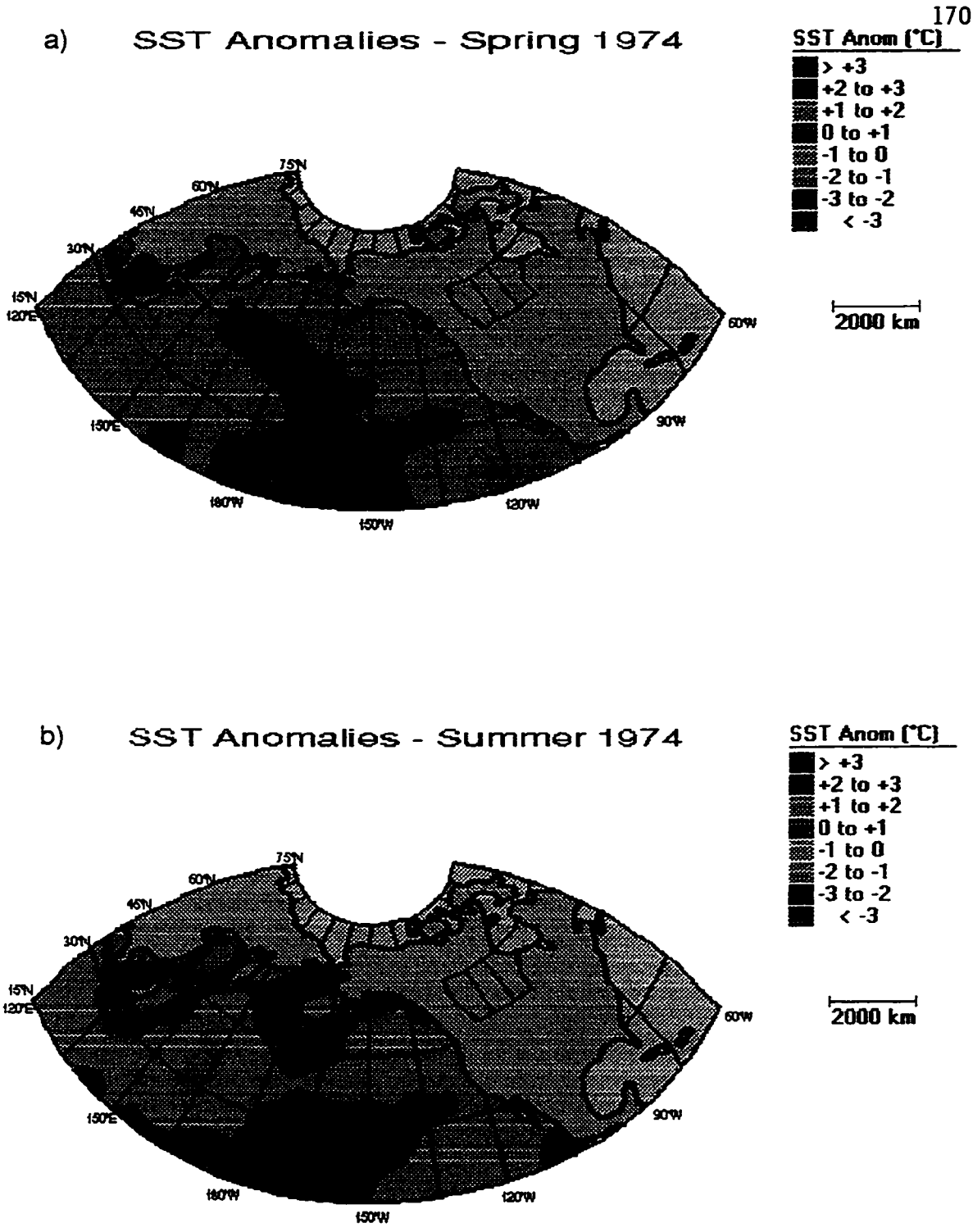

Figure 6.7: North Pacific SST Anomaly Maps Showing the Higher Frequency of Negative SST Anomaly Gradients Associated with the 1973 La Niña: a) Spring 1974 and b) Summer 1974

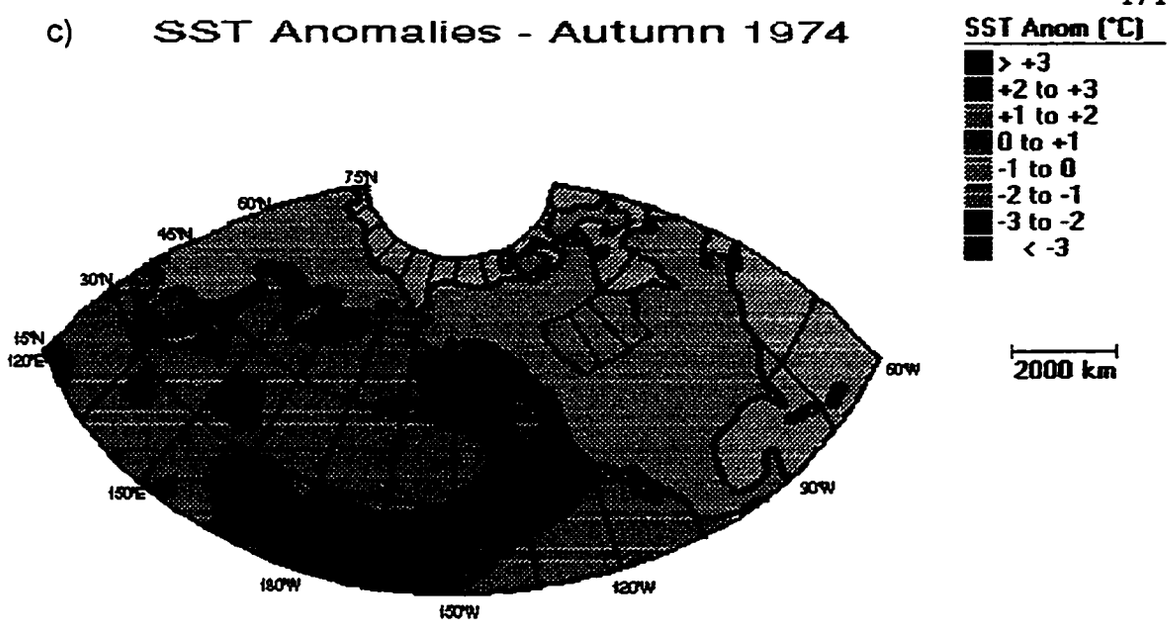

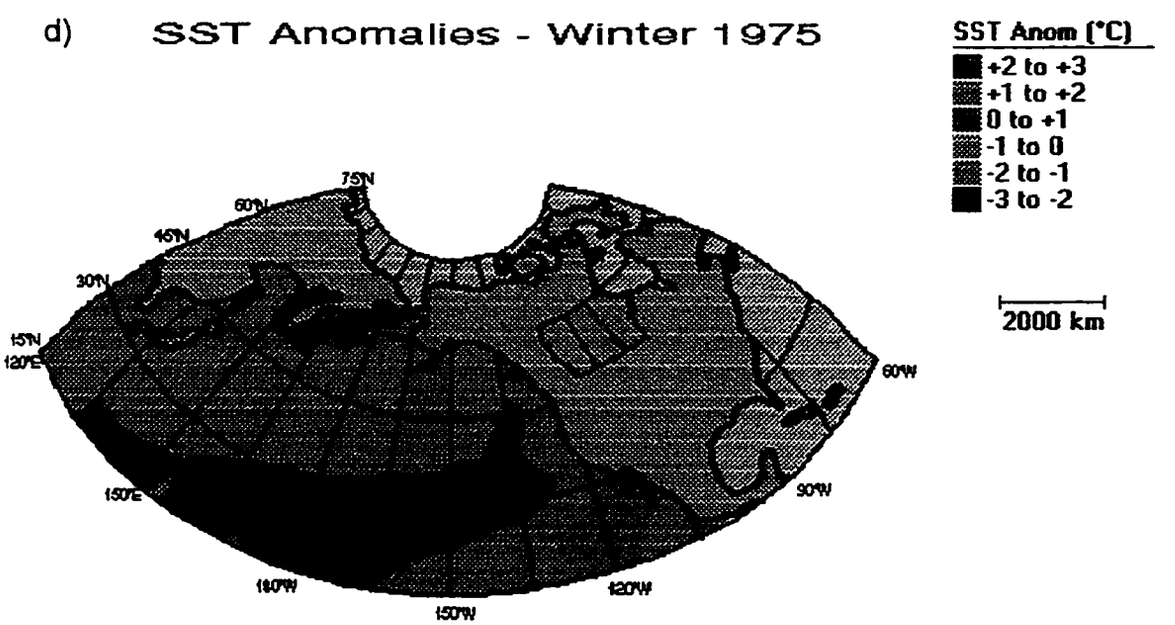

Figure 6.7: Continued: c) Autumn 1974 and d) Winter 1975

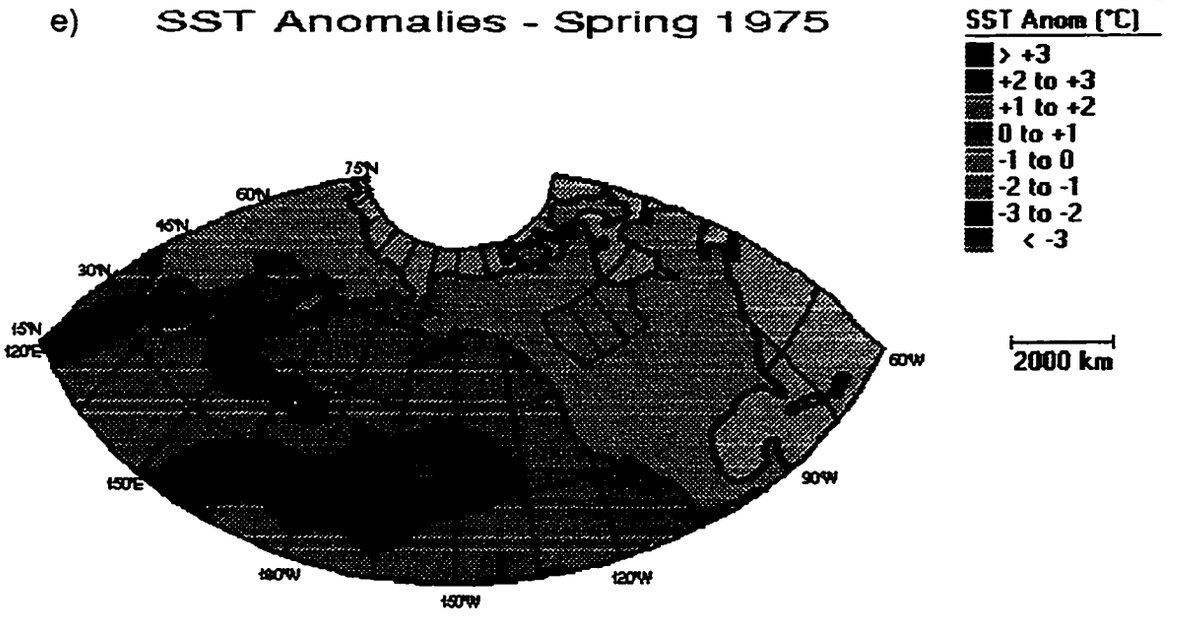

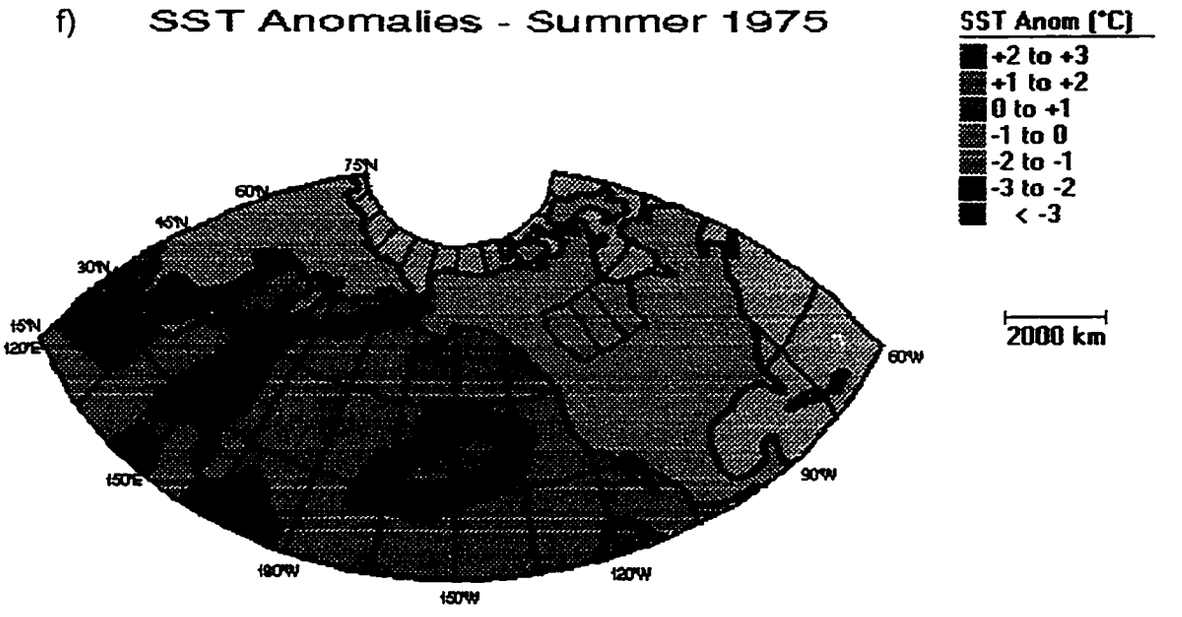

Figure 6.7: Continued: e) Spring 1975 and f) Summer 1975

Table 6.20: Seasonal North Pacific SST Anomaly Gradients Associated with the 1973 La Niña Event.

TIME PERIOD	ACTUAL SST ANOMALY GRADIENT (°C)	STANDARDIZED SST ANOMALY GRADIENT
Winter 1974	-0.57	-0.15
Spring 1974	-1.53	-0.65
Summer 1974	-1.60	-0.90
Autumn 1974	+0.47	+0.33
Winter 1975	-2.10	-0.86
Spring 1975	-2.37	-1.10
Summer 1975	-2.90	-1.72
Autumn 1975	-1.47	-0.85

SST anomaly maps in Figure 6.7 showed a higher frequency of negative SST anomaly gradients during spring 1974 to summer 1975 and also, a persistent strong negative gradient from winter to summer 1975 (three seasons).

6.3.2.4 GROWING-SEASON AREALLY-AVERAGED 50 KPA ANOMALIES OVER THE CANADIAN PRAIRIES

As suggested previously, if the higher frequency of negative North Pacific SST anomaly gradients is associated with negative 50 kPa anomalies over the Canadian Prairies during June(+10), July(+10) and August(+10) (i.e. June, July and August 1975), then fewer extended dry spells will occur during these periods. Table 6.21 presents actual and standardized areally-averaged 50 kPa anomalies over the Prairies for June, July and August 1975. Both June and August had very strong negative 50 kPa anomalies and July had weak positive anomalies.

Therefore, the 1973 La Niña event was associated with very strong negative 50 kPa anomalies over the Prairies during June and August 1975.

Table 6.21: Growing-Season Areally-Averaged 50 kPa Anomalies over the Canadian Prairies Associated with the 1973 La Niña Event.

TIME PERIOD	ACTUAL 50 KPA ANOMALY (dam)	STANDARDIZED 50 KPA ANOMALY
June 1975	-2.89	-1.21
July 1975	+0.51	+0.33
August 1975	-4.16	-1.63

To visualize the upper-atmospheric anomaly pattern during one of these months, the Northern Hemisphere 50 kPa anomaly map of June 1975 is shown in Figure 6.8. The map clearly shows negative 50 kPa anomalies over the Canadian Prairies. It also shows a region of positive anomalies over the east-central North Pacific Ocean. It appears these positive anomalies were associated with the positive SST anomalies in Figure 6.7(d) through (f). Therefore, in this case, the SST anomaly pattern may have played a role in initiating or amplifying the upper-atmospheric circulation pattern. Furthermore, the 50 kPa anomaly map of June 1975 is almost exactly opposite to the one of June 1988 (Figure 6.5) with respect to the locations of positive and negative 50 kPa anomalies over the eastern North Pacific/western North American region. The only exception was that the 50 kPa anomalies during June 1988 were displaced westward. The 50 kPa anomaly pattern of June 1975 also corresponds quite closely to the hypothesized upper-atmospheric flow pattern shown in stage four of the La Niña conceptual model (Figure 6.2). This included ridging (positive 50 kPa anomalies) over the eastern North Pacific and troughing (negative 50 kPa anomalies) over the Canadian Prairies.

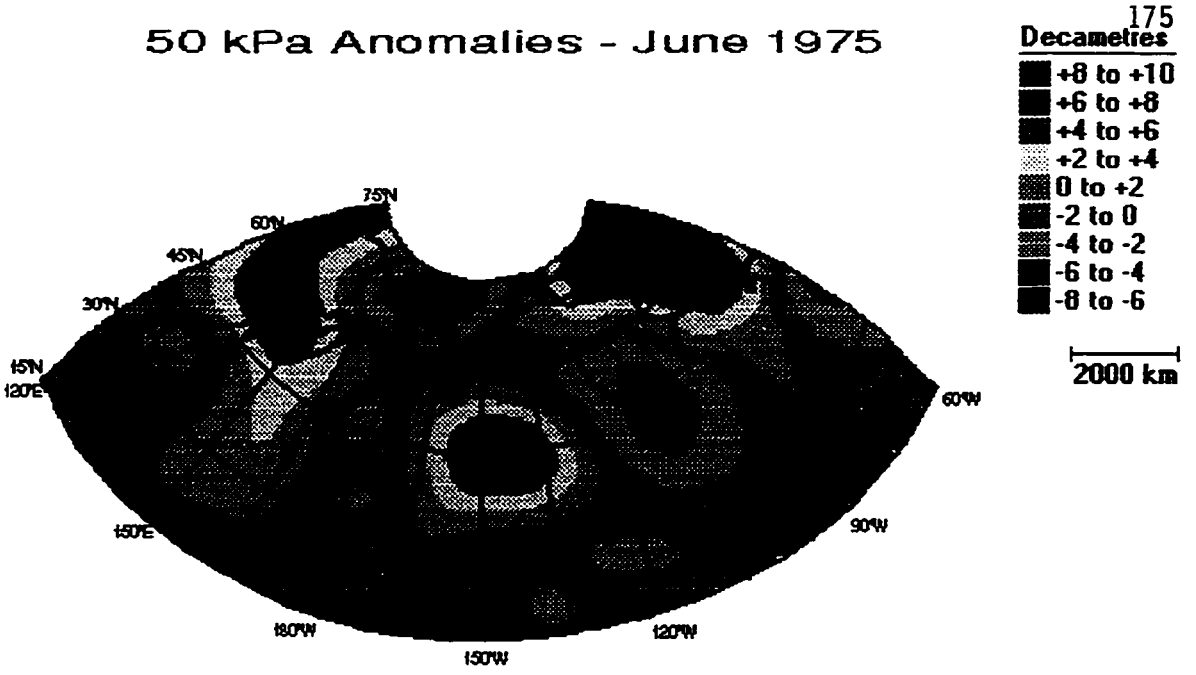

Figure 6.8: Northern Hemisphere 50 kPa Anomaly Map Showing the Negative 50 kPa Anomalies over the Canadian Prairies Associated with the 1973 La Niña: (June 1975)

6.3.2.5 GROWING-SEASON TOTAL NUMBER OF 10-DAY DRY SPELLS ON THE CANADIAN PRAIRIES

The higher frequency of negative SST anomaly gradients along with negative 50 kPa anomalies should lead to fewer extended dry spells on the Canadian Prairies. Table 6.22 presents the percentage of average total number of 10-day dry spells and standardized values on the Prairies for the June, July, August and the total growing season of 1975. June, August and the total growing season all experienced strong negative standardized values. In fact, June had only 43.8% of its normal 10-day dry spells, August 28.8% and the total growing season 58.0%. This result is likely due to the very strong negative 50 kPa anomalies during

Table 6.22: Growing-Season Total Number of 10-Day Dry Spells on the Canadian Prairies Associated with the 1973 La Niña Event.

TIME PERIOD	PERCENTAGE OF AVERAGE TOTAL NUMBER OF 10-DAY DRY SPELLS	STANDARDIZED TOTAL NUMBER OF 10-DAY DRY SPELLS
Total 1975	58.0	-0.76
June 1975	43.8	-0.69
July 1975	99.0	-0.01
August 1975	28.8	-0.73

June and August. On the other hand, July showed near normal 10-day dry spells.

6.3.2.6 SUMMARY

The preceding examined the 1973 La Niña event as a case study showing relationships between La Niña events and growing-season precipitation variations on the Canadian Prairies through a series of atmosphere - ocean teleconnections over the Pacific Ocean. The event began during spring to summer 1973, matured during winter 1974 and terminated around autumn 1974. This was similar to a typical La Niña with the exception that it began approximately one season later and lasted a couple of seasons longer. During winter 1974, a very strong negative PNA pattern developed. It is suggested the circulation associated with this pattern aided in the development of a stronger negative North Pacific SST anomaly gradient observed during spring 1974. This negative gradient weakened slightly during summer 1974 and was positive during the next autumn. However, it became strong negative during winter 1975 and persisted through summer 1975. Therefore, there

was a higher frequency of negative SST anomaly gradients during spring 1974 to summer 1975 and even the presence of a persistent strong negative gradient from winter through summer 1975.

This higher frequency and persistence of negative gradients was associated with very strong negative 50 kPa anomalies over the Canadian Prairies during June and August 1975. These periods (along with the total growing season) also experienced many fewer 10-day dry spells, a situation representative of non-drought conditions on the Prairies.

CHAPTER 7

DISCUSSION

This chapter discusses atmosphere - ocean teleconnections over the Pacific Ocean associated with ENSO events and growing-season precipitation on the Canadian Prairies. It considers the physical processes involved and proposes explanations why some ENSO events corresponded very well to the conceptual models presented in chapter 6, while others did not. It also suggests areas of further research to improve our understanding of atmosphere - ocean teleconnections as they relate to ENSO events and growing-season precipitation on the Prairies. The first two sections discuss the teleconnections associated with El Niño and La Niña events respectively. The chapter concludes with a brief discussion of the timing of ENSO events and why May tends to differ from the rest of the growing season.

7.1 TELECONNECTIONS BETWEEN EL NIÑO EVENTS AND GROWING-SEASON PRECIPITATION VARIATIONS ON THE CANADIAN PRAIRIES

The analysis presented in the preceding chapters suggested a relationship between El Niño and growing-season precipitation variations on the Canadian Prairies. It was proposed this occurred through a series of atmosphere - ocean teleconnections over the Pacific Ocean. These teleconnections and possible physical explanations for their existence are detailed in chapter 6 (section 6.1.1 and Figure 6.1). This section further discusses these teleconnections as they pertain to this study.

7.1.1 EL NIÑO EVENTS AND POSITIVE PNA PATTERNS

The first atmosphere - ocean teleconnection (i.e. stage one of Figure 6.1) involved the development of positive PNA patterns during the autumn or winter following the onset of El Niño events (i.e. autumn(+3) to winter(+4)). The physical basis for this teleconnection was detailed in chapter 6. Of the ten El Niño events occurring between 1948 and 1991, eight were associated with strong or very strong positive PNA patterns during autumn(+3) to winter(+4) indicating a consistent response between the two variables.

Two events were associated with negative PNA patterns. There may be several reasons for this occurrence. Firstly, differences between El Niño events in terms of onset, evolution, amplitude, duration and spatial extent are significant in determining the teleconnection patterns associated with individual events (Rasmusson et al., 1983; Fu et al., 1986; Ropelewski and Halpert, 1986,1987,1989; Philander, 1990; Diaz and Kiladis, 1992). Secondly, the Rossby wave trains generated (due to anomalous heating over the eastern tropical Pacific associated with El Niño) are often sensitive to the atmospheric flow onto which they are superimposed. Therefore, the circulation prior to the forcing can affect the atmospheric response (Wallace and Gutzler, 1981). For example, an El Niño can amplify an already existing positive PNA pattern making it even stronger. Conversely, a negative PNA pattern can be dampened by the atmospheric forcing from the El Niño.

There are several factors (other than tropical forcing due to El Niño) that affect upper-atmospheric flow patterns over the North Pacific/North American region and thus the development of positive PNA

patterns. These include regional scale orography, land/sea heating contrasts and barotropic instability (Lau, 1981; Wallace and Gutzler, 1981; Leathers et al., 1991) and the presence of other larger scale teleconnection patterns such as the North Pacific Oscillation (Wallace and Gutzler, 1981). These factors could explain the many occurrences of stronger positive PNA patterns during autumns and winters not associated with El Niño (see Appendix C). Therefore, strong positive PNA patterns are not exclusive to El Niño events. However, the effect of these factors on the development of positive PNA patterns is outside the scope of this analysis and as a result, additional research in this area is required. Even though these research needs exist, it was shown that when El Niño events occurred, the majority (80%) were associated with stronger positive PNA patterns during the autumn or winter following their onset indicating a consistent response between El Niño events and positive PNA patterns.

7.1.2 POSITIVE PNA PATTERNS AND POSITIVE NORTH PACIFIC SST ANOMALY GRADIENTS

The second atmosphere - ocean teleconnection (i.e. stage two of Figure 6.1) included a relationship between positive PNA patterns and North Pacific SST anomaly patterns consisting of anomalously cold water in the east-central North Pacific and anomalously warm water along the central-west coast of North America (i.e. positive North Pacific SST anomaly gradients). It was suggested that the circulation associated with positive PNA patterns (in particular, the stronger Aleutian low) (Horel and Wallace, 1981; Yarnal and Diaz, 1986) aided in the

development of these SST anomaly patterns shortly after the occurrence of positive PNA patterns (i.e. winter(+4) to spring(+5)). In fact, all eight El Niño events having positive PNA patterns were also associated with either strong or very strong positive SST anomaly gradients during winter(+4).

Therefore, positive PNA patterns likely aid in the development of positive SST anomaly gradients. However, many complex atmosphere - ocean interactions are involved. For instance, the occurrence of positive SST anomaly gradients prior to the development of positive PNA patterns, suggests the latter only aided in the amplification of the SST patterns. Since mid-latitude SST anomalies also affect overlying atmospheric circulation, the existence of positive SST anomaly gradients likely contributes to the development of positive PNA patterns through positive ocean - atmosphere feedback processes (Namias, 1963; Trenberth, 1975; Davis, 1976; Haworth, 1978; Namias and Cayan, 1981; Frankignoul, 1985; Namias et al., 1988).

In fact, three of eight El Niño events having positive PNA patterns and positive SST anomaly gradients during winter(+4) (i.e. 1957, 1963 and 1969) had positive gradients prior to winter(+4). During these events, positive SST anomaly gradients likely aided the development of positive PNA patterns which in turn amplified the SST gradients (i.e. through ocean - atmosphere feedbacks). However, the other five events (i.e. 1953, 1965, 1976, 1982 and 1986) had negative SST anomaly gradients prior to winter(+4). During these events, positive PNA patterns probably played a role in the initiation of the positive gradients. Even though there is a very consistent relationship between

El Niño events having positive PNA patterns and positive SST anomaly gradients during winter(+4), the physical processes involved are not entirely clear.

Note that strong positive North Pacific SST anomaly gradients (i.e. standardized values greater than +0.50) also occurred during winters not associated with El Niño events having positive PNA patterns. These included the winters of 1960, 1961, 1980 and 1981 (see Appendix D). However, these winters were associated with strong positive PNA patterns (see Appendix C) and therefore, positive PNA patterns likely played a role in the development of these positive gradients.

7.1.3 PERSISTENCE OF POSITIVE NORTH PACIFIC SST ANOMALY GRADIENTS

Once positive SST anomaly gradients associated with El Niño developed, they persisted for several seasons. There were several characteristics of this persistence (i.e. stages three, four and five of Figure 6.1). Firstly, following the development of positive gradients during winter(+4), they weakened (but remained positive) during spring(+5) and summer(+6) (i.e. stage three of Figure 6.1). The weakening was due to the disappearance of the anomalously warm water along the central-west coast of North America.

The eight El Niño events having positive PNA patterns and positive SST anomaly gradients during winter(+4), showed a general tendency of weakening during spring(+5) and summer(+6). However, not all of the events corresponded to the conceptual model. For the events of 1963 and 1969, the gradients became negative during spring(+5) and summer(+6) and remained negative for several seasons. The events of 1953, 1965 and 1976

agreed with the model because the positive gradients weakened, but remained positive, during spring(+5) and summer(+6) (presumably due to the disappearance of anomalously warm water). During the events of 1957, 1982 and 1986, the positive gradients did not weaken (i.e. they continued strong positive). However, the 1986 El Niño case study showed the anomalously warm water weakened during spring 1987 (i.e. spring(+5)) and eventually disappeared during summer (i.e. summer(+6)). The SST anomaly gradient remained strong positive because the anomalously cold water in the east-central North Pacific intensified (see Figure 6.4(b) and (c)).

In most cases, the anomalously warm water likely disappeared and the anomalously cold water persisted. However, there were also cases where the positive gradients became negative. The reasons for the persistence of some SST anomalies and the disappearance of others are not entirely clear. As described in chapter 6, several studies observed that once produced, North Pacific SST anomalies tend to persist for several seasons, or even several years, due to the large thermal capacity and slow movement of the ocean (Davis, 1976; Namias and Cayan, 1981; Namias et al., 1988). This could explain the persistence of cold water in the east-central North Pacific. A possible explanation of the disappearance of the anomalously warm water is that it is much smaller in extent than the anomalously cold pool and therefore, less likely to persist for a long period. Furthermore, (as shown by the correlation and composite analyses), the positive PNA patterns associated with El Niño events disappear following winter(+4). As a result, the circulation around the Aleutian low is weakened, likely aiding in the disappearance

of the anomalously warm water.

Many complex ocean - atmosphere interactions acting on a variety of time and space scales affect the initiation, persistence and decay of mid-latitude SST anomalies. These include heat exchanges with the atmosphere, vertical mixing of the ocean due to turbulence, wind driven vertical and horizontal currents (including meridional temperature advection by anomalous ocean currents), entrainment of deeper water into the mixed layer, etc. (Namias, 1972; Haney, 1980; Frankignoul, 1985). However, the effects of these processes on the generation, persistence and decay of SST anomalies in the North Pacific Ocean associated with El Niño are not part of this study. It is recommended that additional investigation of these processes would aid in the understanding of why the cold water in the east-central North Pacific tends to persist and the warm water along the central-west coast of North America disappears, and also why during some El Niño events (i.e. 1963 and 1969), the positive SST anomaly gradients of winter(+4) became negative during spring(+5) and remained negative for several seasons.

The second characteristic of the persistence of positive SST anomaly gradients included an anomalously warm pool of water detaching from the large region of warm SST anomalies in the eastern tropical Pacific (associated with El Niño) and moving up the west coast of North America during spring(+5) to autumn(+7) (i.e. stage four of Figure 6.1). It was suggested this was due to sub-surface Kelvin waves which often move up the west coast of North America during El Niño (McCreary, 1976; Enfield and Allen, 1980; Clarke, 1983; Emery and Hamilton, 1985; Johnson and O'Brien, 1990). Note that the warm water does not physically move up

the coast but rather, the sub-surface waves act to depress the thermocline and thus inhibit the normal cold upwelling along the west coast of North America. As a result, higher than normal SSTs are associated with these waves. By autumn(+7), the Kelvin waves and associated warm water have reached the central-west coast of North America. During the entire period (i.e. spring(+5) to autumn(+7)), the anomalously cold water in the east-central North Pacific continued to persist. Therefore, by autumn(+7), strong positive SST anomaly gradients should be observed.

Six of eight events having positive PNA patterns and positive SST anomaly gradients during winter(+4), also had positive SST anomaly gradients during autumn(+7). During three events (i.e. 1953, 1965 and 1976), the gradients weakened during spring(+5) and summer(+6) and strengthened during autumn(+7), thus indicating the reappearance of anomalously warm water along the central-west coast of North America. During the events of 1957, 1982 and 1986, strong positive gradients persisted from spring(+5) through autumn(+7). However, the 1986 El Niño case study did show the reappearance of anomalously warm water along the central-west coast of North America during autumn 1987 (i.e. autumn(+7)) (see Figure 6.4(d)).

A tendency for anomalously warm water to reappear along the central-west coast of North America during autumn(+7) was indicated. However, it is not clear whether the reappearance is due to Kelvin waves moving up the west coast of North America. The composite analysis in chapter 5 (Figure 5.2(c), (d) and (e)) indicated that a pool of anomalously warm water became detached from the large region of high

SSTs in the tropical Pacific, and then moved up the west coast of North America during spring(+5), summer(+6) and autumn(+7). However, it was difficult to determine whether this occurred during the 1986 El Niño (see Figure 6.4(b), (c) and (d)).

There is evidence that Kelvin waves can be responsible. For example, the large region of anomalously warm water associated with the 1982 El Niño that moved up the west coast of North America during spring and summer 1983, was attributed in part to northward moving Kelvin waves. However, it was not clear whether the anomalously warm water was due entirely to the presence of Kelvin waves, or if other oceanic and atmospheric processes aided in its development and propagation (Norton et al., 1985). Characteristics such as onset, evolution, amplitude, duration and spatial extent of individual El Niño events could control whether northward moving Kelvin waves are generated. The role of Kelvin waves in the development of North Pacific SST anomaly patterns associated with individual El Niño events clearly requires more investigation.

The final characteristic included the persistence of strong positive gradients from autumn(+7) through summer(+10) (i.e. stage five of Figure 6.1). All six El Niño events with positive PNA patterns and persistent positive SST anomaly gradients from winter(+4) through autumn(+7), were associated with positive gradients during winter(+8). During spring(+9), only four (i.e. 1957, 1976, 1982 and 1986) had positive gradients, however, all were strongly positive. During summer(+10), only the events of 1976 and 1986 had positive gradients. Even though all events did not have positive gradients through

summer(+10), they had persistent positive gradients for very long periods. This included six seasons for the events of 1953 and 1965, seven for those of 1957 and 1982 and eight for those of 1976 and 1986.

The reasons for this North Pacific SST anomaly pattern often persisting for such long periods are not entirely clear, although it has often been observed (Davis, 1976; Namias et al., 1988; Alexander, 1990,1992; Yongping and McBean, 1991; Bonsal et al., 1993). As alluded to previously, several oceanic and atmospheric factors acting on a variety of time and space scales affect the initiation, persistence and decay of mid-latitude SST anomalies. Since six of the eight El Niño events having positive PNA patterns were also associated with persistent positive North Pacific SST anomaly gradients from winter(+4) through at least winter(+8) (and in some cases through summer(+10)), there appears to be a relationship between El Niño and persistent positive gradients.

Persistent positive SST anomaly gradients (i.e. at least four seasons) were also observed during periods not associated with El Niño events. They occurred during autumn 1960 through summer of 1961, winter of 1963 through winter of 1964 and autumn of 1979 through summer of 1981 (see Appendix D). However, at the beginning of each of these, there was a strong positive PNA index that likely aided in the initiation of the persistent gradients.

7.1.4 PERSISTENT POSITIVE NORTH PACIFIC SST ANOMALY GRADIENTS AND GROWING-SEASON UPPER-ATMOSPHERIC CIRCULATION PATTERNS OVER THE CANADIAN PRAIRIES

The final atmosphere - ocean teleconnection suggested that if

persistent positive SST anomaly gradients in the North Pacific Ocean are associated with positive 50 kPa anomalies (ridging) over the Canadian Prairies during June(+10), July(+10) and August(+10), more extended dry spells and thus drier conditions occur on the Prairies (i.e. stage six of Figure 6.1). However, from this analysis, there was no clear evidence that the SST anomaly gradients caused the positive 50 kPa anomalies over the Prairies.

There were some indications of a causal effect. For example, the 1986 El Niño case study showed very strong positive 50 kPa anomalies over the Canadian Prairies during June 1988 (i.e. June(+10)). The upper-atmospheric flow pattern was similar to stage six of Figure 6.1. The similarity included positive 50 kPa anomalies to the east of the positive SST anomalies (i.e. over the Canadian Prairies) and negative 50 kPa anomalies to the east of the negative SST anomalies (see Figure 6.5). The pattern was also indicative of the results of both observational and numerical modelling studies of relationships between North Pacific SST anomalies and upper-atmospheric flow patterns (Davis, 1976; Huang, 1978; Chervin, 1980; Palmer and Sun, 1985; Lau and Nath, 1990; Bonsal et al., 1993). In addition, four of six El Niño events having positive PNA patterns and persistent positive SST anomaly gradients (i.e. 1953, 1965, 1982 and 1986) were also associated with strong positive 50 kPa anomalies over the Prairies during either June(+10), July(+10) or August(+10). However, the strong positive anomalies were not consistent through the entire period.

There are several considerations to take into account. For instance, factors other than North Pacific SST anomaly patterns affect

upper-atmospheric flow patterns and thus ridging or troughing over the Canadian Prairies. These include soil moisture anomalies (Ookouchi et al., 1984; Oglesby and Erickson, 1989; Oglesby, 1991), anomalous snow cover and sea ice conditions over Northern Canada and the Arctic Ocean (Namias, 1962; Roads, 1981; Kukla, 1981; Walsh et al., 1982; Ripley, 1991), solar activities (Johnson and Eunus, 1964; Currie and Venkatarangan, 1978), volcanic eruptions (Skinner, 1985; Shabbar, 1993) and orographic influences generated by the Canadian Rockies (Boffi, 1949; Bolin, 1950).

Another consideration involves the variable used to describe 50 kPa anomalies over the Prairies (i.e. monthly areally-averaged 50 kPa anomalies). As outlined in chapter 5, monthly data (which were used for the correlation and composite analyses) may not accurately describe upper-atmospheric flow patterns because persistent 50 kPa anomalies may not occur during the entire month. For example, a particular month may have strong positive 50 kPa anomalies for the first two weeks and the rest of the month had near normal or even negative anomalies. The overall monthly 50 kPa anomaly is therefore lowered. However, the strong positive anomalies during the first two weeks may have been sufficient to initiate an extended dry spell on the Prairies. Furthermore, in any month, persistent 50 kPa anomalies may not cover the very large Canadian Prairie study area. Since the data are areally-averaged, the overall 50 kPa anomaly value is affected.

Characteristics of the persistent SST anomaly gradients can also be a factor. For example, the region of anomalously cold water in the east-central North Pacific is much larger than the region of warm water

along the central-west coast of North America. Therefore, the cold water likely has a greater influence on upper-atmospheric flow patterns. Many complex atmosphere - ocean feedback interactions are also involved in relationships between mid-latitude SST anomalies and upper-atmospheric circulation patterns. In particular, the role of these persistent SST anomalies in anomalous heat transfers (especially latent and sensible) to the atmosphere (which can have a major effect on upper-atmospheric flow patterns) (Frankignoul, 1985; Zhao and McBean, 1986; Cayan, 1992a,1992b) is unknown. Smaller scale processes including diabatic heating, baroclinic eddies and atmospheric convection, as well as larger scale processes such as meridional and horizontal temperature advection also affect atmosphere - ocean interactions and thus upper-atmospheric circulation patterns (Chervin, 1980; Frankignoul, 1985; Palmer and Sun, 1985; Lau and Nath, 1990).

7.1.4.1 NUMERICAL MODELLING RESULTS

To further examine relationships between North Pacific SST anomalies and upper-atmospheric flow patterns over the Canadian Prairies, numerical model simulations were carried out using the Canadian Meteorological Centre (CMC) Global Spectral numerical weather prediction model in Dorval, Quebec. The model includes 21 atmospheric levels and has a horizontal resolution of approximately 1.4° latitude by 1.4° longitude, carrying out integrations at half-hourly time steps. A more detailed description (including the physics) of the model is given in the *CMC Reference Guide* (1994).

Two simulations were carried out using separate initial

conditions. Each had a prescribed North Pacific SST anomaly pattern consisting of negative SST anomalies in the east-central North Pacific and positive anomalies along the central-west coast of North America (i.e. a positive North Pacific SST anomaly gradient) (Figure 7.1). The centre of the negative and positive SST anomalies had values of -2.5°C and +2.0°C respectively. Therefore, the SST anomaly gradient of this pattern is +4.5°C (i.e. +2.0°C minus -2.5°C) which closely corresponded to the highest seasonal SST anomaly value occurring during the study period (i.e. +3.97°C in spring 1983). To maximize the effect of these SST anomalies, the area encompassed was slightly larger than shown in Figure 1.1 and in stage six of Figure 6.1 (see Figure 7.1).

The first SST anomaly run used the initial conditions of May 19, 1979 while the second those of May 20, 1992. The initial conditions included geopotential height, air temperature, wind components, relative humidity and sea-level pressure. These conditions were used because at the time of the model runs (i.e. March, 1993), they were the only ones archived at CMC that coincided closely with the growing season on the Canadian Prairies. For each simulation, a control run was also carried out and used as comparisons to the SST anomaly runs. Each run was 50 days with output generation once a day. However, the first 20 days were required for the model to adjust to initial conditions (i.e. to reach equilibrium) and therefore, were not considered (Ritchie, 1993). The SSTs were fixed (i.e. they were not allowed to change) and consisted of average May SST values. Therefore, for both control runs, the North Pacific SST anomalies for the entire 50 days were 0°C (i.e. average May) while for both SST anomaly runs, they included the prescribed SST

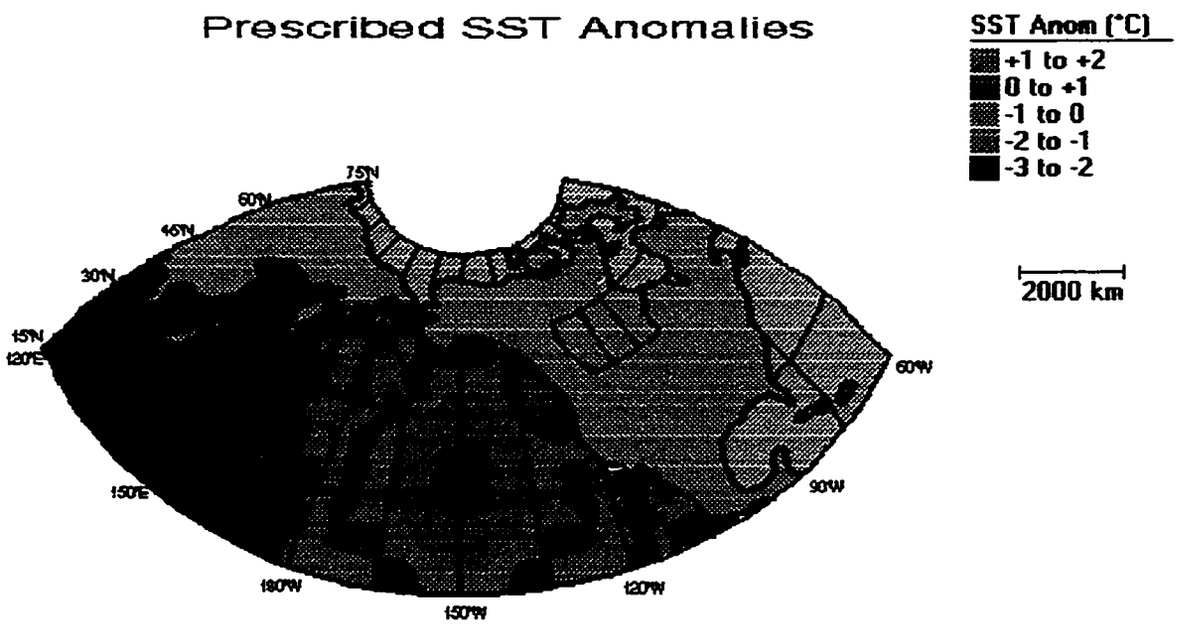

Figure 7.1: Prescribed North Pacific SST Anomalies Used in the CMC Global Spectral Model SST Anomaly Runs

anomaly pattern in Figure 7.1.

The main concern is the relationship between the prescribed SST anomaly pattern and upper-atmospheric circulation patterns over the North Pacific/North American region and in particular, over the Canadian Prairies. Therefore, 50 kPa anomaly maps for both SST anomaly runs are presented (Figure 7.2(a) and (b)). Each map represents average 50 kPa anomalies from day 21 to day 50 (i.e. the first 20 days are not used) and the anomalies are calculated by subtracting the average 50 kPa values of the control run from those of the SST anomaly run.

The comparison of SST anomaly Run #1 with Run #2 shows contrasting results. Run #1 exhibits a pattern consisting of negative anomalies over

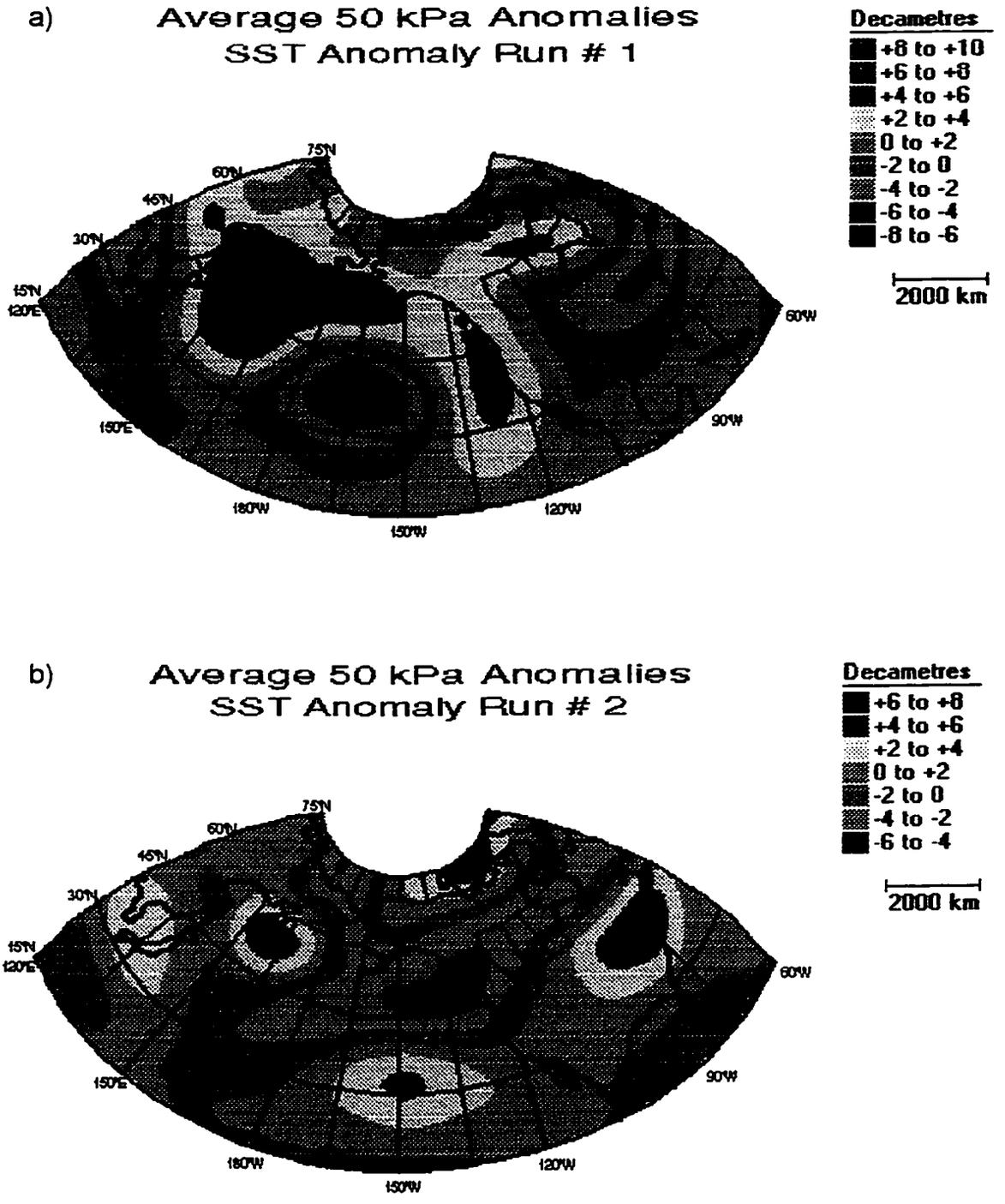

Figure 7.2: Northern Hemisphere Average 50 kPa Anomaly Maps from SST Anomaly Runs of the CMC Global Spectral Model: a) Run # 1 and b) Run # 2

the central North Pacific Ocean and positive anomalies over the eastern North Pacific Ocean and into western North America. It appears the negative 50 kPa anomalies are associated with the negative SST anomalies in Figure 7.1 and the positive 50 kPa anomalies with the positive SST anomalies. However, this is not conclusive.

SST anomaly Run #2 shows a much different pattern. There is a large area of negative 50 kPa anomalies extending from the north-central North Pacific through eastern Canada and a region of positive anomalies over the central North Pacific. Therefore, for this run, the prescribed SST anomaly pattern was not associated with positive 50 kPa anomalies over the Prairies.

There may be several reasons for the large differences between the runs. Firstly, the numerical model analysis included a very small sample size of only two runs. Ideally, many different SST anomaly runs are required and the most consistent response in terms of 50 kPa anomalies over the North Pacific/North American region could be identified. However, due to time restraints and computer time availability, only two SST anomaly runs were performed.

Secondly, this analysis focused on only two regions of SST anomalies in the North Pacific Ocean (mainly because other studies indicated these regions affect upper-atmospheric flow patterns over the North Pacific/North American region and in particular, over the Canadian Prairies (e.g. Namias, 1969,1972,1978,1986; Bonsal et al., 1993)). However, other areas are likely involved. For example, the composite SST anomaly maps associated with El Niño (Figure 5.2) showed other large regions of SST anomalies (especially in the western North Pacific).

Also, the SST anomaly maps associated with the 1986 El Niño case study (Figure 6.4) showed the negative SST anomalies (normally in the east-central North Pacific) extended much further westward to cover a large region of the North Pacific Ocean. Therefore, other regions of SST anomalies in the North Pacific Ocean may also affect upper-atmospheric flow patterns over the North Pacific and North America.

The inconsistent results may also imply that North Pacific SST anomalies alone are not adequate in causing positive 50 kPa anomalies over the Canadian Prairies. In other words, the SST anomalies act in conjunction with other factors (e.g. soil moisture anomalies over North America) to produce ridging over the Prairies. The model runs were only carried out for 50 days using fixed average May SSTs (once again due to time restraints and computer time availability). It was persistent positive SST anomaly gradients occurring during periods other than May that were hypothesized to be associated with positive 50 kPa anomalies over the Prairies. Therefore, if the runs were carried out for longer periods and the SSTs allowed to change, there may be fewer inconsistencies in the model results.

In conclusion, the numerical modelling analysis has shown no clear evidence for a direct relationship between positive SST anomaly gradients in the North Pacific Ocean and strong positive 50 kPa anomalies over the Canadian Prairies during the growing season. This also suggests that the SST anomalies may not necessarily cause 50 kPa anomalies, but rather act in conjunction with these anomalies to produce precipitation variations on the Prairies.

7.1.5 GROWING-SEASON EXTENDED DRY SPELLS ON THE CANADIAN PRAIRIES

The conceptual model of El Niño events suggested the persistent positive SST anomaly gradients in association with positive 50 kPa anomalies during June(+10), July(+10) and August(+10) lead to more extended dry spells and perhaps drought conditions on the Canadian Prairies. The testing of El Niño in chapter 6 showed that if the persistent positive SST anomaly gradients occurred in conjunction with positive or near normal 50 kPa anomalies, strong and consistent positive responses in terms of growing-season extended dry spells were observed on the Prairies (i.e. dry conditions).

Four of six El Niño events having positive PNA patterns and persistent positive SST anomaly gradients were associated with positive or near normal 50 kPa anomalies over the Prairies during June(+10), July(+10) and August(+10) (i.e. 1953, 1965, 1982 and 1986). During all four events, strong positive 10-day dry spell responses were observed. These responses were also consistent (i.e. they covered a period of more than one month and the total growing season(+10)).

Conversely, during the other two events (i.e. 1957 and 1976), strong negative 50 kPa anomalies were observed over the Prairies during June(+10), July(+10) and August(+10). These events were not associated with strong positive responses in terms of extended dry spells. These findings suggest that the SST anomalies have to occur in conjunction with positive or near normal 50 kPa anomalies in order to lead to more extended dry spells on the Prairies.

The reasons for this are not entirely clear. One possibility is that the different 50 kPa anomalies (i.e. positive or near normal versus

strong negative) are representative of different 50 kPa flow patterns over the North Pacific/North American region. This implies that for each case, the air reaching the Canadian Prairies originates from a different part of the North Pacific Ocean. Depending on the North Pacific SST anomaly pattern (e.g. a positive SST anomaly gradient), the amount of moisture advected into the Prairie region (which mainly originates from the North Pacific Ocean (Benton and Estoque, 1954)) can be affected (thus affecting precipitation).

Therefore, from this analysis, it appears that positive North Pacific SST anomaly gradients do not necessarily cause changes in upper-atmospheric flow patterns over the Canadian Prairies. This result does not correspond to the hypothesis of Bonsal et al. (1993) who suggested that positive SST anomaly gradients caused ridging over the Prairies. However, there still appears to be an association between these positive gradients and drier conditions on the Prairies during the growing season (as determined by Bonsal et al. (1993)). The relationships among North Pacific SST anomaly patterns, upper-atmospheric flow patterns and precipitation on the Prairies clearly require further investigation.

Note that several strong positive 10-day dry spell responses also occurred during Junes, Julys, Augusts and total growing seasons not associated with El Niño. Some extreme examples occurred during the growing seasons of 1948, 1960, 1961, 1969, 1970 and 1981 (see Appendix A). These occurrences are likely attributable to the numerous meteorological and climatological factors (including upper-atmospheric flow patterns) that affect growing-season precipitation over the Canadian Prairies. These include sea-level pressure patterns,

atmospheric moisture content, convective instability, soil moisture conditions, air temperature, surface albedo, etc. (Kendrew and Currie, 1955; Kendall and Thomas, 1956; Longley, 1972).

Growing-season precipitation can also be affected by conditions prior to the growing season (i.e. autumn, winter and early spring). For example, persistent dry conditions during these periods often result in low soil moisture levels at the beginning of the growing season. The amount of surface evapotranspiration is therefore reduced. This leads to a reduction of precipitation (especially convective) which is enhanced due to the presence of local surface evapotranspiration (Charney, 1975; Shukla and Mintz, 1982; Namias, 1982). This can be substantial because a large percentage (approximately half) of growing-season precipitation on the Prairies is often convective (especially during June, July and August) (Kendrew and Currie, 1955; Kendall and Thomas, 1956; Chakravarti, 1972).

7.1.5.1 PRECIPITATION VARIABLES IN THIS STUDY

Two variables identified growing-season precipitation variations on the Canadian Prairies including total number of 10-day dry spells and areally-averaged precipitation anomalies. The definitions of these variables were provided in chapter 3 where it was indicated that the former is a temporal representation of precipitation variations, while the latter represents the amount of precipitation on the Prairies. The correlation and composite analyses showed insignificant results for the precipitation anomalies and more significant results for the 10-day dry spells (especially the composite analysis (e.g. Table 5.4)).

To aid in determining reasons for these differences, correlations (using Pearson's product-moment correlation) between monthly total number of 10-day dry spells and areally-averaged precipitation anomalies from 1948-1991 are calculated (Table 7.1). Negative correlations occur for every month which is expected, since a higher number of dry spells suggests negative precipitation anomalies and vice versa. However, the correlation coefficients for May and August are significant while the ones for June and July are not. One possible reason is that a large portion of June and July precipitation on the Canadian Prairies is convective (Kendrew and Currie, 1955; Longley, 1972). As a result, the precipitation anomalies are often strongly influenced by these convective precipitation events. For example, the first three weeks of June receive no precipitation, however, near the end of the month, one or two large convective precipitation events occur. The monthly areally-averaged precipitation anomaly value would be near normal, however, the total number of 10-day dry spells value would be relatively high.

Since the major focus of this study is extended dry periods that could lead to drought conditions, the total number of 10-day dry spells are likely better indicators (i.e. the three week dry period may have been sufficient to initiate drought conditions on the Prairies). Therefore, for the purpose of this investigation, total number of 10-day dry spells (i.e. a measure of extended dry periods) are considered to be more appropriate and therefore, have been the major focus. Furthermore, since more significant results were obtained from this variable, it appears that ENSO events are related more to extended dry periods as opposed to actual precipitation amounts on the Canadian Prairies.

Table 7.1: Correlations Between Total Number of 10-Day Dry Spells and Areally-Averaged Precipitation Anomalies on the Canadian Prairies (1948-1991).

MONTH	R VALUE
May	-0.57***
June	-0.38
July	-0.25
August	-0.73***

*** significant at the 0.01 level

7.2 TELECONNECTIONS BETWEEN LA NIÑA EVENTS AND GROWING-SEASON PRECIPITATION VARIATIONS ON THE CANADIAN PRAIRIES

The second major focus of this study included the analysis of teleconnections between La Niña events and growing-season precipitation variations on the Prairies. These teleconnections and possible physical explanations for their existence are detailed in chapter 6 (section 6.1.2 and Figure 6.2). Generally, the atmosphere - ocean teleconnections are opposite to those associated with El Niño. This agrees with several other studies that observed generally opposite responses between El Niño and La Niña in terms of meteorological variables (e.g. upper-atmospheric circulation patterns, temperature, precipitation) over regions of the world (Yarnal and Diaz, 1986; Ropelewski and Halpert, 1988; Fraedrich and Muller, 1992; Halpert and Ropelewski, 1992). This section further discusses the atmosphere - ocean teleconnections as they relate to La Niña and growing-season precipitation on the Prairies. In many respects, the physical factors are similar to those involved with El Niño events.

7.2.1 LA NIÑA EVENTS AND NEGATIVE PNA PATTERNS

The first atmosphere - ocean teleconnection involved the development of negative PNA patterns during the autumn or winter following the onset of La Niña events (i.e. stage one of Figure 6.2). This was opposite to stage one for El Niño. The physical basis for this teleconnection was detailed in chapter 6. Of the seven La Niña events occurring between 1948 and 1991, all were associated with negative PNA patterns during autumn(+3) to winter(+4) indicating a very consistent response between the two variables.

The strength of these negative patterns was not always consistent (i.e. four events were very strong, two were strong and one was weak). As with El Niño, this could be due to several reasons. These include the following: differences of individual La Niña events in terms of onset, evolution, amplitude, duration and spatial extent (van Loon and Shea, 1985; Ropelewski and Halpert, 1986,1987,1989; Kiladis and Diaz, 1989; Philander, 1990); negative PNA pattern responses to La Niña being sensitive to the atmospheric flow onto which it is superimposed (Wallace and Gutzler, 1981); and the several factors (other than forcing due to La Niña) which affect upper-atmospheric flow patterns over the North Pacific/North American region and thus the development of negative PNA patterns (e.g. orography, land/sea heating contrasts, barotropic instability, the presence of other larger scale teleconnection patterns, etc.) (Lau, 1981; Wallace and Gutzler, 1981; Leathers et al., 1991).

These could also explain the many occurrences of strong negative PNA patterns during autumns and winters not associated with La Niña (see Appendix C) (i.e. negative PNA patterns are not exclusive to La Niña

events). Nonetheless, since every La Niña was associated with a negative PNA pattern during the autumn or winter following the onset, there is a very consistent response between La Niña events and negative PNA patterns.

7.2.2 NEGATIVE PNA PATTERNS AND NEGATIVE NORTH PACIFIC SST ANOMALY GRADIENTS

The second atmosphere - ocean teleconnection (i.e. stage two) included the development of negative North Pacific SST anomaly gradients (i.e. anomalously warm water in the east-central North Pacific and anomalously cold water along the central-west coast of North America). This teleconnection was opposite to stage two for El Niño. It was suggested that the circulation associated with negative PNA patterns (in particular the weaker Aleutian low) (Emery and Hamilton, 1985; Yarnal and Diaz, 1986) aided in the development of these SST anomaly patterns. This occurred shortly after the development of negative PNA patterns (i.e. by spring(+5)). In fact, all seven La Niña events having negative PNA patterns were also associated with negative SST anomaly gradients during spring(+5).

Due to this very consistent result, it was concluded that negative PNA patterns likely aid in the development of negative SST anomaly gradients. However, as with positive PNA patterns and positive SST anomaly gradients, many complex atmosphere - ocean interactions are involved. For example, the occurrence of negative SST anomaly gradients prior to the development of negative PNA patterns suggests the PNA only aided in the amplification of the SST patterns. In fact, five of seven

events having negative PNA patterns and negative SST anomaly gradients during spring(+5) (i.e. 1964, 1970, 1973, 1975 and 1988) had negative gradients prior to spring(+5). During these events, negative PNA patterns likely only aided in the amplification of the negative SST anomaly gradients, or the gradients themselves aided in the development of negative PNA patterns. Only the events of 1949 and 1954 had positive SST anomaly gradients prior to spring(+5). During these events, negative PNA patterns likely played a more important role in initiating the negative SST gradients. Therefore, even though there was a very consistent relationship between La Niña events with negative PNA patterns and negative SST anomaly gradients during spring(+5), the physical processes are not entirely understood.

Strong negative SST anomaly gradients (i.e. standardized values less than -0.50) also occurred during springs not associated with La Niña events having negative PNA patterns. These included the springs of 1948, 1949, 1952, 1962, 1964, 1973, 1979, 1982, 1985 and 1991 (see Appendix D). Most of these were associated with strong negative PNA patterns during the preceding winters (see Appendix C), indicating these patterns aided in the development of the negative gradients. However, there were also strong negative gradients during springs not associated with negative PNA patterns. Therefore, negative SST anomaly gradients can also be produced by factors other than negative PNA patterns.

7.2.3 HIGHER FREQUENCY OF NEGATIVE NORTH PACIFIC SST ANOMALY GRADIENTS

The next stage (stage three) suggested a higher frequency of negative SST anomaly gradients (i.e. more negative than positive) from

spring(+5) to summer(+10). As discussed in chapter 5, this signifies that La Niña are associated with SST anomaly gradients that differ from those of El Niño (i.e. they are not persistently positive). A higher frequency of negative SST anomaly gradients was associated with all seven La Niña events. However, in some cases the negative gradients that occurred during spring(+5) persisted for several seasons while in others, they weakened or became positive for part of the period.

As outlined in chapter 6, the events of 1954 and 1970 had persistent negative gradients during all six seasons from spring(+5) to summer(+10). During the 1973 event, five of six had negative gradients with only autumn(+7) being positive. The events of 1949, 1964 and 1975 showed four negative seasons with autumn(+7) and winter(+8) being positive and 1988 had three seasons with autumn(+7), spring(+9) and summer(+10) being positive.

Therefore, during many of these events (i.e. 1949, 1964, 1973 and 1988), the SST anomaly gradients became positive during autumn(+7), and then negative during winter(+8) or spring(+9). In fact, the 1973 La Niña case study showed this characteristic in that the SST anomaly gradient became positive during autumn 1974 (i.e. autumn(+7)) and negative during winter 1975 (i.e. winter(+8)). The North Pacific SST anomaly maps in Figure 6.7(c) and (d) showed the gradient became positive because the anomalously warm water in the east-central North Pacific during summer 1974, appeared to move northeastward towards the central-west coast of North America. During winter 1975, it then appeared to move back southwestward towards the east-central North Pacific.

It is unknown whether this also occurred during the events of

1949, 1964 and 1988. However, the fact that the gradients also became positive during autumn(+7), and then became negative during winter(+8) or spring(+9), indicates there may be oceanic and/or atmospheric processes occurring during these periods causing the observed changes in SST anomaly gradients. As outlined previously, many complex ocean - atmosphere interactions acting on a variety of time and space scales affect the initiation, propagation, persistence and decay of SST anomalies in the North Pacific Ocean (Namias, 1972; Haney, 1980; Frankignoul, 1985). Nonetheless, the seven La Niña events having negative PNA patterns also had a higher frequency of negative SST anomaly gradients from spring(+5) to summer(+10). Furthermore, in some cases, negative gradients persisted for several seasons (e.g. 1954, 1970 and the 1973 case study). As a result, the SST anomaly gradients associated with La Niña are different from those associated with El Niño.

Higher frequencies of negative SST anomaly gradients during spring(+5) to summer(+10) not associated with La Niña were also observed. They occurred during spring 1948 through summer 1949, spring 1967 through summer 1968 and spring 1972 through summer 1973 (see Appendix D). However, prior to these negative gradients, strong negative PNA indices were observed indicating negative PNA patterns may have aided in initiating or amplifying these negative SST anomaly gradients.

7.2.4 HIGHER FREQUENCY OF NEGATIVE NORTH PACIFIC SST ANOMALY GRADIENTS AND GROWING-SEASON UPPER-ATMOSPHERIC CIRCULATION PATTERNS OVER THE CANADIAN PRAIRIES

The final atmosphere - ocean teleconnection suggested that if the higher frequency of negative SST anomaly gradients are associated with negative 50 kPa anomalies over the Canadian Prairies during June(+10), July(+10) and August(+10), fewer extended dry spells (i.e. wetter conditions) occur on the Prairies (i.e. stage four of Figure 6.2). However, as with El Niño and positive SST anomaly gradients, there was no clear evidence that the SST anomaly gradients caused the negative 50 kPa anomalies over the Prairies.

There were some indications of a relationship. For instance, the 1973 La Niña case study showed the upper-atmospheric flow pattern during June 1975 (i.e. June(+10)) (Figure 6.8) was similar to stage four of the La Niña conceptual model. This included positive 50 kPa anomalies (ridging) over the eastern North Pacific and negative anomalies (troughing) over the Canadian Prairies. Furthermore, six of seven La Niña events having negative PNA patterns and a higher frequency of negative SST anomaly gradients were associated with strong negative 50 kPa anomalies during either June(+10), July(+10) or August(+10). However, the strong negative anomalies were not consistent through the entire period.

As with El Niño, there are several considerations to take into account. These include other factors such as soil moisture anomalies, anomalous snow cover and sea ice conditions over northern Canada and the Arctic Ocean, solar activities, volcanic eruptions and orographic

influences which can affect upper-atmospheric flow patterns over the Prairies; the nature of the areally-averaged 50 kPa anomaly variable; characteristics of negative SST anomaly gradients (e.g. size of the anomalously warm pool versus the anomalously cold pool, latent and sensible heat transfers to the atmosphere, processes such as diabatic heating, baroclinic eddies, atmospheric convection, meridional and horizontal temperature advection, other regions of SST anomalies in the North Pacific Ocean). As outlined previously, the analysis of these factors is outside the scope of this study and therefore, further exploration into their effects on upper-atmospheric flow patterns over the Prairies is needed.

7.2.5 FEWER GROWING-SEASON EXTENDED DRY SPELLS ON THE CANADIAN PRAIRIES

Stage four of Figure 6.2 suggested the higher frequency of negative SST anomaly gradients in association with negative 50 kPa anomalies during June(+10), July(+10) and August(+10), lead to fewer extended dry spells on the Canadian Prairies (which are likely representative of wetter than normal conditions). The testing of La Niña events in chapter 6 showed that if the negative SST anomaly gradients occurred in conjunction with negative or near normal 50 kPa anomalies, strong and consistent negative responses in terms of extended dry spells were observed during the growing season on the Prairies. In fact, during the 1949, 1964, 1970, 1973, 1975 and 1988 La Niña events, a higher frequency of negative SST anomaly gradients occurred in conjunction with negative or near normal 50 kPa anomalies over the Prairies during June(+10), July(+10) and August(+10). During all six events, there were

strong negative 10-day dry spell responses during these periods. The responses were also consistent (i.e. they covered a period of more than one month and in most cases, the total growing season).

Conversely, when the higher frequency of negative gradients occurred in conjunction with strong positive 50 kPa anomalies over the Prairies during June(+10), July(+10) and August(+10), no strong negative extended dry spell responses were observed (i.e. the 1954 La Niña). This also indicates that the SST anomalies have to occur in conjunction with negative or near normal 50 kPa anomalies in order to lead to fewer extended dry spells on the Prairies.

As with the SST anomaly gradients associated with El Niño, the physical basis for this conjunction is unclear. As outlined previously, a possibility is that the different 50 kPa anomalies (i.e. negative or near normal versus strong positive) are representative of different 50 kPa flow patterns over the North Pacific/North American region. This implies that for each case, the air reaching the Canadian Prairies originates from a different part of the Pacific Ocean. Depending on the SST anomaly pattern (e.g. a negative SST anomaly gradient), the amount of moisture advected into the Prairie region (and thus precipitation) can be affected.

Note there were several strong negative total number of 10-day dry spell responses during Junes, Julys, Augusts and total growing seasons not associated with La Niña. Some extreme examples included the growing seasons of 1954, 1957, 1963, 1976, 1982 and 1987 (see Appendix A). As discussed previously, there may be several reasons for this occurrence including the numerous meteorological and climatological

factors (including upper-atmospheric flow patterns) that affect the development of growing-season precipitation over the Canadian Prairies and therefore the number of extended dry spells (e.g. sea-level pressure patterns, atmospheric moisture content, convective instability, soil moisture conditions, air temperature, surface albedo, precipitation conditions prior to the growing season, etc.). Nonetheless, there was a very consistent response between La Niña events having negative PNA patterns and a higher frequency of negative North Pacific SST anomaly gradients and strong negative responses of extended dry spells on the Prairies during June(+10), July(+10) or August(+10) and in most cases, the total growing season(+10).

7.3 TIMING OF ENSO EVENTS

As outlined in chapters 2 and 3, ENSO events occur irregularly throughout the period 1948-1991 (i.e. they are not cyclical). For example, from Table 3.1 it is shown that La Niña events occurred during the year following the onset of El Niño events (e.g. 1963-1964), while El Niño events occurred during the year following the onset of La Niña events (e.g. 1975-1976). As a result, the timing of ENSO events was such that growing season(+10) occasionally coincided with the start of another El Niño or La Niña. However, it was determined that the differences between growing-season 50 kPa anomalies and extended dry spells on the Prairies associated with consecutive ENSO events and those associated with non-consecutive events was insignificant. Therefore, it appears that the timing of ENSO events does not have a significant effect on the growing-season precipitation variations examined in this

study.

7.4 MAY VERSUS THE REST OF THE GROWING SEASON

As shown throughout the entire analysis, May(+10) tended to be opposite from the rest of the growing season in terms of areally-averaged 50 kPa anomalies, total number of 10-day dry spells and even areally-averaged precipitation anomalies over the Prairies. For El Niño, five of six events having positive PNA patterns and persistent positive SST anomaly gradients were associated with negative 50 kPa anomalies during May(+10) including four strong or very strong. The total number of 10-day dry spell response to the same six events showed three associated with strong or very strong negative values during May(+10). The composite analysis also demonstrated that the ten May(+10)s associated with El Niño had significantly fewer extended dry spells than all the other Mays during the study period. For La Niña, five of seven events having negative PNA patterns and a higher frequency of negative SST anomaly gradients were associated with positive 50 kPa anomalies (including two strong and one very strong). However, in terms of extended dry spells, only three showed positive responses indicating that May(+10) was not always different.

As outlined in chapter 6, the reasons for the opposite response are not clear. The fact is that during some years, May weather patterns are characteristic of early spring/late winter, while during others, they resemble summer. This is likely due to April and May often being a transition period between winter and summer upper-atmospheric circulation patterns over the Prairies (Kendrew and Currie, 1955;

Longley, 1972). As a result, over the North Pacific/North American region, May could have a different upper-atmospheric flow pattern from the rest of the growing season. As outlined previously, different flow patterns would imply that the air reaching the Canadian Prairies originates from a different part of the Pacific Ocean. Depending on the North Pacific SST anomaly pattern (e.g. positive gradients versus negative gradients), the amount of moisture advected into the Prairie region can be affected. This could perhaps explain why May generally had opposite precipitation variations on the Prairies.

There have been no studies that have directly cited examples of a major upper-atmospheric circulation change between May and the rest of the growing season for the Canadian Prairies. However, Bell and Janowiak (1995) indicated that the extensive flooding during June-July 1993 in the Midwest United States was attributed in part, to a major upper-atmospheric circulation change during late May 1993. Prior to this period, a stronger than normal ridge persisted over western North America. During late May, the ridge dissipated and negative height anomalies became established over the region. The new pattern was associated with strong zonal flow which provided a "duct" for intense cyclone activity to propagate into the United States Midwest. Prior to this, the strong ridge prevented much of the cyclone activity from entering the area (Bell and Janowiak, 1995). Since these circulation patterns often extend into Canada, it is possible that a change in upper-atmospheric flow patterns during May, could also affect precipitation on the Prairies.

To determine if May areally-averaged 50 kPa anomalies and total

Table 7.2: Correlations Between May and the Rest of the Growing Season during the period 1948-1991.

VARIABLES	R VALUE AREALLY-AVERAGED 50 KPA ANOMALY	R VALUE TOTAL NUMBER OF 10-DAY DRY SPELLS
May vs June	+0.27	-0.07
May vs July	-0.08	+0.01
May vs August	+0.27	+0.03

number of 10-day dry spells were consistently opposite to those of June, July and August, correlations (using Pearson's product-moment correlation) between these two variables for the entire study period of 1948-1991 are determined (Table 7.2). Insignificant results occur for May versus June, July and August for both variables. If May consistently showed an opposite response, the correlation coefficients would be significantly negative. Since they are not, it appears May was not generally opposite to the rest of the growing season in terms of 50 kPa anomalies and number of extended dry spells, but as shown by this analysis, May(+10)s associated with El Niño and La Niña do tend to be opposite. Clearly, more research is required to determine why May(+10) is often different from the rest of the growing season(+10) in terms of 50 kPa anomalies and extended dry spells associated with ENSO events.

CHAPTER 8

SUMMARY AND CONCLUSIONS

8.1 SUMMARY

The objective of this thesis was to determine relationships between ENSO events and growing-season precipitation variations on the Canadian Prairies through a series of atmosphere - ocean teleconnections over the Pacific Ocean. The teleconnections involved PNA patterns, SST anomalies and upper-air circulation anomalies over the Prairies. Two hypotheses were tested: i) El Niño events are related to growing-season extended dry spells and droughts on the Canadian Prairies and ii) La Niña events are related to wet or non-drought conditions during the growing season on the Prairies.

Two main methods were used to analyze these teleconnections. Correlation analysis determined associations between SOI values (i.e. ENSO events) and variables describing the atmosphere - ocean teleconnections. Significant associations were determined for PNA indices, North Pacific SST anomalies and 50 kPa anomalies and number of extended dry spells on the Prairies. The analysis indicated that positive (negative) PNA patterns occur during the winter coinciding with the mature stage of El Niño (La Niña) events. Positive (negative) North Pacific SST anomaly gradients then occur during the same winter and subsequent spring. These gradients persist for several (up to +5 seasons). During the third growing season following the onset of El Niño (La Niña), positive (negative) 50 kPa anomalies and more (fewer)

extended dry spells occur during June, July, and August while May shows an opposite response.

A weakness of the correlation analysis was that all situations (i.e. El Niño, La Niña and periods with no ENSO events) were included. Therefore, a composite analysis was used to analyze the atmosphere - ocean teleconnections associated with actual ENSO events. The findings generally agreed with those of the correlation analysis including significant results with PNA indices, North Pacific SST anomalies and extended dry spells on the Prairies. The analysis indicated that for El Niño events, positive PNA patterns develop during the autumn and winter coinciding with the mature stage of the events. During the same period, North Pacific SST anomaly patterns consisting of anomalously cold water in the east-central North Pacific and anomalously warm water along the central-west coast of North America are observed. These patterns tend to persist for eight seasons. During the third growing season following the onset of the El Niño events, slightly positive 50 kPa anomalies and more extended dry spells are observed during June, July and August and once again, May shows an opposite response.

For La Niña events, generally opposite results were found. Negative PNA patterns develop during the autumn and winter following the mature stage of the events. SST anomaly patterns opposite to those associated with El Niño are observed during the following spring. Though these patterns did not persist, they frequently occur over the next six seasons. The third growing season following the onset of the events shows slightly negative 50 kPa anomalies and fewer extended dry spells during June, July and August.

Two conceptual models (for El Niño and La Niña) were formulated based on the results of the correlation and composite analyses. The models suggested that ENSO events were related to precipitation variations on the Prairies through a series of stages (six for El Niño and four for La Niña).

For El Niño events, the first stage involves the development of positive PNA patterns during the autumn or winter following the onset of the events (i.e. autumn(+3) to winter(+4)). Based on previous studies, it was suggested the positive PNA patterns are due to the propagation of a Rossby wave train initiated by the large area of anomalously warm water in the eastern tropical Pacific associated with El Niño (e.g. Hoskins and Karoly, 1981; Tribbia, 1991).

In stage two, North Pacific SST anomaly patterns consisting of anomalously cold water in the east-central North Pacific and anomalously warm water along the central-west coast of North America (i.e. positive SST anomaly gradients) develop within a season following the development of positive PNA patterns. From previous investigations, it was proposed that the circulation associated with positive PNA patterns and in particular, the stronger Aleutian low, aids in the initiation of these SST anomaly patterns (e.g. Reynolds and Rasmusson, 1983; Yongping and McBean, 1991).

The next three stages are related to the persistence of these SST anomaly patterns. In stage three, for reasons that are unclear, the warm water along the central-west coast of North America cools and eventually disappears during the ensuing winter and spring (i.e. winter(+4) to spring(+5)). During stage four, an anomalous pool of warm water detaches

from the large area of positive SST anomalies in the tropical Pacific Ocean and moves up the west coast of North America. This likely occurs due to sub-surface Kelvin waves which are associated with El Niño (e.g. Norton et al., 1985; Johnson and O'Brien, 1990). By the autumn (i.e. autumn(+7)), this pool reaches the central-west coast of North America. During this entire period (winter(+4) to autumn(+7)), the anomalously cold water in the east-central North Pacific continues to persist. As a result, strong positive SST anomaly gradients are observed. Stage five includes the persistence of strong positive gradients for the next four seasons (i.e. autumn(+7) to summer(+10)).

The final stage indicates that if the persistent strong positive SST anomaly gradients are associated with positive 50 kPa anomalies over the Canadian Prairies, more extended dry spells which could lead to droughts are observed during the following June, July and August. This corresponds to the third growing season following the onset of the El Niño events (i.e. growing season(+10)).

The testing of the El Niño model showed for the ten events occurring between 1948 and 1991, eight were associated with strong or very strong positive PNA patterns during autumn(+3) or winter(+4). Of these eight, six experienced persistent (i.e. at least five seasons) positive North Pacific SST anomaly gradients. Therefore, six of the original ten events had positive PNA patterns and persistent positive SST anomaly gradients. Growing season(+10) showed four of these six events were associated with positive or near normal 50 kPa anomalies and greater than normal extended dry spells during June, July and August over the Prairies. Therefore, four of the original ten events

corresponded to the conceptual model. However, these four events had very strong and consistent positive responses in terms of extended dry spells (i.e. dry conditions) during most of the growing season.

The 1986 El Niño case study showed a very strong positive PNA pattern developed during winter 1987. The same winter was associated with a strong positive SST anomaly gradient which persisted until summer 1988 (seven seasons). The long persistence was associated with an upper atmospheric-circulation pattern that produced very strong positive 50 kPa anomalies over the Canadian Prairies during June 1988. This period was also associated with 178.4% of normal number of 10-day dry spells. Even though July and August had near normal number of extended dry spells, the very dry conditions during June led to very severe drought conditions on the Canadian Prairies during the growing season of 1988.

The La Niña conceptual model consisted of four stages and for the most part, they were generally opposite to those associated with the El Niño model. In stage one, negative PNA patterns develop during the autumn or winter following the onset of the events. Previous studies hypothesized these patterns occur as a result of ocean - atmosphere interactions that stimulate convection over the westward displaced tropical heat source (associated with La Niña). This enhances the east-Asian jet stream setting up a ridge and trough system across the North Pacific/North American region that resembles negative PNA patterns (e.g. Yarnal and Diaz, 1986).

During stage two, North Pacific SST anomaly patterns consisting of anomalously warm water in the east-central North Pacific and anomalously cold water along the central-west coast of North America (i.e. negative

North Pacific SST anomaly gradients) develop during the spring following the development of negative PNA patterns (i.e. spring(+5)). Based on other investigations, it was suggested the SST anomaly patterns develop due to the circulation associated with negative PNA patterns and in particular, the weaker Aleutian low (e.g. Pan and Oort, 1983,1990; Emery and Hamilton, 1985). Stage three includes higher frequencies of negative (i.e. more negative than positive) SST anomaly gradients occurring during the next six seasons (i.e. spring(+5) to summer(+10)). These SST anomaly patterns differ from those associated with El Niño (i.e. they are not persistently positive).

The fourth stage indicates that if the higher frequencies of negative SST anomaly gradients are associated with negative 50 kPa anomalies over the Canadian Prairies, fewer extended dry spells are observed during the following June, July and August. Once again, this corresponds to the third growing season following the onset of the La Niña events (i.e. growing season(+10)). The fewer than normal extended dry spells are indicative of wetter conditions but more importantly, of non-drought conditions on the Prairies.

The testing of the La Niña model showed that all seven La Niña events between 1948 and 1991 were associated with negative PNA patterns during autumn(+3) or winter(+4). These seven events also experienced a higher frequency of negative North Pacific SST anomaly gradients from spring(+5) to summer(+10). During growing season(+10), six of these seven events were associated with negative or near normal 50 kPa anomalies and fewer than normal extended dry spells during June, July and August over the Prairies. These six events also had very strong and

consistently negative responses in terms of 10-day dry spells (i.e. wetter conditions) during most of the growing season. Therefore, six of seven events agreed with this conceptual model suggesting that growing-season precipitation variations and the absence of droughts on the Prairies respond more consistently (than do droughts to El Niño events).

The 1973 La Niña case study showed the development of a very strong negative PNA pattern during winter 1974. Spring 1974 to summer 1975 showed a higher frequency of negative SST anomaly gradients and in fact, strong negative gradients persisted from winter to summer 1975. This was associated with very strong negative 50 kPa anomalies over the Canadian Prairies during June and August 1975. These periods along with the total growing season experienced many fewer than normal 10-day dry spells.

The study concluded with a discussion of the atmosphere - ocean teleconnections over the Pacific Ocean associated with ENSO events and growing-season precipitation variations on the Canadian Prairies. It explained there are many complex relationships that act on a variety of time and space scales affecting the atmosphere - ocean teleconnections in this study. Many of these relationships were outside the scope of this study and therefore, areas of additional research to obtain a better understanding of the physical processes involved in these teleconnections were suggested. A brief discussion of May versus the rest of the growing season indicated that for the entire study period, May did not show an opposite response in terms of 50 kPa anomalies and number of extended dry spells. However, for reasons that were unclear, Mays associated with ENSO events tended to be different.

8.2 CONCLUSIONS

This study indicates a relationship between ENSO events (i.e. El Niño and La Niña) and growing-season precipitation variations on the Canadian Prairies. The relationship occurs through a series of atmosphere - ocean teleconnections which include PNA patterns, North Pacific SST anomalies and upper-atmospheric anomalies over the North Pacific/North American region (and, in particular, over the Canadian Prairies).

The hypothesis that El Niño events are related to more extended dry spells (i.e. dry conditions) on the Prairies was confirmed. These dry conditions tend to occur during June, July and August of the third growing season following the onset of the El Niño events (i.e. a +10 season or +30 month lag). Even though May is often wetter, most of the growing season is drier. This finding is significant for several reasons. Firstly, more frequent extended dry spells are often precursors of droughts on the Prairies. Secondly, the long lags between the onset of El Niño and the occurrence of dry conditions may help form the basis of a long-range forecasting technique of these dry periods which could provide many benefits to the Prairie region.

The hypothesis that La Niña events are related to fewer extended dry spells (i.e. wet conditions) on the Prairies was also confirmed. Fewer extended dry spells tend to occur during June, July and August of the third growing season following the onset of the events. In fact, this relationship is more consistent than that involving El Niño suggesting that growing-season precipitation variations and absence of droughts respond more consistently to La Niña events. This finding is

also significant because not only are fewer extended dry spells indicative of wet periods, they are also non-drought situations. The ability to anticipate or forecast near or above normal periods would also provide many environmental and economic benefits to the Prairies (e.g. agriculture).

The results of the analysis also demonstrate that for all variables examined in this study (i.e. PNA indices, North Pacific SST anomaly gradients and growing-season areally-averaged 50 kPa anomalies and total number of 10-day dry spells on the Prairies), the responses associated with El Niño tend to be opposite to those associated with La Niña. This suggests that similar forcing factors are involved in both relationships.

For the most part, this analysis only provided associations among the variables. However, larger scale physical explanations of the atmosphere - ocean teleconnections were proposed. It is realized there are also many other physical processes that require further investigation to gain a better understanding of these teleconnections. These processes could explain why ENSO events are not always related to growing-season precipitation on the Prairies and also why extreme precipitation variations also occur during growing seasons not associated with these events (e.g. 1961). These areas of suggested research were presented in chapter 7.

However, with regards to precipitation variations on the Canadian Prairies, it is believed that the following research needs are most important:

i) An analysis of relationships between ENSO events and precipitation

on the Canadian Prairies during the first and second growing seasons following the onset of the events and periods other than the growing season.

ii) A more regional analysis of growing-season precipitation variations on the Canadian Prairies as they relate to ENSO events.

iii) An in depth analysis to determine if May precipitation differs from the rest of the growing season on the Canadian Prairies.

iv) A detailed examination of the physical processes involved among persistent North Pacific SST anomaly patterns (both positive and negative gradients), upper-atmospheric flow patterns over the North Pacific/North American region and precipitation on the Canadian Prairies.

v) An analysis to determine the possible role of other factors such as anomalous soil moisture, anomalous snow cover and ice conditions over North America and the Arctic Ocean, solar variability and orographic influences on precipitation on the Canadian Prairies.

In conclusion, this is the first study to directly analyze, model and propose physical explanations of relationships between both El Niño and La Niña and growing-season precipitation variations on the Canadian Prairies through a series of atmosphere - ocean teleconnections for up to a +10 season lag. The study is significant because it can be considered as a preliminary step in identifying potential causes of these growing-season precipitation variations. It has also suggested areas where further research is required to obtain a better understanding of the precipitation variations. Due to the lags involved (i.e. precipitation could be affected during the third growing season

following the onset of an ENSO event), the models formulated could help form the basis of a long-range forecasting technique of growing-season precipitation variations on the Prairies. Since droughts are a major economic and environmental concern, the ability to anticipate or forecast their occurrence (or non-occurrence) could provide many benefits to the Canadian Prairies.

REFERENCES

Aceituno, P. 1992. El Niño, the Southern Oscillation, and ENSO: Confusing names for a complex ocean-atmosphere interaction. *Bull. Amer. Meteorol. Soc.* 73: 483-485.

AES Drought Study Group, 1986. *An Applied Climatology of Drought in the Prairie Provinces.* Report 86-4, Canadian Climate Centre, Downsview, Ont., 197pp.

Alexander, M.A. 1990. Simulation of the response of the North Pacific Ocean to the anomalous atmospheric circulation associated with El Niño. *Climate Dyn.* 5: 53-65.

Alexander, M.A. 1992. Midlatitude atmosphere-ocean interaction during El Niño. Part I: The North Pacific Ocean. *J. Climate* 5: 944-958.

Bell, G.D. and Janowiak, J.E. 1995. Atmospheric circulation associated with the Midwest floods of 1993. *Bull. Amer. Meteorol. Soc.* 76: 681-695.

Benton, G.S. and Estoque, M.A. 1954. Water vapour transfer over the North American continent. *J. Meteorology* 11: 462-477.

Bigg, G.R. 1990. El Niño and the Southern Oscillation. *Weather* 45: 2-8.

Bjerknes, J. 1966. A possible response of the atmospheric Hadley Circulation to equatorial anomalies of ocean temperature. *Tellus* 18: 820-829.

Bjerknes, J. 1969. Atmospheric teleconnections from the equatorial Pacific. *Mon. Wea. Rev.* 97: 163-172.

Blackmon, M.L., Geisler, J.E. and Pitcher, E.J. 1983. A general circulation model study of January climate anomaly patterns associated with the interannual variation of equatorial Pacific sea surface temperatures. *J. Atmos. Sci.* 40: 1410-1425.

Boffi, J.A. 1949. Effect of the Andes mountains on the general circulation over the southern part of South America. *Bull. Amer. Meteorol. Soc.* 30: 242-247.

Bolin, B. 1950. On the influence of the earth's orography on the general character of the westerlies. *Bull. Amer. Meteorol. Soc.* 31: 184-195.

Bonsal, B.R., Chakravarti, A.K. and Lawford, R.G. 1993. Teleconnections between North Pacific SST anomalies and growing season extended dry spells on the Canadian Prairies. *Int. J. Climatol.* 13: 865-878.

Bradley, R.S., Diaz, H.F., Kiladis, G.N. and Eischeid, J.K. 1987. ENSO signal in continental temperature and precipitation records. *Nature* 327: 497-501.

Canadian Meteorological Centre, 1994. *CMC Reference Guide*. Internal Report, Dorval, Que.

Cane, M.A. 1991. Forecasting El Niño with a geophysical model. In Glantz, M.H., Katz, R.W. and Nicholls, N. (eds.), *Teleconnections Linking Worldwide Climate Anomalies*. Cambridge University Press, Cambridge, 345-369.

Cayan, D.R. 1992a. Latent and sensible heat flux anomalies over the northern oceans: The connection to monthly atmospheric circulation. *J. Climate* 5: 354-368.

Cayan, D.R. 1992b. Latent and sensible heat flux anomalies over the northern oceans: Driving the sea surface temperatures. *J. Phys. Oceanogr.* 22: 859-881.

Chakravarti, A.K. 1972. The June - July precipitation patterns in the Prairie Provinces of Canada. *J. Geogr.* 71: 155-160.

Chakravarti, A.K. 1976. Precipitation deficiency patterns in the Canadian Prairies. *Prairie Forum* 1: 95-110.

Charney, J.G. 1975. Dynamics of deserts in the Sahel. *Quart. J. Roy. Meteorol. Soc.* 101: 193-202.

Chen, W.Y. 1982. Assessment of the Southern Oscillation sea level pressure indices. *Mon. Wea. Rev.* 110: 800-807.

Chen, W.Y. 1983. The climate of spring 1983 - a season with persistent global anomalies associated with El Niño. *Mon. Wea. Rev.* 111: 2371-2384.

Chervin, R.M. 1980. Response of the NCAR General Circulation Model to prescribed changes in ocean surface temperature. Part II: Midlatitude and subtropical changes. *J. Atmos. Sci.* 37: 308-332.

Clarke, A.J. 1983. The reflection of equatorial waves from oceanic boundaries. *J. Phys. Oceanogr.* 13: 1193-1207.

Currie, B.W. and Venkatarangan, P. 1978. *Relationships Between Solar Disturbances and the Precipitation and Temperature on the Canadian Prairies*. Institute of Space and Atmospheric Studies, University of Saskatchewan, Saskatoon, Sask., 38pp.

Davis, R. 1976. Predictability of sea surface temperature and sea level pressure anomalies over the North Pacific Ocean. *J. Phys. Oceanogr.* 6: 249-266.

Deser, C. and Wallace, J.M. 1990. Large scale atmospheric circulation features of warm and cold episodes in the tropical Pacific. *J. Climate* 3: 1254-1281.

Dey, B. 1976. The variability of summer precipitation in the Canadian Prairies. *The Albertan Geographer* 12: 16-25.

Dey, B. 1977. Nature and possible causes of heavy summer precipitation in the Canadian Prairies. *Geographical Perspectives* 40: 26-33.

Dey, B. 1979. Application of 700mb synoptic climatology to drought analysis. *Geog. Bull.* 18: 21-29.

Dey, B. 1982. Nature and possible causes of droughts on the Canadian Prairies - case studies. *J. Climatol.* 2: 233-249.

Dey, B. and Chakravarti, A.K. 1976. A synoptic climatological analysis of summer dry spells in the Canadian Prairies. *Great Plains - Rocky Mountain Geogr. J.* 5: 30-46.

Diaz, H.F. and Kiladis, G.N. 1992. Atmospheric teleconnections associated with the extreme phases of the Southern Oscillation. In Diaz, H.F. and Margraf, V. (eds.), *El Niño: Historical and Paleoclimatic Aspects of the Southern Oscillation.* Cambridge University Press, Cambridge, 7-28.

Dixon, K.W. and Harnack, R.P. 1986. The effect of intraseasonal circulation variability on winter temperature forecast skill. *Mon. Wea. Rev.* 115: 208-214.

Ebdon, D. 1985. *Statistics in Geography.* Basil Blackwell Ltd., Oxford, 232pp.

Emery, W.J. and Hamilton, K. 1985. Atmospheric forcing of interannual variability in the northeast Pacific Ocean; connections with El Niño. *J. Geophys. Res.* 90: 857-868.

Enfield, D.B. and Allen J.S. 1980. On the structure and dynamics of monthly mean sea level anomalies along the Pacific coast of North and South America. *J. Phys. Oceanogr.* 10: 557-578.

Fraedrich, K. and Muller, K. 1992. Climate anomalies in Europe associated with ENSO extremes. *Int. J. Climatol.* 12: 25-31.

Frankignoul, C. 1985. Sea surface temperature anomalies, planetary waves, and air-sea feedback in the middle latitudes. *Reviews of Geophysics* 23: 357-390.

Fu, C., Diaz, H.F. and Fletcher, J.O. 1986. Characteristics of the response of sea surface temperature in the central Pacific associated with warm episodes in the Southern Oscillation. *Mon. Wea. Rev.* 114: 1716-1738.

Glantz, M.H. 1991. Introduction. In Glantz, M.H., Katz, R.W. and Nicholls, N. (eds.), *Teleconnections Linking Worldwide Climate Anomalies*. Cambridge University Press, Cambridge, 1-12.

Hamilton, K. 1988. A detailed examination of the extratropical response to tropical El Niño/Southern Oscillation events. *J. Climatol.* 8: 67-86.

Halpert, M.S. and Ropelewski, C.F. 1992. Surface temperature patterns associated with the Southern Oscillation. *J. Climate* 5: 577-593.

Handler, P. 1990. USA corn yields, the El Niño and agricultural drought: 1867-1988. *Int. J. Climatol.* 10: 819-828.

Haney, R.L. 1980. A numerical case study of the development of large scale thermal anomalies in the North Pacific Ocean. *J. Phys. Oceanogr.* 10: 541-556.

Hanna, A.F., Stevens, D.E. and Reiter, E.R. 1984. Short-term climatic fluctuations forced by thermal anomalies. *J. Atmos. Sci.* 41: 122-141.

Hansen, A.R., Pandolfo, J.P. and Sutera, A. 1993. Mid-tropospheric flow regimes and persistent wintertime anomalies of surface-layer pressure and temperature. *J. Climate* 6: 2136-2143.

Harnack, R.P. 1979. A further assessment of winter temperature prediction using objective methods. *Mon. Wea. Rev.* 107: 250-267.

Harnack, R.P and Broccoli, A.J. 1979. Associations between sea surface temperature gradient and overlying mid-tropospheric circulation in the North Pacific region. *J. Phys. Oceanogr.* 9: 1232-1242.

Haurwitz, B. 1940. The motion of atmospheric disturbances on the spherical earth. *J. Marine Res.* 3: 254-267.

Haworth, C. 1978. Some relationships between sea surface temperature anomalies and surface pressure anomalies. *Quart. J. Roy. Meteorol. Soc.* 104: 131-146.

Henderson, K.G. and Robinson, P.J. 1994. Relationships between the Pacific/North America teleconnection patterns and precipitation events in the south-eastern USA. *Int. J. Climatol.* 14: 307-323.

Horel, J.D. and Wallace, J.M. 1981. Planetary scale atmospheric phenomena associated with the Southern Oscillation. *Mon. Wea. Rev.* 110: 1863-1878.

Hoskins, B.J. and Karoly, D.J. 1981. The steady linear response of a spherical atmosphere to thermal and orographic forcing. *J. Atmos. Sci.* 38: 1179-1196.

Hoskins, B.J., Simmons, A.J. and Andrew, D.G. 1977. Energy dispersion in a barotropic spherical atmosphere. *Quart. J. Roy. Meteorol. Soc.* 103: 553-567.

Huang, J.C.K. 1978. Response of the NCAR General Circulation Model to North Pacific sea surface temperature anomalies. *J. Atmos. Sci.* 35: 1164-1179.

Iwasaka, N., Hanawa, K. and Toba, Y. 1987. Analysis of SST anomalies in the North Pacific and their relation to 500 mb height anomalies over the Northern Hemisphere during 1969-1979. *J. Meteorol. Soc. Jpn.* 65: 104-114.

Johnson, L.P. and Eunus, A.M. 1964. A note on the relation of relative sunspot number to precipitation. *Roy. Astronomical Soc. Can. J.* 58: 250-252.

Johnson, M.A. and O'Brien, J.J. 1990. The northeast Pacific Ocean response to the 1982-1983 El Niño. *J. Geophys. Res.* 95: 7155-7166.

Kendall, R.G. and Thomas, M.K. 1956. *Some Characteristics of Precipitation in the Canadian Prairies.* Meteorological Services of Canada, 311-323.

Kendrew, W.G. and Currie, B.W. 1955. *The Climate of Central Canada.* Edmond Cloutier, Ottawa, 194pp.

Keshavamurty, R.N. 1982. Response of the atmosphere to sea surface temperature anomalies over the equatorial Pacific and the teleconnections of the Southern Oscillation. *J. Atmos. Sci.* 39: 1241-1259.

Kiladis, G.N. and Diaz, H.F. 1989. Global climatic anomalies associated with extremes of the Southern Oscillation. *J. Climate* 2: 1069-1090.

Kiladis, G.N. and van Loon, H. 1988. The Southern Oscillation Part VII: Meteorological anomalies over the Indian and Pacific sectors associated with the extremes of the oscillation. *Mon. Wea. Rev.* 116: 120-136.

Kiladis, G.N., von Storch, H. and van Loon, H. 1989. Origin of the South Pacific Convergence Zone. *J. Climate* 2: 1185-1195.

Knox, J.L. 1991. *Personal communication.*

Knox, J.L., Higuchi, K., Shabbar, A. and Sargent, N.E. 1988. Secular variation of Northern Hemisphere 50 kPa geopotential height. *J. Climate* 1: 500-511.

Knox, J.L. and Lawford R.G. 1990. The relationship between Canadian Prairie dry and wet months and circulation anomalies in the mid-troposphere. *Atm. Ocean* 28: 189-215.

Kukla, G. 1981. Climatic role of snow covers. In: *Sea level, Ice and Climatic Change*. Proceedings of the Canberra Symposium, December, 1979, IASH Publication No. 131: 79-107.

Kushnir, Y. and Lau, N.C. 1992. The general circulation model response to a North Pacific SST anomaly: Dependence on time scale and pattern polarity. *J. Climate* 5: 271-283.

Lanzante, J.R. 1984. A rotated eigenanalysis of the correlation between 700 mb heights and sea surface temperatures in the Pacific and Atlantic. *Mon. Wea. Rev.* 112: 2270-2280.

Lau, K.M and Chan, P.H. 1983a. Short-term climate variability and atmospheric teleconnections from satellite observed outgoing longwave radiation. Part I: Simultaneous relationships. *J. Atmos. Sci.* 40: 2735-2750.

Lau, K.M and Chan, P.H. 1983b. Short-term climate variability and atmospheric teleconnections from satellite observed outgoing longwave radiation. Part II: Lagged correlations. *J. Atmos. Sci.* 40: 2751-2767.

Lau, K.M. and Lim, H. 1984. On the dynamics of equatorial forcing of climate teleconnections. *J. Atmos. Sci.* 41: 161-176.

Lau, K.M. and Sheu, P.J. 1988. Annual cycle, quasi-biennial oscillation, and Southern Oscillation in global precipitation. *J. Geophys. Res.* 93: 10975-10988.

Lau, N.C. 1981. A diagnostic study of recurrent meteorological anomalies in a 15 year simulation with a GFDL general circulation model. *Mon. Wea. Rev.* 109: 2287-2311.

Lau, N.C. and Nath, M.J. 1990. A General Circulation Model study of the atmospheric response to extratropical SST anomalies observed in 1950-1979. *J. Climate* 3: 965-989.

Lawford, R.G. 1992. Research implications of the 1988 Canadian Prairie Provinces drought. *Natural Hazards* 6: 109-129.

Leathers, D.J. and Palecki, M.A. 1992. The Pacific/North American teleconnection pattern and United States climate. Part II: Temporal characteristics and index specification. *J. Climate* 5: 707-716.

Leathers, D.J., Yarnal, B. and Palecki, M.A. 1991. The Pacific/North American teleconnection pattern and United States climate. Part I: Regional temperature and precipitation associations. *J. Climate* 4: 517-528.

Lim, H. and Chang, C.P. 1983. Dynamics of teleconnections and Walker Circulations forced by equatorial heating. *J. Atmos. Sci.* 40: 1897-1915.

Longley, R.W. 1972. *The Climate of the Prairie Provinces*. Climatological Studies #13, Toronto, 79pp.

Maybank, J., Bonsal, B., Jones, K., Lawford, R., O'Brien, E.G., Ripley, E.A. and Wheaton, E. 1995. Drought as a natural disaster. *Atm. Ocean* 33: 195-222.

McCreary, J. 1976. Eastern tropical ocean response to changing wind systems: with application to El Niño. *J. Phys. Oceanogr.* 6: 632-645.

McKay, G.A., Godwin, R.B and Maybank, J. 1989. Drought and hydrological drought research in Canada. *Can. Water Res. J.* 14: 71-84.

Meehl, G.A. 1987. The annual cycle and interannual variability in the tropical Pacific and Indian Ocean regions. *Mon. Wea. Rev.* 115: 27-50.

Mysak, L.A. 1986. El Niño, interannual variability and fisheries in the northeast Pacific Ocean. *Can. J. Fish. Aquat. Sci.* 43: 464-497.

Namias, J. 1962. Influence of abnormal surface heat sources and sinks on atmospheric behaviour. *Proceedings of the International Symposium on Numerical Weather Prediction*. Meteorological Society of Japan, Tokyo, 615-629.

Namias, J. 1963. Large scale air-sea interactions over the North Pacific from summer 1962 through the subsequent winter. *J. Geophys. Res.* 68: 6176-6186.

Namias, J. 1969. Seasonal interactions between the North Pacific Ocean and the atmosphere during the 1960s. *Mon. Wea. Rev.* 97: 173-192.

Namias, J. 1970. Macroscale variations in sea surface temperatures in the North Pacific. *J. Geophys. Res.* 75: 565-582.

Namias, J. 1972. Experiments in objectively predicting some atmospheric and oceanic variables for the winter of 1971-72. *J. Appl. Meteorol.* 71: 1164-1174.

Namias, J. 1978. Multiple causes of the North American abnormal winter 1976-77. *Mon. Wea. Rev.* 106: 279-295.

Namias, J. 1981. State of the art predicting short period climatic variations. In Bach, W., Pankrath, J. and Schneider, S.H. (eds.), *Food-Climate Interactions*. Dordrecht: D. Reidel, 399-422.

Namias, J. 1982. Anatomy of the Great Plains protracted heat waves. *Mon. Wea. Rev.* 110: 825-838.

Namias, J. 1986. Persistence of flow patterns over North America and adjacent ocean sectors. *Mon. Wea. Rev.* 114: 1368-1383.

Namias, J. 1991. Spring and summer 1988 drought over the contiguous United States - Causes and prediction. *J. Climate* 4: 54-65.

Namias, J. and Cayan, D. 1981. Large scale air-sea interactions and short period climatic fluctuations. *Science* 214: 869-876.

Namias, J., Yuan, X. and Cayan, D. 1988. Persistence of North Pacific sea surface temperatures and atmospheric flow patterns. *J. Climate* 1: 682-703.

Norton, J., McLain, D., Brainard, R. and Husby, D. 1985. The 1982-83 El Niño event off Baja and Alta California and its ocean climate context. In Wooster, W.S. and Fluharty, D.L. (eds.), *El Niño North*. University of Washington, 44-72.

Oglesby, R.J. 1991. Springtime soil moisture, natural climatic variability, and North American drought as simulated by the NCAR Community Climate Model 1. *J. Climate* 4: 890-897.

Oglesby, R.J. and Erickson III, D.E. 1989. Soil moisture and the persistence of North American drought. *J. Climate* 2: 1362-1380.

Ookouchi, Y., Segal, M., Kessler, R.C. and Pielke, R.A. 1984. Evaluation of soil moisture effects on the generation and modification of mesoscale circulations. *Mon. Wea. Rev.* 112: 2281-2292.

Opsteegh, J.D. and van den Dool, H. 1980. Seasonal differences in the stationary response of a linearized primitive equation model: prospects for long-range forecasting? *J. Atmos. Sci.* 37: 2169-2185.

Palmer, T.N. and Sun, Z. 1985. A modelling and observational study of the relationship between sea surface temperatures in the north west Atlantic and the atmosphere general circulation. *Quart. J. Roy. Meteorol. Soc.* 111: 947-975.

Pan, Y.H. and Oort, A.H. 1983. Global climate variations connected with sea surface temperature anomalies in the eastern equatorial Pacific Ocean for the 1958-73 period. *Mon. Wea. Rev.* 111: 1244-1258.

Pan, Y.H. and Oort, A.H. 1990. Correlation analyses between sea surface temperature anomalies in the eastern equatorial Pacific and the world ocean. *Climate Dyn.* 4: 191-205.

Perry, A.H. and Walker, J.M. 1977. *The Ocean - Atmosphere System.* Longman Press, New York, 160 pp.

Philander, S.G.H. 1985. El Niño and La Niña. *J. Atmos. Sci.* 42: 2652-2662.

Philander, S.G.H. 1990. *El Niño, La Niña, and the Southern Oscillation.* Academic Press Inc., Toronto, 289pp.

Pitcher, E.J., Blackmon, M.L., Bates, G.T. and Munoz, S. 1988. The effect of North Pacific sea surface temperature anomalies on the January climate of a general circulation model. *J. Atmos. Sci.* 45: 173-188.

Quinn, W.H., Zopf, D.O., Short, K.S. and Kuo-Yang, R.T.W. 1978. Historical trends and statistics of the Southern Oscillation, El Niño, and the Indonesian droughts. *Fish. Bull.* 76: 663-678.

Ramage, C.S. 1986. El Niño. *Scientific American* 254: 76-83.

Rasmusson, E.M., Arkin, P.A., Krueger, K.F., Quiroz, R.S. and Reynolds, R.W. 1983. The equatorial Pacific atmospheric climate during 1982-83. *Trop. Ocean-Atmos. Newslett.* 21: 2-3.

Rasmusson, E.M. and Carpenter, T.H. 1982. Variations in tropical sea surface temperature and surface wind fields associated with the Southern Oscillation/El Niño. *Mon. Wea. Rev.* 110: 354-384.

Rasmusson, E.M., Wong, X. and Ropelewski, C.F. 1990. The biennial component of ENSO variability. *J. Marine Sys.* 1: 71-96.

Reynolds, R.W. and Rasmusson, E.M. 1983. The North Pacific sea surface temperature associated with El Niño events. *Proc. of the Seventh Annual Climate Diagnostic Workshop.* Boulder, Colorado, NOAA, 298-310.

Ripley, E.A. 1988. *Drought Prediction on the Canadian Prairies.* Report 88-4, Canadian Climate Centre, AES, National Hydrology Research Centre, Saskatoon, Sask., 137pp.

Ripley, E.A. 1991. *Study of the Arctic Heat Sink.* Report 91-5, Canadian Climate Centre, AES, National Hydrology Research Centre, Saskatoon, Sask., 95pp.

Ritchie, H. 1993. *Personal communication.*

Roads, J.O. 1981. Linear and nonlinear aspects of snow albedo feedbacks in atmospheric models. *J. Geophys. Res.* 86: 7411-7424.

Ropelewski, C.F. and Halpert, M.S. 1986. North American precipitation and temperature patterns associated with El Niño/Southern Oscillation (ENSO). *Mon. Wea. Rev.* 114: 2352-2362.

Ropelewski, C.F. and Halpert, M.S. 1987. Global and regional scale precipitation associated with El Niño/Southern Oscillation. *Mon. Wea. Rev.* 115: 1606-1626.

Ropelewski, C.F. and Halpert, M.S. 1989. Precipitation patterns associated with the high index phase of the Southern Oscillation. *J. Climate* 2: 268-284.

Shabbar, A. 1993. *Explosive Volcanoes, ENSOs and the Canadian Climate.* Report 93-6, Canadian Climate Centre, AES, Downsview, Ontario. 36pp.

Shukla, J. and Mintz, Y. 1982. The influence of land surface evapotranspiration on the earth's climate. *Science* 215: 1498-1501.

Shukla, J. and Wallace, J.M. 1983. Numerical simulation of the atmospheric response to equatorial Pacific sea surface temperature anomalies. *J. Atmos. Sci.* 40: 1613-1630.

Simmons, A.J. 1982. The forcing of stationary wave motion by tropical diabatic heating. *Quart. J. Roy. Meteorol. Soc.* 108: 503-534.

Simmons, A.J., Wallace J.M. and Branstator, G.W. 1983. Barotropic wave propagation and instability, and atmospheric teleconnection patterns. *J. Atmos. Sci.* 40: 1363-1392.

Simpson, J.J. 1983. Large-scale thermal anomalies in the California Current during the 1982-1983 El Niño. *Geophys. Res. Lett.* 10: 937-940.

Skinner, W.R. 1985. The effects of major volcanic eruptions on Canadian climate. In: Harington, C.R. (ed), *Climatic Change in Canada.* National Museums of Canada, Ottawa. 75-106.

Trenberth, K.E. 1975. A quasi-biennial standing wave in the Southern Hemisphere and interrelations with sea surface temperature. *Quart. J. Roy. Meteorol. Soc.* 101: 55-74.

Trenberth, K.E. 1976. Spatial and Temporal variations in the Southern Oscillation. *Quart. J. Roy. Meteorol. Soc.* 102: 639-653.

Trenberth, K.E. 1984. Signal versus noise in the Southern Oscillation. *Mon. Wea. Rev.* 112: 326-332.

Trenberth, K.E. 1991. General characteristics of El Niño-Southern Oscillation. In Glantz, M.H., Katz, R.W. and Nicholls, N. (eds.), *Teleconnections Linking Worldwide Climate Anomalies.* Cambridge University Press, Cambridge, 13-42.

Trenberth, K.E., Branstator, G.W. and Arkin P.A. 1988. Origins of the 1988 North American drought. *Science* 242: 1640-1645.

Tribbia, J.J. 1991. The rudimentary theory of atmospheric teleconnections associated with ENSO. In Glantz, M.H., Katz, R.W. and Nicholls, N. (eds.), *Teleconnections Linking Worldwide Climate Anomalies.* Cambridge University Press, Cambridge, 285-308.

van Loon, H. and Madden, R.A. 1981. The Southern Oscillation Part I: Global associations with pressure and temperature in the northern winter. *Mon. Wea. Rev.* 109: 1150-1162.

van Loon, H. and Shea, D.J. 1985. The Southern Oscillation Part IV: The precursors south of 15°S to the extremes of the oscillation. *Mon. Wea. Rev.* 113: 2063-2074.

Wagner, A.J. 1984. Possible mid-latitude atmospheric generation of anomalously warm surface waters in the Gulf of Alaska from autumn 1982 to spring 1983. *Trop. Ocean-Atmos. Newslett.* 26: 15-16.

Walker, G.T. 1924. Correlations in seasonal variations in weather. VIII: Preliminary study of world weather. *Mem. Ind. Meteorol. Dept.* 24: 275-332.

Walker, G.T. and Bliss, E.W. 1932. World Weather V. *Mem. Roy. Meteorol. Soc.* 4: 53-84.

Wallace, J.M and Gutzler, D.S. 1981. Teleconnections in the geopotential height field during the Northern Hemisphere winter. *Mon. Wea. Rev.* 109: 784-812.

Wallace, J.M and Jiang, Q. 1987. On the observed structure of interannual variability of the atmosphere/ocean climate system. In Cattle, H. (ed.), *Atmospheric and Oceanic Variability.* Royal Meteorological Society, 17-43.

Wallace, J.M., Smith, C. and Jiang, Q. 1990. Spatial patterns of atmosphere - ocean interaction in the northern winter. *J. Climate* 3: 990-998.

Walsh, J.E., Jasperson, W.H. and Ross, B. 1985. Influences of snow cover and soil moisture on monthly air temperature. *Mon. Wea. Rev.* 113: 756-768.

Walsh, J.E., Tucek, D.R. and Peterson, M.R. 1982. Seasonal snow cover and short term climatic sensitivity. *Mon. Wea. Rev.* 110: 1474-1485.

Weare, B.C., Navator, A.R. and Newell, R.E. 1976. Empirical orthogonal analysis of Pacific sea surface temperature. *J. Phys. Oceanogr.* 6: 671-678.

Weber, G.R. 1990. North Pacific circulation anomalies, El Niño and anomalous warmth over the North American continent in 1986-1988: Possible causes of the 1988 North American drought. *Int. J. Climatol.* 10: 279-289.

Webster, P.J. 1981. Mechanisms determining the atmospheric response to sea surface temperature anomalies. *J. Atmos. Sci.* 38: 554-571.

Webster, P.J. 1982. Seasonality in the local and remote atmospheric response to sea surface temperature anomalies. *J. Atmos. Sci.* 39: 41-52.

Webster, P.J. and Holton, J.R. 1982. Crossequatorial response to middle-latitude forcing in a zonally varying basic state. *J. Atmos. Sci.* 39: 722-733.

Wheaton, E.E., Arthur, L.M., Chorney, B., Shewchuk, S., Thorpe, J., Whiting, J. and Wittrock, V. 1992. The Prairie Drought of 1988. *Clim. Bull.* 26: 188-205.

Wick, G. 1973. Where Poseidon courts Aeolus. *New Scientist* 18: 123-126.

Wyrtki, K. 1975. El Niño - the dynamic response to the equatorial Pacific Ocean to atmospheric forcing. *J. Phys. Oceanogr.* 9: 1223-1231.

Yarnal, B. 1985. Extratropical teleconnections associated with El Niño/Southern Oscillation (ENSO) events. *Progress Phys. Geogr.* 9: 315-352.

Yarnal, B. and Diaz, H.F. 1986. Relationships between extremes of the Southern Oscillation and the winter climate of the Anglo-American Pacific coast. *J. Climatol.* 6: 197-219.

Yeh, T. 1949. On energy dispersion in the atmosphere. *J. Meteorology* 6: 1-16.

Yongping, Z. and McBean, G.A. 1991. Seasonal North Pacific sea surface temperature patterns and their relations to the atmospheric circulation. *Marine Sciences* 3: 27-33.

Zhao, Y.P. and McBean, G.A. 1986. Annual and interannual variability of the North Pacific ocean-to-atmosphere total heat transfer. *Atm. Ocean* 24: 265-282.

APPENDIX A

PRECIPITATION

TABLE A.1: Stations Used in This Study.

ALBERTA:

Station	Number	Time Period
1. Elk Point *	3012280	1948-1991
2. Edmonton	3012208	1948-1991
3. Ranfurly	3015400	1948-1989
	3015405	1990-1991
4. Camrose	3011240	1948-1991
	3011241	July 1979
5. Rocky Mtn House	3015520	1948-1977
	3015522	1978-1991
6. Lacombe	3023720	1948-1991
7. Olds *	3024920	1948-1991
8. Drumheller	3022120	1948-1968
	3022136	1969-1991
9. Empress *	3022400	1948-1991
10. Calgary	3031093	1948-1991
11. Gleichen *	3032800	1948-1991
12. Brooks	3030840	1948-1954
	3030856	1955-1988
	3030862	1989-1991
13. Medicine Hat	3034480	1948-1991
14. Lethbridge	3033880	1948-1991
15. Foremost *	3032640	1948-1991
16. Fort Macleod	3032680	1948-1988
	30326QF	1989-1991
17. Manyberries *	3044200	1948-1991
18. Goose Mountain *	3062880	1948-1991
19. Campsie	3061200	1948-1991
20. Lovett *	3064040	1948-1991
21. Carrot Creek *	3061360	1948-1991
22. Fairview *	3072520	1948-1991
23. Beaver Lodge	3070560	1948-1991

* denotes station had some missing data.

TABLE A.1 (Continued)

SASKATCHEWAN:

Station	Number	Time Period
1. Humboldt *	4013400	1948-1973
	4013401	1974-1991
2. Yorkton	4019080	1948-1991
3. Tugaske	4018160	1948-1991
4. Dilke *	4012200	1948-1991
5. Indian Head	4013480	1948-1991
6. Regina	4016560	1948-1991
7. Moose Jaw *	4015320	1948-1991
8. Moosomin	4015360	1948-1991
9. Willmar *	4018960	1948-1991
10. Estevan	4012400	1948-1991
11. Semans *	4017320	1948-1991
12. Midale	4015160	1948-1991
13. Leader *	4024160	1948-1969
	4024161	1970-1991
14. Swift Current	4028040	1948-1991
15. Maple Creek *	4024920	1948-1957
	4024936	1958-1991
16. Shaunavon *	4027480	1948-1978
	4027485	1979-1991
17. Aneroid *	4020160	1948-1991
18. Gravelbourg	4022960	1948-1991
19. Consul *	4031760	1948-1969
	4031776	1970-1991
20. North Battleford	4045600	1948-1991
21. Scott	4047240	1948-1991
22. Kindersley	4043888	1948-1971
	4043920	1972-1988
	4043900	1989-1991
23. Prince Albert	4056240	1948-1991
24. Melfort	4055080	1948-1961
	4055085	1962-1991
25. Saskatoon	4057120	1948-1991
26. Outlook *	4055720	1948-1971
	4055736	1972-1991
27. Lost River	4074640	1948-1991

TABLE A.1 (Continued)

MANITOBA:

	Station	Number	Time Period
1.	Russell *	5012520	1948-1991
2.	Birtle *	5010240	1948-1991
3.	Virden *	5012960	1948-1991
4.	Brandon	5010480	1948-1991
5.	Pierson	5012080	1948-1991
6.	Cypress River *	5010640	1948-1991
7.	Portage La Prairie	5012280	1948-1971
		5012320	1972-1991
8.	Morden	5021848	1948-1991
9.	Winnipeg	5023222	1948-1991
10.	Emerson *	5020880	1948-1991
11.	Indian Bay	5031320	1948-1991
12.	Swan River *	5042800	1948-1991
13.	Dauphin	5040680	1948-1991

TABLE A.2: Replacement Stations.

ALBERTA:

STATION	REPLACEMENT STATION	TIME PERIOD	DISTANCE (km)
Elk Point	Marwayne	Jun,Jul 1963 Jul 1964	60
	Tulliby Lake	May 1978 Aug 1981	53
	Cold Lake	Jun 1961	80
Empress	Pollockville	Jul 1961	113
Olds	Bowden	May,Jun 1963	16
	Madden	Jul 1963	42
Gleichen	Queenstown	Jun 1962 May,Jul,1963	27
Goose Mountain	High Prairie	May 1948,1951	64
	Sweathouse	May,Jun 1955 Aug 1961	77
Fairview	Berwyn	Aug 1956	50
Lovett	Entrance	Jun 1950 Jun,Jul 1953	115
Carrot Creek	Edson	Jun,Jul 1954 May 1956 Aug 1965	39
Foremost	Taber	Aug 1955	61
Manyberries	Altawan	May,Jun,Jul Aug 1991	35

SASKATCHEWAN:

Dilke	Lumsden	May,Jun,Jul,Aug 1949, Aug 1950	36
Moose Jaw	Caron	Jul 1953	22
Humboldt	Muenster	May 1977	9
Maple Creek	Klintonel	Jul 1951, May 1987, Jun 1989	65

TABLE A.2 (Continued)

Aneroid	Hazenmore	May,Jun,Jul 1962	12
	Limerick	May, Jun 1989	79
Shaunavon	Instow	Jun 1956	14
Consul	Claydon	Jun,Jul,Aug 1983, Aug 1984 May,Jul 1985 May,Jun,Jul 1986 1990, 1991	43
Outlook	Glenside	Jun 1986	16
Semans	Nokomis	Aug 1961 Jul 1962 May,Jun,Jul 1964	24
	Duval	May,Aug 1963 Aug 1964	31
Leader	Abbey	Jul 1962	58
Willmar	Arcola	Jun 1961	16
MANITOBA:			
Birtle	Hamiota	May 1952	45
Virden	Reston	Jun 1956	35
Cypress River	St. Alphonse	May 1964	15
Emerson	Morden	May 1979	68
Russell	Birtle	May 1953	40
	Binscarth	1991	23
Swan River	Durban	Jul 1964	24

TABLE A.3: Total Number of 10-Day Dry Spells

YEAR	TOTAL	MAY	JUNE	JULY	AUGUST
1948	854	248	283	246	77
1949	686	301	103	180	102
1950	545	108	177	166	94
1951	456	177	135	128	16
1952	603	316	20	156	111
1953	701	32	129	331	209
1954	228	99	67	59	3
1955	964	43	169	444	308
1956	534	172	89	173	100
1957	421	246	67	81	27
1958	838	413	52	255	118
1959	541	175	140	202	24
1960	950	72	376	427	75
1961	1956	249	436	729	542
1962	361	89	53	116	103
1963	217	63	52	62	40
1964	637	278	121	161	77
1965	514	96	50	232	136
1966	463	205	69	136	53
1967	1485	208	281	603	393
1968	571	213	191	131	36
1969	996	115	184	375	322
1970	990	146	45	450	349
1971	874	226	48	396	204
1972	479	105	44	191	139
1973	710	167	168	280	95
1974	505	2	304	179	20
1975	353	59	56	216	34
1976	336	103	44	130	59
1977	181	8	83	59	31
1978	283	22	65	139	57
1979	639	39	94	282	224
1980	761	636	52	50	23
1981	750	185	44	287	234
1982	137	26	46	42	23
1983	334	51	38	157	88
1984	758	8	327	339	84
1985	612	119	326	150	17
1986	482	109	12	185	176
1987	229	171	36	19	3
1988	683	187	228	211	97
1989	332	38	113	131	50
1990	314	19	55	141	99
1991	501	4	81	252	164
AVE	608.3	144.3	127.8	218.1	118.1
STD	335.6	121.9	104.1	146.4	115.0

TABLE A.3: Continued (Standardized)

YEAR	TOTAL	MAY	JUNE	JULY	AUGUST
1948	+0.73	+0.85	+1.49	+0.19	-0.36
1949	+0.23	+1.29	-0.24	-0.26	-0.14
1950	-0.19	-0.30	+0.47	-0.36	-0.21
1951	-0.52	+0.27	+0.07	-0.62	-0.89
1952	-0.02	+1.41	-1.04	-0.42	-0.06
1953	+0.28	-0.92	+0.01	+0.77	+0.79
1954	-1.13	-0.37	-0.58	-1.09	-1.00
1955	+1.06	-0.83	+0.40	+1.54	+1.65
1956	-0.22	+0.23	-0.37	-0.31	-0.16
1957	-0.56	+0.83	-0.58	-0.94	-0.79
1958	+0.68	+2.20	-0.73	+0.25	0.00
1959	-0.20	+0.25	+0.12	-0.11	-0.82
1960	+1.02	-0.59	+2.39	+1.43	-0.36
1961	+4.02	+0.86	+2.96	+3.49	+3.69
1962	-0.74	-0.45	-0.72	-0.70	-0.13
1963	-1.17	-0.67	-0.73	-1.07	-0.68
1964	+0.09	+1.10	-0.07	-0.39	-0.36
1965	-0.28	-0.40	-0.75	+0.10	+0.16
1966	-0.43	+0.50	-0.57	-0.56	-0.57
1967	+2.61	+0.47	+1.47	+2.63	+2.39
1968	-0.11	+0.56	+0.61	-0.60	-0.71
1969	+1.16	-0.24	+0.54	+1.07	+1.77
1970	+1.14	+0.01	-0.80	+1.58	+2.01
1971	+0.79	+0.67	-0.77	+1.22	+0.75
1972	-0.39	-0.32	-0.81	-0.19	+0.18
1973	+0.30	+0.19	+0.39	+0.42	-0.20
1974	-0.31	-1.17	+1.69	-0.27	-0.85
1975	-0.76	-0.70	-0.69	-0.01	-0.73
1976	-0.81	-0.34	-0.81	-0.60	-0.51
1977	-1.27	-1.12	-0.53	-1.09	-0.76
1978	-0.97	-1.00	-0.60	-0.48	-0.49
1979	+0.09	-0.86	-0.33	+0.44	+0.92
1980	+0.46	+4.03	-0.73	-1.15	-0.83
1981	+0.42	+0.33	-0.81	+0.47	+1.01
1982	-1.40	-0.97	-0.79	-1.20	-0.83
1983	-0.82	-0.77	-0.86	-0.42	-0.26
1984	+0.53	-1.12	+1.91	+0.83	-0.30
1985	+0.01	-0.21	+1.90	-0.47	-0.88
1986	-0.38	-0.29	-1.11	-0.23	+0.50
1987	-1.13	+0.22	-0.88	-1.36	-1.00
1988	+0.52	+0.35	+1.03	+0.05	-0.27
1989	-0.82	-0.87	-0.14	-0.60	-0.59
1990	-0.88	-1.03	-0.70	-0.53	-0.17
1991	-0.32	-1.15	-0.45	+0.23	+0.40

TABLE A.4: Areally-Averaged Precipitation Anomalies (mm)

YEAR	TOTAL	MAY	JUNE	JULY	AUGUST
1948	-43.3	-11.4	-28.6	+12.2	-15.5
1949	-20.4	+4.0	-23.6	+10.2	-11.0
1950	-22.3	-10.4	-11.1	+16.4	-17.2
1951	-1.6	-2.9	-8.5	-12.9	+22.7
1952	+17.5	-14.7	+18.8	+7.2	+6.2
1953	+66.8	+21.1	+32.3	+10.3	+3.1
1954	+81.3	+11.2	+26.9	-12.2	+55.4
1955	-31.1	+6.0	-19.4	+12.0	-29.7
1956	+22.8	-19.6	+32.8	+1.7	+7.9
1957	-15.7	-24.6	-11.4	-3.6	+23.9
1958	-86.6	-25.2	-28.0	-13.7	-19.7
1959	-15.3	-9.6	+17.1	-29.2	+6.4
1960	-23.4	+5.8	-5.3	-25.5	+1.6
1961	-107.7	-10.0	-30.8	-19.6	-47.3
1962	+26.1	+11.1	-7.2	+9.0	+13.2
1963	+8.9	-9.1	+23.4	+4.4	-9.8
1964	+6.8	+7.4	-18.5	+2.2	+15.7
1965	+61.5	+27.7	+30.5	-2.6	+5.9
1966	+8.2	-18.9	-2.1	-0.6	+29.8
1967	-110.9	-26.6	-34.6	-23.4	-26.3
1968	+14.5	+4.9	-14.4	+0.2	+23.8
1969	-39.9	-8.7	-24.0	+9.0	-16.2
1970	-5.2	-11.0	+32.2	+6.8	-33.2
1971	+9.2	-23.8	+32.6	+21.8	-21.4
1972	-29.6	-6.0	-2.9	-10.1	-10.6
1973	+21.4	-6.9	+31.2	-12.5	+9.6
1974	+78.5	+33.0	+32.3	-5.4	+18.6
1975	+22.2	+2.6	+19.2	-21.3	+21.7
1976	+18.9	-16.7	+43.8	-13.1	+4.9
1977	+48.6	+63.7	-27.5	+15.2	-2.8
1978	-3.4	+16.9	-10.6	-5.5	-4.2
1979	-36.2	+3.5	-12.0	-6.4	-21.3
1980	+9.4	-15.3	+4.6	-15.8	+35.9
1981	-13.4	-3.6	-0.6	+13.1	-22.3
1982	+28.7	+12.2	-37.0	+45.5	+8.0
1983	+12.9	-10.3	+17.3	+33.0	-27.1
1984	-35.1	+6.8	+10.7	-36.5	-16.1
1985	-16.5	+3.1	+18.6	-36.7	+31.5
1986	+14.5	+14.6	-13.0	+45.3	-32.4
1987	+19.1	-7.5	-22.0	+37.6	+11.0
1988	-3.5	-0.3	-5.5	-11.3	+13.6
1989	+27.7	+7.7	+6.2	-16.0	+29.8
1990	+17.4	+7.2	+8.1	+15.7	-13.6
1991	+47.6	+28.4	+42.8	-7.2	-16.4
AVE	+1.42	+0.13	-0.43	-0.28	-0.32
STD	40.81	17.43	23.04	19.13	21.87

TABLE A.4: Continued (Standardized)

YEAR	TOTAL	MAY	JUNE	JULY	AUGUST
1948	-1.10	-0.66	-1.22	+0.65	-0.69
1949	-0.53	+0.22	-1.01	+0.55	-0.49
1950	-0.58	-0.60	-0.46	+0.87	-0.77
1951	-0.07	-0.18	-0.35	-0.66	+1.05
1952	+0.39	-0.85	+0.83	+0.39	+0.30
1953	+1.60	+1.20	+1.42	+0.45	+0.15
1954	+1.96	+0.63	+1.18	-0.62	+2.55
1955	-0.80	+0.34	-0.82	+0.64	-1.34
1956	+0.52	-1.13	+1.44	+0.10	+0.38
1957	-0.42	-1.42	-0.47	-0.17	+1.11
1958	-2.16	-1.46	-1.20	-0.70	-0.89
1959	-0.41	-0.56	+0.76	-1.51	+0.31
1960	-0.61	+0.32	-0.21	-1.32	+0.09
1961	-2.67	-0.58	-1.32	-1.01	-2.15
1962	+0.60	+0.63	-0.29	+0.48	+0.62
1963	+0.18	-0.53	+1.03	+0.24	-0.44
1964	+0.13	+0.42	-0.79	+0.13	+0.73
1965	+1.47	+1.58	+1.34	-0.12	+0.29
1966	+0.17	-1.09	-0.07	+0.02	+1.38
1967	-2.75	-1.53	-1.48	-1.21	-1.19
1968	+0.32	+0.27	-0.61	+0.02	+1.10
1969	-1.01	-0.51	-1.02	+0.49	-0.72
1970	-0.16	-0.64	+1.42	+0.37	-1.50
1971	+0.19	-1.37	+1.43	+1.15	-1.06
1972	-0.76	-0.36	-0.11	-0.49	-0.47
1973	+0.49	-0.41	+1.37	-0.64	+0.45
1974	+1.89	+1.89	-1.38	-0.27	+0.86
1975	+0.51	+0.14	+0.85	-1.10	+1.00
1976	+0.43	-0.96	+1.92	-0.67	+0.24
1977	+1.16	+3.65	-1.17	+0.81	-0.11
1978	-0.12	+0.96	-0.54	-0.27	-0.18
1979	-0.92	+0.19	-0.50	-0.32	-0.96
1980	+0.20	-0.88	+0.22	-0.81	+1.65
1981	-0.36	-0.21	-0.01	+0.70	-1.01
1982	+0.67	+0.69	-1.59	+2.39	+0.38
1983	+0.28	-0.60	+0.77	+1.74	-1.22
1984	-0.90	+0.38	+0.48	-1.89	-0.72
1985	-0.37	+0.17	-0.79	-1.90	+1.46
1986	+0.32	+0.83	-0.55	+2.38	-1.47
1987	+0.43	-0.44	-0.94	+1.98	+0.52
1988	-0.12	+0.02	-0.22	-0.58	+0.64
1989	+0.64	+0.43	+0.29	-0.82	+1.38
1990	+0.39	+0.41	+0.37	+0.84	-0.61
1991	+1.13	+1.62	+1.88	-0.36	-0.74

APPENDIX B

50 KPA HEIGHTS

TABLE B.1: Areally-Averaged 50 kPa Height Anomalies (dam)

YEAR	MAY	JUNE	JULY	AUGUST
1948	+5.80	+5.95	+0.63	+1.27
1949	+2.16	-1.14	+0.83	+3.17
1950	-1.74	+0.72	+0.31	-0.53
1951	+3.53	-1.57	+1.16	+0.85
1952	+2.61	-0.43	-0.57	-0.94
1953	-0.06	-0.13	+1.25	+2.21
1954	+1.64	-1.43	+2.38	+1.87
1955	-1.39	+3.09	+0.75	+0.54
1956	+1.33	+2.14	+2.33	+0.01
1957	+1.91	-3.55	-1.22	+1.19
1958	+2.97	-0.97	-1.65	+0.07
1959	-3.69	-1.20	-0.39	-4.76
1960	-2.67	-1.28	+2.68	-1.89
1961	+1.80	+6.17	+2.45	+4.16
1962	-2.83	+0.65	-1.40	-2.17
1963	-1.67	-1.24	-0.97	+2.58
1964	-1.64	-1.27	+0.82	-3.82
1965	-3.94	-0.43	+0.15	-0.75
1966	+0.12	-2.09	-0.70	-0.32
1967	-3.45	-0.58	-0.47	+3.14
1968	-1.50	-2.46	-1.64	-3.26
1969	-0.48	-2.49	-2.21	-0.73
1970	-0.17	+4.04	-0.04	+0.06
1971	+1.02	-0.75	-1.14	+3.29
1972	+3.22	+0.97	-2.69	+1.85
1973	+1.86	-1.60	-0.46	-0.63
1974	-6.32	-1.07	-0.88	-2.72
1975	-1.42	-2.89	+0.51	-4.16
1976	+1.14	-1.71	+0.56	+0.77
1977	+0.63	+1.67	-2.33	-5.10
1978	-0.95	-1.05	-2.33	-2.96
1979	-2.82	-0.63	+2.27	-0.71
1980	+3.31	+1.84	-0.80	-3.91
1981	+2.24	-4.81	+0.45	+5.42
1982	+0.89	+0.27	+0.40	+0.06
1983	-2.70	-0.76	-0.63	+3.22
1984	-3.73	-1.07	+0.07	+1.18
1985	+0.60	-1.21	+0.41	-2.05
1986	+1.81	+0.96	-2.99	+0.50
1987	+1.95	+2.83	-1.12	-3.09
1988	+0.99	+6.36	+0.22	-0.32
1989	-0.55	+1.51	+4.28	+1.07
1990	-0.78	-2.13	+1.57	+1.76
1991	+2.12	+1.17	+0.08	+4.32
AVE	-0.01	0.00	0.00	-0.01
STD	2.48	2.39	1.56	2.54

TABLE B.1: Continued (Standardized)

YEAR	MAY	JUNE	JULY	AUGUST
1948	+2.34	+2.49	+0.40	+0.50
1949	+0.88	-0.48	+0.53	+1.25
1950	-0.70	+0.30	+0.20	-0.20
1951	+1.43	-0.66	+0.74	+0.34
1952	+1.06	-0.18	-0.37	-0.37
1953	-0.02	-0.05	+0.80	+0.87
1954	+0.67	-0.60	+1.53	+0.74
1955	-0.56	+1.29	+0.51	+0.22
1956	+0.54	+0.90	+1.49	-0.01
1957	+0.77	-1.49	-0.78	+0.47
1958	+1.20	-0.41	-1.06	+0.03
1959	-1.48	-0.49	-0.25	-1.87
1960	-1.07	-0.54	+1.72	-0.74
1961	+0.73	+2.58	+1.57	+1.64
1962	-1.14	+0.27	-0.90	-0.85
1963	-0.67	-0.52	-0.62	+1.02
1964	-0.66	-0.53	+0.53	-1.50
1965	-1.58	-0.18	+0.10	-0.29
1966	+0.05	-0.87	-0.52	-0.12
1967	-1.39	-0.24	-0.30	+1.24
1968	-0.60	-1.03	-1.05	-1.28
1969	-0.19	-1.04	-1.42	-0.28
1970	-0.06	+1.69	-0.03	+0.03
1971	+0.42	-0.31	-0.73	+1.30
1972	+1.30	+0.41	-1.72	+0.73
1973	+0.75	-0.67	-0.29	-0.24
1974	-2.54	-0.45	-0.46	-1.07
1975	-0.57	-1.21	+0.33	-1.63
1976	+0.46	-0.72	-0.36	+0.31
1977	+0.26	+0.70	-1.49	-2.00
1978	-0.38	-0.44	-1.49	-1.16
1979	-1.13	-0.26	+1.46	-0.28
1980	+1.34	+0.77	-0.51	-1.54
1981	+0.91	-2.01	+0.29	+2.14
1982	+0.36	+0.11	+0.26	+0.03
1983	-1.08	-0.32	-0.40	+1.27
1984	-1.50	-0.45	+0.04	+0.52
1985	+0.25	-0.51	+0.26	-0.80
1986	+0.73	+0.40	-1.92	+0.20
1987	+0.79	+1.18	-0.72	-1.21
1988	+0.40	+2.66	+0.14	-0.12
1989	-0.22	+0.63	+2.74	+0.43
1990	-0.31	-0.89	+0.98	+0.70
1991	+0.86	+0.49	+0.05	+1.70

APPENDIX C

PNA INDICES

TABLE C.1: Seasonal PNA Indices

YEAR	WINTER	SPRING	SUMMER	AUTUMN
1948	-0.29	-0.67	-0.02	-0.28
1949	-1.42	+0.19	-1.25	+0.15
1950	-1.25	-0.09	+0.69	+0.16
1951	-0.17	+0.33	-0.38	-0.41
1952	-0.83	-0.14	-1.46	+0.48
1953	+0.45	-0.05	-0.62	+0.58
1954	-0.14	-0.82	-0.48	+0.22
1955	-0.32	-0.85	+0.03	-0.60
1956	-0.36	-0.01	+0.83	-0.26
1957	-0.82	+0.46	+0.50	+0.90
1958	+0.94	+0.41	+0.45	-0.59
1959	-0.12	-0.36	-0.19	-0.13
1960	+0.42	+0.48	+0.23	+0.02
1961	+0.98	+0.26	+1.31	-0.91
1962	-0.31	-0.65	-0.33	+0.74
1963	+0.73	-1.11	-0.20	+0.99
1964	+0.67	-1.70	-0.11	-0.20
1965	-0.55	-0.42	+1.00	-0.24
1966	-0.27	-0.13	+0.44	+0.02
1967	+0.15	-1.53	+0.15	+0.84
1968	+0.43	+0.38	+0.47	+0.43
1969	-0.34	+1.15	-0.06	+1.01
1970	+1.29	+0.08	+0.61	-0.66
1971	-0.30	+1.00	+0.08	-0.72
1972	-1.04	+0.44	+0.72	-0.43
1973	+0.32	+0.60	+0.26	+0.12
1974	-0.84	-0.13	+0.14	-0.33
1975	+0.54	-0.33	+0.09	-0.35
1976	+0.04	+0.34	+0.52	+1.44
1977	+1.24	-0.31	+0.27	-0.11
1978	+1.03	+0.55	-0.31	-0.32
1979	-0.67	-0.12	-0.64	+0.72
1980	+0.60	+1.02	-1.27	+0.79
1981	+1.15	+1.15	+0.76	+0.30
1982	-0.31	-0.75	+0.22	-0.02
1983	+1.30	+0.83	+0.22	-0.16
1984	+0.40	+0.87	+0.16	-0.20
1985	-0.40	-0.58	-0.34	-2.12
1986	+1.26	+0.36	+0.14	-0.35
1987	+0.96	+0.13	-0.10	-0.28
1988	-0.29	-0.67	-0.02	-0.28
1989	-1.42	+0.19	-1.25	+0.15
1990	-1.25	-0.09	+0.69	+0.16
1991	-0.17	+0.33	-0.38	-0.41
AVE	+0.03	0.00	+0.04	0.00
STD	0.76	0.66	0.60	0.63

TABLE C.1: Continued (Standardized)

YEAR	WINTER	SPRING	SUMMER	AUTUMN
1948	-0.43	-1.01	-0.09	-0.44
1949	-1.91	+0.28	-2.16	+0.24
1950	-1.68	-0.13	+1.08	+0.25
1951	-0.26	+0.50	-0.70	-0.64
1952	-1.13	-0.21	-2.50	+0.77
1953	+0.56	-0.08	-1.10	+0.92
1954	-0.23	-1.25	-0.86	+0.35
1955	-0.46	-1.28	-0.01	-0.96
1956	-0.51	-0.02	+1.32	-0.41
1957	-1.12	+0.70	+0.77	+1.44
1958	+1.20	+0.63	+0.68	-0.94
1959	-0.19	-0.55	-0.39	-0.21
1960	+0.51	+0.73	+0.32	+0.03
1961	+1.25	+0.39	+2.12	-1.45
1962	-0.45	-0.99	-0.61	+1.18
1963	+0.92	-1.68	-0.40	+1.57
1964	+0.84	-2.58	-0.25	-0.32
1965	-0.76	-0.64	+1.60	-0.38
1966	-0.40	-0.19	+0.67	+0.03
1967	+0.16	-2.32	+0.18	+1.33
1968	+0.53	+0.57	+0.71	+0.68
1969	-0.49	+1.75	-0.16	+1.61
1970	+1.66	+0.12	+0.95	-1.05
1971	-0.43	+1.52	+0.07	-1.15
1972	-1.41	+0.67	+1.13	-0.69
1973	+0.38	+0.91	+0.37	+0.11
1974	-1.13	-0.19	+0.17	+0.76
1975	-0.68	-0.31	+0.09	-0.55
1976	-0.01	+0.51	+0.79	+2.29
1977	+1.59	-0.48	+0.38	-0.17
1978	+1.31	+0.83	-0.58	-0.50
1979	-0.92	-0.17	-1.14	+1.14
1980	+0.75	+1.55	-2.18	+1.26
1981	+1.48	+1.74	+1.19	+0.48
1982	-0.45	-1.14	+0.30	-0.02
1983	+1.67	+1.25	+0.30	-0.25
1984	+0.49	+1.32	+0.21	-0.31
1985	-0.56	-0.88	-0.63	-3.37
1986	+1.62	+0.55	+0.17	-0.55
1987	+1.23	+0.20	-0.24	-0.44
1988	-0.43	-1.01	-0.09	-0.44
1989	-1.91	+0.28	-2.16	+0.24
1990	-1.68	-0.13	+1.08	+0.25
1991	-0.26	+0.50	-0.70	-0.64

APPENDIX D

NORTH PACIFIC SST ANOMALIES

TABLE D.1: Seasonal North Pacific SST Anomaly Gradients (°C)

YEAR	WINTER	SPRING	SUMMER	AUTUMN
1948	-1.40	-1.93	+0.97	-0.93
1949	-4.63	-1.33	+1.37	+0.43
1950	-1.63	-2.93	-2.17	+1.43
1951	+1.20	-1.63	-0.77	-1.43
1952	-2.50	-1.73	-0.30	+0.47
1953	+1.83	+1.17	-0.90	+1.80
1954	+1.87	-0.60	-0.10	+2.20
1955	+0.93	-2.30	-1.33	-2.87
1956	-2.17	-1.13	+0.60	-0.33
1957	-2.97	-1.23	+2.17	+1.37
1958	+2.03	+2.63	+3.37	+1.83
1959	+2.53	+1.57	-1.00	-1.83
1960	+2.47	+1.97	-0.27	+0.33
1961	+2.80	+2.00	+2.70	-0.87
1962	-1.90	-1.47	-2.13	-0.27
1963	+1.70	+1.77	+1.93	+2.83
1964	+0.87	-1.83	-0.90	-0.63
1965	-1.80	-1.80	-2.07	+0.90
1966	+1.80	-0.37	+0.33	+0.77
1967	+0.47	-1.27	-0.43	+2.53
1968	-1.53	-0.87	-0.43	-1.03
1969	-0.57	+0.47	+1.00	+0.43
1970	+2.00	+0.53	-2.87	-2.70
1971	-0.90	-2.13	-2.60	-1.53
1972	-4.47	-2.53	-0.53	-2.73
1973	-2.73	-1.37	-1.63	-1.57
1974	-0.57	-1.53	-1.60	+0.47
1975	-2.10	-2.37	-2.90	-1.47
1976	-2.40	-2.40	-1.07	+1.23
1977	+2.40	+0.60	+0.20	+0.40
1978	+0.80	+2.20	+1.23	-0.93
1979	-2.70	-1.77	+0.67	+2.67
1980	+2.00	+1.77	+0.37	+0.43
1981	+2.77	+2.70	+1.93	-0.80
1982	-2.40	-2.40	-1.07	+1.23
1983	+1.10	+3.97	+3.00	+2.27
1984	+1.47	+0.80	-1.00	+0.53
1985	-1.43	-1.70	-0.70	-2.27
1986	+0.77	-0.73	-0.73	-0.37
1987	+2.97	+1.92	+1.85	+2.57
1988	+2.17	+2.17	+0.57	-0.57
1989	-2.07	-0.63	+0.63	-2.60
1990	-1.90	+0.70	+1.87	-0.87
1991	-2.37	-2.03	-2.76	-2.53
AVE	-0.25	-0.35	-0.18	-0.07
STD	2.14	1.82	1.58	1.64

TABLE D.1: Continued (Standardized)

YEAR	WINTER	SPRING	SUMMER	AUTUMN
1948	-0.54	-0.87	+0.73	-0.53
1949	-2.05	-0.54	+0.98	+0.31
1950	-0.65	-1.42	-1.26	+0.92
1951	+0.68	-0.71	-0.37	-0.83
1952	-1.05	-0.76	-0.08	+0.33
1953	+0.97	+0.83	-0.46	+1.14
1954	+0.99	-0.14	+0.05	+1.38
1955	+0.55	-1.07	-0.73	-1.71
1956	-0.90	-0.43	+0.49	-0.16
1957	-1.27	-0.49	+1.49	+0.88
1958	+1.07	+1.64	+2.24	+1.16
1959	+1.30	+1.05	-0.49	-1.08
1960	+1.27	+1.27	-0.05	+0.25
1961	+1.43	+1.29	+1.82	-0.49
1962	-0.77	-0.61	-1.24	-0.12
1963	+0.91	+1.16	+1.34	+1.77
1964	+0.52	-0.82	-0.46	-0.34
1965	-0.72	-0.80	-1.19	+0.59
1966	+0.96	+0.01	+0.10	+0.51
1967	+0.33	-0.49	-0.16	+1.59
1968	-0.60	-0.28	-0.16	-0.59
1969	-0.15	+0.45	+0.75	+0.31
1970	+1.05	+0.49	-1.70	-1.60
1971	-0.30	-0.98	-1.53	-0.89
1972	-1.97	-1.20	-0.22	-1.62
1973	-1.16	-0.56	-0.92	-0.91
1974	-0.15	-0.65	-0.90	+0.33
1975	-0.86	-1.11	-1.72	-0.85
1976	-1.00	-1.13	-0.56	+0.79
1977	+1.24	+0.14	+0.14	+0.29
1978	+0.50	+1.40	+0.89	-0.53
1979	-1.14	-0.78	+0.54	+1.67
1980	+1.05	+1.16	+0.35	+0.31
1981	+1.41	+1.68	+1.34	-0.45
1982	-1.00	-1.13	-0.56	+0.79
1983	+0.63	+2.37	+2.01	+1.42
1984	+0.80	+0.63	-0.48	+0.37
1985	-0.55	-0.74	-0.33	-1.34
1986	+0.48	-0.21	-0.35	-0.18
1987	+1.50	+1.25	+1.28	+1.61
1988	+1.13	+1.38	+0.50	-0.30
1989	-0.85	-0.16	+0.51	-1.54
1990	-0.77	+0.58	+1.30	-0.49
1991	-0.99	-0.92	-1.59	-1.50

APPENDIX E

SOI VALUES

TABLE E.1: Seasonal SOI Values

YEAR	WINTER	SPRING	SUMMER	AUTUMN
1948	-0.67	-0.04	-0.39	+0.17
1949	-0.79	+0.10	-0.82	+0.13
1950	+2.01	+2.00	+2.81	+1.97
1951	+2.81	-1.24	-1.05	-1.73
1952	-1.59	+0.06	+0.41	+0.10
1953	-1.09	-1.60	-1.05	-0.90
1954	-0.26	+0.26	+0.58	+0.37
1955	+1.48	+0.36	+2.28	+2.50
1956	+2.21	+1.66	+1.68	+1.23
1957	+0.78	-0.70	-0.45	-1.13
1958	-1.86	-0.50	+0.58	-0.43
1959	-1.99	+0.86	-0.69	+0.87
1960	+0.48	+0.86	+0.48	+0.80
1961	+0.68	-0.97	-0.15	+0.17
1962	+2.31	-0.37	-0.15	+1.07
1963	+0.14	+0.66	-0.75	-1.60
1964	-1.16	+1.23	+1.35	+1.67
1965	-0.36	-0.34	-2.22	-2.23
1966	-1.06	-1.50	+0.25	-0.20
1967	+1.64	+0.16	+0.58	+0.07
1968	+0.54	+0.26	+0.85	-0.40
1969	-1.36	-0.67	-0.62	-1.20
1970	-1.29	-0.04	+0.35	+2.30
1971	+2.38	+2.43	+0.95	+2.23
1972	+0.88	-0.77	-1.75	-1.57
1973	-2.02	+0.03	+1.45	+2.90
1974	+3.64	+2.10	+1.05	+1.00
1975	-0.09	+1.50	+2.78	+2.93
1976	+2.91	+0.90	-1.25	-0.03
1977	+0.08	-1.47	-2.19	-1.93
1978	-2.69	-0.04	+0.61	-0.33
1979	+0.08	-0.30	-0.45	-0.27
1980	-0.22	-1.24	-0.19	-0.50
1981	-0.16	-0.94	+1.31	+0.20
1982	+0.94	-0.37	-3.02	-3.80
1983	-5.96	-2.24	-0.59	+0.77
1984	+0.44	-0.37	-0.22	+0.07
1985	+0.21	+0.86	-0.09	+0.20
1986	-0.16	-0.24	-0.15	-0.63
1987	-1.64	-2.23	-1.07	-0.23
1988	+0.10	+0.40	+0.73	+1.77
1989	+1.17	+1.13	+0.17	+0.27
1990	-1.10	-0.03	-0.03	-0.47
1991	0.00	-1.30	-0.53	-1.37
AVE	0.00	-0.04	+0.02	+0.09
STD	1.71	1.09	1.24	1.41

TABLE E.1: Continued (Standardized)

YEAR	WINTER	SPRING	SUMMER	AUTUMN
1948	-0.39	0.00	-0.33	+0.06
1949	-0.46	+0.13	-0.68	+0.03
1950	+1.18	+1.87	+2.25	+1.33
1951	+1.64	-1.10	-0.86	-1.29
1952	-0.93	+0.09	+0.31	+0.01
1953	-0.64	-1.43	-0.86	-0.70
1954	-0.15	+0.28	+0.45	+0.20
1955	+0.87	+0.37	+1.82	+1.71
1956	+1.29	+1.56	+1.34	+0.81
1957	+0.46	-0.61	-0.38	-0.87
1958	-1.09	-0.42	+0.45	-0.37
1959	-1.16	+0.83	-0.57	+0.55
1960	+0.28	+0.83	+0.37	+0.50
1961	+0.40	-0.85	-0.14	+0.06
1962	+1.35	-0.30	-0.14	+0.70
1963	+0.08	+0.64	-0.62	-1.20
1964	-0.68	+1.17	+1.07	+1.12
1965	-0.21	-0.28	-1.81	-1.65
1966	-0.62	-1.34	+0.19	-0.21
1967	+0.96	+0.18	+0.45	-0.01
1968	+0.32	+0.28	+0.67	-0.35
1969	-0.80	-0.58	-0.52	-0.91
1970	-0.75	0.00	+0.27	+1.57
1971	+1.39	+2.27	+0.75	+1.52
1972	+0.51	-0.67	-1.43	-1.18
1973	-1.18	+0.06	+1.15	+1.99
1974	+2.13	+1.96	+0.83	+0.72
1975	-0.05	+1.41	+2.23	+2.01
1976	+1.70	+0.86	-1.02	-0.09
1977	+0.05	-1.31	-1.78	-1.43
1978	-1.57	0.00	+0.48	-0.30
1979	+0.05	-0.24	-0.38	-0.26
1980	-0.13	-1.10	-0.17	-0.42
1981	-0.09	-0.83	+1.04	+0.08
1982	+0.55	-0.30	-2.45	-2.76
1983	-3.49	-2.02	-0.49	+0.48
1984	+0.26	-0.30	-0.19	-0.01
1985	+0.12	+0.83	-0.09	+0.14
1986	-0.09	-0.18	-0.10	-0.51
1987	-0.96	-2.01	-0.88	-0.23
1988	+0.06	+0.40	+0.57	+1.19
1989	+0.68	+1.07	+0.12	+0.13
1990	-0.64	+0.01	-0.04	-0.40
1991	0.00	-1.16	-0.44	-1.04